



**HAL**  
open science

**Approches micro-macroscopiques pour l'évaluation des mécanismes fongiques impliqués dans la dégradation des mortiers biosourcés : impact sur les propriétés hygrothermiques**

Dmytro Kosiachevskyi

► **To cite this version:**

Dmytro Kosiachevskyi. Approches micro-macroscopiques pour l'évaluation des mécanismes fongiques impliqués dans la dégradation des mortiers biosourcés : impact sur les propriétés hygrothermiques. Civil Engineering. Université Paris-Saclay, 2021. English. NNT : 2021UPAST124 . tel-04510270

**HAL Id: tel-04510270**

**<https://theses.hal.science/tel-04510270>**

Submitted on 18 Mar 2024

**HAL** is a multi-disciplinary open access archive for the deposit and dissemination of scientific research documents, whether they are published or not. The documents may come from teaching and research institutions in France or abroad, or from public or private research centers.

L'archive ouverte pluridisciplinaire **HAL**, est destinée au dépôt et à la diffusion de documents scientifiques de niveau recherche, publiés ou non, émanant des établissements d'enseignement et de recherche français ou étrangers, des laboratoires publics ou privés.

Micro-macroscopic approaches for the  
evaluation of fungal mechanisms involved  
in the degradation of bio-based mortars:  
impact on hygrothermal properties

**Thèse de doctorat de l'université Paris-Saclay**

École doctorale n° d'accréditation, dénomination et sigle

Spécialité de doctorat : génie civil

Unité de recherche : Université Paris-Saclay, ENS Paris-Saclay, CNRS, LMT - Laboratoire de Mécanique et Technologie, 91190, Gif-sur-Yvette, France

Référent : ENS Paris-Saclay

**Thèse présentée et soutenue à Paris-Saclay,  
le 08/12/2021, par**

**Dmytro KOSIACHEVSKYI**

**Composition du Jury**

<b>Stephanie STAQUET</b> Professeur, Université Libre de Bruxelles	Présidente
<b>Sofiane AMZIANE</b> Professeur, Université Clermont Auvergne	Rapporteur
<b>Antonin FABBRI</b> Professeur, Université de Lyon	Rapporteur
<b>Isabelle TRINSOUTROT-GATTIN</b> Professeur, UniLaSalle	Examinatrice
<b>Stephane POYET</b> Maître de conférences, HDR, CEA	Examineur
<b>Lisa CASTEL</b> Ingénieur d'études, UniLaSalle	Invitée

**Direction de la thèse**

<b>Mohend CHAOUCHE</b> Professeur, ENS Paris-Saclay	Directeur de thèse
<b>Kamilia ABAHRI</b> Maître de conférences, ENS Paris- Saclay	Co-encadrante de thèse
<b>Anne DAUBRESSE</b> Responsable Laboratoire, ParexGroup	Tutrice en entreprise



# CONTENTS

<b>CONTENTS</b> .....	<b>3</b>
<b>LIST OF FIGURES</b> .....	<b>7</b>
<b>LIST OF TABLES</b> .....	<b>12</b>
<b>GENERAL INTRODUCTION</b> .....	<b>14</b>
<b><i>CHAPTER I. GENERAL INFORMATION ON HEMP MORTAR: FROM ANATOMY TO HYGRO-MECHANICAL BEHAVIOR AND DURABILITY</i></b> .....	<b>17</b>
<b>I.1. INTRODUCTION</b> .....	<b>17</b>
<b>I.2. ECOLOGICAL AND THERMAL INTEREST IN USING BIO-BASED MATERIALS</b> .....	<b>17</b>
<b>I.3. HEMP MORTAR</b> .....	<b>20</b>
I.3.1. Composition of hemp mortar .....	20
I.3.1.1. Hemp particles and their characteristics .....	21
I.3.1.2. Mineral binder .....	24
I.3.1.2.1. Lime .....	24
I.3.1.2.2. Portland cement .....	26
I.3.1.2.3. Calcium Sulfoaluminate Cements (CSA) .....	29
I.3.2. Applications of hemp mortars in construction .....	31
I.3.2.1. Different formulations of hemp mortars .....	31
I.3.2.2. Application techniques .....	32
I.3.2.3. Cure conditions .....	34
<b>I.4. PROPERTIES OF THE HEMP MORTARS</b> .....	<b>35</b>
I.4.1. Mechanical properties of hemp fibers and hemp mortars .....	35
I.4.2. Thermal properties .....	37
I.4.3. Hydric properties.....	39
I.4.3.1. Sorption-desorption curves .....	40
I.4.3.2. Water vapor permeability .....	41
I.4.3.3. Moisture buffer value (MBV) .....	42
I.4.4. Acoustic properties.....	44
<b>I.5. DURABILITY AND AGING OF THE HEMP MORTARS</b> .....	<b>45</b>
I.5.1. Concept of the durability .....	45
I.5.2. Factors of hemp mortar’s durability .....	46
I.5.2.1. Impact of agricultural methods: retting .....	47
I.5.2.2. Interconnexion mineral binder / hemp shivs .....	49
I.5.2.2.1. Influence of the mineral binder on organic granulates .....	50
I.5.2.2.2. Influence of organic compounds on the mineral binder .....	51
I.5.3. Hemp dimensional variations at hygric loads .....	55
I.5.4. Degradation of hemp mortar and their properties during its service life.....	57
I.5.5. Microbiological contamination .....	60
I.5.5.1. Concept of bioreceptivity for building materials .....	60
I.5.5.2. Microbiological degradation of different building materials .....	61
I.5.5.3. Microbiological contamination of hemp mortars .....	62

<b>I.6. CONCLUSION.....</b>	<b>63</b>
<b>CHAPTER II. ANALYZE OF THE HEMP MORTAR DURABILITY: IMPLEMENTATION OF NEW TOTAL WEATHERING AGING PROTOCOL.....</b>	<b>65</b>
<b>II.1. INTRODUCTION.....</b>	<b>65</b>
<b>II.2. CHOICE OF ACCELERATED AGING EXPERIMENTAL PROTOCOL.....</b>	<b>66</b>
<b>II.3. EXPERIMENTAL PROTOCOL.....</b>	<b>68</b>
<b>II.3.1. Hemp mortar’s composition and fabrication.....</b>	<b>68</b>
<b>II.3.2. Accelerated weathering aging cycles.....</b>	<b>69</b>
<b>II.3.3. Experimental procedure.....</b>	<b>71</b>
<b>II.3.3.1. Microstructural characteristics and chemical analysis.....</b>	<b>72</b>
<b>II.3.3.2. Hygrothermal properties evolution.....</b>	<b>75</b>
<b>II.4. EVOLUTION OF MICROSTRUCTURE, CHEMICAL COMPOSITION AND HYGROTHERMAL PROPERTIES OF HEMP MORTAR.....</b>	<b>78</b>
<b>II.4.1. Microstructural characteristics and chemical analysis.....</b>	<b>79</b>
<b>II.4.2. Hygrothermal properties evolution.....</b>	<b>83</b>
<b>II.5. CONCLUSION.....</b>	<b>86</b>
<b>CHAPTER III. INFLUENCE OF THE MOLD GROWTH ON THE CRYSTALLOGRAPHIC COMPOSITION OF HEMP MORTAR.....</b>	<b>90</b>
<b>III.1. INTRODUCTION.....</b>	<b>90</b>
<b>III.2. GENERAL INFORMATION ON MOLDS.....</b>	<b>90</b>
<b>III.2.1. Molds strains in the world.....</b>	<b>90</b>
<b>III.2.2. Mold classification and phylogeny.....</b>	<b>91</b>
<b>III.2.3. Fungal reproduction.....</b>	<b>92</b>
<b>III.2.4. Biological characteristics of molds.....</b>	<b>93</b>
<b>III.2.5. Conditions for mold growth.....</b>	<b>94</b>
<b>III.2.5.1. Physicochemical factors.....</b>	<b>94</b>
<b>III.2.5.2. Nutritive conditions.....</b>	<b>97</b>
<b>III.2.6. Interactions of molds with the environment.....</b>	<b>98</b>
<b>III.2.7. Ability of mold to degrade a material.....</b>	<b>99</b>
<b>III.2.8. Effects of moulds on human health.....</b>	<b>100</b>
<b>III.2.8.1. Allergens.....</b>	<b>100</b>
<b>III.2.8.2. Volatile Organic Compound (VOC).....</b>	<b>101</b>
<b>III.2.8.3. Mycotoxins.....</b>	<b>101</b>
<b>III.2.8.4. Glucans.....</b>	<b>101</b>
<b>III.3. BIBLIOGRAPHIC STUDY OF THE MOLDS’ IMPACT ON THE HEMP MORTAR.....</b>	<b>102</b>
<b>III.4. EXPERIMENTAL PROTOCOL.....</b>	<b>103</b>
<b>III.4.1. Materials and conditioning.....</b>	<b>103</b>

III.4.2. Methods of characterization .....	104
III.4.2.1. Mold growth observation .....	104
III.4.2.2. Chemical characterization.....	105
III.5. MOLD GROWTH OBSERVATION .....	105
III.6. CHEMICAL CHARACTERIZATION.....	107
III.7. CONCLUSION.....	110
<b>CHAPTER IV. FUNGAL RISK ANALYSIS IN HEMP MORTARS: IDENTIFICATION OF FUNGAL SPECIES .....</b>	<b>113</b>
IV.1. INTRODUCTION.....	113
IV.2. PREDICTION AND QUANTIFICATION OF MOLD GROWTH.....	113
IV.3. IDENTIFICATION OF FUNGAL SPECIES .....	115
IV.3.1. Identification methods of molds strains.....	115
IV.3.2. Phenotypic methods.....	115
IV.3.3. Mass spectrometry method .....	117
IV.3.4. Molecular methods .....	118
IV.4. EXPERIMENTAL PROTOCOL .....	119
IV.4.1. Materials formulation and conditioning .....	119
IV.4.2. Conditioning.....	120
IV.4.3. Cultivation conditions.....	122
IV.4.4. Fungal identification procedure.....	122
IV.5. HEMP SHIVE FUNGAL CONTAMINATION ANALYSIS .....	123
IV.6. HEMP MORTAR FUNGAL CONTAMINATION ANALYSIS.....	125
IV.6.1. Morphology analysis and interface observation.....	125
IV.6.2. Fungal species identification.....	127
IV.7. ANALYSIS OF IDENTIFIED FUNGAL SPECIES .....	128
IV.7.1. <i>Rhizopus sp.</i> .....	128
IV.7.2. <i>Aspergillus niger</i> .....	129
IV.8. CONCLUSION.....	131
<b>CHAPTER V. METAGENOMIC ANALYSIS OF HEMP MORTAR AND HEMP SHIVE FUNGAL CONTAMINATION.....</b>	<b>133</b>
V.1. INTRODUCTION.....	133
V.2. BIBLIOGRAPHIC STUDY .....	133
V.3. EXPERIMENTAL PROCEDURE .....	134
V.3.1. In situ conditioning and sample preparation.....	134
V.3.2. Total DNA extraction and quantification .....	136
V.3.3. Real-time PCR amplification .....	137
V.3.4. Metagenomic analysis of microbial community .....	137
V.3.4.1. Library construction and metagenomic sequencing .....	137
V.3.4.2. Data metagenomic sequencing analyses .....	137
V.4. FUNGAL DNA SEQUENCING DATA ANALYSIS .....	138
V.4.1. DNA extraction.....	138

V.4.2.	Rarefaction analysis .....	138
V.4.3.	Mold species identified .....	139
V.5.	ANALYSIS OF MAJOR FUNGI GENERA AND DISCUSSION .....	143
V.6.	CONCLUSION.....	144
<b><i>CHAPTER VI. EVALUATION OF HEMP MORTAR AND HEMP SHIV BACTERIAL CONTAMINATION BY METAGENOMIC INVESTIGATION</i></b> .....		<b>147</b>
VI.1.	INTRODUCTION.....	147
VI.2.	BIBLIOGRAPHIC STUDY .....	147
VI.3.	EXPERIMENTAL PROCEDURE .....	148
VI.3.1.	In situ conditioning.....	149
VI.3.2.	Sample preparation .....	150
VI.3.3.	Total DNA extraction and quantification .....	151
VI.3.4.	Real-time polymerase chain reaction (PCR) amplification.....	152
VI.3.5.	Metagenomic analysis of microbial community .....	153
VI.3.5.1.	Library construction, and metagenomic sequencing .....	153
VI.3.5.2.	Data metagenomic sequencing analyses.....	153
VI.4.	BACTERIAL DNA SEQUENCING DATA ANALYSIS .....	154
VI.4.1.	DNA extraction.....	154
VI.4.2.	Rarefaction analysis .....	154
VI.4.3.	Identification of bacterial species.....	155
VI.5.	ANALYZE OF MAJOR BACTERIAL GENERA AND DISCUSSION.....	161
VI.5.1.	Hemp shives bacterial contamination.....	161
VI.5.2.	Hemp shives and hemp mortar contamination .....	162
VI.5.3.	Hemp mortar contamination .....	166
VI.6.	CONCLUSION.....	167
<b><i>CONCLUSIONS AND PERSPECTIVES</i></b> .....		<b>170</b>
<b>REFERENCES</b> .....		<b>173</b>

## LIST OF FIGURES

Figure 1. Final energy consumption by sector in France: 140 megatons of oil equivalent in 2016 (ADEME, 2018).....	18
Figure 2. CO <sub>2</sub> emissions by sector in France in 2016 (ADEME, 2018).....	18
Figure 3. Carbon footprint of different building materials .....	20
Figure 4. Hemp cultivated surface and processing units by regions in France (Scrucca et al., 2020).....	22
Figure 5. Schematic representation of the general structure of a plant fibre cell wall displaying the distribution of cellulose microfibrils with hemicellulose and lignin (Shuvo, 2020) .....	23
Figure 6. Structure of lignocellulosic tissue.....	23
Figure 7. Manufacture and setting mechanisms of natural hydraulic lime.....	25
Figure 8. Couvrot cement plant (France): (1) preparation of raw materials, (2) baking and (3) treatment of clinker.....	26
Figure 9. Typical Portland cement heat flow (mW/g) as a function of time given by isothermal calorimetry measurements (Bullard et al., 2011) .....	28
Figure 10. Different application of hemp mortars in construction (roof and wall insulation) (Chabannes et al., 2018).....	31
Figure 11. Hemp mortar techniques: (a) bricklaying, (b) casting monolithic walls, (c) prefabrication, (d) spraying.....	33
Figure 12. Diagram of the influence of the curing conditions on the mechanical performances of the lime-based plant mortars (Chabannes, 2015) .....	35
Figure 13. Compressive strength tests on the hemp mortar after 28 days of setting in curing conditions of 20 °C and various relative humidities (Arnaud and Gourlay, 2012).....	35
Figure 14. Two representative diagrams of the typical behavior of hemp-lime mortar under a compressive axial load (Walker et al., 2014).....	37
Figure 15. Evolution of thermal conductivity depending on the water content of the material at 23 °C, and 30 days of age (Bennai et al., 2017).....	38
Figure 16. Comparison of thermal conductivity as a function of hemp mortar temperature at 30 and 60 days of age (Bennai et al., 2017).....	39
Figure 17. Thermal conductivity of sprayed hemp mortar wall versus dry density and water content (Collet and Pretot, 2014).....	39
Figure 18. Stages of water vapor adsorption under rising relative humidity .....	40
Figure 19. Comparison of water vapor adsorption-desorption isotherm of hemp mortar at 7, 30 and 60 days hemp concrete age at 25 °C (Bennai et al., 2017).....	41
Figure 20. Sound absorption of hemp concrete according to the binder content (Glé et al., 2011) .....	44
Figure 21. Sound absorption of hemp shiv in bulk for 3 different sizes of the particles (Glé et al., 2011) .....	44
Figure 22. Representation of the concepts of performance and service life (ISO 15686, 2011; Talon, 2006) .....	46
Figure 23. Diagram representing different parameters and their interconnections that affect the durability of hemp mortars.....	47
Figure 24. SEM images of the transverse sections two types of hemp stems (a, c, e, g and b, d, f, h) during retting. Before retting (a,b), after 14 (c,d), 28 (e,f) and 42 days (g,h) of retting; (ba) bacteria, (bf) biofilm, (co) conidiophore, (ef) elementary fibre, (ep) epidermis, (fb) fibre bundle,	



(fbd) fibre bundle decohesion, (fl) fibre lumen, (hy) hyphae, (mc) microbial colonization, (p) parenchyma, (tr) trichome and (xy) xylem. Scale bar =200 $\mu\text{m}$ .....	49
Figure 25. Organic fiber degradation (sisal example) mechanisms in a Portland cement environment (Melo Filho et al., 2013).....	50
Figure 26. Diagrammatic sketch of natural fiber's alkaline degradation process (Wei and Meyer, 2015).....	51
Figure 27. Representation of the flow of mortar with admixed lignin samples from different organic fibers (flax, hemp, wheat straw) obtained with the small-scale testing apparatus (Nadif et al., 2002) .....	52
Figure 28. SEM micrographs of cortical fibers before (a and b) and after immersion in a lime-saturated solution (c and d) for 24h (Sedan et al., 2008).....	54
Figure 29. Variations in the concentrations of calcium ( $\square$ ), silicon ( $\Delta$ ), aluminium (+) and iron ( $\times$ ) as a function of the amount of hemp fibres introduced into a diluted cement paste ( $W / C = 2$ ). Measurements made 30 min after the start of mixing (Sedan et al., 2008) .....	54
Figure 30. Heat flow for pastes of CEM I, CEM I mixed with hemp shiv powder and hemp concrete (Delannoy et al., 2020b).....	55
Figure 31. Evolution of the middle slice of hemp during water absorption as seen by MRI, higher brightness means higher water content (Fourmentin et al., 2016) .....	56
Figure 32. Water to hemp mass ratio in time as measured by T1 relaxometry (squares) and by weighing of an immersed sample (crosses). The inset shows the additional water to hemp mass ratio in phase 2 of imbibition as a function of time in logarithmic scale. The continuous line has a slope 1/2 (Fourmentin et al., 2016).....	56
Figure 33. Hemp mortar's sample at (a) dry state, and strains equivalent to 76% RH (b) $\epsilon_{xx}$ (d) $\epsilon_{yy}$ and (d) $\epsilon_{xy}$ (Bennai et al., 2019).....	57
Figure 34. Swelling of hemp concrete (%) as a function of relative humidity (%) .....	57
Figure 35. Evolution of the thermal conductivity of the lime-based (FL-HC) and natural cement-based (NC-HC) binders of the reference samples $A_{REF}$ and aged samples $A_{WD}$ (Delannoy et al., 2020a) .....	59
Figure 36. Lime carbonatation kinetics, followed by the intensity of the (104) X-ray diffraction peak of calcite (Elfordy et al., 2008) .....	59
Figure 37. Visualization of the conceptualization of bioreceptivity proposed by (Sanmartín et al., 2021) .....	60
Figure 38. Observation of molds on shiv by scanning electron microscopy (Marceau et al., 2017) .....	62
Figure 39. Example of wetting/ drying cycles (a) and immersion and drying cycles (b) (Abahri et al., 2020) .....	67
Figure 40. Hemp shives .....	68
Figure 41. Granulometric curve of hemp mortar by image analysis .....	68
Figure 42. Mass ratios of hemp mortar composition .....	69
Figure 43. Hemp mortar samples laboratory drying.....	69
Figure 44. Diagram of the total accelerated aging cycles (A) with detailed heat-rain (B) and heat-cold (C) cycles.....	70
Figure 45. Disposition of the hemp mortar specimens in the climatic room before accelerated aging cycles .....	70
Figure 46. Experimental protocol schema .....	71
Figure 47. Hemp mortar samples without (A) and with (B) protective cotton tissue .....	72
Figure 48. Hemp mortar samples in the Hitachi S-3400N.....	73
Figure 49. Preparation of hemp mortar samples (coverage with carbon).....	73

Figure 50. Measurement of the surface pH level using a WTW Sentix Sur electrode.....	74
Figure 51. Bruker D8 diffractometer used for crystallography analysis .....	75
Figure 52. Hemp mortar sample sealed on the experimental cup .....	76
Figure 53. CT-Metre measurement device .....	77
Figure 54. Moisture buffer value (g/%RH.m <sup>2</sup> ) standardization according to Nordtest protocol (NORDTEST project, 2005).....	78
Figure 55. Total water porosity values (%) evolution of hemp mortar samples before and after the weathering aging cycles .....	79
Figure 56. W-SEM observation of the surface of the specimens before (a) and after (b) the weathering aging cycles.....	80
Figure 57. Mean size (µm) of the hemp particles / cementitious matrix interface cracks for 2 samples before and after the weathering aging cycles (10 measurements for 10 interfaces) .....	81
Figure 58. X-ray diffraction patterns of: (a) interior part of the hemp mortar samples before the weathering aging cycles; (b) interior part of the hemp mortar samples after the weathering aging cycles; (c) surface part of the hemp mortar samples before the weathering aging cycles; (d) surface part of the hemp mortar samples after the weathering aging cycles .....	82
Figure 59. Zoomed X-ray diffraction patterns for ettringite (I), portlandite (II) and calcite (III) evolution: (a) interior part of the hemp mortar samples before the weathering aging cycles; (b) interior part of the hemp mortar samples after weathering aging cycles; (c) surface part of the hemp mortar samples before the weathering aging cycles; (d) surface portion of the hemp mortar samples after the weathering aging cycles.....	82
Figure 60. Diagram of pH level evolution on the surface and in the middle of the samples before and after the weathering aging cycles.....	83
Figure 61. Water vapor permeability (kg.s <sup>-1</sup> .m <sup>-1</sup> .Pa <sup>-1</sup> ) evolution of hemp mortar samples before and after the weathering aging cycles.....	84
Figure 62. Thermal conductivity (W/m.K) evolution of hemp mortar samples before and after the accelerated aging cycles.....	84
Figure 63. Masse (g) and relative humidity (%RH) evolution in function of the time .....	85
Figure 64. Moisture buffer value (g/%RH.m <sup>2</sup> ) evolution of hemp shives and hemp mortar samples before and after the accelerated aging cycles .....	86
Figure 65. Phylogeny and classification of fungi based on the analysis of several genes (Hibbett et al., 2007).....	92
Figure 66. Diagram of fungal sexual and asexual reproduction .....	93
Figure 67. Metabolism scheme (aerobic and anaerobic) .....	96
Figure 68. Distribution of Ascomycetes and Basidiomycetes strains according to the final pH of the growth medium after 6 days of incubation (Liaud et al., 2014) .....	99
Figure 69. Hemp mortar samples before aging .....	104
Figure 70. High humidity desiccator weathering (23 ± 2 °C, 97 ± 2% RH) of hemp mortar samples.....	104
Figure 71. ATR-FTIR spectra obtained from hemp mortar samples conditioned during two years at high humidity and laboratory conditions .....	106
Figure 72. W-SEM observations of mould growth on the hemp mortar sample conditioned in a high humidity environment for two years at different depths: at the surface (a); at 1 mm (b); at 2 mm (c); and at 4 mm from the surface (d).....	107
Figure 73. X-ray diffraction patterns of: interior part (a) and surface part (b) of the hemp mortar reference sample (23 °C and 50% RH); interior part (c) and surface part (d) of the hemp mortar sample conditioned at high humidity environment (23 °C and 97% RH).....	108

Figure 74. Diagram of pH level evolution on the surface and in the middle of the samples conditioned for two years at the laboratory and high humidity conditions .....	109
Figure 75. TG and DTG analysis performed in samples of two types of conditioning after 2 years: LI – interior part of laboratory conditioned sample, LS – surface part of laboratory conditioned sample, HI – interior part of the sample conditioned at high humidity, HS – surface part of the sample conditioned at high humidity .....	110
Figure 76. Granulometric curves of four hemp shives types: (A) HS-1, (B) HS-2, (C) HS-3, (D) HS-4 .....	120
Figure 77. Conditioning schema of the hemp shives and hemp mortar samples .....	121
Figure 78. Electric burner .....	123
Figure 79. Isolation of molds .....	123
Figure 80. Representation of the scotch tape method for fungal identification .....	123
Figure 81. Monitoring of mold growth in a Petri dish (left - first day, right - after 5 days).....	124
Figure 82. Images of Petri dishes with the shives of 4 hemp types after 8 days of cultivation: HS-1 (a), HS-2 (b), HS-3 (c), HS-4 (d).....	124
Figure 83. Numerical microscope photos of the hemp mortar (F2) before (a) and after (b) mold growth .....	126
Figure 84. SEM images of the morphological structures of the mold present on the hemp concrete of the first formulation (F1) .....	126
Figure 85. SEM images of the morphological structures of the mold present on the hemp concrete of the second formulation (F2).....	126
Figure 86. Image of Petri dish with F1 particles after 8 days at laboratory conditions.....	127
Figure 87. Image of Petri dish with isolated white fungal strain (identified as <i>Rhizopus sp.</i> ) after 8 days at 25 °C and 50 %RH.....	127
Figure 88. Image of Petri dish with isolated white fungal strain (identified as <i>Aspergillus niger</i> ) after 8 days at 25 °C and 50 %RH.....	128
Figure 89. Microscopical observation of <i>Rhizopus sp.</i> : (A) magnification 1:200 and (B) magnification 1:600 .....	129
Figure 90. Isolated <i>Rhizopus sp.</i> after 8 days at 5°C .....	129
Figure 91. Isolated <i>Rhizopus sp.</i> after 8 days at 35°C .....	129
Figure 92. Microscopical observation of <i>Aspergillus niger</i> : (A) magnification 1:300, (B) magnification 1:400, (C) magnification 1:1000 .....	130
Figure 93. Isolated <i>Aspergillus niger</i> after 8 days at 5°C.....	130
Figure 94. Isolated <i>Aspergillus niger</i> after 8 days at 35°C .....	131
Figure 95. Images of mold proliferation on hemp mortar (A), in the optical microscope (B), and the electronic microscope (C) .....	135
Figure 96. Mass ratios of hemp mortar composition.....	135
Figure 97. DNA extraction protocol schema .....	136
Figure 98. Rarefaction analysis of the observed OTUs for the hemp shives, the hemp mortar, and the negative control as a function of an increasing number of sequences .....	139
Figure 99. Relative abundance levels of each fungal phylum for hemp shives (a) and hemp mortar (b) .....	140
Figure 100. Fungal community analysis in hemp shives (18S rDNA).....	141
Figure 101. Fungal community analysis in hemp mortar (18S rDNA) .....	141
Figure 102. Venn Diagram evaluating the concentration of mold contamination of hemp shives, hemp mortar and both.....	142
Figure 103. Study case: stone masonry castle in the region of Pau (France) .....	149

Figure 104. Image of the wall before the hemp mortar insulation (a) and the application process (b).....	149
Figure 105. Example of two samples: hemp mortar (left) and hemp shivs (right) .....	150
Figure 106. In situ mold proliferation on inside insulation hemp mortar.....	150
Figure 107. Images of bacterial proliferation on hemp mortar (A), in optical microscope (B) and in electronic microscope (C) .....	151
Figure 108. DNA extraction protocol schema .....	152
Figure 109. Rarefaction analysis of the observed OTUs for the hemp shivs, the hemp mortar and the negative control as a function of an increasing number of sequences .....	155
Figure 110. Relative abundance levels of each bacterial phylum for hemp shivs (left) and hemp mortar (right) .....	156
Figure 111. Bacterial community analysis in hemp shivs (16S rDNA) .....	158
Figure 112. Bacterial community analysis in hemp mortar (16S rDNA).....	159
Figure 113. Venn Diagram evaluating the concentration of bacterial contamination of hemp shivs, hemp mortar and both hemp shivs and mortar .....	160

---

## LIST OF TABLES

---

Table 1. Examples of the hemp mortar formulations in function of the application type .....	31
Table 2. Composition and performances of hemp mortars in function of its application .....	32
Table 3. Mechanical properties of natural fibers compared to conventional reinforcement available from the literature (Bentur and Mindess, 2006; Bledzki and Gassan, 1999; Lewin and Pearce, 1998; Li et al., 2000) .....	36
Table 4. Description of one cycle of different aging protocols.....	67
Table 5. Total water porosity values (%) evolution of hemp mortar samples before and after the weathering aging cycles .....	79
Table 6. Fungi categories according to their development temperature range .....	94
Table 7. Moulds in building materials and their water activity (Li and Yang, 2004).....	95
Table 8. Mass ratios of hemp mortar composition .....	104
Table 9. Oxide analysis of used lime-based binder with hydraulic additions.....	104
Table 10. Classification of mold growth index .....	114
Table 11. Values of the coefficients representing the material sensitivity class (Ojanen et al., 2010; Viitanen et al., 2010).....	114
Table 12. Formulations of the studied hemp mortar .....	120
Table 13. Results of hemp shive mold identification .....	125
Table 14. Results of hemp mortar mold identification .....	128
Table 15. Mass ratios of hemp mortar composition .....	151

---

GENERAL INTRODUCTION

---

## GENERAL INTRODUCTION

---

Today, the use of materials with a low environmental impact, such as bio-based mortars, which are already recognized for their thermal and acoustic insulation qualities, is attracting increasing attention in the construction sector. Unlike conventional building materials, they present a renewable resource derived from plant biomass. Thus, they are low-cost materials that save energy and are responsible for low CO<sub>2</sub> emissions and therefore they are environmentally friendly.

Hemp mortars are one of the bio-based materials that are widely used in Europe and especially in France. Thermally, hemp shivs have a low thermal conductivity, which makes them suitable as insulating materials well adapted to function with mineral binders making light mortars. In fact, hemp mortars exhibit double porosity (having both intra- and interparticle porosity), which provides better insulating performance. The porous parts can contain a very variable proportion of water vapor that are subject to external excitations such as moisture sources and temperature. The combination of these phenomena will create a coupled transfer of heat, air and moisture within the material, which has a significant influence on the durability of buildings and represents one of the major causes of their degradation. Simultaneously, the durability of these materials with respect to internal and external environmental excitations is essential. Indeed, during their life cycle, bio-based mortars are exposed to various factors, such as microorganisms that can cause their degradation and affect the air quality of the buildings.

The objective of this thesis is the study and the analysis of the properties evolution and durability of biosourced materials, and particularly hemp mortar. Different aspects of durability are approached by taking into account various phenomenon during the life cycle of hemp mortar, as the hygro-thermal durability and the microbiological proliferation.

To do so, this work consists firstly in experimental characterization the microscopic, hygrothermal and chemical durability of the material. Particular attention was devoted to the choice of the experimental aging protocol taking into account the literature data and previously proposed protocols. In second part, this work consists in complete analyzing of microbiological contamination: its influence on the chemical composition of the mortar and precise, elaborated analysis of the proliferation. This approach allows a better understanding of the hemp mortar / microorganisms interconnection and the main sources of the microbiological contamination of the bio-based building materials.

To address these issues, this research paper has been organized into six interconnected chapters:

In CHAPTER I, the general context of this work is presented. It includes an evaluation of the multiscale and anisotropic structure of bio-based materials, in particular hemp mortars, as well as a bibliographic study of its behavior and its thermo-hygro-mechanical properties. Particular attention was devoted to the overview of the works available in the literature dealing with the durability and microorganism proliferation of hemp mortars. This chapter gives a critical vision on the need to consider the coupled behavior of this material and includes all the essential concepts for the realization of the present work.

In CHAPTER II, the experimental investigation of the durability of hemp mortar was proposed. The first part of this chapter describes the choice of the experimental aging protocol. In a second step, chosen aging protocol was applied to the material and the microstructural, chemical and hygro-thermal properties were analyzed before and after the aging. Finally, all these results were analyzed and interpreted, linking the various microstructural quantities characteristic of hemp mortar and their variation due to proposed accelerated aging protocol.

In next chapters the complete precise analysis of microbiological proliferation was conducted. CHAPTER III represents the study of the fungal proliferation influence on the chemical composition of the hemp mortar. Different techniques allowed to identify the fungal growth of the hemp mortar specimens and to analyze the chemical composition of the hemp mortar mineral matrix.

CHAPTER IV deals with the fungal species identification and is complementary to the study presented in the CHAPTER III. Indeed, for more precise risk assessment, the species identification of the fungal growth is necessary. To do so, in the first part of this chapter the choice of the fungal identification technique was conducted. The method consists in microscopic observation of the molds present in hemp mortars and their comparison to the catalogs. The results showed that this phenotypical method is not reliable enough to ensure the exhaustive analysis of the fungal growth.

That is why, CHAPTER V and VI propose the metagenomic analyze of the fungal and bacterial contamination of hemp mortar and hemp shivs. In the first parts of both chapters, the principle of DNA extraction and sequencing are proposed. Obtained results allowed to make the conclusion on the main source of the microbiological contamination of bio-based materials.



CHAPTER I.

GENERAL INFORMATION ON HEMP MORTAR:  
FROM ANATOMY TO HYGROTHERMAL  
BEHAVIOR AND DEGRADATION

---

# **CHAPTER I. GENERAL INFORMATION ON HEMP MORTAR: FROM ANATOMY TO HYGRO-MECHANICAL BEHAVIOR AND DURABILITY**

---

## **I.1. INTRODUCTION**

In this chapter, the context and the problematic in which this work is carried out are presented. Thus, a bibliographical study is presented in a structured way for a better description of the environmental conditions of hemp mortars and their influence on their properties and durability. Then, a description of the current environmental challenges and possible solutions is made to underline the need to reduce energy consumption and carbon impact in the building sector using bio-based materials. Then, the anatomical structure and composition of hemp mortar was presented with emphasis on the chemical composition of organic fibers. Thereafter, the thermal, hygroscopic, acoustic and mechanical properties of hemp mortars will be presented. Finally, a bibliographical review of the durability studies carried out on hemp mortars will reveal the limits and the lack of knowledge of the work already existing in the literature. Particular attention was devoted to the research of hemp mortars degradation under hygrothermal and microbiological stresses.

## **I.2. ECOLOGICAL AND THERMAL INTEREST IN USING BIO-BASED MATERIALS**

Since the beginning of the age of industrialization and the first use of fossil energy sources (e.g., coal, oil), human activities have provoked climate changes. These last ones have been accelerating since the second half of the 20<sup>th</sup> century and are manifested in rising of global temperatures. This can cause more frequent meteorological events, melting of glaciers, or rising of ocean levels. This, in turn, is leading to a shortage of drinking water, the migration of large populations, and the disappearance of biological species (IPCC, 2013).

The goal of reduction of emissions is to avoid a global temperature rise of more than 1.5 degrees by 2100. Numerous subsequent climate conferences have emphasized the importance of the path taken and tightened control measures. Proposed solutions vary by the sector of activity.

The last climate conference in Madrid in 2019 emphasized different solutions to reduce the rate of global warming. In the construction sector, several solutions could be adopted, such as:

using of materials with low carbon footprint, using of local building materials that decrease the necessity of the transport, decreasing of the energy consumption at all stages of construction. As regards the building sector in France, 45% of final energy was consumed (see Figure 1) and 22% of CO<sub>2</sub> was emitted (see Figure 2) due to the functioning of the residential and tertiary sectors in 2016 (ADEME, 2018).

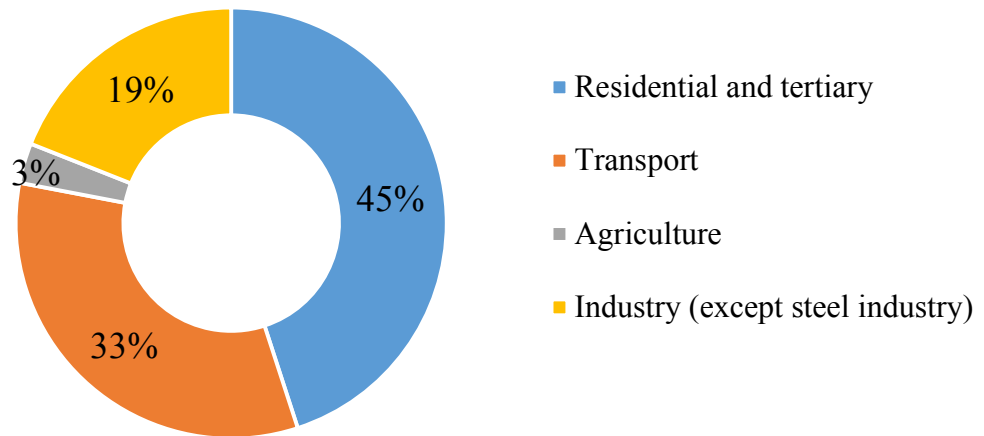


Figure 1. Final energy consumption by sector in France: 140 megatons of oil equivalent in 2016 (ADEME, 2018)

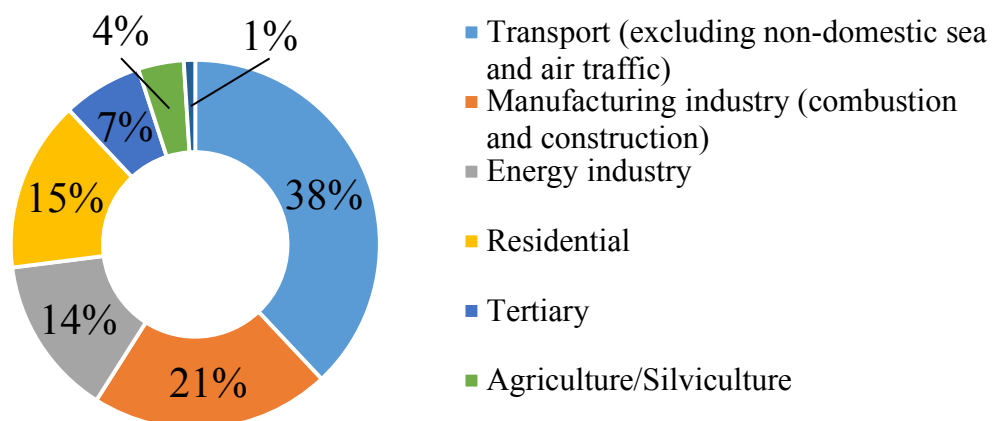


Figure 2. CO<sub>2</sub> emissions by sector in France in 2016 (ADEME, 2018)

A design phase is critical for the construction of low-energy buildings. From 1974, as a consequence of the oil shock, several thermal regulations were regularly adopted. Over time, different thermal regulations have been implemented in 1974 (RT 1974), 1982 (RT 1982), 1988 (RT 1988), 2000 (RT 2000), 2005 (RT 2005), 2012 (RT 2012) and 2022 (RT 2020). They all contributed to the reduction of the maximum authorized consumption in new buildings. The new thermal regulation RT 2020 is based on the concept of a low energy building. It lies on three main pillars: decrease of the energetic price of the building, summer comfort and decarbonation of the elements (materials and energy consumption). Nevertheless, all the thermal regulations could be applied for new buildings but not for the existing building park.

Nowadays, the main idea of the building insulation is the total reduction of thermal bridges in order to eliminate heat loss. This technique represents a risk for old buildings whose external walls are often made of stones, bricks, wood, rammed earth or daub. These are materials that have the ability to absorb moisture from the atmosphere (e.g., wood) or the rising damp (e.g., stone, rammed earth) that increase the moisture content in the walls and can provoke mold proliferation and structural degradation (Agence Qualité Construction, 2016). That is why it is so important to choose the appropriate insulation materials that allow moisture and water vapor pass through. The need to both to reduce the amount of greenhouse gas emissions and to properly insulate the existing old houses leads us to use of new unconventional materials that respond to today's ecological challenges.

The development of new building materials with low environmental impact requires the analysis and comparison of the impact of these materials on ecology and the environment. To do so, different methods were proposed in the literature. We can distinguish Carbon Footprint evaluation (CF) (ISO 14067, 2018), Life Cycle Analysis (LCA) (ISO 14040, 2006; ISO 14044, 2006), Eco-Efficiency Analysis (EEA) (Kounetas, 2021). All of them allow to evaluate different impacts of the product on the environment, the main difference being the number of parameters. According to quantitative comparison of various building materials used in construction, bio-based materials represent lower carbon footprint (Figure 3). Similarly, it was approved by the results of other studies (Magwood, 2014; Tettey et al., 2014) for different types of structural insulation (roof, floor, walls). Indeed, as organic fibers being the by-product of the agricultural industry, they represent a low carbon footprint at the production stage. Additionally, the bio-based materials are the natural stock of CO<sub>2</sub> that allow to decrease its quantity in the atmosphere. All of these aspects make bio-based materials a good solution for environmentally friendly insulation.

First of all, it is advisable to define what are bio-based materials. In fact, bio-based materials are materials derived from biomass (plant or animal). These materials can be transformed or contain a part of non-organic materials. The use of local materials is also important as it decreases the impact of transportation and thus reduce the embodied energy of the material (Akbarnezhad and Xiao, 2017). Also, they are interesting from the point of view of their thermal, acoustic and hydric properties (El Hachem et al., 2019, 2017; Garikapati and Sadeghian, 2020; Jerónimo et al., 2020; Ren et al., 2019; Walker et al., 2014).

Nowadays, different organic fibers, such as straw, cork, flax or hemp, are used for bio-based thermal insulation. Also, we can distinguish different types of applications of materials. We can use bio-based materials in bulk or fabricate insulation boards (flax boards), organic wools (i.e., wood, flax, hemp, sheep) or mortars (i.e., hemp mortar, wood mortar). Concerning the bio-based mortars, they are characterized by the presence of mineral matrix that enrobe organic particles and

allow to ensure their cohesion to protect them from environmental impacts of different nature (i.e., hygrothermal solicitations, insects, rodents). One of the most promising bio-based mortars in France is hemp mortar that is the object of this study.

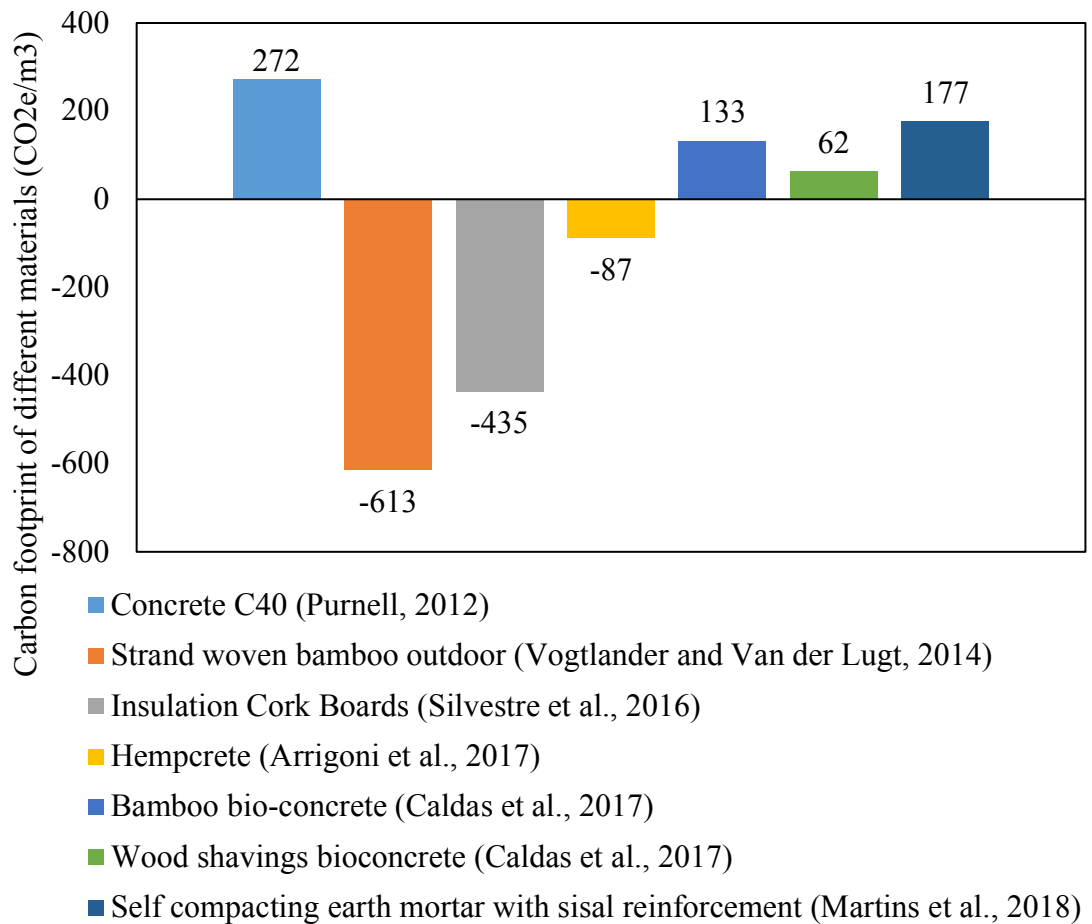


Figure 3. Carbon footprint of different building materials

### I.3. HEMP MORTAR

In this section, the general information on hemp mortars will be presented. Firstly, the chemical composition and the structural analysis of hemp shivs and mineral matrix is detailed in order to better understand interconnection of the microstructure and properties. Then, different applications' methods of this material will be presented.

#### I.3.1. Composition of hemp mortar

The hemp mortar is obtained by mixing hemp particles, mineral binder, water and possible additives. It could be used as the layer of insulation or as a filling material for a supporting structure.

Hemp concrete has a very high and essentially "open" porosity (more than 70% in volume for a "wall" type formulation (Collet et al., 2008; Evrard and De Herde, 2005)) with several characteristic pore sizes:

- macropores (about 1 cm in diameter) due to the imperfect arrangement of the various hemp particles in the mixture;

- mesopores (0.1 mm to 1 mm) between the particles and the binder;

- interhydrate micropores (less than 0.01  $\mu\text{m}$ ) in the binder matrix.

As hemp mortar is a composite material, first we must study the components separately in order to better understand the microstructure and properties of the total material.

### **I.3.1.1. Hemp particles and their characteristics**

The hemp (*Cannabis sativa L.*), that has been used as a source of organic particles, has been well known in agriculture for over 8000 years for its textile fibers and oleaginous seeds (Terres Inovia, 2020). In France, after reaching its peak in the middle of 19th century (176,000 ha) with outlets for paper mills and the sailing navy, the surface area was reduced to a few hundred hectares in 1960 (700 ha) due to the emergence of cotton, synthetic fibers and the arrival of the motorized navy. Never abandoned, the crop has seen a revival since the 1970s for paper markets. In 2019, the hemp cultivated surface reached 15,200 ha, which represents 40% of the total European hemp production. This is due to the increased interest towards hemp industry and agricultural advantages (Amaducci et al., 2015; Horne, 2020). Data on cultivated hemp by regions and main processing units are represented in Figure 4. It is cultivated mainly for its fibrous stem, being widely used in paper, textiles, construction, isolation, agriculture, composites, automotive, medicine, etc. Nowadays, the global hemp market is estimated to consist of more than 25,000 products (Salentijn et al., 2015) and new applications for hemp products are continually emerging (Adesina et al., 2020).

Hemp is composed of two products that generate three raw materials: straw, separated into fiber and hemp particles and hemp seeds. Also, it is possible to distinguish the third product of defibering of hemp straw – an organic powder. All these materials could be valorized (Amaducci et al., 2015). The seeds are rich in protein, fibers, fatty acids and others minerals. Thus, they are interesting from the point of view of their use for food or cosmetics. They represent about 11% of the plant mass. The fibers that represent 24% of plant's total mass are widely used for textiles, composites or organic wool insulation. Hemp particles are the most abundant product of hemp (44% of total mass). They are used for animal bedding, horticultural mulch or in construction (in bulk or in hemp mortars). The organic powder represents 21% of total hemp mass but only 2% of

its economic value. It is composed of small particles of organic fibers as well as mineral materials. It can be used as cow bedding or fuel in industrial boilers after compression (Terres Inovia, 2020).

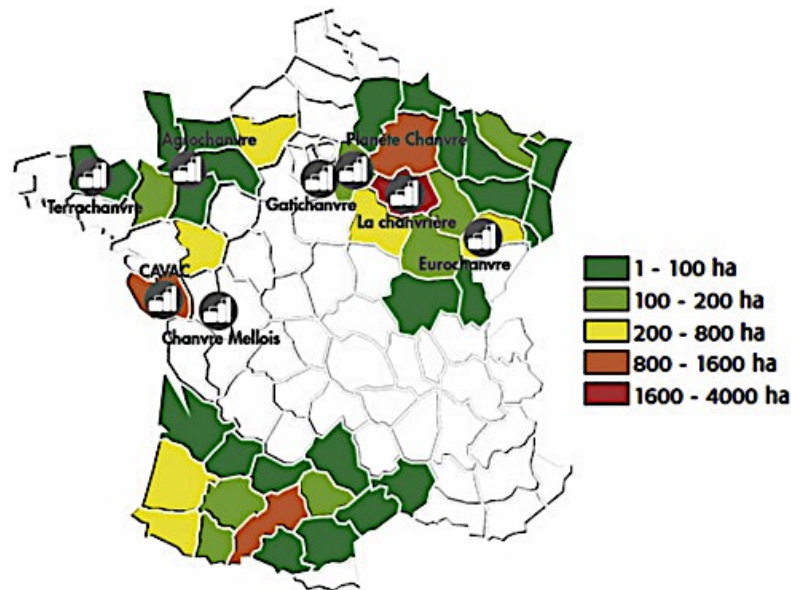


Figure 4. Hemp cultivated surface and processing units by regions in France (Scrucca et al., 2020)

Hemp particles that are used in construction are technically composed of hemp particles themselves and organic powder. Because of its high absorbent capacity, the quantity of organic powder must be regulated. It allows to control the difference between the properties of final hemp mortar. Nevertheless, the main part is hemp particle.

Organic hemp particles are natural composites with a cellular structure. They are composed of several elements, at different scales. The hemp particle at a first scale (the largest) consists of cell walls with lumens (voids). As can be seen in Figure 5, from the outside to the inside, the hemp fibers consist of a middle lamina (a), a primary wall (b), a secondary wall (c), a tertiary wall, and a lumen (Shuvo, 2020).

The middle lamina is mainly composed of pectins (galacturonic acid macromolecules) which hold the fibers together in a bundle. Next to the middle lamella, the primary cell wall is made up of disorganized fibers (a polymer based on glucose units) consisting of fibrils in an organic matrix of hemicelluloses, lignin and proteins. The secondary cell wall is composed of three layers of cellulose fibrils with different axial orientation bound by lignin (Mohanty et al, 2000).

On a finer scale, lignocellulosic materials refer to plants composed of cellulose, hemicellulose and lignin. Cellulose microfibrils (formed by ordered polymer chains that contain tightly packed crystalline regions) are incorporated into the hemicellulose and lignin matrix, as shown in Figure 6.

The strength and stiffness of the fibers are mainly provided by hydrogen bonds between the different chemical components. Other characteristics such as thermal stability, UV resistance or

biodegradation depend on the concentration of each component characterized by its individual properties. Hemicellulose is responsible for biodegradation, moisture absorption and thermal degradation of the fiber (Sahed and Jog, 1999). Lignin is mainly a structural material that adds strength and rigidity to cell walls and constitutes between 15% by total weight and 40% by weight of the dry matter of plants. It is a cross-linked macromolecular material based on a phenylpropanoid monomer structure. Typical molecular weights of isolated lignin are between 1000 and 20,000 g/mol, but the degree of polymerization in nature is difficult to measure, as lignin is always fragmented during extraction and consists of several types of substructures that repeat in an apparently disordered manner (Doherty, 2011). Indeed, lignin is more resistant to most forms of biological attack than cellulose and other structural polysaccharides (Akin and Benner, 1988, Baurhoo et al., 2008, and Kirk, 1971).

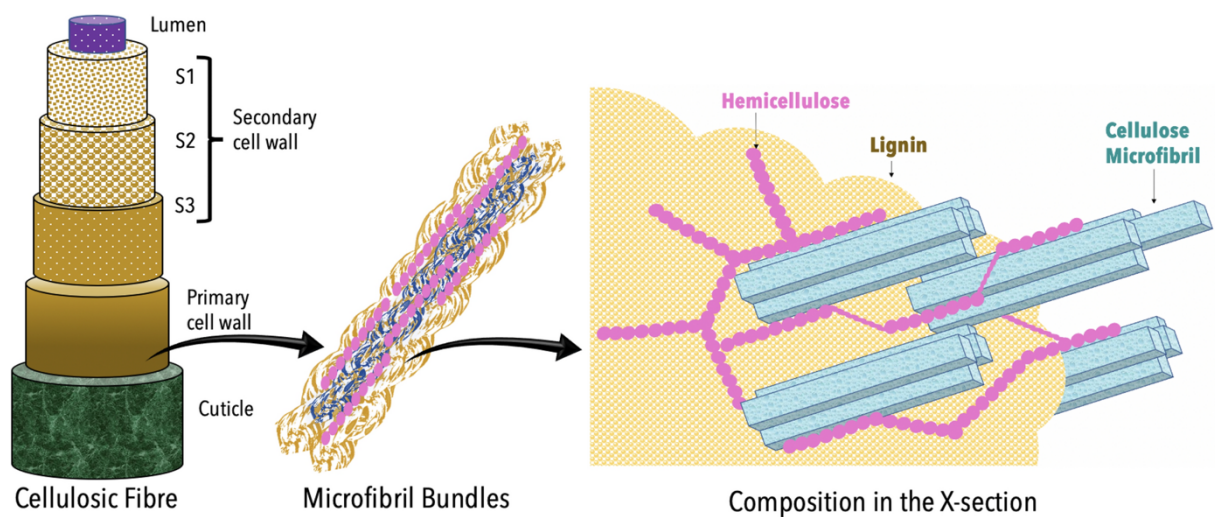


Figure 5. Schematic representation of the general structure of a plant fibre cell wall displaying the distribution of cellulose microfibrils with hemicellulose and lignin (Shuvo, 2020)

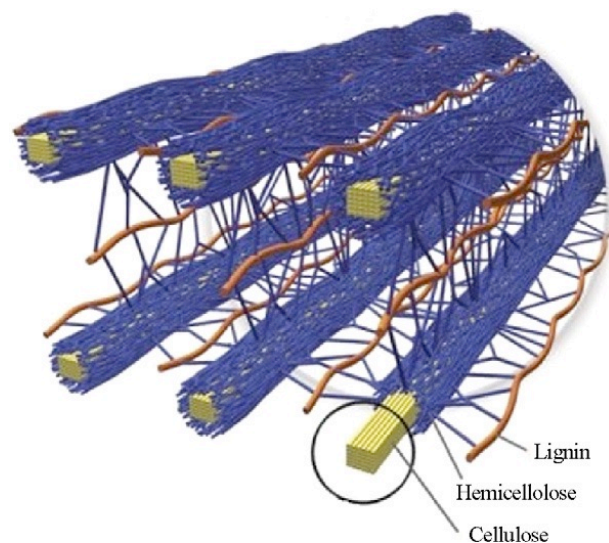


Figure 6. Structure of lignocellulosic tissue



Thus, plants with higher lignin content are more resistant to direct sunlight and frost (Miidla, 1980). In vitro, lignin extracts and lignin have antimicrobial and antifungal activity (Cruz et al., 2001), act as antioxidants (Ugartondo et al., 2008), absorb radiation (Toh et al., 2005; Zschiegner, 1999) and have flame retardant properties (Reti et al., 2008).

### **I.3.1.2. Mineral binder**

The second component of hemp mortar is a binder or a mixture of binders. It binds all hemp particles together, ensures their mechanical properties and protects them against insects and animals. It also can contain certain additives.

Various types of binders were used for hemp mortar as cement (Bütschi et al., 2004; de Bruijn et al., 2009) or different mixes of hydraulic lime, hydrated lime and pozzolanic admixtures (Arizzi et al., 2015; Chabannes et al., 2018). According to (SEBTP, 2012), 4 types of binders could be used, such as lime (according to NF EN 459-1), quick-setting cement (NF P 15-314), ordinary cement (NF EN 197-1) or another material with a pozzolanic effect.

The most adapted binders are those which represent the aerial hydration. This is explained by the high absorbance that negatively affect the hydraulic setting. The use of lime-based binders allows to get the biobased mortars with lower density and enhance their hygrothermal properties. Nevertheless, other hydraulic binders are used to get the minimum of mechanical performances that will be sufficient to resist against drying shrinkage. The main mineral binders used in the present work are listed in following paragraphs.

#### **I.3.1.2.1. Lime**

##### **Calcic and dolomitic lime (CL and DL according to EN 459-2)**

Calcic lime is fabricated by the decarbonation of the limestone at 900°C:

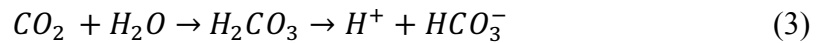


Then, the quicklime (CaO) is slaked by adding water:

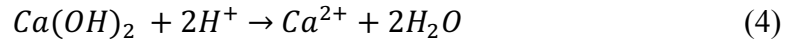


Calcic limes contain more than 80% of Ca(OH)<sub>2</sub> and about 5% of CaCO<sub>3</sub>. Their hardening occurs due to the reaction of carbonation, that needs the access of air (specifically, CO<sub>2</sub>). It is the best type of binder from the point of view of the bio-based mortars. In fact, from the first moment of adding of water in the mortar, organic particles absorb water because of their hygroscopicity. It decreases the quantity of water available for binder hydration that is important for hydraulic binders. As for carbonation reaction, the presence of water speeds up but is not critical. A carbonation reaction occurs between 30 and 90% RH and proceeds in three steps (Cizer et al., 2012; Rackley, 2017):

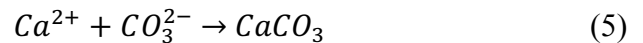
1.  $\text{CO}_2$  dissolves in water to form carbonic acid containing protons ( $\text{H}^+$ ) and bicarbonate ions ( $\text{HCO}_3^-$ ):



2. The presence of free protons ( $\text{H}^+$ ) enables the release of Ca from the mineral matrix:



3. The metal and bicarbonate ions combine to precipitate carbonate:



This setting starts quickly but then the phenomenon slows down and takes several years.

### Hydraulic lime

Another type of lime is hydraulic one. It is obtained from limestones that contain silicates. The  $\text{CaO}/\text{SiO}_2$  ratio influences the quantity of the  $\text{C}_2\text{S}$  that give their hydraulic properties. Natural limestones are often composed of siliceous and silicate minerals known as reactive minerals. At the temperature around  $1200^\circ\text{C}$ , calcium oxide  $\text{CaO}$  combines with these elements to form calcium silicates. The schema of the hydraulic and calcic lime is represented in Figure 7 (Martinet and Souchu, 2009).

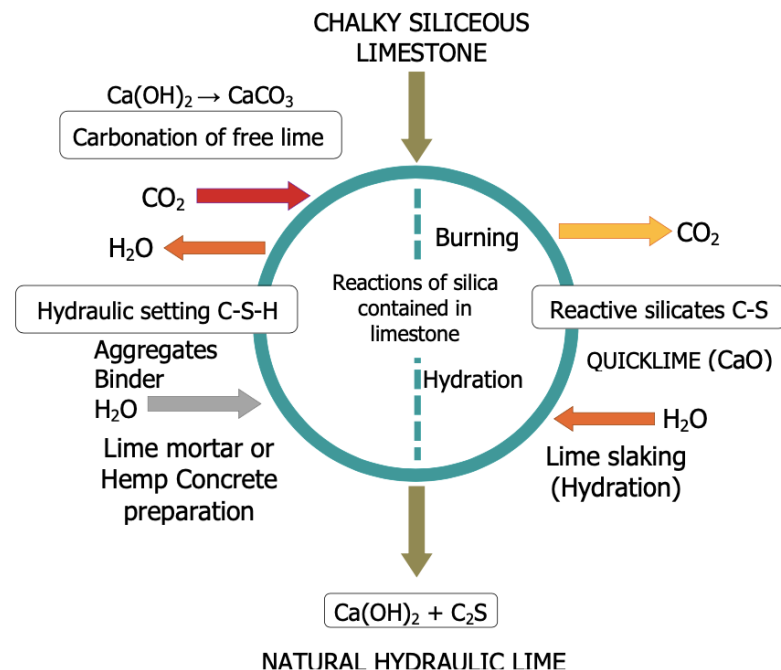
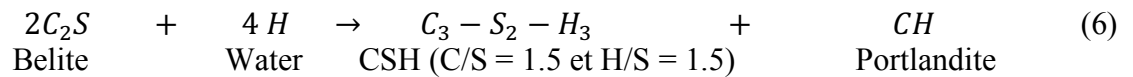


Figure 7. Manufacture and setting mechanisms of natural hydraulic lime<sup>1</sup>

<sup>1</sup> <http://www.stastier.co.uk/nhl/info/hydraul.htm>

Natural hydraulic limes (NHL) are composed of Portlandite  $\text{Ca}(\text{OH})_2$  (30-50%), belite  $\text{C}_2\text{S}$  (20-40%) and calcite  $\text{CaCO}_3$  (5-20%). They have the property of setting and hardening both by hydration reaction with the mixing water (hydraulic setting) and by reaction with  $\text{CO}_2$  from the air (non-hydraulic setting). The hydration of  $\text{C}_2\text{S}$  for hydraulic and natural hydraulic limes is carried out according to the following reaction:



### I.3.1.2.2. Portland cement

Portland cement is the most used mineral binder in construction. It is composed of clinker, gypsum and different additives. Its production consists of three main stages: preparation of the raw materials, baking and treatment. In the first stage, the raw materials (clay and limestone) are dosed, dried, ground, homogenized to  $800^\circ\text{C}$  and fed into the rotating cement kiln. In the kiln, raw materials are heated up to  $1450^\circ\text{C}$ . The resulting Portland clinker is mainly composed of alite ( $\approx 60\%$ ,  $\text{Ca}_3\text{SiO}_5$ ), belite ( $\approx 20\%$ ,  $\text{Ca}_2\text{SiO}_4$ ), tricalcium aluminate ( $\approx 5$  to  $15\%$ ,  $\text{Ca}_3\text{Al}_2\text{O}_6$ ) and tetracalcium aluminoferrite ( $\approx 0$  to  $15\%$ ,  $4\text{CaO}\cdot\text{Al}_2\text{O}_3\cdot\text{Fe}_2\text{O}_3$ ). Clinker is also composed of a few percent alkali sulphates, free lime or periclase. Later, during the last stage, the obtained Portland clinker is ground with different additives. These steps are illustrated in Figure 8:

1. Preparation of raw materials: a mixture of clay (20%) and limestone (80%) is dried, ground, homogenized and preheated to  $800^\circ\text{C}$ . About a ton and a half of raw materials are used to produce a ton of cement;
2. Baking: It takes place in a rotary oven at  $1450^\circ\text{C}$ . We thus obtain the clinker;
3. Treatment of clinker: The clinker is finely ground with additions (gypsum, limestone, ash, slag, etc.) whose properties and quantities determine the quality of the cement.

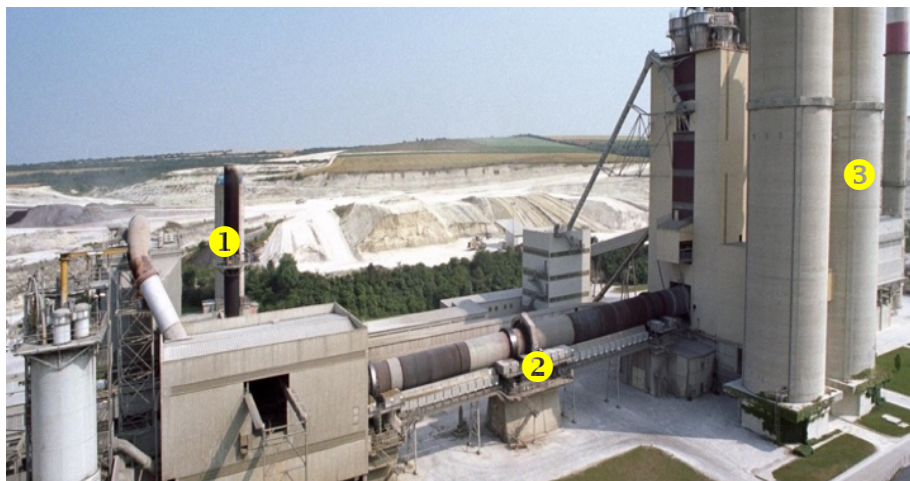


Figure 8. Couvrot cement plant (France): (1) preparation of raw materials, (2) baking and (3) treatment of clinker

As for hydration process, it is based on the dissolution. In fact, after adding water to the cement, the anhydrous clinker compounds that are soluble dissolve and enrich the solution with ions, mainly calcium, silicon, aluminium and sulphur (Bullard et al., 2011). When the solution becomes supersaturated, hydrates that are less soluble than clinker precipitate and become in thermodynamic equilibrium with the interstitial solution. These reactions are called heterogeneous because they take place in two distinct media: a liquid medium (water) and a solid medium (hydrates). These chemical equilibria have enabled the thermodynamic modeling of cement hydration.

Dissolution reactions are exothermic phenomena that can be monitored by calorimetry. Schematically, under standard conditions, four periods of hydration of a Portland cement can be distinguished as indicated in Figure 9:

1. Initial reaction (during the first few minutes). When Portland clinker compounds are mixed with water, a strong release of heat occurs; it corresponds to the rapid dissolution of the clinker, especially the alkaline sulfates ( $\text{Na}_2\text{SO}_4$ ,  $\text{K}_2\text{SO}_4$ );
2. Period of slow reaction is of almost one hour (between 1 and 2 hours after mixing) during which the heat flow is low. The anhydrous compounds then dissolve very slowly. Several theories (formation of a metastable hydrate barrier or slow activation of dissolution) are proposed to explain this phenomenon. During this period, the cement has not yet hardened, allowing it to be used;
3. Acceleration period of almost 9 hours when reactions accelerate abruptly and release a large amount of heat. This acceleration can be explained by the breaking of the metastable hydrate barrier, nucleation and growth of amorphous gel (CSH) or Portlandite. The hydrates formed (CSH and Portlandite) cover the aggregates, form a porous network and ensure the cohesion of the concrete, leading to hardening and an increase in strength;
4. Deceleration period (after 9 hours) during which the heat flow gradually decreases. Hydration is then controlled by diffusion and continues for several months. The lack of water, the formation of the cementitious matrix and the exhaustion of the finest grains explain this slowing down, which also results in a slow rise in resistance.

Hydration of Portland cement leads to the formation of Portlandite ( $\text{Ca}(\text{OH})_2$  or CH) and CSH "gel". CSH is a hydrate whose crystallinity is very low (amorphous compounds) and whose composition can vary greatly depending on Ca/Si ratio, alkali, aluminum and quantity of water. The main hydration reactions of calcium silicates are proposed below. They are written in cementitious notation.

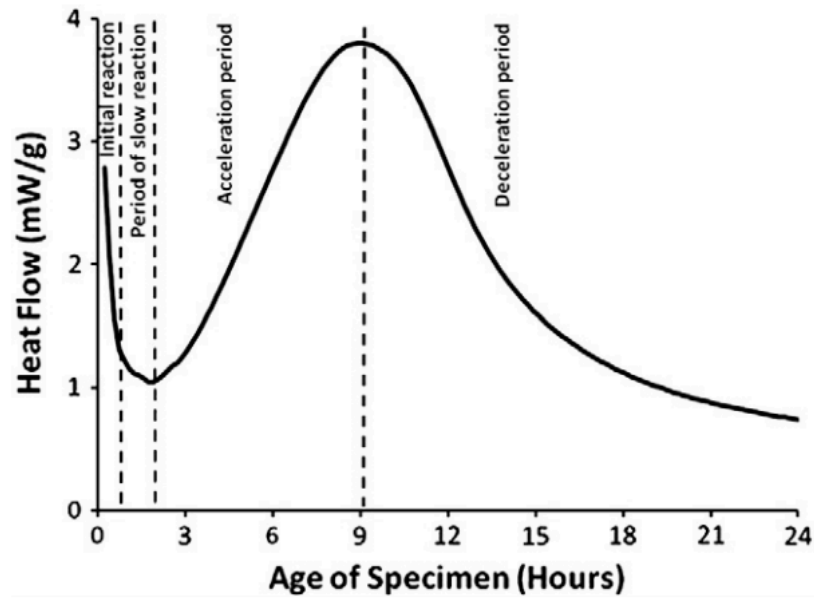
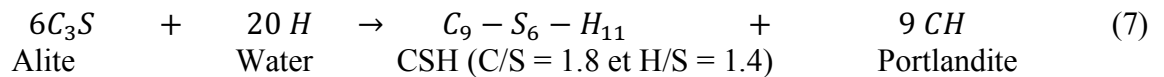
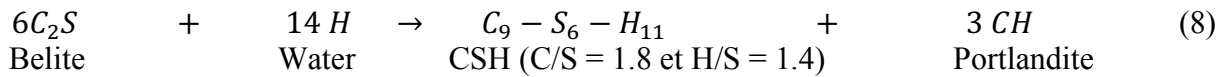


Figure 9. Typical Portland cement heat flow (mW/g) as a function of time given by isothermal calorimetry measurements (Bullard et al., 2011)

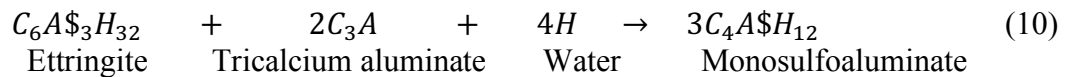
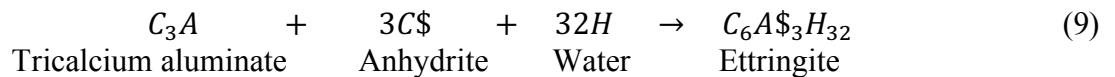
An alite is the most reactive and starts the hydration before others forming the CSH and portlandite:



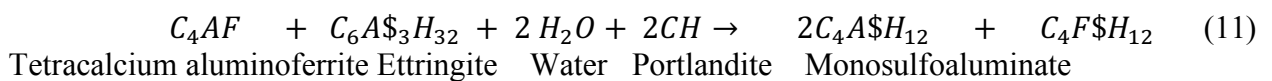
A belite starts its reaction later but it also results in forming of CSH and portlandite:



A tricalcium aluminate reacts with the formation of ettringite and a monosulfoaluminate. In fact, ettringite formation occurs early in the hydration of cement (Eq. 9). When a calcium sulfate is consumed, the monosulfoaluminate formation starts (Eq. 10):

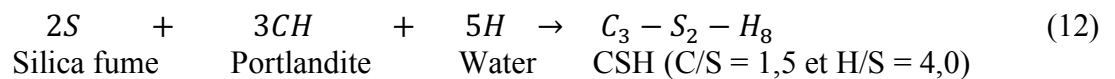


The hydration of the last phase,  $C_4AF$ , tetracalcium ferroaluminate involves calcium aluminoferrite and is very similar to that of  $C_3A$ . However, the reaction kinetics are much slower and the formed hydration products will substitute some of their aluminum with iron, the microstructure being the same.

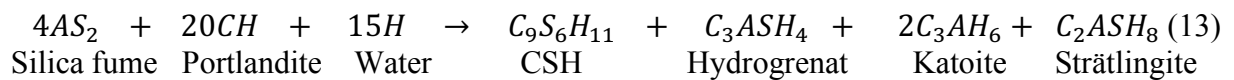


The volume occupied by the hydrates formed during these 5 reactions is smaller than that occupied by their respective anhydrous compounds and water. That is why Portland cement exhibits a volume contraction which can be the cause of chemical shrinkage and cracking.

Besides classical composition of the Portland cement, mineral binder could consist of some additives. They could decrease the mechanical properties because of the dilution effect (Hamidi, 2013). At the same time, they are known for their ability to improve the binder performance due to their granulometry or hydration reactions (Bucher et al., 2021). In fact, granulometry of the additives is very important as smaller size of the additive particles increases the contact surface between the water and the aggregates and therefore the number of possible nucleation sites. Also, it allows them to optimize stacking, fill small pores and improve the mechanical performances. Among such additives we can distinguish additives with pozzolanic properties such as silica fume, flue ash or metakaolin. The Portlandite formed by the hydration of Portland cement enables the binding properties of these additives. However, these compounds generally react slowly and affect short-term strength. Essentially siliceous additions, such as silica fume, lead to the formation of CSH:



Another pozzolanic additive is a metakaolin. It can contain significant proportions of aluminum or calcium. The metakaolin is metastable and presents a strong pozzolanic activity, whose reaction in the presence of lime leads to the formation of CSH, strätlingite (C<sub>2</sub>ASH<sub>8</sub>) or katoite (C<sub>3</sub>AH<sub>6</sub>) or hydrogrenat (C<sub>3</sub>ASH<sub>x</sub>):



### I.3.1.2.3. Calcium Sulfoaluminate Cements (CSA)

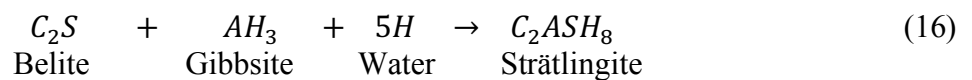
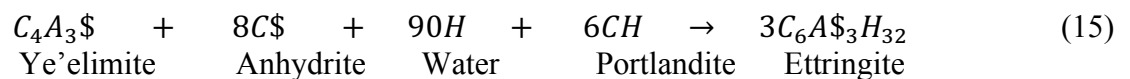
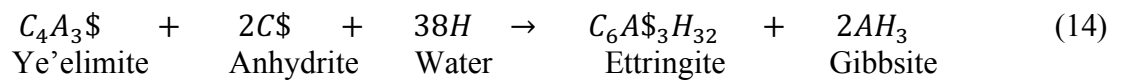
Calcium sulfoaluminate cement is made from about 40% of limestone (instead of 80% for Portland cement), a source of aluminum such as bauxite (40%) and a source of sulfate (20%). The obtained sulfoaluminous clinker is mainly composed of ye'elimite (≈ 65%) and belite (≈ 20%). Nevertheless, these proportions could change depending on the manufacturer. For example, (Le-Bihan et al., 2012) studied the CSA cement with 73.3% of ye'elimite and 16.12% of belite, or (Khalil et al., 2017) had 54.3% of ye'elimite and 29.1% of belite.

In order to better understand the origins of the different hydration kinetics, it is important to discuss the hydration of pure stoichiometric ye'elimite. Five steps of pure ye'elimite hydration can be distinguish (Bullerjahn et al., 2019a):

1. The initial period is characterized by the rapid dissolution of a small amount of ye'elimite. This results in a rapid increase in solution concentrations, resulting in a constant slowing down of the dissolution, starting in a few seconds. During the first step, only the formation of an amorphous phase is detected by X-ray.

2. The period of slow reaction is marked by the slow dissolution of ye'elimite. Ettringite, the only crystalline phase detected by XRD, forms progressively throughout this stage. This leads to a slow but constant decrease in sulfate ion concentration.
3. The acceleration period is marked by the rapid depletion of sulfate ions from the solution and the reacceleration of ye'elimite dissolution. These effects coincide with an increase in pH, an increase in the concentration of aluminum ions and the beginning of monosulfate formation in conjunction with microcrystalline aluminium hydroxide.
4. The main hydration period is characterized by the rapid rise in conductivity and pH, linked to the reaction of all the hydrated phases and the massive precipitation of hydrates. The degree of hydration is almost complete at the end of this stage, but its fall is slightly slowed down. On the contrary, the pH remains relatively constant at a high level.
5. The last stage represents a slow and constant decrease in the concentration of aluminum ions and a slight increase in pH. The formation of monosulphate and microcrystalline aluminium hydroxide continues, apparently at the expense of ettringite and amorphous phases.

These steps for hydration of ye'elimite in the presence of sulfates can be presented by the following equations:



Moreover, the importance of the mayenite for ye'elimite hydration was stated. In fact, the rapid dissolution of mayenite alters the Ca/Al ratio in solution. This results in acceleration of ettringite formation and faster depletion of primarily sulphate from solution. Consequently, the duration of the other hydration periods is shortened. However, the impact of mayenite depends on the w/b ratio. It was also shown, that the addition of 1% mayenite to the stoichiometric ye'elimite is sufficient to accelerate its hydration and a bigger quantity results in a delay of the main hydration peak (Bullerjahn et al., 2019b).

## I.3.2. Applications of hemp mortars in construction

### I.3.2.1. Different formulations of hemp mortars

Hemp mortar is generally used for thermal or acoustic insulation of different parts of buildings. According to (Chabannes et al., 2018), hemp mortars could be used in different structures in buildings, such as a roof or a floor insulation, non-load bearing walls or a coating for walls. The examples of such applications are represented in Figure 10. Different formulations have been proposed in the literature, some of them are referenced in Table 1.



Figure 10. Different application of hemp mortars in construction (roof and wall insulation) (Chabannes et al., 2018)

Table 1. Examples of the hemp mortar formulations in function of the application type

Reference	Binder / shivs ration (%w/w in total dry)	Water / binder ratio (%w/w)	Density (kg/m <sup>3</sup> )			
			Wall	Roof	Floor	Coating
(Gourlay et al., 2017)	2	1.3	573-700 (fresh), 340-415 (dry)	-	-	-
(Marceau et al., 2017)	2	1.5	573-578 (fresh), 325-327 (at 100 days)	-	-	-
(Sinka et al., 2014)	1.66	1.5	330-540	-	-	-
(Cerezo, 2005)	-	-	391	256	460	782

The formulations depend on the type of application, as a compromise between mechanical and thermal properties must be achieved. For example, roof insulation is applied on a pitched or



flat roof. It is not intended to bear any loads, so it could be formulated with less of binder (to fix hemp shivs together) and be lighter. Hemp mortar is also used for filling the walls in the buildings which is called non-load bearing walls. Hence, hemp mortar needs to save the form and support its own weight. In this case, the amount of binder and density must be higher than for the roof insulation. A compromise between mechanical and thermal properties must be achieved. The hemp mortar floor insulation is made in multiple layers including an abrasion protection. For this material, it is crucial to bear the effective load of the floor. That is why the quantity of binder is to be higher than for the walls. As for the coating, hemp mortar is applied with a thickness from 2 to 8 cm. It must therefore be sufficiently adhesive to remain on the support and retain its shape that needs more binder.

Table 2. Composition and performances of hemp mortars in function of its application

Hemp mortar application	Binder dosage (%w/w in total dry)	Hemp particles dosage (%w/w in total dry)	Dry density (kg/m <sup>3</sup> )	Modulus of elasticity (MPa)	Compressive strength (MPa)
Wall	50-90	10-50	200-1000	> 15	> 0,2
Roof				> 3	> 0,05
Floor				> 15	> 0,3
Coating				> 20	> 0,3

In order to match the type of application of hemp mortar, the dosage of components must be selected. Formulations are regulated by the professional construction rules (SEBTP, 2012). The rules identify limits of the hemp mortar formulation and performances for each application. The main characteristics of hemp mortar for four different applications are represented in the table 2. The minimal performances must be identified in standard conditions (20°C and 50% HR) at 60 at 90 days after hemp mortar fabrication. Also, the formulation of hemp mortar depends on the application technic.

### **I.3.2.2. Application techniques**

There are different technics for fabrication of hemp mortar structures. Four technics can be distinguished: bricklaying, casting of monolithic walls, prefabrication and spraying, as indicated in Figure 11. Every type of application represents different advantages.

Prefabricated blocs or structures are transported to a construction site already prepared for use. They don't need the time for drying and the rendering could be applied directly after their installation. This technic is used to for non-load bearing walls with thermal insulating properties and could be used for new building (Figure 11-a-b).

Another way of manufacturing is a casting monolithic wall. In this case, the fresh hemp mortar is mixed on site and then placed in a formwork that creates and compacts a structure. The disadvantage of this method is the time of drying of hemp mortar. In fact, in order to allow the hydration of the binder a great amount of water is added. This is why the drying of monolithic walls takes several months. This technic is used for internal or external insulation or even for non-load bearing walls of new or existing buildings (Figure 11-c).



(a)



(b)



(c)



(d)

Figure 11. Hemp mortar techniques: (a) bricklaying<sup>2</sup>, (b) casting monolithic walls<sup>3</sup>, (c) prefabrication<sup>4</sup>, (d) spraying<sup>5</sup>

<sup>2</sup> <https://www.solution-biosys.fr/>

<sup>3</sup> <http://www.technichanvre.com/techniques/conseils-techniques/banchage-chanvre-et-chaux/>

<sup>4</sup> <https://www.batirama.com/article/15380-le-beton-de-chanvre-passe-a-la-prefa.html>

<sup>5</sup> <https://www.lemoniteur.fr/photo/une-coque-en-beton-de-chanvre-pour-l-arche-des-petites-betes-du-parc-animalier-de-thoiry.1196994/projection.3>

Spraying is an interesting technic that allow to apply large surfaces of hemp mortar using special rendering machines. Even if it could be used for new buildings as internal or external insulation, this application method is well adapted to old building. These walls are often of irregular thickness and the spraying allows to level the surfaces and to compact the hemp mortar under the pressure. Moreover, as the quantity of water is lower, the time of drying is less than during casting of monolithic walls (Figure 11-d).

There two main methods of spraying: dry- and wet-mix process shotcrete. In the case of dry-mix process shotcrete, the dry or slightly moist mixture with a powdery consistency is fed into the blending machine. The mixture is transferred from the machine to the lance by a compressed air flow (high speed transfer). Water is added to the lance. In the case of wet-mix process shotcrete, the mixture, of plastic consistency, already contains all the necessary water. The transfer is mechanical: the concrete is pumped, possibly with the addition of compressed air to facilitate its transit (this is called diluted flow). The projection is ensured by adding compressed air to the lance. The consistency of the two mixes is therefore not comparable. It induces differences in terms of behavior during spraying, concrete compaction, production of losses and dust, and output.

When talking about hemp mortar spraying, the quality of supports must be controlled to ensure the durability of insulation. Walls before application must be scraped and brushed to remove dust or insufficiently cohesive parts. Supports must not be waterlogged or frozen. Existing coatings must be completely removed. All external hemp mortar insulation must be protected by finishing layer and coating to reduce the influence of the environment.

### **I.3.2.3. Cure conditions**

Available research results show that hemp mortars provide adequate mechanical and interesting insulating properties if properly designed and cured (SEBTP, 2012; Arnaud and Gourlay, 2012). Nevertheless, the improper curing cause some problems like hemp mortar cracking, dissociation or microbiological proliferation (Agence Qualité Construction, 2016; Kosiachevskyi et al., 2018; Parexlanko, 2020). All these factors decrease the durability of the hemp mortar structure, that is why the curing conditions must be controlled to allow the hydration of the binder. Hemp mortars represent an important quantity of water which cause a significant mass loss after drying. According to (Nguyen, 2014), the mass loss of a hemp mortar could be more than 30% in 3 months (at 20°C and 75% RH) depending on the formulation. As for mineral binder, hydraulic ones need enough water for their hydration. Non-hydraulic binders set during the action of carbonatation, which is not a quick phenomenon and is ideally done between 45% and 75% RH. Figure 12 indicates the influence of the curing conditions on the mechanical performances of the lime-based plant mortars.

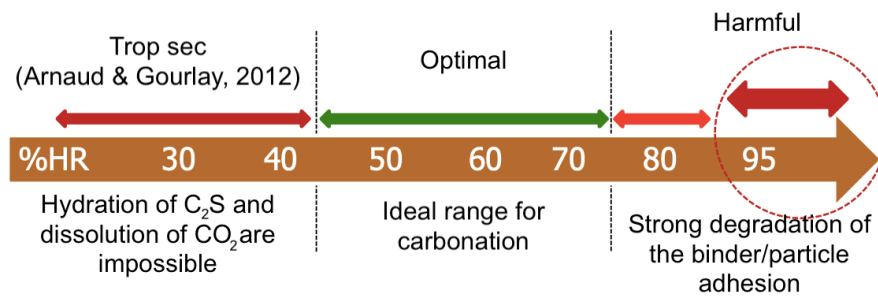


Figure 12. Diagram of the influence of the curing conditions on the mechanical performances of the lime-based plant mortars (Chabannes, 2015)

(Arnaud and Gourlay, 2012) and (Colinart et al., 2012) investigated the influence of the cure mode and the formulation on final properties of hemp mortars. Figure 13 shows an example of results of compressive strength tests on the hemp mortar after 28 days of setting in curing conditions of 20 °C and various relative humidities. These results revealed that the treatment at 20 °C and 50% RH is the best from the point of view of mechanical performances of hemp mortar.

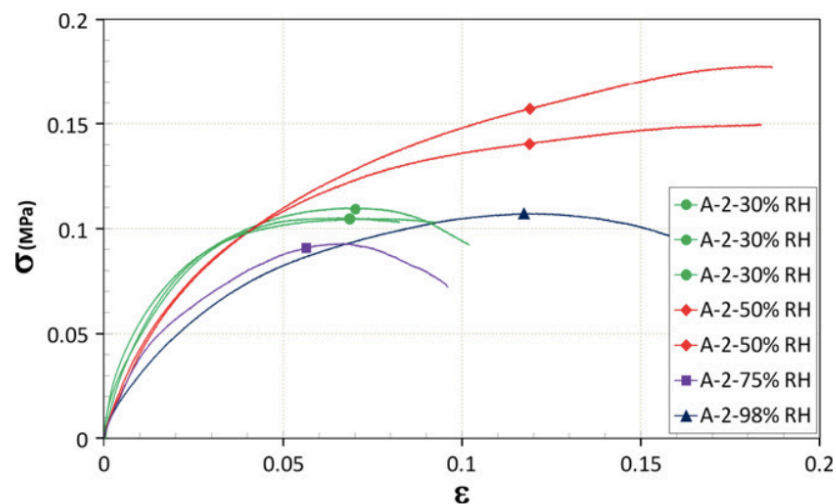


Figure 13. Compressive strength tests on the hemp mortar after 28 days of setting in curing conditions of 20 °C and various relative humidities (Arnaud and Gourlay, 2012)

## I.4. PROPERTIES OF THE HEMP MORTARS

All points described previously (formulation, cure conditions, etc.) influence the characteristics of hemp mortar and are critical for creating of the functional material. This section presents a description of the hemp mortar's mechanical and hygrothermal and acoustics properties.

### I.4.1. Mechanical properties of hemp fibers and hemp mortars

Since hemp mortars are used additionally as non-load bearing insulation materials, their mechanical properties are not the most important characteristic. There is a lot of research in the

literature that focuses on the mechanical properties of hemp mortars. They investigate compressive and flexural strengths (Arnaud and Gourlay, 2012; Chabannes, 2015). Unlike synthetic fibers, organic particles have lower mechanical properties (Table 3) due to the presence of surface defects and hierarchical internal microstructure (Luo et al., 2014). That is why their use needs detailed investigation.

Concerning hemp mortar, its mechanical strength under compression is similar to the most of cellular materials, e.g. wood (Gibson, 2003). (Walker et al., 2014) stated that under compressive loading, the stress-strain curve represents three regions: linear, plateau and densification, as it is shown in Figure 14. There are two cases: (a) with more distinct plateau region (large deformation for small increase in stress) and (b) with no plateau region. Figure 14-a demonstrates that initially, the curve is linear and the concrete behavior is quasi-elastic. Later, a cracking noise and binder powder appear indicating that the binder is failing. The behavior then departs from linearity and deformation significantly increases for a small stress increase (plateau region). During this phase, the hemp cells begin to collapse and the intensity of the cracking noise increases indicating that binder failure is becoming greater. Following the plateau region, there is a strain densification where the stress increases rapidly in relation to the strain. This is attributed to the collapse of the hemp particles which increases the stiffness of the concrete as the contact between cell walls provides additional mechanical strength. Hemp mortars of different formulations showed compressive strengths between 0.25 and 1.15 MPa with a corresponding elastic modulus between 4 and 160 MPa (Cerezo, 2005).

Table 3. Mechanical properties of natural fibers compared to conventional reinforcement available from the literature (Bentur and Mindess, 2006; Bledzki and Gassan, 1999; Lewin and Pearce, 1998; Li et al., 2000)

Fibre	Density (g/cm <sup>3</sup> )	Tensile strength (MPa)	Young's modulus (GPa)	Specific Young's modulus (GPa x cm <sup>3</sup> /g)
Flax	1.20–1.50	345–1035	28–90	19–75
Hemp	1.14–1.51	500–900	30–80	20–57
Sisal	1.45–1.50	67–635	4–22	3–15
E-Glass	2.50–2.60	2000–3500	70–80	27–32
Carbon	1.40–1.78	4000–5000	230–240	129–171
Steel	7.75–8.05	500–2000	200–210	25–27

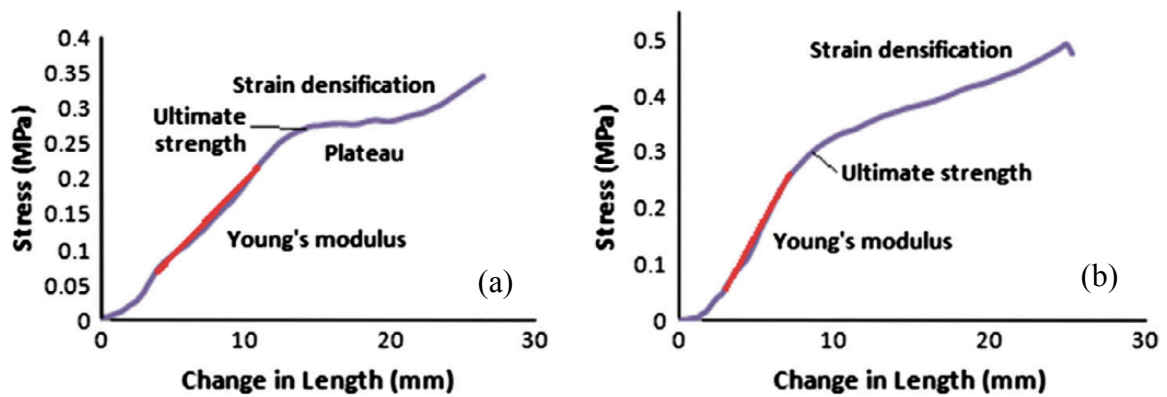


Figure 14. Two representative diagrams of the typical behavior of hemp-lime mortar under a compressive axial load (Walker et al., 2014)

As for flexural load, results are low comparing to ordinary concrete. For most of compositions they do not exceed 0.2 MPa at 1 year (Costigan and Pavia, 2012). At the same time, there are also some exceptions investigated for example by (Brümmer et al., 2017). Nevertheless, hemp mortars show a similar pattern of bending deformation as rigid materials – constant , and then the formation of a crack between the underside of the sample and the main axis (Sinka et al., 2014).

#### I.4.2. Thermal properties

Hemp mortars are known for their insulating properties (Chabannes et al., 2018; Elfordy et al., 2008). Indeed, the main thermal characteristic is thermal conductivity  $\lambda$  ( $\text{W}\cdot\text{m}^{-1}\cdot\text{K}^{-1}$ ). It shows the ability of the material to conduct heat as a function of a given temperature difference. It is one of the intrinsic properties that most affect the hygrothermal behavior of the building.

There is a multitude of methods for the experimental evaluation of thermal conductivity. They can be regrouped according to different criteria. One of these criteria is the thermal regime. Using this characteristic, a distinction can be made between steady-state and variable-state measurements. The steady-state regime concerns the test made at the medium subjected to a flow independent of time (stationary). Some examples are the hot plate method and the hot box method. The second regime is represented by the measurements made under transient flow (e.g., the hot wire or hot disk method).

Another criterion of classification of thermal conductivity identification methods is the type of measurements. They can be relative and absolute. In the first case, the measurements are relative when the thermal conductivity of a material is determined in relation to a reference specimen whose thermal conductivity is known. Measurements are absolute in the opposite case.

There are many scientific works on the subject of thermal conductivity of hemp mortars. Different aspects have been shown to be important when talking about prediction and preservation

of thermal properties. Such parameters as fiber orientation, compaction and application method must be taken into account as they affect thermal conductivity of a material (Nguyen et al., 2016). It was shown that the type of the binder has a little effect on the thermal properties (Nguyen et al., 2010). Hemp mortars can have up to 30% greater thermal conductivity in the perpendicular direction of compaction because of the anisotropic pore structure of hemp shivs (Dartois et al., 2017; Williams et al., 2016).

Thermal conductivity also increases as a function of moisture content and temperature of hemp mortar as indicated in Figures 15 and 16, respectively. In fact, (Bennai et al, 2017), investigated the influence of aging on the thermal conductivity of hemp mortars. They reveal that with aging, after 30 days, the thermal conductivity increases due to the microstructure evolution of the material.

Also, mechanical properties improve with increasing density (Collet and Pretot, 2014; Delannoy et al., 2018). Typical hemp-lime formulation exhibits a moderate thermal conductivity from 0.06 to 0.12  $\text{W}\cdot\text{m}^{-1}\cdot\text{K}^{-1}$  (Latif et al., 2015). Lower values could be obtained by spray application or use of organic binders (Hussain et al., 2019). (Stevulova et al., 2012) showed that the smaller hemp particles have a minimal effect on the thermal conductivity of hemp mortars.

The thermal conductivity values of hemp insulation mortars are not as good as those of traditional insulating materials (polystyrene and glass wool with values of  $0.04 \text{ W}\cdot\text{m}^{-1}\cdot\text{K}^{-1}$ ). In fact, hemp mortars hygroscopic behavior contributes to better thermal performance associated with the latent heat transfer caused by the process of liquid phase to vapor transition of water contained in its porous structure in solid, liquid and gaseous phases (Tran Le, 2010). The absorption abilities of hemp particles and fibers vary considerably due to differences in their physical structure and chemical composition (Sáez-Pérez et al., 2020).

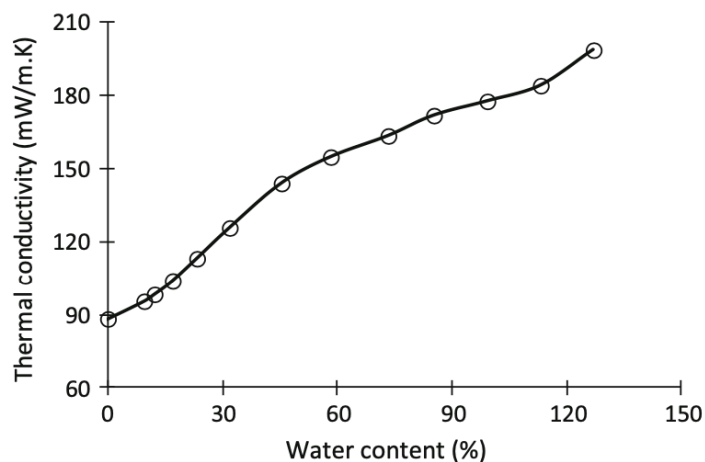


Figure 15. Evolution of thermal conductivity depending on the water content of the material at 23 °C, and 30 days of age (Bennai et al., 2017)

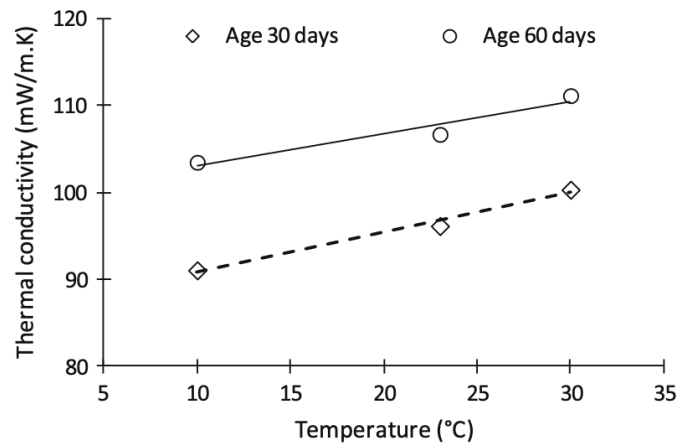


Figure 16. Comparison of thermal conductivity as a function of hemp mortar temperature at 30 and 60 days of age (Bennai et al., 2017)

Further, (Collet and Pretot, 2014) indicated that the increase in the moisture content decrease the thermal performance of hemp mortar, especially the thermal conductivity as indicated in Figure 17. As it is indicated in this figure, thermal conductivity of sprayed hemp mortar wall increases with the increase of the water content and dry density.

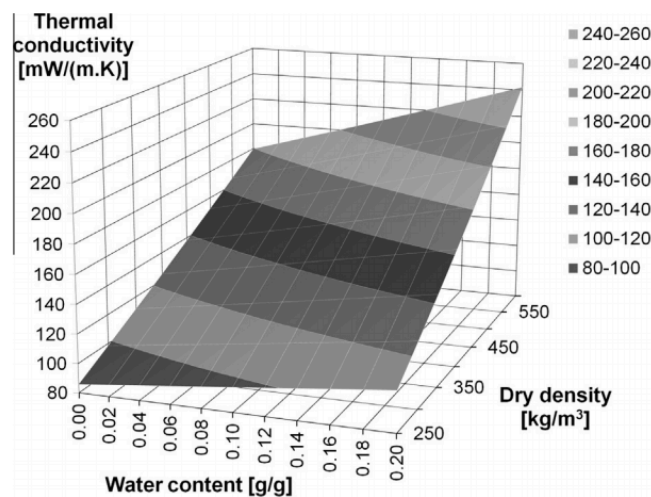


Figure 17. Thermal conductivity of sprayed hemp mortar wall versus dry density and water content (Collet and Pretot, 2014)

### I.4.3. Hydric properties

Hemp mortars are known for their ability to absorb significant quantity of water because of the hygroscopicity of hemp particles and the high open porosity of hemp mortar. There are a lot of different technics and methods to evaluate the hydric performance of hemp mortars, such as sorption-desorption curves, water vapor permeability or moisture buffer value (MBV).



### I.4.3.1. Sorption-desorption curves

Sorption-desorption isotherms describe the amount of vapor adsorbed at equilibrium in a material at a given relative humidity and temperature. In fact, the adsorption of water proceeds in 4 steps as shown in Figure 18. Firstly, isolated sites on the surface begin to adsorb gas molecules. Then, the water molecules cover the surface of the pores in a single layer. They are maintained under the effect of the forces of VAN DER WAALS: it is monolayer or monomolecular adsorption. Then, when humidity becomes more important, other layers of molecules are adsorbed. This is known as multilayer or polymolecular adsorption. Finally, at higher relative humidities, the polymolecular layers bind together, join and form a liquid bridge separated from the gaseous phase by a meniscus. The water is retained on the surface of the pores by capillary forces. This results in the filling from the thinner pores to the larger pores: this is capillary condensation (Chamoïn, 2013).

In order to predict the adsorption isotherms there are a lot of different models that were proposed, for example models of Henry, Freundlich (1909), Langmuir (1918), a Brunauer–Emmett–Teller (BET) model (1938) or Guggenheim–Anderson–de Boer (GAB) model. Two last models are the most commonly used for the determination of the sorption isotherms for different materials.

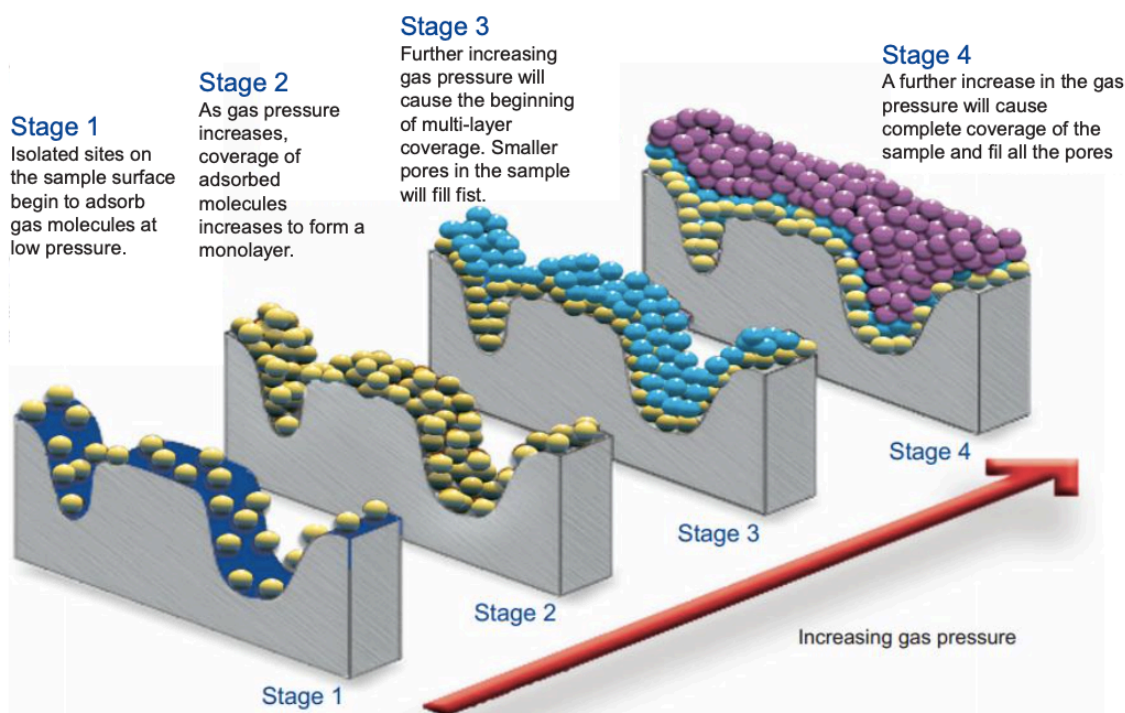


Figure 18. Stages of water vapor adsorption under rising relative humidity<sup>6</sup>

<sup>6</sup> <https://www.micromeritics.com/>

The relationship between water content and relative humidity in experimental practice is not unique but depends on the direction of change of the relative humidity RH, showing a "hysteresis". Different forms of buckles can be schematized. They are grouped by (IUPAC, 1985). In addition, hysteresis may be related to the shape of the pores ("bottles") or to the structuring of the pores (interconnections).

A lot of studies were conducted to evaluate the sorption-desorption isotherm (Collet et al., 2013; Gourlay et al., 2017; Piot et al., 2017a). Most of researches reveal that hemp mortar has high moisture content as wood (~27%). (Bennai et al., 2017) investigated the sorption-desorption isotherm of hemp mortar in function of the samples age, after 7, 30 and 60 days (Figure 19). This curve represents the change in the water content of the material depending on the water activity or relative humidity of air in equilibrium. The presence of hysteresis was observed between absorption and desorption that extends to the lower pressures. The effect of the material age was noted on the sorption behavior of hemp concrete. In fact, the adsorption-desorption rate decreases with increasing material age. For example, at 89% of relative humidity, the adsorption decreases from 21.51% between 7 and 60 days. At early-age, the binder hydrates do not form a connected network yet, over time, the hydrates connect together, and the volume of the solid phase increases which causes a change in the internal structure of hemp concrete and reduces the material porosity and its water adsorption capacity.

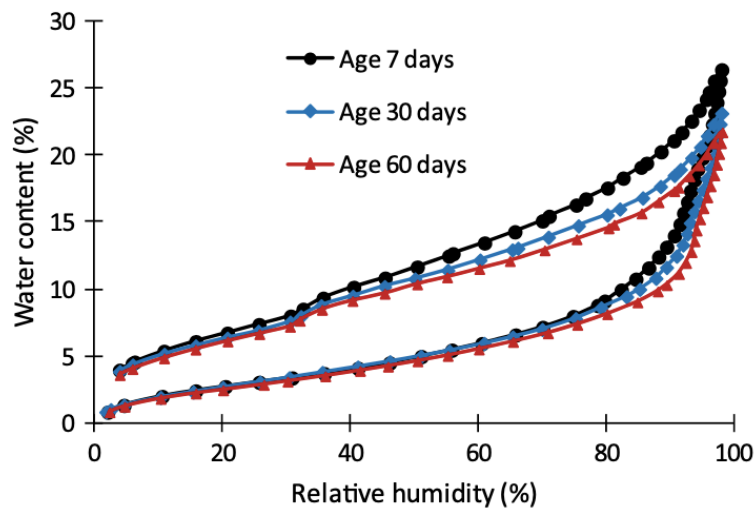


Figure 19. Comparison of water vapor adsorption-desorption isotherm of hemp mortar at 7, 30 and 60 days hemp concrete age at 25 °C (Bennai et al., 2017)

#### I.4.3.2. Water vapor permeability

In the building, relative humidity is one of the most important factors to consider when assessing hygrothermal comfort. High indoor humidity influences air quality and can cause structural degradation of the building structure and significantly shorten their durability

(Kosiachevskiy et al., 2018; Roulet, 2004). That is why the question of water vapor permeability is so important. Indeed, hemp mortar, as insulating material, is applied as a structural part of the wall. It means that this material should be permeable to water vapor in order to avoid any problems during its life cycle.

Environments with open porosity represent an ability to transfer a moisture flow when they are subjected to gradients of different potentials (total pressure, vapor pressure, temperature). The total moisture flow  $g_h$  is then the sum of vapor flow  $g_v$  and liquid flow  $g_l$  according to (Eq. 17).

$$g = g_v + g_l = -\delta_p \frac{dp}{dx} - D_{w,l} \frac{dw}{dx} \quad (17)$$

Where

$g_v$  - vapour flux density;

$g_l$  - liquid moisture flux density;

$\delta_p$  - water vapor permeability [ $\text{kg}\cdot\text{m}^{-1}\cdot\text{s}^{-1}\cdot\text{Pa}^{-1}$ ];

$D_{w,l}$  - moisture content - driven liquid diffusion coefficient [ $\text{m}^2/\text{s}$ ].

The criterion that characterizes a material's ability to allow the water vapor to pass through is water vapor permeability  $\delta_p$ . This value is the sum of three terms relating to the transport of vapor by diffusion, vapor by effusion and liquid by capillarity. As for hemp mortars, their water vapor permeability value is at the range of  $10^{-11} \text{ kg}\cdot\text{m}^{-1}\cdot\text{s}^{-1}\cdot\text{Pa}^{-1}$  -  $10^{-10} \text{ kg}\cdot\text{m}^{-1}\cdot\text{s}^{-1}\cdot\text{Pa}^{-1}$  (Hussain et al., 2019; Moujalled et al., 2018). It is several times higher than for a conventional concrete. This makes the use of this material interesting, especially for ancient buildings, where the question of the durability of the walls arises.

#### **I.4.3.3. Moisture buffer value (MBV)**

Many authors (Hussain et al., 2019; Rahim et al., 2015) have shown that hygroscopic materials contribute to moderate indoor relative humidity variations, thus improving the comfort of the occupants and reducing energy consumption. That is why the Nordtest project (NORDTEST project, 2005) proposed an experimental protocol to evaluate the hygroscopic inertia of hygroscopic materials through the definition of the Moisture Buffer Value (MBV).

According to (NORDTEST project, 2005), the MBV of a material is measured experimentally by its exposition to the cycles of relative humidity (8 hours at 75% RH and 16 hours at 33% RH at constant temperature of 23°C). These cycles are repeated until reaching the constant mass. Then, the MBV value is calculated using the following expression:

$$MBV_{practical} = \frac{\Delta m}{S(RH_{max} - RH_{min})} \quad (18)$$

Where,  $\Delta m$  – mass change [kg];

$S$  – exposition surface of the sample [ $\text{m}^2$ ];

$HR_{max}$  – maximal relative humidity (75% RH);

$HR_{min}$  – minimal relative humidity (33% RH).

Apart from experimental value of MBV, the Nordtest project defines also the theoretical MBV. It proposes the equation for identification of  $MBV_{ideal}$ , basing on the material's properties (Eq. 19) (NORDTEST project, 2005).

$$MBV_{ideal} = 0,00568 \cdot P_{vs} \cdot b_m \cdot \sqrt{t_p} \quad (19)$$

Where,  $P_{vs}$  – saturation vapor pressure [Pa] ;  
 $b_m$  – moisture effusivity [ $\text{kg}\cdot\text{m}^{-2}\cdot\text{Pa}^{-1}\cdot\text{s}^{-1/2}$ ];  
 $t_p$  – time [s].

Moisture effusivity value  $b_m$  is identified basing on the water vapor permeability (Eq. 20).

$$b_m = \sqrt{\frac{\delta_p \cdot \rho_0 \cdot \frac{\partial u}{\partial RH}}{P_{vs}}} \quad (20)$$

Where,  $\delta_p$  – water vapor permeability [ $\text{kg}\cdot\text{m}^{-1}\cdot\text{s}^{-1}\cdot\text{Pa}^{-1}$ ];  
 $\rho_0$  – dry density [ $\text{kg}\cdot\text{m}^{-3}$ ],  
 $u$  – moisture content by mass [%],  
 $RH$  – relative humidity [%].

This  $MBV_{ideal}$  identification model requires that the measurements be performed in a semi-infinite environment. It means that the thickness of the sample must be higher than the distance between the exposed surface and the point where the amplitude of change in water vapor concentration does not exceed 1% of that at the surface. This distance is named penetration depth and is calculated using the Eq. 21 (NORDTEST project, 2005).

$$d = 4,61 \sqrt{\frac{D_{w,v} \cdot t_p}{\pi}} \quad (21)$$

Where,  $d$  – penetration depth [m],  
 $D_{w,v}$  – hydric diffusivity [ $\text{m}^2\cdot\text{s}^{-1}$ ],  
 $t_p$  – time [s].

As the mass convection coefficient at the boundary plays an important role, technically the MBV value is an intrinsic property of the material. Nevertheless, this value can be assimilated to an intrinsic property of the material when this coefficient tends towards infinity.

A lot of studies were conducted to evaluate the MBV value of hemp mortars. For example, (Tran Le, 2010) studied the moisture buffer value of cast hemp concrete from analytical and experimental points of view. The moisture buffer values obtained are 2.35 ( $\text{kg}/(\text{m}^2 \cdot \%RH)$ ) for the analytical value, 1.99 ( $\text{kg}/(\text{m}^2 \cdot \%RH)$ ) and 1.89 ( $\text{kg}/(\text{m}^2 \cdot \%RH)$ ) for experimental value for the 6 cm and 3 cm thick sample respectively. It should be mentioned that the penetration depth calculated by this author was of 3.7 cm. Thus, the 3 cm thick sample is too thin to give a representative MBV value. (Collet and Pretot, 2012) studied the moisture buffer value of sprayed hemp concrete. The determined MBV value was  $2.15 \pm 0.06$  ( $\text{kg}/(\text{m}^2 \cdot \%RH)$ ) with the penetration depth of 5,8 cm.

#### I.4.4. Acoustic properties

Acoustic properties of building materials are important when talking about everyday comfort. Indeed, 86% of French people say that they are bothered by noise in their homes. 67 % and 65% stated being bothered by road traffic and by neighborhood noise respectively (Bendavid and Chasles-Parot, 2014). These nuisances have negative effects on our health, leading to sleep disorders, reduced performance at work and increased stress (AFSSE, 2004).

When talking about acoustic performance of a building, we note two main types of consideration:

- Acoustic insulation is used to reduce as much as possible the noise transmitted by the external environment.
- Acoustic correction concerns all the methods used to control the response to acoustic excitations of the same room.

Depending on the objectives, insulation or acoustic correction, the means can be very different. Thus, a massive and impermeable structure is preferred for good insulation, while porous and permeable materials are used for acoustic correction. Thus, the performance of building materials is generally described by two quantities, the sound transmission loss noted TL, and the sound absorption coefficient noted  $\alpha$  (Glé, 2013).

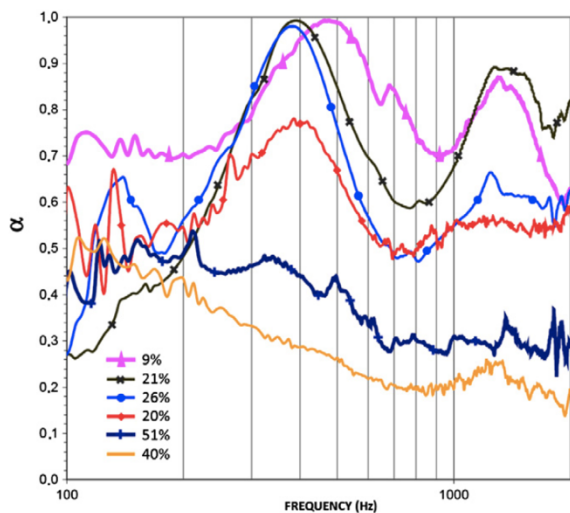


Figure 20. Sound absorption of hemp concrete according to the binder content (Glé et al., 2011)

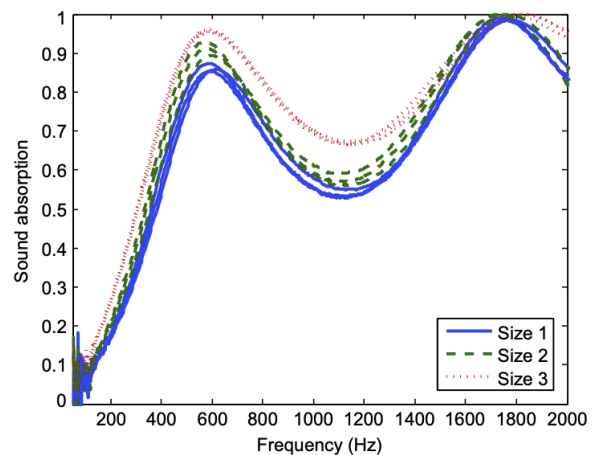


Figure 21. Sound absorption of hemp shiv in bulk for 3 different sizes of the particles (Glé et al., 2011)

The main factor that affect the acoustic properties of hemp mortars is the porous microstructure (Glé, 2013). Therefore, the question of the finishes of hemp mortar walls is important. Indeed, the surface rendering decrease significantly the sound absorption coefficient.

As for unrendered hemp mortars, they represent a sound absorption at the range between 40 and 50% for certain frequencies (Kinnane et al., 2016). Additionally, it was stated that the sound absorption increases with the increase of amount of binder (Figure 20) or use smaller hemp particles in bulk (Figure 21) (Cerezo, 2005; Glé et al., 2011). Also it is greater for mortars made with lime-pozzolanic binders than hydraulic ones (Kinnane et al., 2016). Further retting and aging can affect the acoustic absorption capacity of the hemp aggregate by changing the pore size distribution (Delannoy et al., 2018). When the hemp shivs are aged via exposure to real weather conditions they tend to swell up. Greater open porosity was found to have an important influence on acoustic absorption (Delannoy et al., 2018; Sáez-Pérez et al., 2020).

## **I.5. DURABILITY AND AGING OF THE HEMP MORTARS**

Hemp mortar is very interesting material from ecological and economical points of view. Also, their mechanical, acoustical and hygrothermal properties make them one of the reliable solutions for sustainable construction. At the same time, the use of this bio-based material raises a large number of questions, especially with regard to the durability of materials. Indeed, their hygroscopic aspect means that there are complex interactions between the microstructure of hemp shivs and humidity. Thus, the solid and porous phases of such materials present local thermal, hygro-mechanical and mechanical phenomena, which are at the origin of various dimensional variations due to hygroscopic stresses. Moreover, multiscale factor and anisotropy of hemp mortar represents some difficulties when predicting the evolution of their properties over time. In order to ensure the proper life cycle of hemp mortar, its durability need to be mastered.

### **I.5.1. Concept of the durability**

According to the international standard ISO 15686, the durability of a building or its components is an ability to perform its required functions during a specified period under the influence of climatic agents and intended use (ISO 15686, 2011). This specified period is named “service life” which is defined as a period of time after implementation during which a building or building components meet or exceed the performance requirements. The expected service life identified at a particular assembly or/and service conditions that can be basic for prediction of service life during real use is named reference service life (ISO 15686, 2011).

The modification of the performance comparing to initial properties during service life is named the “degradation of a material”. It is characterized by a phenomenon and a state of degradation. The moment when one or more properties are below the level of their requirements is called the level of failure. All these notions are presented in Figure 22 (ISO 15686, 2011; Talon, 2006).

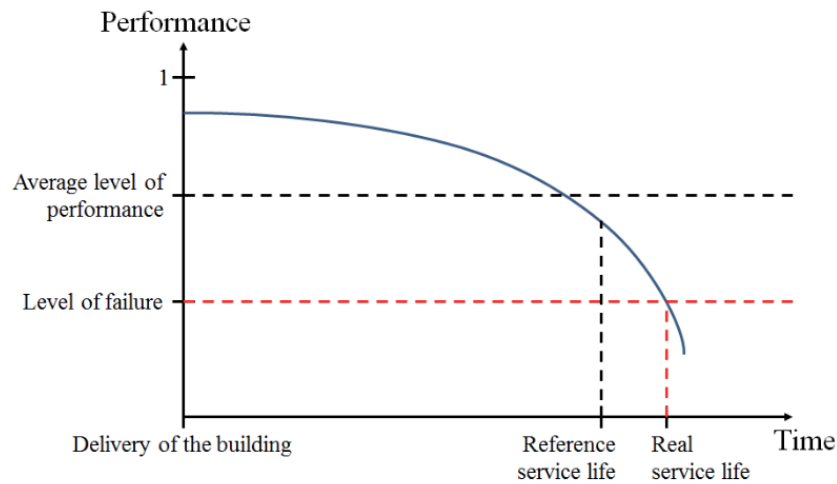


Figure 22. Representation of the concepts of performance and service life (ISO 15686, 2011; Talon, 2006)

### **I.5.2. Factors of hemp mortar's durability**

Many factors affect the durability and service life of building materials. They depend on the performance requirements for the material. This varies depending on the type of material and its destination. For example, the durability requirements for precast concrete structures differ from those for interior finishes.

As a thermal insulation material, hemp mortar must perform its insulating function. However, the question of durability is a more complex subject that depends on their microstructural characteristics, mechanical, hygrothermal and acoustic properties and their behavior towards the air quality and hygiene (moisture content, microorganism's proliferation). Also, these factors affect each other, as indicated in Figure 23. For example, an evolution of hemp mortar's porosity affects its acoustic and hygrothermal properties. The properties, such as hygroscopicity, of a material can provoke a high moisture content and, thus, microorganisms' proliferation. In their turn, microbiological agents (mold and bacteria) can change the properties by changing, at the same time, hemp mortar's microstructure (chemical composition and porosity). Also, some characteristics of microstructure can be more favorable for mold and bacteria growth (i.g. low pH level or surface roughness).

Various studies have been conducted to examine hemp concrete's durability across these parameters (Arizzi et al., 2016; Bourdot et al., 2020; Delannoy et al., 2018, 2020a; Rima et al., 2021). Moreover, durability can be investigated at different periods not only of service life, but even before. This is because the organic granulate is a material whose composition and properties are formed before the hemp mortar is made - during the growing period of the hemp. There are different stages: harvesting of hemp, its preparation and grinding, storage, hemp mortar manufacturing and service life. At all stages there are different interactions with the environment

and other compound of hemp mortar that can provoke a degradation resulting in decrease of the material's performance. That is why, all periods and interconnections must be mastered.

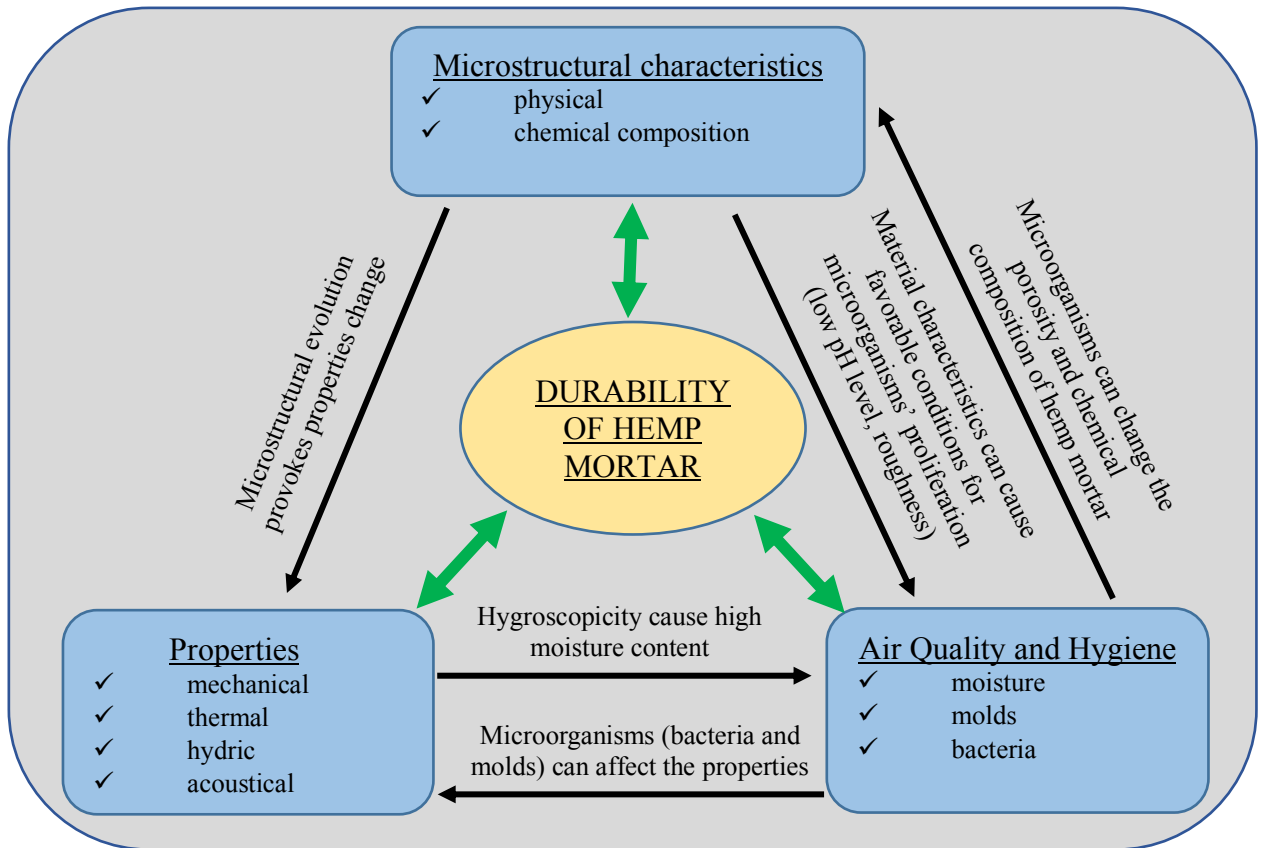


Figure 23. Diagram representing different parameters and their interconnections that affect the durability of hemp mortars

### I.5.2.1. Impact of agricultural methods: retting

After harvesting the hemp, hemp stems are exposed to so-called period of retting. It This period allows to naturally occurring organisms (fungi, bacteria, enzymes) to break down the pectic compounds (a glue-like substance made up from galacturonic acid units) of the middle lamellae binding the plant cells together (Bengtsson, 2009). This then facilitates the subsequent grinding of the hemp (Zhao et al., 2016). Retting method had a significant influence on fiber chemical composition (Jankauskienė et al., 2015). Without retting, there can be significant fiber loss during the subsequent refinement processes (Bócsa and Karus, 1998).

There different technics of retting:

- Water-retting
- Dew-retting (field retting)
- Dam-retting
- Chemical retting



Water-retting is a method where stalk bundles are submerged in water (normally in tanks, streams or ponds) for about 10 days (Ranalli, 1999). As a result, the water becomes rich in pectin-degrading bacteria. This method is not sustainable from ecological point of view due to the high quantity of used water and the pollution of water with high concentration of bacteria (Ranalli, 1999). Nevertheless, according to (Östbom, 2007), the water retting method provides a better quality of hemp fibers (length, color and smoothness). Dew-retting is also named field method. Hemp stalks are left in the field after harvest for exposure to climatic phenomenon (rain and dew) for about 2-3 weeks (Bócsa and Karus, 1998). Available researches on the subject of dew-retting showed the chemical evolution and degradation of hemp stems at different periods of retting (Bleuze et al., 2020, 2018) , as shown in Figure 24, by SEM images of the transverse sections two types of hemp stems. This method is environmentally friendly which gives good quality fiber which is strong yet fine (Haugaard-Nielsen et al., 2003). Dam-retting consists in immersing of the stems into dams or ponds for about 10 days and is no longer practiced except Egypt. Chemical retting is done by boiling the hemp with alkali or oxalic acid at atmospheric. It is quicker process but costly. The most widely used are dew- and water-retting methods, both carried out by pectic enzymes secreted by indigenous microflora (Bengtsson, 2009).

Drying is important to halt the retting process (Ranalli, 1999). Over-retting adversely affects fiber thickness and leads to discoloration of the fibers which turn dark grey or brown (Östbom, 2007). Under-retting where the humidity is insufficient, can also lead to reduction in fiber quality (Bengtsson, 2009).

Fibers from unretted hemp stalks become cheaper since the handling time is shorter. They also contain a lower degree of microorganisms and do not require bleaching, which is more environmentally safe (Bengtsson, 2009).

After the process of the retting, hemp is dried and grinded. Then, in the case of hemp mortar, hemp shivs are transported and incorporated with mineral binder on the construction site. Conditions must be regulated in order to protect hemp shivs from wetting and possible degradation. Nevertheless, the next stage where durability must be assessed is the hemp mortar manufacturing because of the intercommunion between mineral binder and hemp shivs.

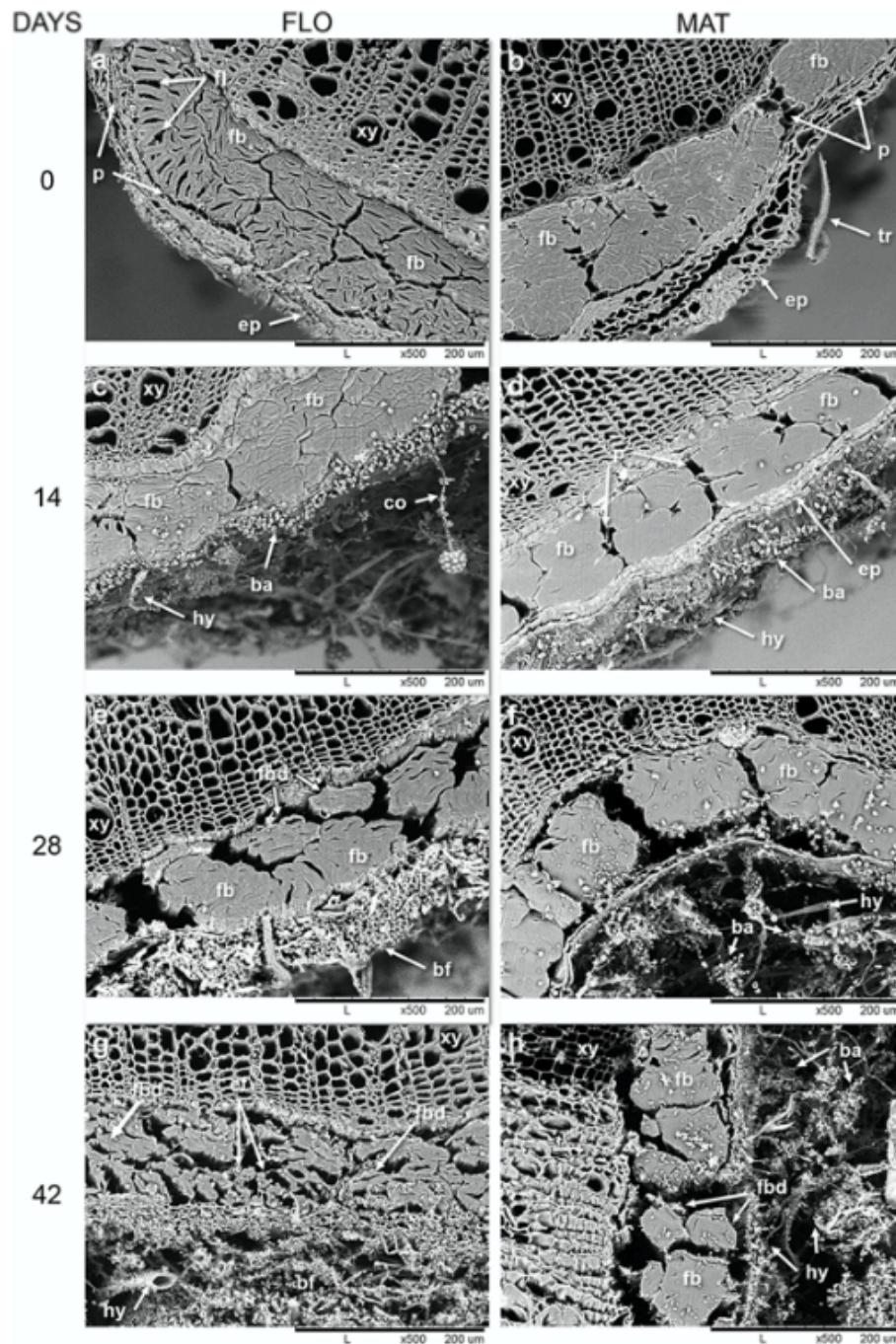


Figure 24. SEM images of the transverse sections two types of hemp stems (a, c, e, g and b, d, f, h) during retting. Before retting (a,b), after 14 (c,d), 28 (e,f) and 42 days (g,h) of retting; (ba) bacteria, (bf) biofilm, (co) conidiophore, (ef) elementary fibre, (ep) epidermis, (fb) fibre bundle, (fbd) fibre bundle decohesion, (fl) fibre lumen, (hy) hyphae, (mc) microbial colonization, (p) parenchyma, (tr) trichome and (xy) xylem. Scale bar =200  $\mu\text{m}$

### I.5.2.2. Interconnexion mineral binder / hemp shivs

Hemp shivs represent some quantity of organic particles (sugars, lignin, other organic compounds), that affect hemp mortar setting and properties during the manufacturing process. At the same time, mineral binders represent aggressive environment for organic tissue of hemp. It is

characterized by high pH level and saturation with minerals that provoke degradation of hemp shivs. This, in turn, leads to more emission of organic compounds.

### I.5.2.2.1. Influence of the mineral binder on organic granulates

Several studies have focused on the influence of the mineral binder on the organic particles (Melo Filho et al., 2013; Wei and Meyer, 2015). (Elfordy et al., 2008) worked on hemp-lime mortar and determined the presence of calcium on the entire external surface of the hemp particles using energy-dispersive X-ray spectroscopy (EDS) analysis. This shows that the mixing process is effective in completely covering the hemp particles with the binder. Other researchers investigated the degradation of molecular chains and the reduction in the degree of polymerization and the tensile strength due to the dissolution of lignin and hemicellulose in a cement pore solution and alkaline hydrolysis of cellulose molecules (Tolêdo Filho et al., 2000). Also, it was demonstrated that mineralization of lime in lumens decrease the fiber flexibility and strength (Tolêdo Filho et al., 2000). Further, (Melo Filho et al., 2013) basing on their studies of sisal-Portland mortars suggest two mechanisms for the organic fiber degradation (Figure 25). The first step is the deposition of calcium hydroxide crystals at the fiber surface that leads to a mineralization process. It provokes the reduce of the quantity of cellulose in the fibers and decrease of fiber's ductility and strength. The second step consists in hemicellulose and lignin degradation. It is provoked by adsorption of calcium and hydroxyl ions by the organic fiber surface. These elements are known to remove from the surface amorphous materials, like waxes, fats, hemicelluloses and lignin that, therefore, leads to a reduction in the macro mechanical properties of the organic fiber.

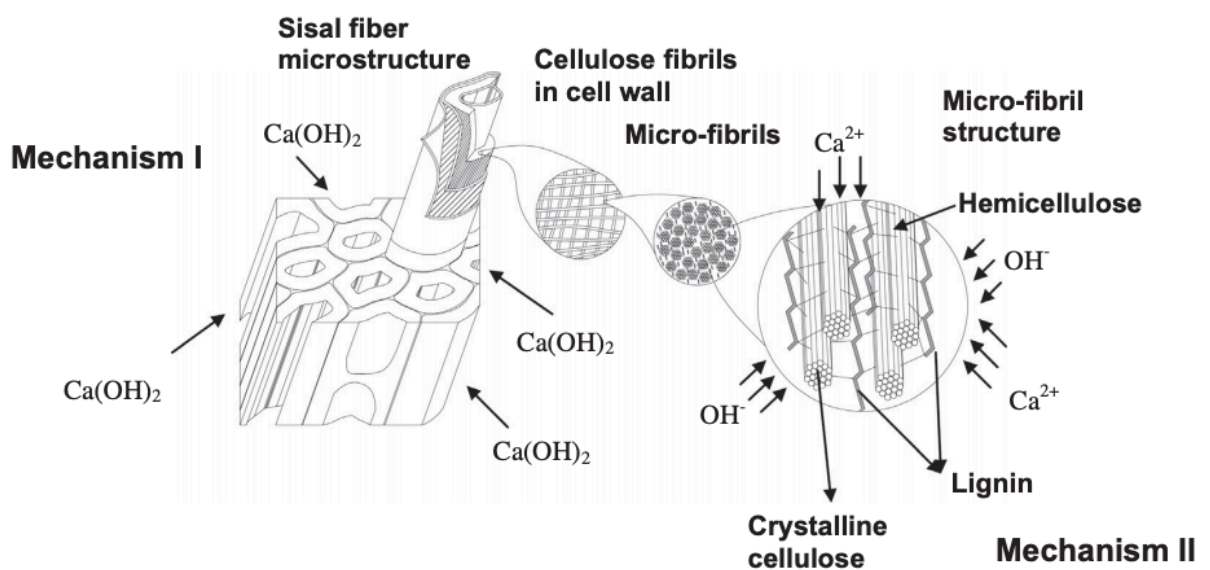


Figure 25. Organic fiber degradation (sisal example) mechanisms in a Portland cement environment (Melo Filho et al., 2013)

(Wei and Meyer, 2015) demonstrated the organic particles' mineralization. Also, in their study, they proposed a more detailed four-stages schema of alkaline degradation of natural fiber in a cement matrix, due to the high alkalinity of cement solid phase and pore solution (Figure 26):

- Degradation of lignin and part of hemicellulose, which leads to the exposure of holocellulose in the pore solution and solid phase of the matrix;
- Degradation occurs mainly on hemicellulose, which causes the decrease of integrity and stability of the cell wall of natural fiber;
- After the degradation of lignin, hemicellulose and intra-molecular hydrogen bonding, there remains no binding for cellulose micro-fibrils, and as a result cellulose fiber disperse in the pore solution of the matrix, which in turn, accelerates the degradation of cellulose;
- The last step is the failure of cellulose micro-fibrils, which is caused by alkaline hydrolysis of amorphous regions containing non-reducing end and leads to the complete degradation of natural fiber. As the degradation proceeds, the hydration products, such as C-S-H and soluble Portlandite, gradually infiltrate into the cell wall, which in turn leads to mineralization and embrittlement of organic particles.

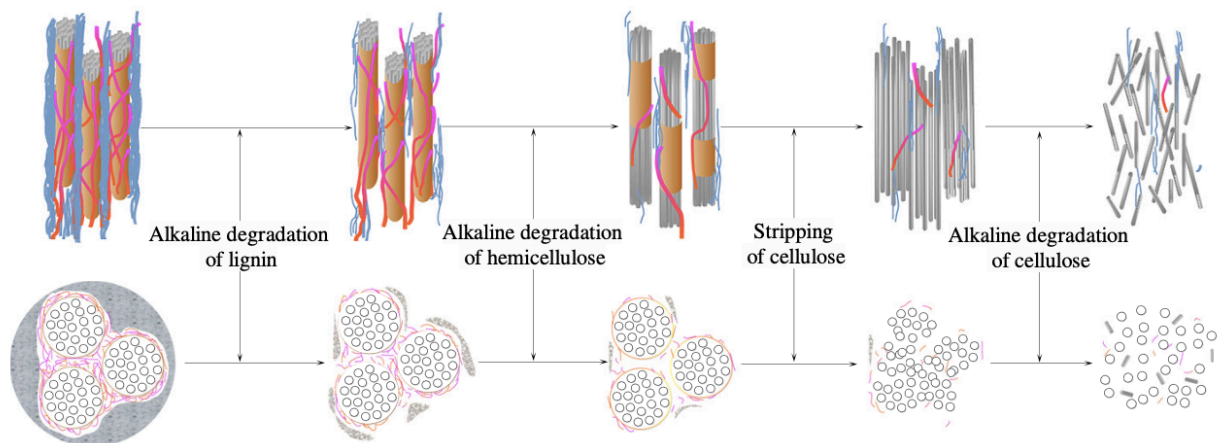


Figure 26. Diagrammatic sketch of natural fiber's alkaline degradation process (Wei and Meyer, 2015)

#### **I.5.2.2.2. Influence of organic compounds on the mineral binder**

Apart from the degradation of hemp by mineral binder, there is another aspect – the influence of organic compounds on the reactivity and properties of the binder. There are several studies on this subject. Some authors investigated the influence of the organic compounds on the properties of hemp mortars (Delannoy et al., 2020b; Nadif et al., 2002), others showed their influence on the setting (Delannoy et al., 2020b; Sedan et al., 2008).

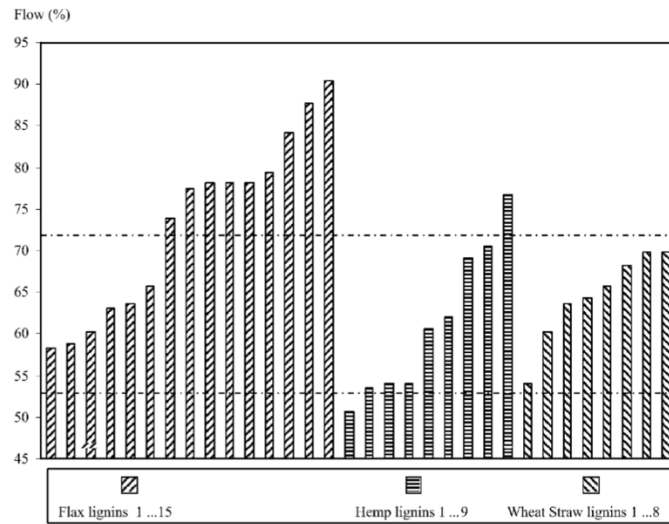


Figure 27. Representation of the flow of mortar with admixed lignin samples from different organic fibers (flax, hemp, wheat straw) obtained with the small-scale testing apparatus (Nadif et al., 2002)

(Nadif et al., 2002) showed the influence of lignin extracted from organic fibers (flax, hemp, wheat straw) on the flow of the mortars. Every sample of lignin improved the mortar flow, that in the reference state was calculated for the sample without additives at 49%. Two proposed levels of 53% and 72% demonstrate the limits for the 10% and 50% improvement towards the reference mortar's flow (Figure 27). The effect of increasing of mortar's flow was explained by other researches (Delannoy et al., 2020b; Sedan et al., 2008).

(Sedan et al., 2008) investigated the influence of the presence of hemp particles on the Portland cement-based binder setting. Firstly, they were interested in the trapping of calcium by organic particles. To study this phenomenon, they observed organic fibers before and after the immersion for 24h into the lime-saturated solution as shown in the SEM micrographs of cortical fibers in Figure 28. These images indicate the formation of spherical nodules after the immersion. The EDS analysis shows that these nodules are calcium rich compared to a nodule free region. (Sedan et al., 2008) explains this result by the organic particles' adsorption of a high quantity of  $\text{OH}^-$  ions, that, then, attract the calcium from the solution. Indeed, the free carboxylate and alcohol functions found in the chemical structure of the fiber compounds (in particular in the pectin) trap  $\text{OH}^-$  ions, become ionized in alkaline media and carries an electrical negative charge. They, later, attract calcium ions to form  $\text{Ca}(\text{OH})_2$  nodules. Pectin contained in the fibers can also react with calcium ions in an alkaline environment and form a very stable "egg box" structure responsible of the decrease of  $\text{Ca}^{2+}$  concentration in lime-saturated solutions.

The decrease in the quantity of  $\text{Ca}^{2+}$  affects the setting as it depends on the concentrations of calcium, silicon, aluminium and iron. Figure 29 shows that the increase in the quantity of fibers

decreases the concentration of calcium that cannot produce calcium silicate hydrates (CSH) responsible for setting (Sedan et al., 2008).

(Delannoy et al., 2020b) investigated the influence of the hemp shivs extractives on hydration of Portland cement. In their study they used the isothermal calorimetry to assess the hydration process. Figure 30 demonstrates the heat flows over time of pure CEM I and CEM I / hemp shiv powders admixtures in different proportions (hemp shivs/cement = 0.01; 0.02; 0.05; 0.1; 0.5). These results show the same pattern - the increase of the quantity of organic particles slow down significantly the hydration time. Indeed, the first peak of hydration for CEM I sample is observed at about 9 hours after the beginning of the hydration and is connected with the  $C_3S$  reaction and precipitation of the Portlandite and the CSH (Delannoy et al., 2020b). The hydration of the mixtures with hemp shivs are slowed by 3.5 hours, 13 hours, 26 hours for the samples with ratios hemp shivs/cement of 0.01; 0.02; 0.05 respectively. No heat flow peak during first six days was seen for the samples of the mixture with hemp shivs/cement ratio of 0.1 and hemp mortar with the ration 0.5.

Given the risks of the interaction between organic fibers and mineral binders, several works have been carried out to increase the durability of natural fibers in inorganic matrices, different approaches have been proposed in the literature. (Gram, 1983) proposed different treatments of fibers with blocking agents, such as sodium silicate, magnesium sulphate, iron or copper compounds and others, but the durability of the fibers did not increase significantly. (Melo Filho et al., 2013) proposed the use of silica fume products to reduce degradation due to alkaline attack. (Bilba and Arsene, 2008) studied a silane coating of natural fibers to reduce the external aggressions and then the degradation of the mechanical properties.

Latex coating is also proposed as one of possible solutions to overcome the problem of degradation of physical and mechanical properties (Asprone et al., 2011). The objective is to provide external protection, to isolate the fibers from alkaline agents and moisture. The results show that latex coating can improve the durability of hemp fiber in the mortar environment and that the bonding behavior between hemp fibers and mortar is improved by latex coating.

Another possible technic is a treatment with aqueous NaOH solution. It removes certain hemicelluloses, waxes and impurities from the surface of the fibers. The surface is chemically more homogeneous. In the literature it has also been observed that treatment with NaOH tends to roughen the fiber surface (Sedan et al., 2008). Therefore, in the case of the study conducted by (Sedan et al., 2008) the gain in flexural strength can be attributed not only to the improved adhesion at the interface but also to the improved tensile strength of the fiber. For fibers treated with  $AlCl_3$ , the effect of the treatment on the flexural strength of the composite is less noticeable. Indeed, it

only removes impurities or waxy substances on their surface and has little effect on the morphology of the fibers.

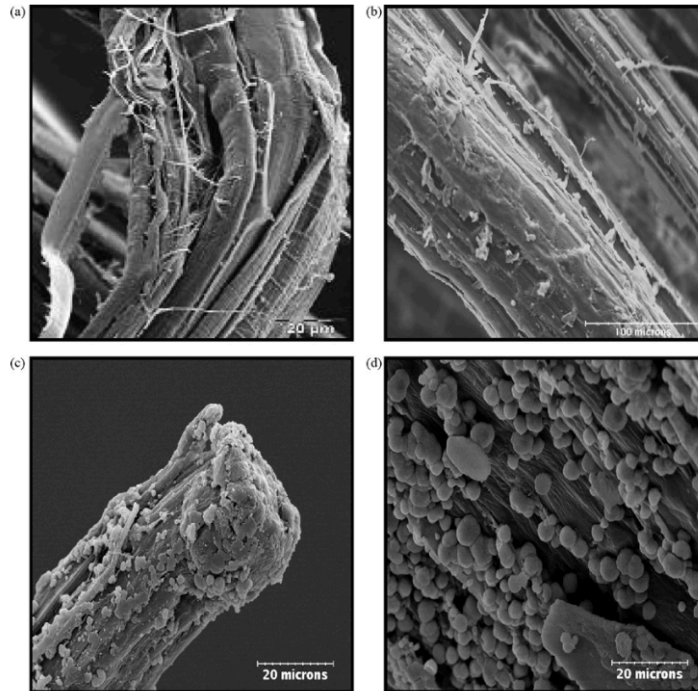


Figure 28. SEM micrographs of cortical fibers before (a and b) and after immersion in a lime-saturated solution (c and d) for 24h (Sedan et al., 2008)

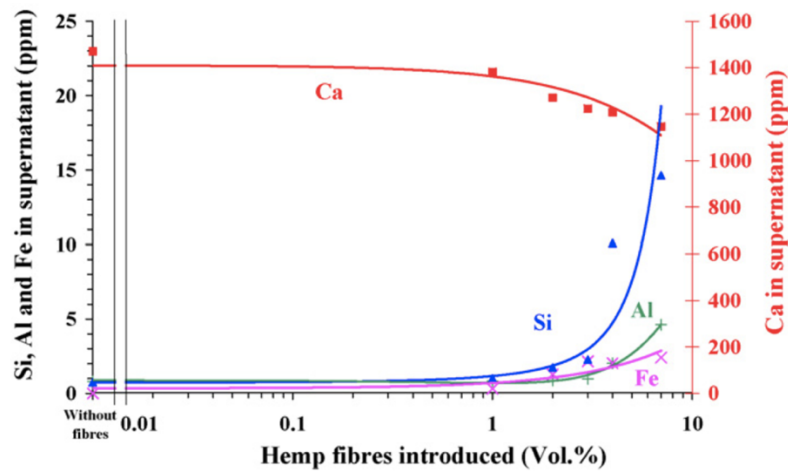


Figure 29. Variations in the concentrations of calcium ( $\square$ ), silicon ( $\Delta$ ), aluminium ( $+$ ) and iron ( $\times$ ) as a function of the amount of hemp fibres introduced into a diluted cement paste ( $W / C = 2$ ). Measurements made 30 min after the start of mixing (Sedan et al., 2008)

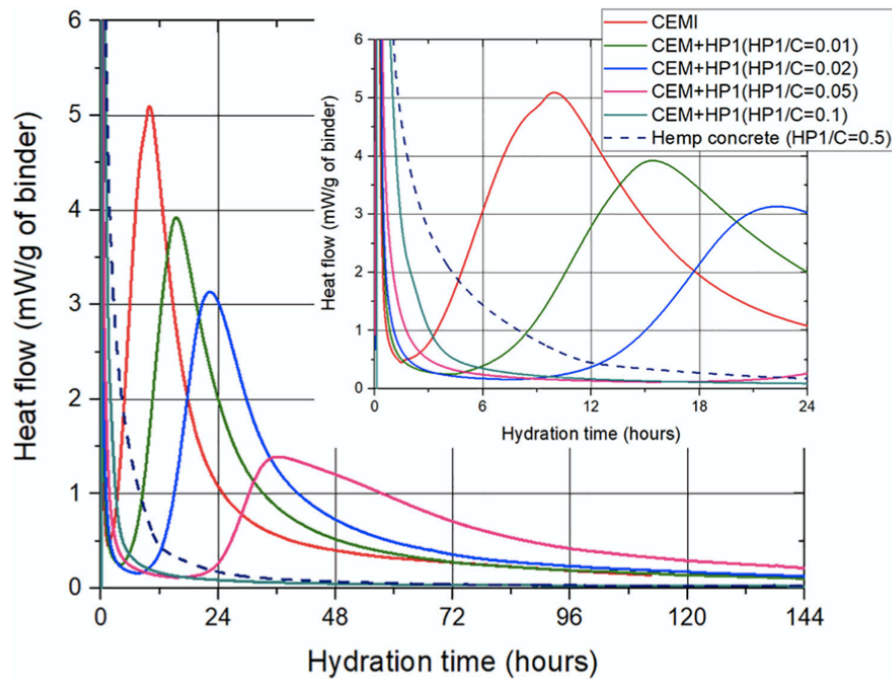


Figure 30. Heat flow for pastes of CEM I, CEM I mixed with hemp shiv powder and hemp concrete (Delannoy et al., 2020b)

### I.5.3. Hemp dimensional variations at hygric loads

As hemp is hygroscopic, their particles, start to absorb the high quantity of water when exposed to water during hemp mortar manufacturing (Fourmentin et al., 2016). It leads to the swelling of hemp shivs (as shown in section I.4.3.1). Then, during the period of the setting and drying of hemp mortar structures, hemp shivs liberate stocked water and shrink. It provokes dimensional variations that cause the damage of the material. This effect was noted also during hygroscopic solicitation not only at early-age but also at the whole period of service life of organic-based mortars (Abahri et al., 2020; Bennai et al., 2019; Fourmentin et al., 2016).

There are several studies that are interested at the hemp shivs' water absorption and their dimensional variations (Rima et al., 2021). For example, (Fourmentin et al., 2016) followed the evolution of the distribution of NMR relaxation time to quantify the effective amount of water entering the hemp (Figure 31). They showed that water intake occurs in two steps, a fast one taking place in less than two minutes, corresponding to water entering the pith, and a slow one, taking place over days, corresponding to water diffusing into the woody part of the shiv (Figure 32).

(Bennai et al., 2019) used another technic, digital image correlation, to study the 2D hygromorphic behavior of hemp mortar to better understand the swelling and shrinkage of the material due to variations in its hydric status. Results showed that humidification of the hemp mortar leads to swelling of the vegetable particles and decrease of the porosity present between the binder and the hemp shiv. In addition, hydric drying causes shrinkage of vegetable aggregates



and the dilation of interparticle porosity. For example, figure 33 shows the hemp mortar sample at the dry state (a) and the strain fields for the passage from dry state to 76% RH (b,c,d).

Recently, (Rima et al, 2021) studied the microscopic estimation of swelling and shrinkage of hemp concrete in response to relative humidity variations. This work is based on the analysis of the 2D microstructure of both hemp concrete and hemp shiv aggregates, in order to estimate these dimensional variations for sorption and desorption cycles. In this context, a new experimental optical setup was investigated to quantify the hemp shiv and hemp concrete swelling and shrinking by analyzing variations in their microstructure at different relative humidity levels. The findings of this study underline the real influence of relative humidity on the hemp concrete, that present a hysteretic swelling (Figure 34) due to the porous structure and hygroscopic behavior of this material.

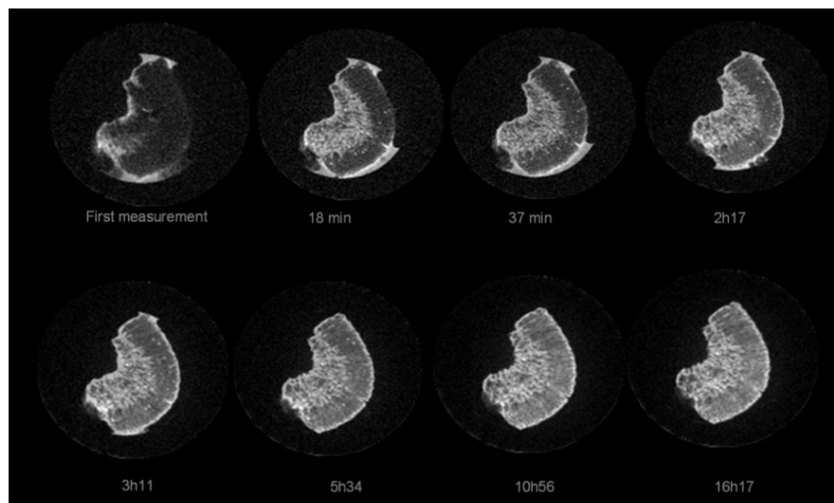


Figure 31. Evolution of the middle slice of hemp during water absorption as seen by MRI, higher brightness means higher water content (Fourmentin et al., 2016)

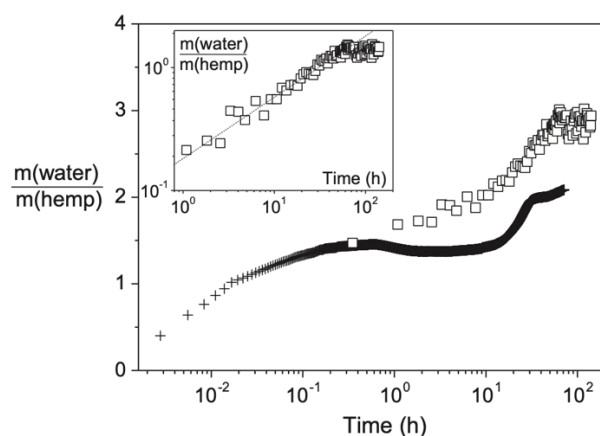


Figure 32. Water to hemp mass ratio in time as measured by T1 relaxometry (squares) and by weighing of an immersed sample (crosses). The inset shows the additional water to hemp mass ratio in phase 2 of imbibition as a function of time in logarithmic scale. The continuous line has a slope 1/2 (Fourmentin et al., 2016)

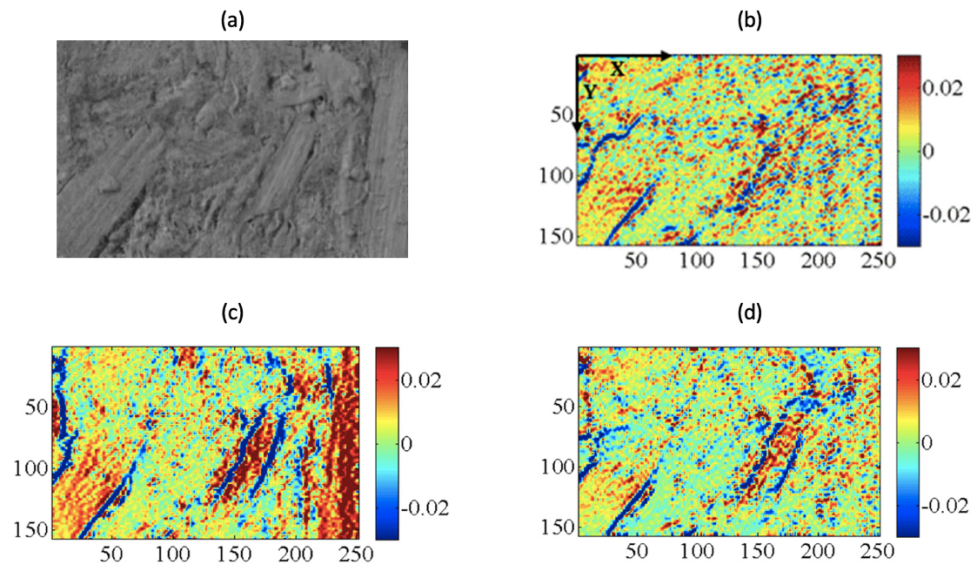


Figure 33. Hemp mortar's sample at (a) dry state, and strains equivalent to 76% RH (b)  $\epsilon_{xx}$  (c)  $\epsilon_{yy}$  and (d)  $\epsilon_{xy}$  (Bennai et al., 2019)

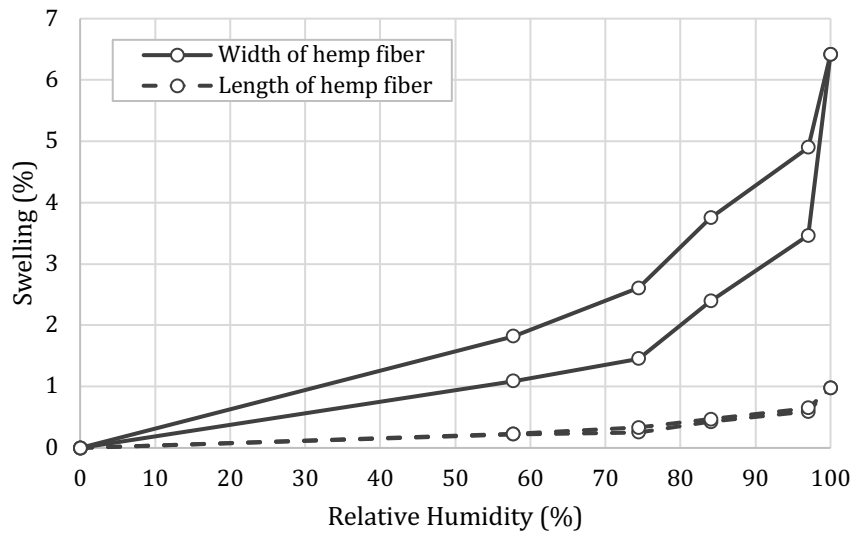


Figure 34. Swelling of hemp concrete (%) as a function of relative humidity (%)

#### I.5.4. Degradation of hemp mortar and their properties during its service life

Several works in the literature show that the physical and mechanical properties of natural fibers can be affected by important modifications due to environmental factors (Gram, 1983). In particular, works of (Tolêdo Filho et al., 2000) showed that problems of durability are associated with an increase in fibre damage and a decrease in pull-out force due to a combination of fibre weakening as result of the inorganic matrix environment and high-water absorption. Indeed, alkaline attack and mineralization of the fibers caused by the migration of hydration products to the lumens can induce a significant degradation of the fiber properties and provoke the mechanical properties' degradation (Tolêdo Filho et al., 2000). It was found that hemp shivs do not completely

decompose within the composite because of the mineralization, which takes place as a result of the precipitation of calcium carbonate on the individual elementary fibers, following an alkaline degradation mechanism. Such mineralized hemp particles become inert within the composite, but also brittle, less porous, and weak in tension (Marceau and Delannoy, 2017). Further, (Walker et al., 2014) studied the mechanical properties and durability of hemp-lime concretes of various mixes. Different parameters were investigated, such as resistance to freeze-thaw or salt exposure. It was found that hemp concrete had poor resistance to freeze-thaw due to the washout of mass during the freeze and thaw cycle, thereby leading to a reduction in compressive strength. Hemp concretes had good resistance to sodium chloride salt exposure as the large pores did not allow crystallization to occur.

In other aging tests such as wetting and drying cycles, and full immersion and drying cycles, it was found, especially with calcic lime binders, that the binder leaches out and the mass reduces, leading to a reduction in compressive strength. In cases of hydraulic binders, the cyclic wetting and drying has improved the compressive strength of the composite (Jami et al., 2019; Marceau and Delannoy, 2017).

(Benmahiddine et al., 2020) used the total immersion/drying weathering cycles that have shown a significant influence on the mechanical performances. Indeed, the compressive strength of hemp mortar samples decreased by 51% after the weathering cycles. Apart from mechanical properties, these authors investigated the evolution of hygrothermal properties. Results highlighted the cracking of the binder/hemp shivs interfaces the degradation of hygric properties as for example the MBV.

As for hygrothermal properties, a lot of researchers stated the influence of the environmental conditions (humidity, temperature, etc.) on the hemp mortar performance (Abahri et al., 2020; Collet and Pretot, 2014; Gourlay et al., 2017; Kosiachevskiy et al., 2017). Other researchers demonstrated the evolution of hygrothermal properties under different types of aging (Abahri et al., 2020; Benmahiddine et al., 2020; Delannoy et al., 2020a). For example, (Delannoy et al., 2020a) followed the evolution of different properties of hemp mortar using the accelerated environmental aging. Results show that the samples at the stable environmental conditions (50% RH and 20°C) do not represent any significant changes of microstructure, thermal, acoustic, hydric or mechanical properties. As for samples under accelerated aging cycles, they showed the increase in the thermal conductivity and water vapor sorption capacity (Bourdot et al., 2020; Delannoy et al., 2020a). In fact, in their investigation, (Delannoy et al., 2020a) studied the evolution of the thermal conductivity of the lime-based (FL-HC) and natural cement-based (NC-HC) binders of the reference samples  $A_{REF}$  and aged samples  $A_{WD}$  in function of time. Figure 35 demonstrates that no significant variation in thermal conductivity was observed for two years. In contrast, with aging

$A_{WD}$ , the thermal conductivity increase is about 19% for FL-HC after 24 months and 7% for NC-HC.

Another problem that was often noted and affect directly the durability is a carbonation of the mineral matrix over time. In a modern hemp mortar the pH-value of the pore water normally exceeds 12 (depending on the binder). This high alkalinity occurs due to the formation of calcium hydroxide,  $Ca(OH)_2$ , during the hydration of mineral binder. However, calcium hydroxide can be consumed by the carbon dioxide to form calcium carbonate ( $CaCO_3$ ) as it was described in the paragraph I.3.1.2.1.

(Elfordy et al., 2008) studied the carbonation kinetics of lime-hemp mortar. He detected by X-ray diffraction that a mortar contains significant amounts of calcite ( $CaCO_3$ ) already after mixing (Figure 36). The carbonation then follows a classical evolution and the saturation of the calcite content during the setting of the lime appears approximately after 20 days of drying.

Carbonation opens another durability question, as several studies showed the interconnection between the level of pH and other characteristics of hemp mortar and the microbiological activity (molds, bacteria and other microorganisms) (Kosiachevskiy et al., 2018; Sinka, M. et al., 2019; Viel et al., 2019).

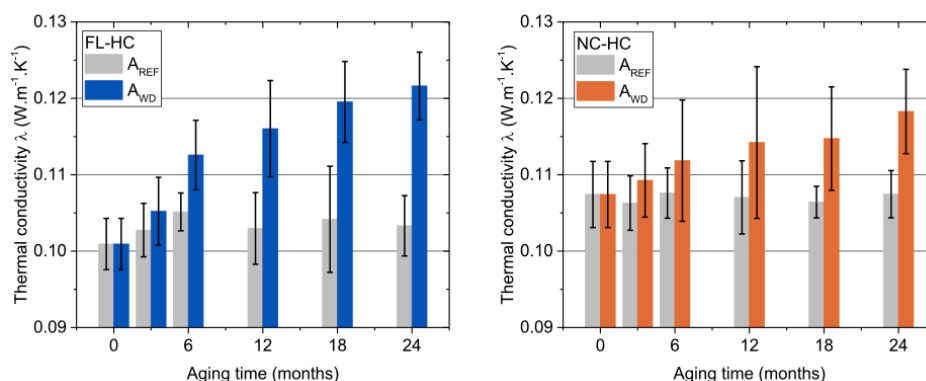


Figure 35. Evolution of the thermal conductivity of the lime-based (FL-HC) and natural cement-based (NC-HC) binders of the reference samples  $A_{REF}$  and aged samples  $A_{WD}$  (Delannoy et al., 2020a)

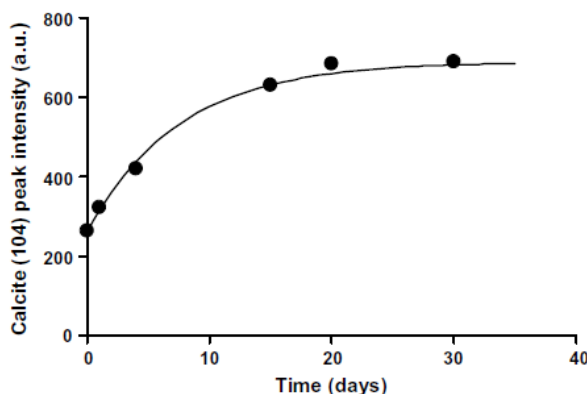


Figure 36. Lime carbonation kinetics, followed by the intensity of the (104) X-ray diffraction peak of calcite (Elfordy et al., 2008)

## I.5.5. Microbiological contamination

### I.5.5.1. Concept of bioreceptivity for building materials

The microbiological colonization of building materials is a complex process as it is dynamic in time and space due to the interrelationships among the colonizing organisms, as well as between their populations, the inorganic substrate and the surrounding heterogeneous environment (Sanmartín et al., 2021).

The microbiological growth depends on three sets of factors to be considered which relate to the properties of the organisms themselves (including dispersal mechanisms, growth requirements, etc.), the characteristics of the environment (including climatic conditions and microclimatic parameters, such as solar exposure, shading and water availability), and the properties of the building materials (including physical and chemical characteristics) (Sanmartín et al., 2021). (Guillitte, 1995) proposed to regroup intrinsic properties of materials and name them the “bioreceptivity” of material. This term is defined as the “ability of a material to be colonized by living organisms” and is consists of physical (porosity, roughness and hydrodynamic properties) and chemical properties (chemical composition, pH surface).

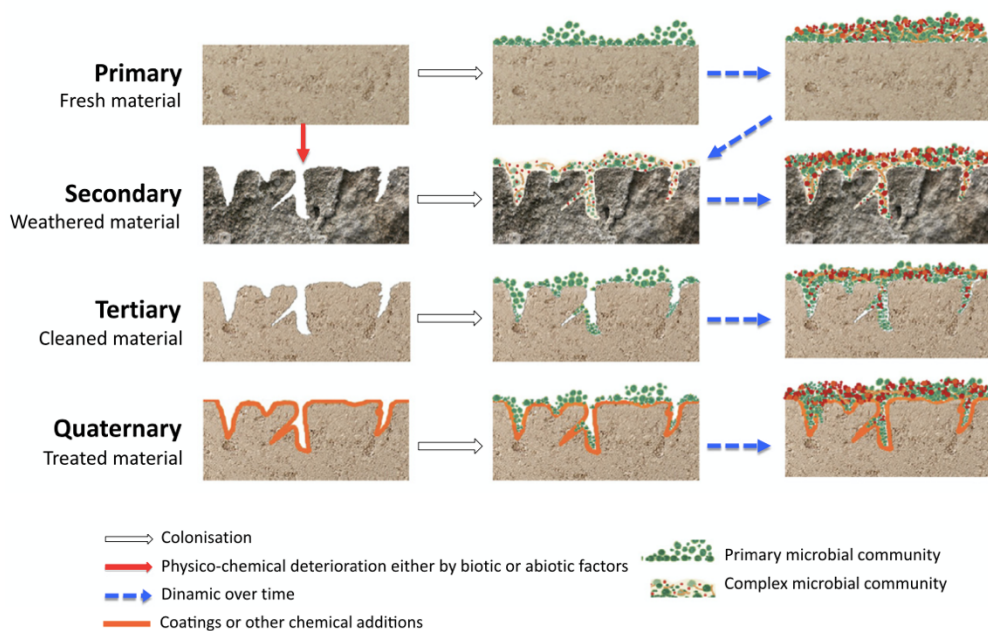


Figure 37. Visualization of the conceptualization of bioreceptivity proposed by (Sanmartín et al., 2021)

Additionally, (Guillitte, 1995) proposed the classification of bioreceptivity by types: primary, secondary and tertiary ones. The primary is related to the intrinsic properties of fresh material after its implementation for final function (concrete casting, montage or manufacturing of structures). Secondary bioreceptivity’ appears when the material properties change due to aging

by different environmental and microbiological factors. Tertiary bioreceptivity' appears after any human activity affecting the material, like cleaning or restoration of the material. At the same time, (Sanmartín et al., 2021) proposed to split the tertiary bioreceptivity into two types, with “tertiary bioreceptivity” regrouping the human actions that provoked the physical changes of the material (mechanical (with abrasives) and laser cleaning treatments) and “quaternary bioreceptivity” regrouping different treatments when new materials are added (coatings, chemical products, biocides) as shown in Figure 37.

#### **I.5.5.2. Microbiological degradation of different building materials**

Several studies were conducted to evaluate the influence of different properties on the bioreceptivity of the material. For example, (Guillitte and Dreesen, 1995) aimed to make a comparison of the influence of different materials' properties on the ability to be colonized. Results demonstrated that the bioreceptivity of building materials is highly variable and that it is mainly controlled primarily by their surface roughness, initial porosity and mineralogical nature.

Although the relative importance of each property on the bioreceptivity of the building material is not clarified, there are some studies that try to systemize them. It was demonstrated that physical properties affect more the bioreceptivity than chemical composition. For example, such parameters as high open porosity, capillary water content or roughness facilitate the colonization of granite by phototrophs (Vázquez-Nion et al., 2018). Other researchers (Dubosc, 2000; Tran et al., 2014, 2012) interested in bioreceptivity of building mortars and concrete also confirmed the high influence of the roughness that provides many asperities which allow the physical anchorage of the microorganisms. Nevertheless, for the most of building materials, the key factors remain unclear (Coutinho et al., 2016; Rodrigues et al., 2014). For limestone there is no consensus about intrinsic properties most influencing the bioreceptivity (Miller et al., 2012). (Coutinho et al., 2016; Rodrigues et al., 2014) used the concept for ceramic tiles and glass. Results showed that water absorption by capillarity and water vapor permeability affect the most the bioreceptivity of tiles. As for stained glass, chemical composition is a key factor for fungal growth (Rodrigues et al., 2014).

Additionally, microbiological colonization is various in time, different taxonomic groups can be involved in it depending on the conditions. For example, results of the study conducted on different materials by (Guillitte and Dreesen, 1995) demonstrated that after two weeks the first dominant microorganism were green algae on concrete. After four weeks, the green algae on concrete was replaced by cyanobacteria and mosses. At the same time, sandy limestone, brick and mortar just started to be colonized by algae. After one month, cyanobacteria became the most

abundant colonizer on all materials. After 6 months, the concrete and sandy limestone represented the highest colonization and brick and mortar were hardly colonized.

### I.5.5.3. Microbiological contamination of hemp mortars

The use of hemp mortars requires the consideration of several criteria towards microbiological contamination that make them vulnerable. The mold growth is one of the most important criteria when assessing the degradation of bio-based materials (Lähdesmäki et al., 2011). Also, there are other types of microorganisms (bacteria, lichens, algae) that can be involved into the material's contamination and, thus, affect hemp mortars. Several researches were conducted to evaluate the ability of hemp mortars to be colonized by these microorganisms.

(Viel et al., 2019) studied the resistance of hemp mortars towards the mold development. Results demonstrated the inhibition of the microbiological proliferation by high pH of material surface. It was also confirmed by other studies in case of mold growth for mortars (Tran et al., 2014) and hemp mortars (Sinka, M. et al., 2019) and algal growth for different materials (Grant, 1982). Several researchers state the resistance of hemp mortar towards mold growth because the alkalinity of mineral binder (Bevan and Woolley, 2008; Walker et al., 2014). Also, (Jami et al., 2019) note the importance of a good quality, non-water absorbing render shall to prevent the mold growth.

(Marceau et al., 2017) investigated the mold growth on hemp mortars subjected to the wetting/drying cycles and mold inoculation. Figure 38 shows SEM observation of molds on hemp shivs. Results demonstrated high dependence on the high relative humidity (98% RH was used in the study) the pH level of the material surface (lower than 10 that was also stated by (Sinka, M. et al., 2019)).

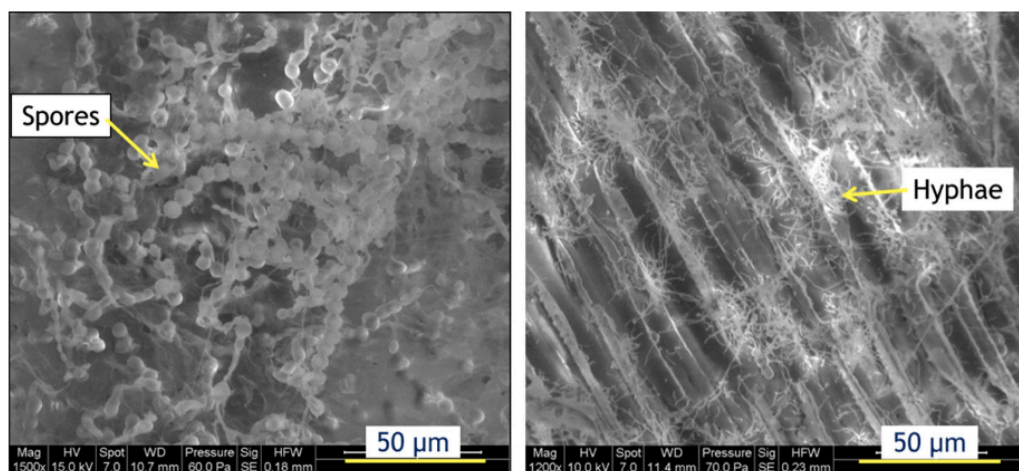


Figure 38. Observation of molds on shiv by scanning electron microscopy (Marceau et al., 2017)

## **I.6. CONCLUSION**

As time goes by, construction sector and especially building insulation industry face new challenges and requires new sustainable, eco-responsible and economically profitable solutions. One of such materials that are interesting for their low CO<sub>2</sub> emissions, renewability and functional properties are bio-based materials. Among different types of organic fibers, hemp attracts great interest of researchers because of its high abundance, simplicity of cultivation and the advantageous hygrothermal properties when mixing to mineral binder. Nevertheless, the anisotropy, hygroscopicity and heterogeneity of hemp provoke the evolution of microstructure and functional properties. Also, it can lead to the dimensional variations of hemp shivs and, thus, degradation of the material. That is why a reliable characterization of the durability of hemp mortars is therefore necessary.

In this chapter, a detailed bibliographical study was presented that allowed to highlight the real situation of the hemp mortars in the industry, their mechanical, acoustical and hygrothermal properties and hemp mortar durability. Also, literature analysis demonstrated the characteristics of hemp shivs as hygroscopicity, presence of different types of water, multiscale composition and complex interactions with the mineral binder matrix. Within the scope of representing hemp mortar durability, different parameters of durability were identified from the stage of the gathering of hemp in the fields to the aspects that need to be taken into account during the service life of hemp mortars. The results of the literature analyze demonstrated that the subject of the hemp mortar durability is under-researched and need further investigations. In the next parts of the document, different aspects of hemp mortar durability will be investigated. Chapter 2 proposes the analyze of the influence of the organic compounds on the setting of mineral binders.



CHAPTER II.

ANALYZE OF HEMP MORTAR DURABILITY:  
IMPLEMENTATION OF NEW TOTAL  
WEATHERING AGING PROTOCOL

---

## **CHAPTER II. ANALYZE OF THE HEMP MORTAR DURABILITY: IMPLEMENTATION OF NEW TOTAL WEATHERING AGING PROTOCOL**

---

### **II.1. INTRODUCTION**

Hemp mortar is represented as a constitutive part of the envelope or as a multiphase material with interphases between hemp particles and a cementitious matrix to the nanoscale of organic cell walls tissues or cement hydrates. This multiphase nature offers a double porosity to the material: intra- (hemp particles porosity) and inter-particular (hemp/matrix interface), that improves the performances of the insulating hemp-based mortar. Consequently, such compositional and structural complexity complicates the investigation of hemp mortar when talking about the durability.

Another important point to be considered, when talking about the durability, is the hygroscopicity of hemp mortar and its sensibility to thermal and hygric loads and to the environmental conditions of its life cycle. In fact, directly after the hemp mortar cast at early-age, cracks appear at the interfaces between the hemp particles and the cementitious matrix. Later, these cracks increase due to dimensional variations of hemp particles caused by the relative humidity and temperature solicitations and leads to the degradation of the material. Thus, the evolution of the microstructural properties must be investigated in order to understand the behavior and durability of the bio-based composite as regards to the hygrothermal stresses.

Aging tests of biobased materials are very slow. To overcome this constraint, part of this research work was devoted to accelerated ageing tests. The objective of this part is to study the response of the materials to extreme climatic constraints carried out in the laboratory (humidification/drying cycles). This step will allow to evaluate in detail the impact of these stresses on the materials after their degradation by making comparisons with the morphological and hygrothermal properties of the materials in their initial state.

For this purpose, a literature review is first presented in this chapter. It will clarify the limits of knowledge in the literature, regarding the experimental aging protocols and the resulting changes in the properties of hemp mortar. Basing on the literature review, a representative

accelerated aging experimental protocol is proposed. It is described along with the composition and manufacturing technique of the studied hemp mortar.

In a second step, the experimental investigations related to the aging of microstructural characteristics, chemical composition and hygrothermal properties of hemp mortar are presented, specifying experimental protocols adopted for this study. The evaluation of total porosity, the pH level and crystallographic composition is also investigated before and after aging. Special attention was devoted to the cracking at the interface between hemp mortar particles and the mineral matrix and the carbonation of hemp mortar.

Finally, all these results were analyzed and interpreted, linking the various microstructural quantities characteristic of hemp mortar and their variation due to proposed accelerated aging protocol.

## **II.2. CHOICE OF ACCELERATED AGING EXPERIMENTAL PROTOCOL**

Before carrying out the study on the evolution of hemp mortar's properties under hygrothermal stresses, an appropriate accelerated aging protocol must be chosen. Indeed, natural aging takes a long time, the protocol of real conditions can last several years, is not reproducible because of climate changes and depends on the region. To decrease the time of experimental procedure, the accelerated aging protocols are used. At the same time, the choice of the aging procedure is important as it must be the most representative of the real-life.

When talking about the durability of hemp mortars, few researchers studied the hygrothermal stresses impact on the hemp mortar properties. For example, (Sentenac et al., 2017) studied the performance and durability of treated hemp mortar. To estimate the evolution of the different properties and physical characteristics, the full immersion test was used. The conditioning represents 12 to 15 cycles of water immersion at 20 °C during 48 hours and drying at 40 °C during 48 °C depending on the samples. (Benmahiddine et al., 2020) adopted another protocol of immersion during 48 hours followed by drying in an oven at 50 °C for 72 h, over a period of 40 days. This immersion protocol has often been criticized because it is highly aggressive and also not very representative of the real aging conditions of the materials.

Other researchers used accelerated wetting and drying cycles to investigate the aging of hemp mortars. For example, (Marceau et al., 2017) adopted the wet/dry cycles protocol at constant temperature of 30°C (each cycle lasts 8 hours). Each conditioning consists of 8 cycles: 4 cycles of 40% / 90% RH and 4 cycles of 40% / 98% RH. They studied the changes in the microstructure (density evolution, hemp particles / cementitious matrix interface) and physical properties (thermal and acoustical performance). Delannoy et al. (Delannoy et al., 2020a) proposed another

accelerated aging protocol consisting of 5 days at 98% RH and 2 days of 40% RH constantly at 30 °C. Their study examines the evolution of the different properties of hemp mortar and its chemical composition.

(Bourdot et al., 2020) used 6 cycles of immersion in water for 48 h followed by freezing at -18 °C and drying in oven at 50 °C for 72 h. (Abahri et al., 2020) adopted the immersion/drying test of (Sentenac et al., 2017), the immersion/freeze test, and the wet/dry cycles (using a climatic chamber) of (Marceau et al., 2017) (Figure 39). These protocols allow both to make aggressive accelerated aging, and less-aggressive tests, as indicated in Table 4.

Table 4. Description of one cycle of different aging protocols

Protocol	Conditioning	Reference
Immersion/Drying (ID)	Immersion in water for 48 hours. Drying in an oven at 40 °C for 48 hours	(Sentenac et al., 2017)
Immersion/Freeze (IF)	Immersion in water for 48 hours. Freezing during 24 hours. Drying in an oven at 50 °C for 72 hours	(Abahri et al., 2020; Bourdot et al., 2020)
Climatic Chamber (CC)	5 days of wetting (HR=98 %, T=30 °C) and 5 days for drying (HR=40 %, T=30 °C)	(Delannoy et al., 2020a; Marceau et al., 2017)

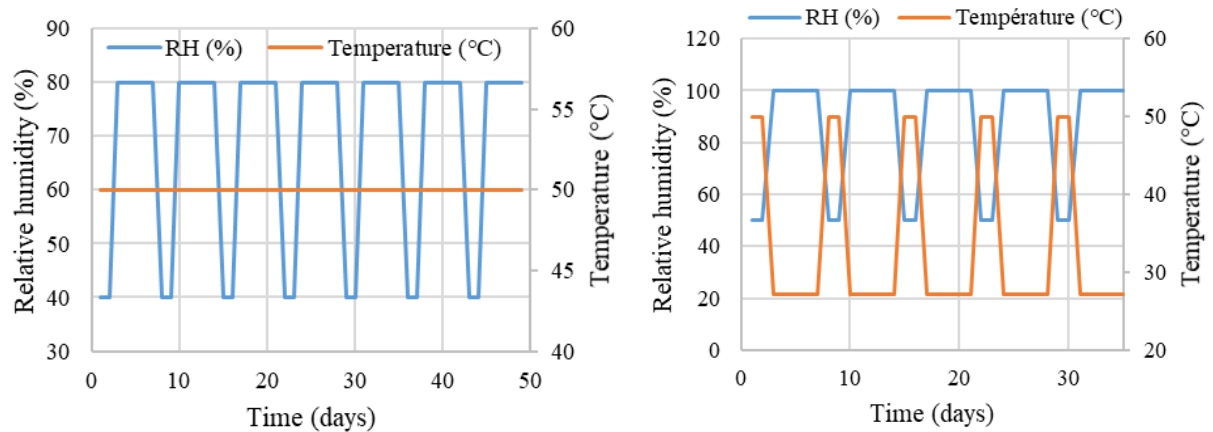


Figure 39. Example of wetting/ drying cycles (a) and immersion and drying cycles (b) (Abahri et al., 2020)

In all of the proposed literature works, non-standardized accelerated aging protocols were adopted that are not representative of the real-life cycle conditions of hemp mortar insulation. This is explained by the direct contact with water in the case of the protocol of (Sentenac et al., 2017) or high relative humidity in the works of (Marceau et al., 2017) and (Delannoy et al., 2020a), that do not appear under standard conditions of application and use (Piot et al., 2017b).

Therefore, in this chapter we adapt and propose the accelerated aging protocol basing on the standardized one used for External Thermal Insulation Composite Systems (ETICS) with rendering (EOTA, 2013). Experimentally, microstructural characteristics, chemical composition and hygrothermal properties are investigated.

### II.3. EXPERIMENTAL PROTOCOL

This section presents the studied material formulation, the accelerated weathering aging cycles conditions and the experimental characterization methods. The studied hemp mortar can be used for both external and internal insulation. Characterization of hemp mortar was conducted on two benchmarks: before and after the exposure to aging protocol. This allows to compare the results and study the influence of the conditioning on hemp mortar microstructure, chemical composition and hygrothermal properties.

#### II.3.1. Hemp mortar's composition and fabrication

The hemp shives of France origin were used for manufacturing the hemp mortar samples. Their photo and granulometric curve are presented in Figure 40 and 41 respectively. The granulometric curve demonstrates that shives are mainly composed of the particles of the size lower than 1 mm.



Figure 40. Hemp shives

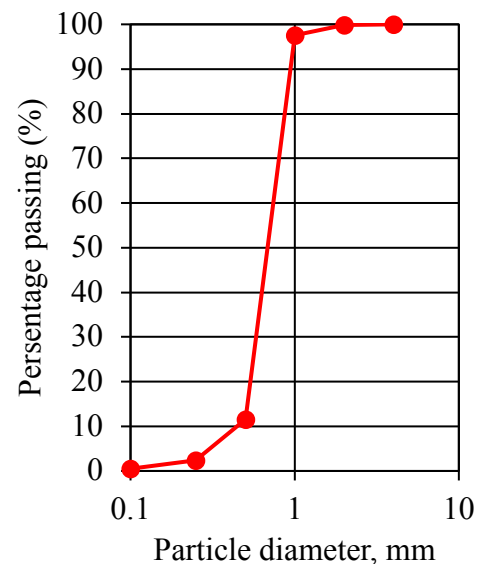


Figure 41. Granulometric curve of hemp mortar by image analysis

The binder represents a commercial mix designed by ParexGroup SA. Its composition is not disclosed by the manufacturer for commercial confidentiality. The mix proportion ratios of the used hemp mortar are represented in the Figure 42. The mixing was done in two stages: firstly,

hemp shives (initially conditioned at  $23 \pm 2^\circ\text{C}$  and  $50 \pm 5\%\text{RH}$  during one month) were premixed with water during 1 minute at 140 rpm, secondly, the binder was added and it was mixed during 5 minutes at 140 rpm. After their manual manufacture, the specimens were dried for 28 days at laboratory conditions ( $23 \pm 2^\circ\text{C}$ ,  $50 \pm 5\%\text{RH}$ ) as shown in Figure 43. The adopted sample sizes depend on experimental procedure and are presented for every type of test in section 2.3.

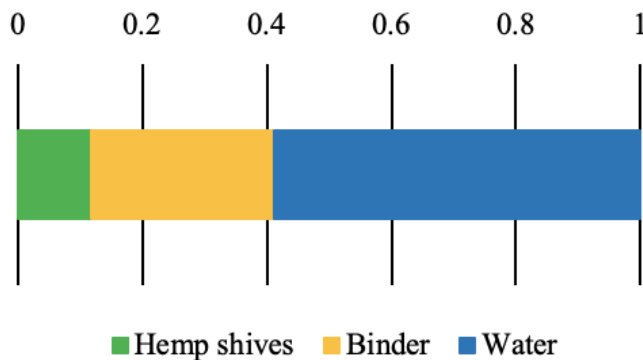


Figure 42. Mass ratios of hemp mortar composition



Figure 43. Hemp mortar samples laboratory drying

### II.3.2. Accelerated weathering aging cycles

After the 28 days of drying, the hemp mortar samples were conditioned in two different ambiances. Total weathering protocol is represented in Figure 44-A as is explained in the following:

- The first batch of specimens was subjected to the laboratory conditions ( $23 \pm 2^\circ\text{C}$ ,  $50 \pm 5\%\text{RH}$ ) for the whole period of the aging cycles. These samples were used later as a reference.
- The second part of the specimens was exposed to the accelerated aging cycles that consist of two parts: heat – rain and heat – cold cycles that are described below:
  - ✓ Heat - rain cycles: Samples are subjected to a series of 80 cycles, comprising the following phases: 1- heating to  $70^\circ\text{C}$  (rise for 1 hour) and maintaining at  $(70 \pm 5)^\circ\text{C}$  and 10 to 30% RH for 2 hours, 2 - spraying for 1 hour (water temperature at  $+ 15 \pm 5^\circ\text{C}$ , and amount of water  $1 \text{ l/m}^2 \text{ min}$ ), 3 – leave for 2 hours (drainage). These cycles are represented in Figure 44-B.
  - ✓ Heat-cold cycles: After a subsequent conditioning of at least 48 hours at temperatures between  $10$  and  $25^\circ\text{C}$  and a minimum relative humidity of 50 %, the same test rig is exposed to 5 heat/cold cycles of 24 hours comprising the following phases: 1- exposure to  $(50 \pm 5)^\circ\text{C}$  (rise for 1 hour) and maximum 30% RH for 7 hours (total of 8 hours), 2-

exposure to  $(-20 \pm 5)^{\circ}\text{C}$  (fall for 2 hours) for 14 hours (total of 16 hours) (Figure 44-C).

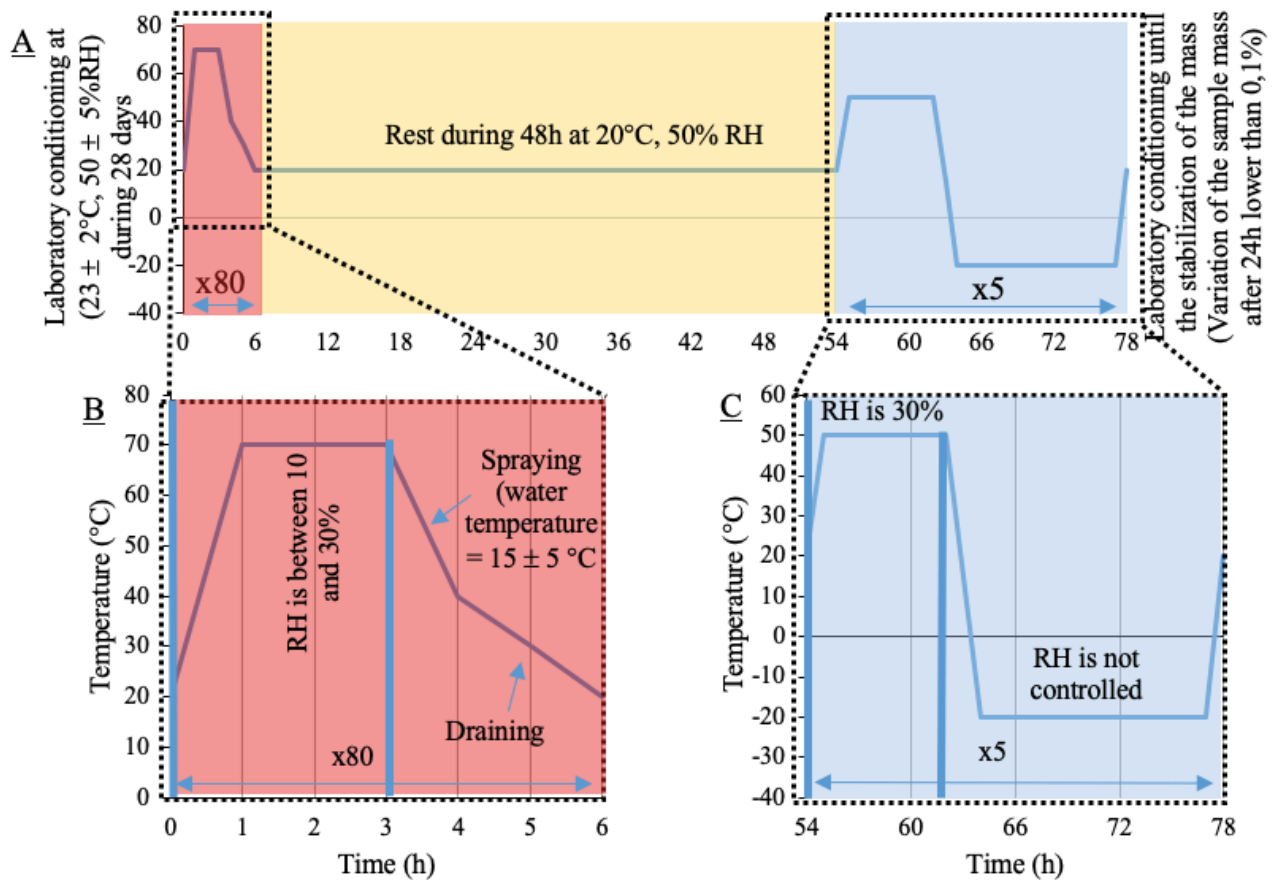


Figure 44. Diagram of the total accelerated aging cycles (A) with detailed heat-rain (B) and heat-cold (C) cycles



Figure 45. Disposition of the hemp mortar specimens in the climatic room before accelerated aging cycles

Specimens from two batches were characterized later after aging cycles. As hemp mortar is used as insulation material with rendering, it is protected against direct access of water. That's why, in this study, we used a roofing to avoid direct spraying of water on the samples, as shown in figure 45.

### II.3.3. Experimental procedure

This paper investigates the evolution of the hygrothermal properties, the microstructural and the chemical composition of the hemp mortar before and after aging cycles. Thermal conductivity, water vapor permeability and moisture buffer value (MBV) tests were conducted to analyze the evolution of the properties of the material. Identification of total porosity, pH level values, scanning electron microscope SEM and X-ray crystallography analysis provided more information about microstructural evolution. Experimental protocols for each test are proposed further. For each type of characterization test, three specimens were analyzed before and after the weathering aging cycles. The overall protocol schema is presented in the figure 46.

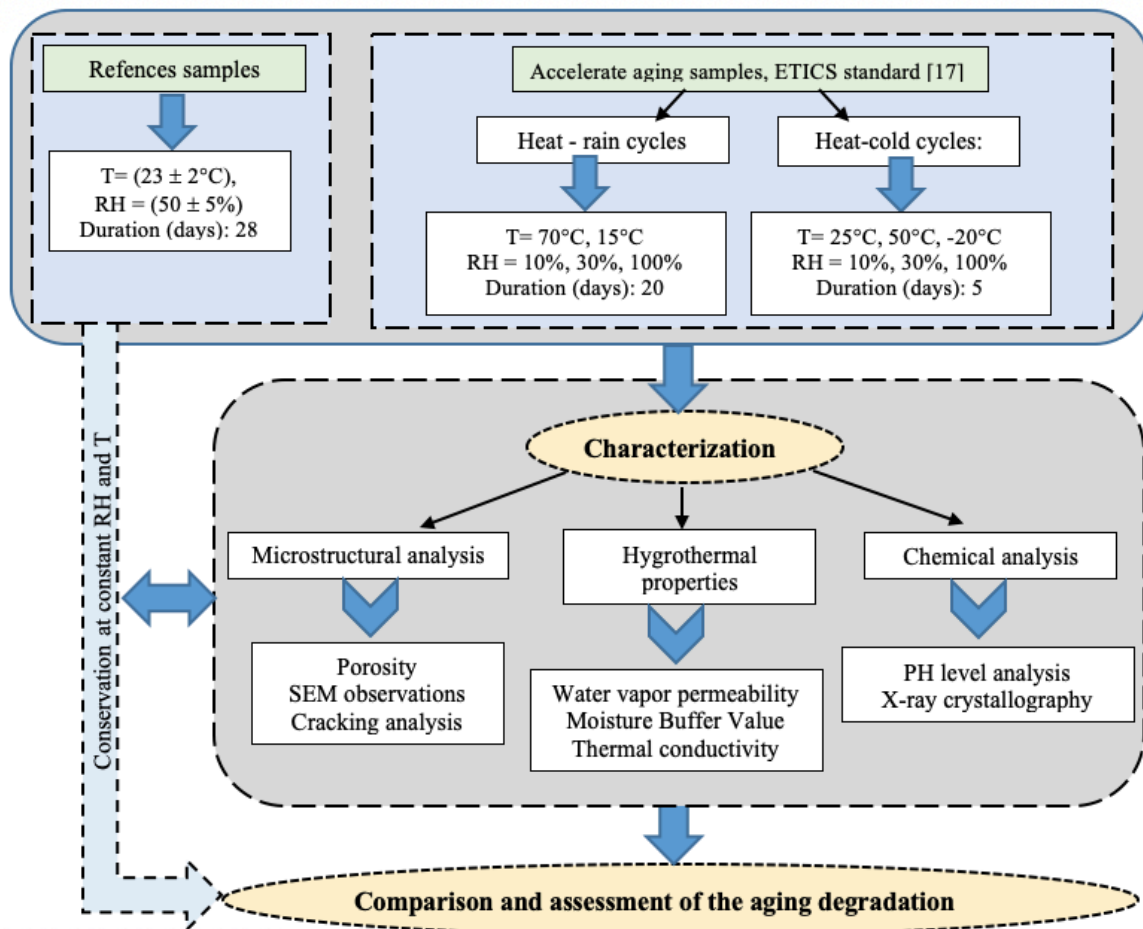


Figure 46. Experimental protocol schema



### II.3.3.1. Microstructural characteristics and chemical analysis

#### The total porosity tests

In order to measure the total porosity, the water porosity test was used accordingly the NFP 18-459 standard (AFN, 2010). Measurements of water-accessible porosity were carried out because, in addition to being one of the main indicators of durability, these tests provide information on the total porosity which is thought to affect the microstructure after aging.

Measuring this porosity involves determining by weighing the apparent mass in water after immersion in water (hydrostatic weighing) of a concrete test body previously impregnated with water under vacuum; dry samples masses. The standard required to put samples in desiccators under vacuum at a constant pressure of during 4 hours and then gradually inject water inside the desiccator ensuring that samples are covered by a minimum of 20 mm of water level during 48h. Hydrostatic whetting at 0.01 % were carried out ( $M_w$ ) accompanied with air weighing ( $M_a$ ). Finally, the mass after drying ( $M_d$ ) (at 100°C) was determined for all samples and when the mass becomes stable (no variation up to 0.05% between two successive weightings in an interval of 24h) we calculate the porosity according Eq. 22:

$$\epsilon = \frac{M_a - M_d}{M_a - M_w} \cdot 100 \quad (22)$$

It is based on the hemp concrete saturation in water under vacuum. Then different weightings were done to calculate the total porosity of the samples. The scales reading is 0.01 g. One of the weightings is the weighting of wet sample. As hemp mortar becomes fragile after wetting, we used a cotton tissue in order to protect the wet sample from damage (Figure 47). Three specimens (15x15x7 cm<sup>3</sup>) were tested for each time of conditioning to warranty the repeatability of the test.

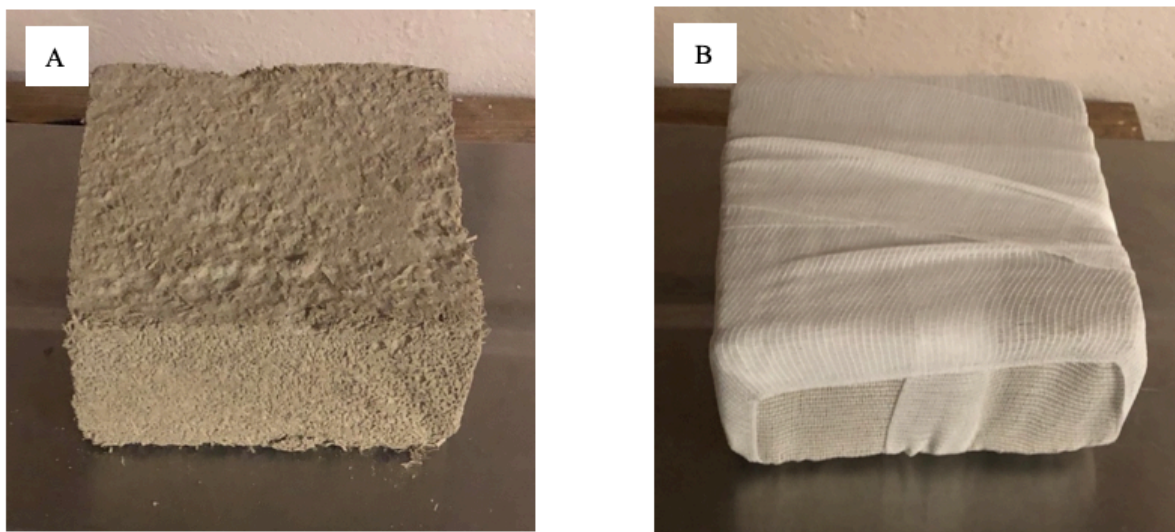


Figure 47. Hemp mortar samples without (A) and with (B) protective cotton tissue

## Scanning Electron Microscopy (W-SEM) microstructural analysis

The microstructure of hemp mortars was analyzed before and after aging using Scanning Electron Microscope (W-SEM). All observations were performed using a Hitachi S-3400N device (Figure 48). The surface of the hemp mortar and the interface zone between cementitious matrix and hemp particles were observed and analyzed before and after aging. Particular attention has been devoted to the identification of the same observation area for these two states. Micrographs are recorded by using secondary electrons detectors at an acceleration voltage of 15 kV, in high vacuum mode (pressure <1Pa). Previously to observations, the specimens were covered by carbon in order to improve the image quality (Figure 49).

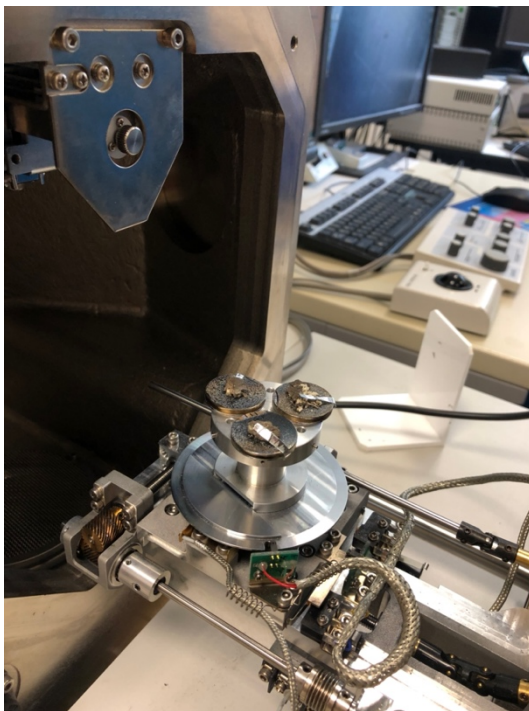


Figure 48. Hemp mortar samples in the Hitachi S-3400N



Figure 49. Preparation of hemp mortar samples (coverage with carbon)

## PH level evolution

Measuring the pH of biobased materials is an important step to assess their durability. In fact, pH is one of the critical parameters for the molds proliferation that is one of the most important aspects that degrade the biobased materials (Marceau et al., 2017; Sinka, M. et al., 2019). There are a lot of different methods of the identification of a pH level. Measuring the pH of hemp mortar is a difficult task due to the high heterogeneity of this material. Some authors identify a pH level of interstitial solution by compression that allow to get the most reliable results as we don't modify the pH level adding water (Alonso et al., 2007). Nevertheless, this method is a heavy procedure that requires special equipment and a large quantity of cement. Others propose another method – of cementitious suspensions (Codina, 2007). It consists of suspending of some part of

the mortar in water and measuring a pH level of obtained suspension. At the same time, the use of suspensions implies problems of dissolution of the solid phases but especially of dilution, moreover if talking about hygroscopic composite material. That is why in this work a surface electrode WTW Sentix Sur was used (Tran et al., 2014). It allowed us to get a reliable result and especially on different parts of samples to evaluate a chemical degradation of the mineral matrix.

In order to better understand the degradation of the samples, we have investigated two different areas for the measurement of pH: the surface and the middle of the sample. The idea is to understand whether or not the degradation caused by hygrothermal stresses has actually propagated inside the sample or not. In fact, most of the works in the literature studying hemp mortars do not pay attention to the position of pH measurement in the sample. Nevertheless, it is important as the chemical degradation starts from the surface and is a long process.

For this test the specimens of the same composition, made with the same raw materials, of the size 16x4x4 cm<sup>3</sup> were used. For each value three measures were performed at different positions on the specimen. As the pH level measurements are possible just in solution, the constant volume of demineralized water (0.2 ml) was deposited on the studied surfaces. Then, the electrode was kept on the sample surface, so that the electrode's membrane remains in contact with the hemp mortar (Figure 50). At equilibrium, the WTW Sentix Sur displays a constant value of PH which will be subsequently recorded. For the inner pH level measures the protocol is the same, but the measurements were conducted in the middle of the specimen.



Figure 50. Measurement of the surface pH level using a WTW Sentix Sur electrode

### **X-ray diffraction (XRD) crystallography analysis**

Prior to XRD crystallography analysis, hemp mortar samples of the size 16x4x4 cm<sup>3</sup> were grinded and sieved to remove organic fibers. This step allowed us to decrease the influence of the dilution on the final result as in this case we analyze only mineral matrix. To link the results of

chemical composition to the pH level, the crystallography at the surface and in the middle was analyzed.

Free water was removed using the acetone. Then, the specimens were dried at 50°C in order not to modify the composition of the sample. XRD crystallography patterns were obtained using Cu K $\alpha$  anode tube ( $\lambda = 1.54182 \text{ \AA}$ ) radiation at 40kV and 20mA with a Bruker D8 diffractometer (Bruker, Karlsruhe, Germany) (Figure 51). The diffractometer was scanned from 5° to 60° (2 $\theta$ ) in step size of 0.015° and the counting time per step was 1.2 s.



Figure 51. Bruker D8 diffractometer used for crystallography analysis

### **II.3.3.2. Hygrothermal properties evolution**

#### **The water vapor permeability (WVP) (wet cup method)**

The water vapor permeability is the ability of a material to transfer or retain water vapor due to a difference in the partial pressure of water vapor at the same atmospheric pressure on both sides of the material. It was identified according to the NF EN ISO-12572 standard using the wet cup method (ISO 12572, 2016). Firstly, specimens of diameter 11 cm and thickness of 2.4 cm (3 samples for each test) were dried at 23°C, 50% RH during 28 days. Then, they were sealed on cups containing a saturated salt solution that ensures constant relative humidity in the cup (Figure 52). In the case of wet cup, ammonium dihydrogen phosphate was used that maintains the relative humidity at 93 $\pm$ 1%. The cups are conditioned in a constant ambiance of 23°C and 50% RH.

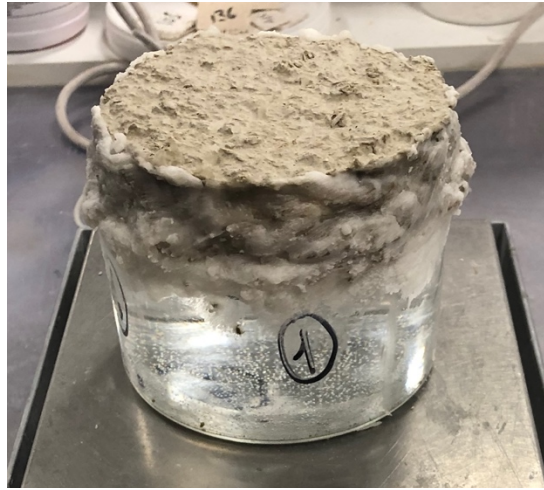


Figure 52. Hemp mortar sample sealed on the experimental cup

The water vapor permeability value was determined in function of the vapor transmission through the specimen. To do so, the mass monitoring was conducted every day during 18 days for each cup to calculate the kinetics of mass variation:

$$\Delta\dot{m}_{12} = \frac{m_1 - m_2}{t_1 - t_2} \quad (23)$$

where  $\Delta\dot{m}_{12}$  is a mass variation velocity (kg/s);  $m_1$  and  $m_2$  are masses of the cups with hemp mortar samples at the time  $t_1$  and  $t_2$  respectively (kg);  $t_1$  and  $t_2$  are the successive times of weighting (s).

Then, the water vapor flux density was calculated:

$$g = \frac{G}{A} \quad (24)$$

where  $G$  is an average value of five successive measurements of  $\Delta\dot{m}_{12}$  and  $A$  is an exposed area (m<sup>2</sup>).

The water vapor permeance was calculated as

$$W = \frac{G}{A \cdot \Delta p} \quad (25)$$

where  $\Delta p$  is difference of water vapor during the test.

The water vapor resistance is an inverse value to permeance:

$$Z = \frac{1}{W} \quad (26)$$

In fact, there are several resistances in the experimental montage:

$$Z_m = Z_a + Z_s + Z_1 + Z_2 \quad (27)$$

where  $Z_m$  is an experimental calculated value of resistance,  $Z_a$  is a water vapor resistance of air,  $Z_1$  and  $Z_2$  are the water vapor resistances that take into account the interface diffusion at the sample/air and air/saline solution interfaces respectively.

Finally, the water vapor permeability value was calculated:

$$\delta = \frac{d}{Z_s} \quad (28)$$

where  $d$  is a thickness of our sample (mm).

### The thermal conductivity tests

For measuring thermal conductivity, there are two types of experimental methods: steady-state and non-steady-state ones. When talking about measurement setups, we can distinguish four main types: the guarded hot plate (GHP), the heat-flow meter (HFM), the hot wire, and laser flash diffusivity (Yüksel, 2016). In this work the method of hot wire is used as it is well adapted for bio-based materials. Thermal conductivity measurements were taken on three different pairs of the  $15 \times 15 \times 7 \text{ cm}^3$  samples under transitory conditions using the device CT-Metre (Figure 53). Before measurements, these samples were conditioned at  $23^\circ\text{C}$  and 50 % RH until a constant mass, according to (ISO 12571, 2000).

Measurements were made according to the device precautions on the measurements. The used protocol consists of placing a probe between two samples keeping the maximal parallelism of the surfaces to avoid the distortion of results. The thermal conductivity values were calculated by the CT-Metre automatically, coefficients of correlation of presented results were 0,999.



Figure 53. CT-Metre measurement device

### Moisture buffer value (MBV) tests

The moisture buffer value represents the ability of the material to mitigate the relative humidity changes in ambient air. It refers to the amount of water that could be absorbed/released

when exposed to relative humidity change. In this paper, the Nordtest protocol was used to investigate the MBV of the studied hemp mortar. During this test the samples of hemp shives placed in the aluminum recipient of 10x10x3 cm<sup>3</sup> size and hemp mortar samples of 15x15x7 cm<sup>3</sup> size were used. To do this, variable cycles of relative humidity of 75% (for 8h) and 33% (for 16h) were applied. Samples were weathered at laboratory conditions (23 ± 2°C, 50 ± 5%RH) beforehand. The MBV value was calculated:

$$MBV = \frac{\Delta m}{S \cdot (HR_{max} - HR_{min})} \quad (29)$$

where  $\Delta m$ : sample mass variation [kg],

S: exposed area of sample [m<sup>2</sup>],

$HR_{max}$ : maximal relative humidity [%],

$HR_{min}$ : minimal relative humidity [%].

According to (NORDTEST project, 2005), building materials are classified using the MBV range represented in Figure 54.

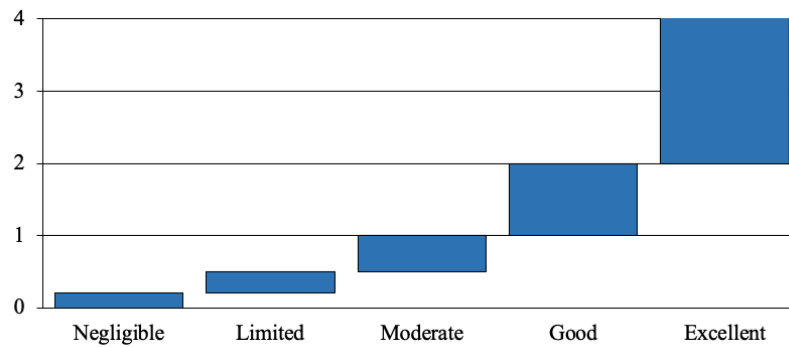


Figure 54. Moisture buffer value (g/%RH.m<sup>2</sup>) standardization according to Nordtest protocol (NORDTEST project, 2005)

## II.4. EVOLUTION OF MICROSTRUCTURE, CHEMICAL COMPOSITION AND HYGROTHERMAL PROPERTIES OF HEMP MORTAR

Hygrothermal stresses have a great impact on the hemp mortar's microscopic morphology, its chemical composition and hygrothermal properties. In fact, microscopic degradation of hemp mortar, especially cracking, and the total porosity or crystallographic composition evolution, affect significantly its macroscopic behavior and functions.

In this section, the assessment of the microstructure, the chemical composition and its hygrothermal performance evolution under the accelerated aging cycles are presented.

### II.4.1. Microstructural characteristics and chemical analysis

In order to study the microstructure evolution, firstly the total porosity was analyzed before and after the accelerated aging cycles. Then, the interface between cement matrix and hemp particles was observed and the evolution of the chemical composition was studied. The analysis of these results was complemented by SEM.

We note that the studied hemp mortar has a porosity of 85.2% which is more important than the other mortars, presented in literature (Bennai et al., 2017). This is explained by the organic fibers porosity and the properties of the cementitious matrix that ensure good insulation properties.

In order to ensure repeatability of the porosity measurement, there samples of hemp mortars were tested and the results are presented in Table 5 and the average total water porosity value (%) are presented in Figure 55.

Table 5. Total water porosity values (%) evolution of hemp mortar samples before and after the weathering aging cycles

Values	Before the weathering aging cycles	After the weathering aging cycles
Total water porosity value of the sample 1 (%)	83.9	87.7
Total water porosity value of the sample 2 (%)	86.5	84.8
Total water porosity value of the sample 3 (%)	85.2	84.9
Standard deviation (%)	$\pm 0.87$	$\pm 1.23$

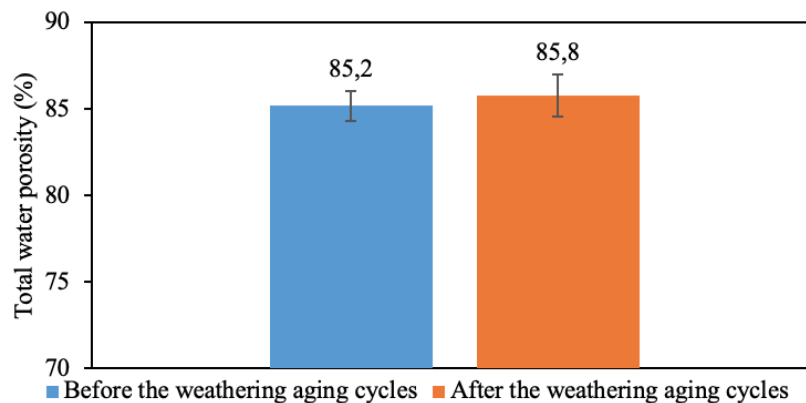


Figure 55. Total water porosity values (%) evolution of hemp mortar samples before and after the weathering aging cycles

According to the results given in Figure 55 weathering aging cycles affect very slightly the total porosity, increasing the value from 85.2% to 85.8%. This result remains in the range of a standard deviation. Such slight evolution of porosity could be explained by the dimensional



variation of the hemp mortar due to hygrothermal solicitations. In fact, hygrothermal stresses cause swelling or shrinkage of the organic fiber causing cracking of the interface and, consequently, an increase in porosity. At the same time there is another effect – a carbonation of mineral matrix and such porosity change could be explained by competition between these two phenomena. Both effects are investigated in detail.

In order to study the hemp mortar cracking before and after proposed weathering aging cycles, the W-SEM observation of the hemp particles / cementitious matrix interface was conducted. To do this, the surface areas of 2 samples for each type of conditioning were observed. For each sample, 10 interfaces were examined and the crack sizes were measured in 10 spots all along the crack. example of the image before and after aging are present in Figure 56. We notice the cracking of the hemp mortar and mineral matrix interface that show the nature of the hemp mortar damage. That explains the results of the water vapor permeability evolution. Moreover, the mean results of the crack size show the important increase of the crack size from 5.5 to 24.8  $\mu\text{m}$  (Figure 57) in the longitudinal direction of fibers. These results emphasize the influence of hygrothermal solicitations on the morphology of the hemp mortar.

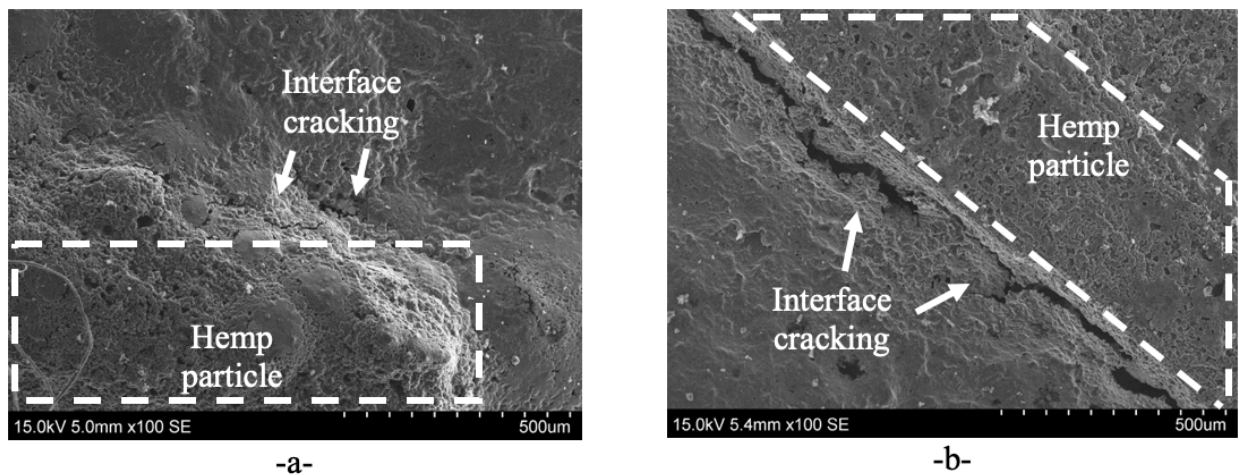


Figure 56. W-SEM observation of the surface of the specimens before (a) and after (b) the weathering aging cycles

The carbonation of the cementitious matrix was investigated by the X-ray diffraction crystallography (XRD). It was conducted for the samples before and after the weathering aging cycles which allowed estimate the chemical composition evolution. For each specimen the analysis of the composition on the surface and in the middle of the studied samples was performed.

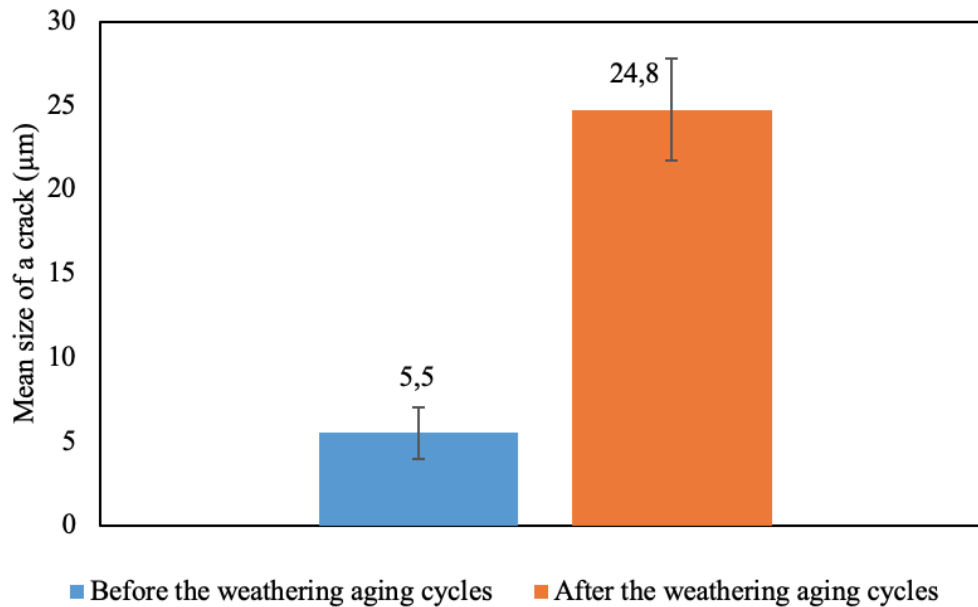


Figure 57. Mean size ( $\mu\text{m}$ ) of the hemp particles / cementitious matrix interface cracks for 2 samples before and after the weathering aging cycles (10 measurements for 10 interfaces)

The XRD patterns presented in Figure 58 showed the main mineralogical compounds of the hemp mortar as  $\text{Mg}_4\text{Si}_6\text{O}_{15}(\text{OH})_2 \cdot 6\text{H}_2\text{O}$  (sepiolite),  $\text{Ca}_6\text{Al}_2(\text{SO}_4)_3(\text{OH})_{12} \cdot 26\text{H}_2\text{O}$  (ettringite),  $\text{Ca}(\text{OH})_2$  (portlandite),  $\text{CaCO}_3$  (calcite),  $\text{SiO}_2$  (quartz),  $\text{Ca}_3\text{SiO}_5$  (tricalcium silicate),  $\text{Ca}_2\text{SiO}_4$  (dicalcium silicate) and  $\text{Ca}_3\text{Al}_2\text{O}_6$  (tricalcium aluminate). Figures 58 (a) and 58 (c) present the crystallographic analysis of the hemp mortar specimen before the weathering aging cycles in the middle and on the surface, respectively. We note that after one month of drying at  $23^\circ\text{C}$  and 50% RH there is non-hydrated  $\text{Ca}_3\text{SiO}_5$  (tricalcium silicate),  $\text{Ca}_2\text{SiO}_4$  (dicalcium silicate) and  $\text{Ca}_3\text{Al}_2\text{O}_6$  (tricalcium aluminate), which means that hydration is not completed. As for carbonatation of the cementitious matrix, we note that the quantity of the ettringite and portlandite is lower on the surface, is more visible in Figures 59 (I (a and c)) and 59 (II (a and c)) respectively. On contrary, Figure 59 (III (a and c)) shows the increase of calcite.

The same pattern was noted for the sample after the weathering aging cycles. The results show that the ettringite and portlandite almost vanished in the middle and on the surface of the sample (Figure 59 (I) and (II)), and calcite quantity increased (Figure 59 (III)). This shows that after the aging protocol the matrix is almost carbonated.

The carbonation of the calcium hydroxide is accompanied by a decrease in pH. That is why the measurements of the pH level were carried out to study the influence of the pH on the crystallographic composition. The results presented in Figure 60 show that the pH levels on the surface and in the middle of the sample were equal to 8.46 and 12.18 respectively before the weathering aging cycles and 8.71 and 8.69 – after. It demonstrates the effect of the carbonatation of the cementitious matrix. In fact, the diffusion of the air dioxide carbon in the hemp concrete

provokes its reaction with the portlandite and decrease the pH level. As the surface of the sample is exposed to the air, the quantity of portlandite at the surface is lower because of the carbonation. Later, that leads to the degradation of the ettringite, as it is very sensible to the ambient pH level.

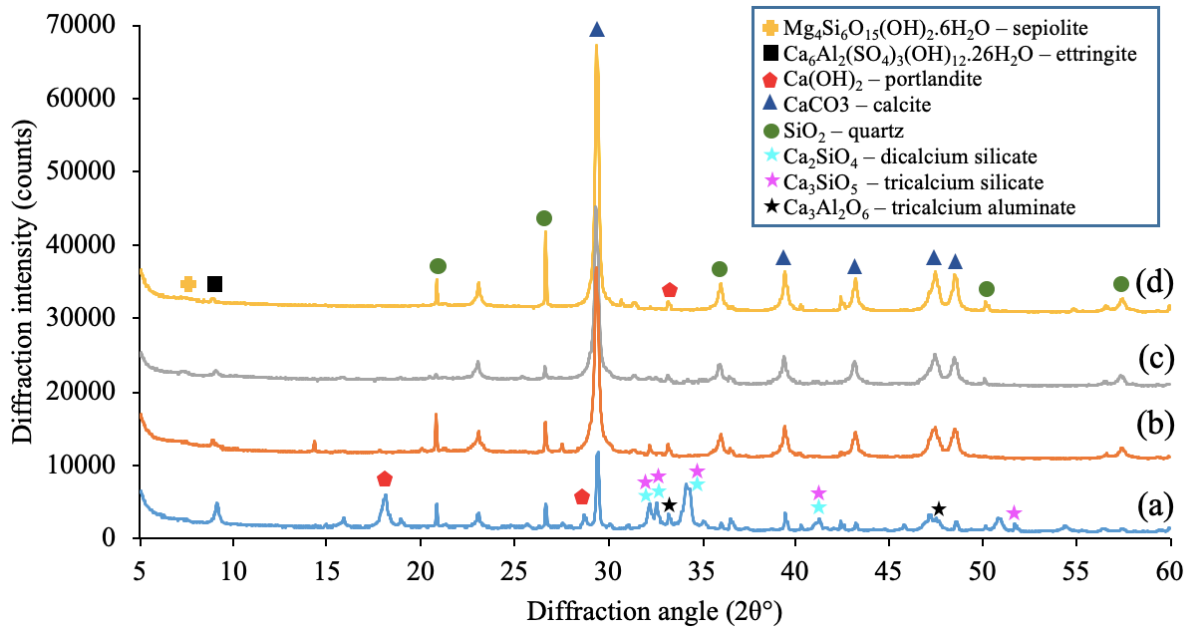


Figure 58. X-ray diffraction patterns of: (a) interior part of the hemp mortar samples before the weathering aging cycles; (b) interior part of the hemp mortar samples after the weathering aging cycles; (c) surface part of the hemp mortar samples before the weathering aging cycles; (d) surface part of the hemp mortar samples after the weathering aging cycles

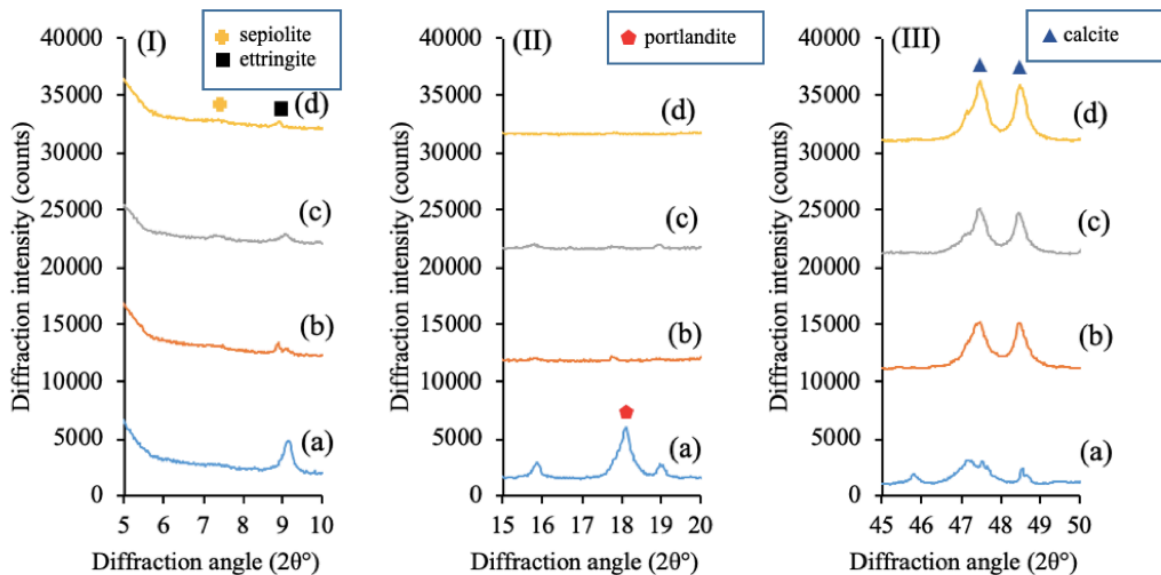


Figure 59. Zoomed X-ray diffraction patterns for ettringite (I), portlandite (II) and calcite (III) evolution: (a) interior part of the hemp mortar samples before the weathering aging cycles; (b) interior part of the hemp mortar samples after weathering aging cycles; (c) surface part of the hemp mortar samples before the weathering aging cycles; (d) surface portion of the hemp mortar samples after the weathering aging cycles.

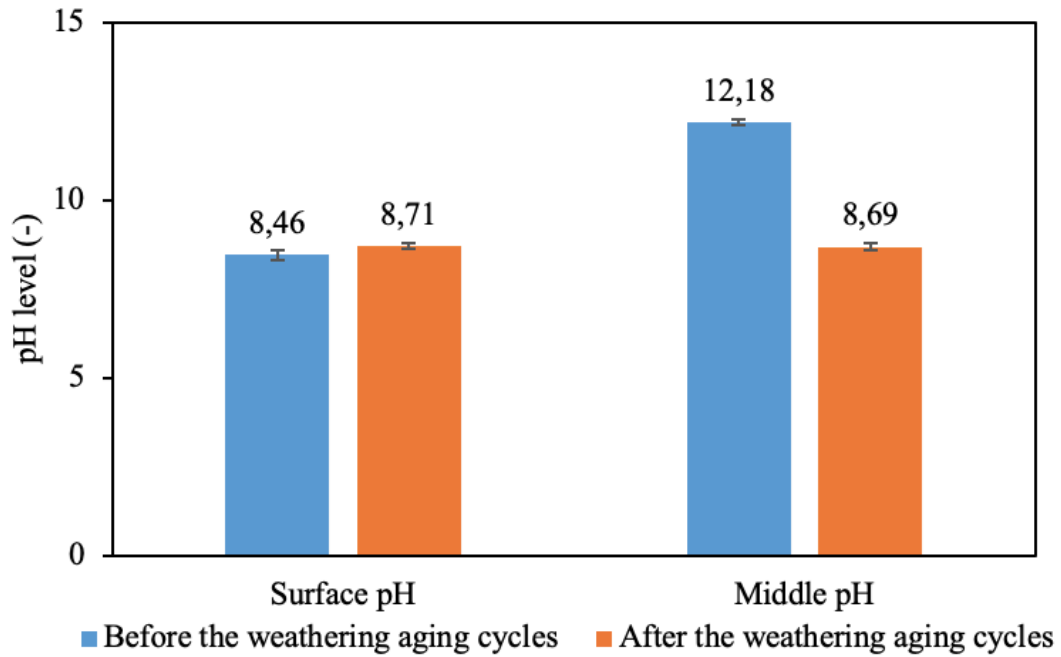


Figure 60. Diagram of pH level evolution on the surface and in the middle of the samples before and after the weathering aging cycles

#### II.4.2. Hygrothermal properties evolution

Hemp mortar is used for external or internal insulation applications. It is also considered as a hygroscopic material with a good ability to moderate variations in relative humidity of the external environment. The results of their evolution investigation are present below.

##### Water vapor permeability

First, the water vapor permeability evolution due weathering aging cycles was investigated. This parameter expresses the quantity of water vapor that passes through sample's porosity. Thus, the evolution of this parameter also gives information on the evolution of the porosity and cracking caused by the hygrothermal dimensional variations after aging. The results of water vapor permeability before and after the weathering aging cycles are present in Figure 61. Firstly, one can notice that the results obtained from this study are much higher than the values measured for other formulation of the hemp mortar in the literature (Bennai et al., 2017). In fact, [Bennai et al., 2017] using the methods of dry (3% RH inside) and wet (93% RH inside) caps got different values in function of the sample age. Experimental conditions for the method values. The measured value at the age of 30 days for wet cup method was  $2,38E^{-11} \text{ kg.s}^{-1}.\text{m}^{-1}.\text{Pa}^{-1}$ . That is explained by the composition, the particle size of hemp, and different binder types that allow to produce more aerated hemp mortar in case of our formulation. Also, we notice the increase of the average water vapor permeability after aging from  $2,02E^{-10}$  to  $3,41E^{-10} \text{ kg.s}^{-1}.\text{m}^{-1}.\text{Pa}^{-1}$ , that justify the results of

the increase of the porosity. This is explained also by the cracking of the hemp mortar, which increases its vapor diffusion capacity and thus its permeability.

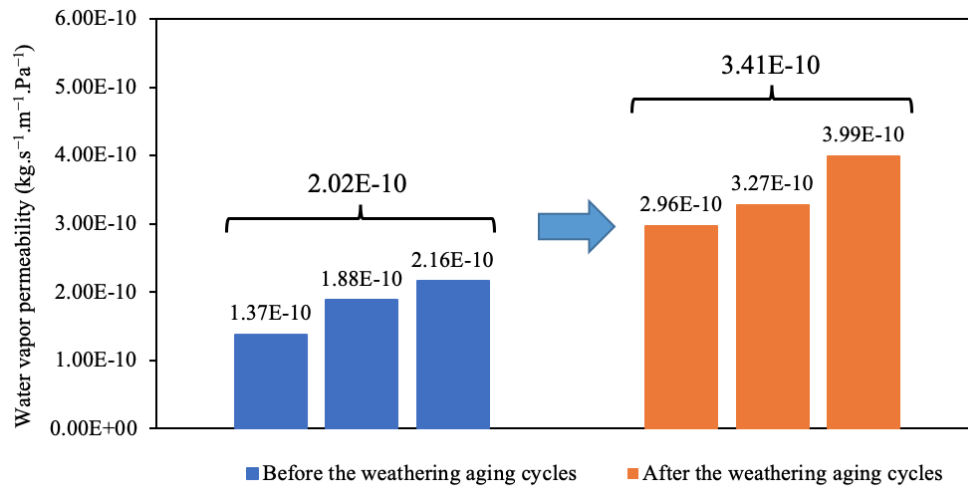


Figure 61. Water vapor permeability ( $\text{kg.s}^{-1}.\text{m}^{-1}.\text{Pa}^{-1}$ ) evolution of hemp mortar samples before and after the weathering aging cycles

### Thermal conductivity

The result of the evolution of the thermal conductivity before and after aging are presented in Figure 62. The thermal conductivity was slightly increased after aging from 0.087 W/m.K to 0.091 W/m.K. In fact, this parameter is very dependent on the porosity. Thermal conductivity increased after aging because of the degradation of the plant fibers which consequently reduces the thermal performance of this material.

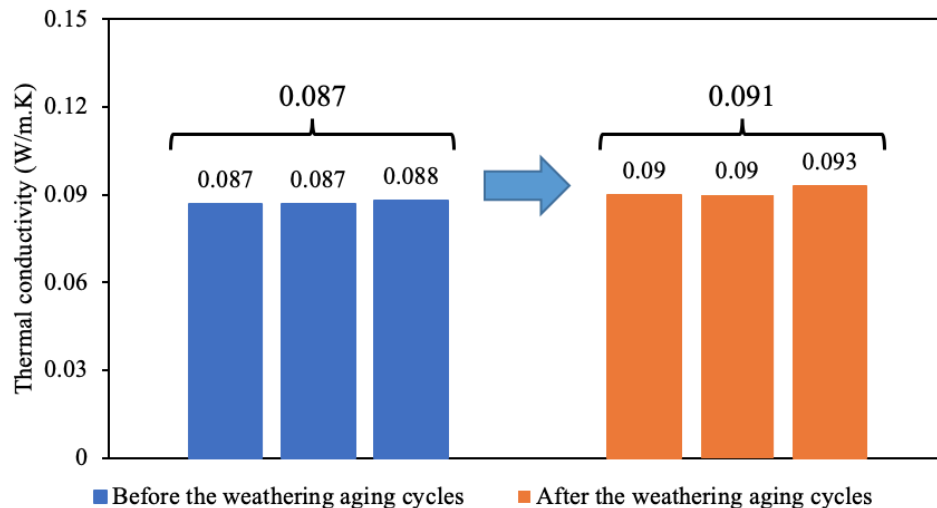


Figure 62. Thermal conductivity (W/m.K) evolution of hemp mortar samples before and after the accelerated aging cycles

An increase in thermal conductivity of 11% was also observed after natural aging (60 days in constant temperature and relative humidity) in the work of (Bennai et al., 2017). They explained this behavior by the evolution of the porous structure of the material. However, (Benmahiddine et al., 2020) obtained a reduction of 6.67% of thermal conductivity between the reference state and

after immersion/drying aging. These authors explained this result by to the modification of the microstructure of the material and the increase of its total porosity after aging.

### Moisture Buffer Value MBV

Figure 63 shows the mass and relative humidity evolution that occurred during the first 5 MBV experimental cycles for the second sample of hemp mortar before the weathering aging cycles. The temperature was held constant at 23 °C.

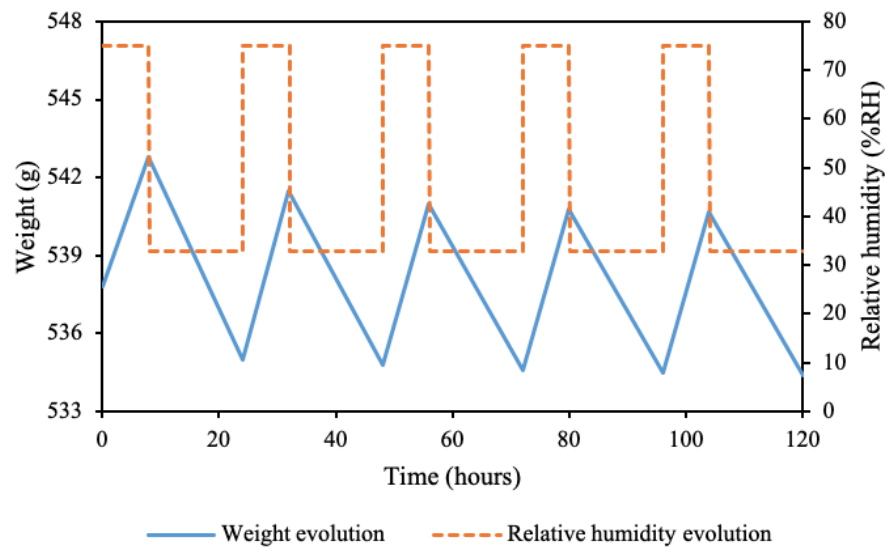


Figure 63. Masse (g) and relative humidity (%RH) evolution in function of the time

Concerning the moisture buffer value, one can note that the MBV of hemp mortar is bigger than the MBV of hemp shives before aging cycles. It is explained by the fact that the studied hemp mortar is much more aerated and lightweight than conventional hemp mortars that allows it to preserve the hygric properties of hemp shives. Nevertheless, we notice that the accelerated aging cycles did not affect the hemp shives moisture buffer value. It stays excellent with 2.25 moisture buffer value according to Nordtest protocol (Figure 54) (NORDTEST project, 2005). Unlike hemp shives, hemp mortar represents the degradation of its MBV value. It decreased from 2.22  $\text{g}/\%RH.m^2$  to 2  $\text{g}/\%RH.m^2$  (Figure 64). In fact, there is the competition between the interface damage of the hemp mortar samples and the carbonatation of the mineral matrix during the hygrothermal solicitations caused by the accelerated aging cycles. So, the carbonatation of the matrix caused the closing of the microporosity and complicated the air access to the hemp particles that finally led to the moisture buffer value decrease. Despite the decrease of the moisture buffer value, we note that the MBV of the hemp mortar stays excellent.

The same behavior was observed with (Benmahiddine et al., 2020) where the MBV of hemp mortar decreased of 11 % after immersion/drying aging. This decrease was explained by the aging

of the hemp shiv which has caused a degradation of its capacity to adsorb and restore moisture (natural moisture regulation).

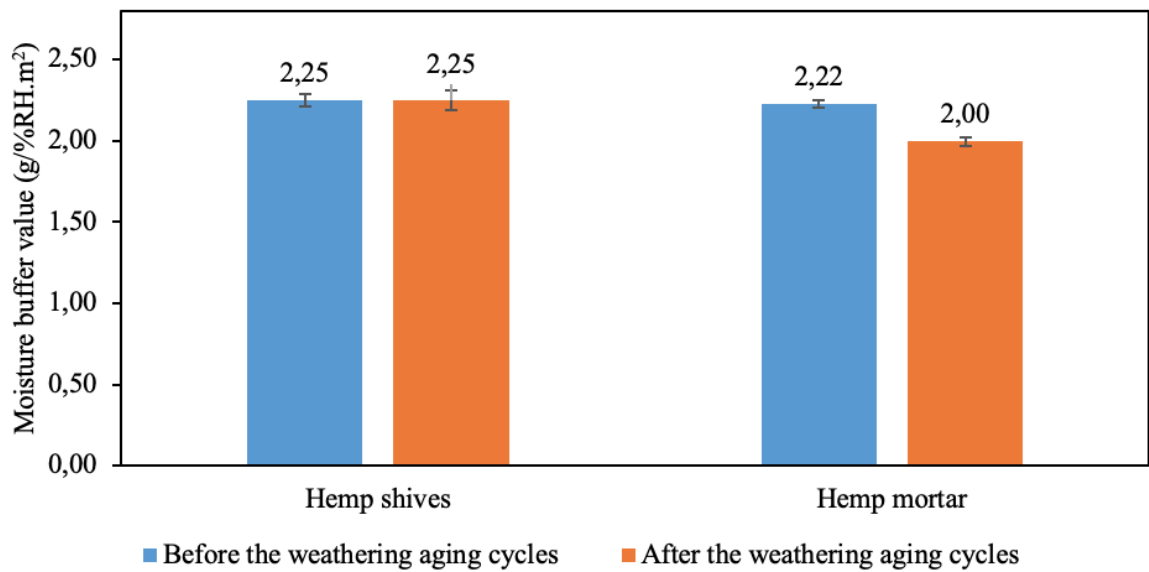


Figure 64. Moisture buffer value (g/%RH.m<sup>2</sup>) evolution of hemp shives and hemp mortar samples before and after the accelerated aging cycles

## II.5. CONCLUSION

In this chapter, an original accelerated weathering aging protocol inspired by the standardized one was proposed. Experimentally, the hemp mortar microstructure, its composition and properties evolution were investigated. To do this, all characteristics were studied before and after the hemp mortar exposure to accelerated aging cycles. Firstly, the hemp mortar total water porosity, its water vapor permeability, its mineralogical composition and pH level evolutions were analyzed. Also, the SEM observation of the hemp particles / cementitious matrix interface was realized. Then, the characterization of evolution of the hygrothermal properties as thermal conductivity and moisture buffer value was conducted.

Results of the total porosity evaluation show a slight increase of the porosity but it remains in a standard deviation range. This is explained by a compensation of two processes that occurs and are in contest during the hygrothermal stresses: the cracking of the hemp particles / cementitious matrix interface that increase the hemp mortar porosity and the carbonatation that provoke the filing of the porosity by calcite. To study the cracking effect the evolution of water vapor permeability was analyzed. It increased from  $2.02E^{-10}$  to  $3.75E^{-10}$   $\text{kg}\cdot\text{s}^{-1}\cdot\text{m}^{-1}\cdot\text{Pa}^{-1}$  that shows the increase of the ability to transfer a water vapor. This change was also noticed using a SEM observation because of the increase of the interface cracks on the surface of the mortar. The XRD analysis demonstrated the carbonatation of the mineral matrix – the increase of the quantity of the calcite and decrease of the quantity of the portlandite and ettringite due to the aging cycles. The carbonatation was also demonstrated by the study of pH level evolution since the pH level of the

samples decreased to 8.69 in the middle and to 8.71 on the surface after the weathering cycles. As for the hygrothermal properties, the value of thermal conductivity dependent on the porosity follows the same as total porosity pattern – it slightly increases at the range of the standard deviation. The moisture buffer value decreases from 2.22 g/%RH.m<sup>2</sup> to 2 g/%RH.m<sup>2</sup> that is explained by the closing of the hemp mortar microporosity and complication of the air access to the hemp particles. Obviously, both the interface cracking and the carbonatation processes present the considerable influence on the durability of the hemp insulating mortar. At the same time, we note that the studied hemp mortar saves their previously declared hygrothermal properties (as the thermal conductivity and the moisture buffer value). It is primordial when talking about the durability of the insulating material.

This chapter highlighted the influence of the hygrothermal solicitations on the evolution of the microstructural characteristics and functional properties of the hemp mortar. The results reveal that the main properties are saved. Therefore, the following chapter is devoted to the evaluation of another important factor of durability – the influence of mold on hemp mortar.



CHAPTER III.

INFLUENCE OF THE MOLD GROWTH ON THE  
CRYSTALLOGRAPHIC COMPOSITION OF HEMP  
MORTAR

## NOTATIONS

**Holocellulose** is a water-insoluble carbohydrate fraction of wood materials.

**Macrophages** are white blood cells whose job is to destroy invading microorganisms.

**Mesophilic** is an organism that grows best in moderate temperature, neither too hot nor too cold.

**Neutrophils** are the most abundant type of granulocytes and make up 40% to 70% of all white blood cells in humans. They form an essential part of the innate immune system, with their functions varying in different animals.

**Ribosomal RNA** is a type of non-coding RNA which is the primary component of ribosomes, essential to all cells. rRNA is a ribozyme which carries out protein synthesis in ribosomes.

---

## **CHAPTER III. INFLUENCE OF THE MOLD GROWTH ON THE CRYSTALLOGRAPHIC COMPOSITION OF HEMP MORTAR**

---

### **III.1. INTRODUCTION**

CHAPTER II was dedicated to the study of hygrothermal properties, chemical composition and microstructure of hemp mortar under accelerated aging cycles representative of the environmental solicitations. In addition to the degradation by hygrothermal stresses, the organic nature of biobased building materials leads to another phenomenon: the risk of microbiological contamination, which is one of the most encountered on different types of hemp-based building materials in France (Agence Qualité Construction, 2016). Apart from the influence of the microorganisms on air quality, they can also affect the substrate where they grow as they produce different metabolites (organic acids, etc.).

Therefore, this chapter deals with the fungal influence on the crystallographic composition of hemp mortar. First, bibliographical study was carried out, on the molds including their: classification and phylogeny, reproduction and biological characteristics, nutritive conditions, interactions with the environment, ability to degrade a material, conditions of growth, effect on the human health. Then, the completed literature works on the molds influence on the crystallographic characteristics of hemp mortars was collected, and which highlights the lack of knowledge regarding this aspect.

To do so, experimentally, different methods were performed to verify the presence of the molds on the surface of the hemp mortar samples exposed to high relative humidity conditions, for two years. Then, chemical composition was studied using XRD and TGA analysis. Finally, all these results were analyzed and interpreted, linking the evolution of the hemp mortar chemical composition and the mold growth.

### **III.2. GENERAL INFORMATION ON MOLDS**

In this section, the bibliographic study of general information on molds was presented. Different aspects of fungal species were reported, special attention was dedicated to the influence of molds on a human health.

#### **III.2.1. Molds strains in the world**

Fungi are eukaryotic, heterotrophic, generally aerobic, immobile, multicellular or unicellular organisms. Like plants and animals, their genetic constitution is confined in a nucleus. At the same

time, they possess a number of characteristics that make them a special group: walls containing cellulose and chitin, absence of chlorophyll (the main assimilating pigments of photosynthetic plants) and mobility. All these characteristics have led taxonomists to classify fungi in a distinct kingdom. The theoretical number of different species of fungi has been estimated at 1.5 million (Hawksworth, 2001). Among the fungi a distinction is made between “macromycetes” (the sporophores of which are visible with the naked eye and are (commonly called higher fungi)) and “micromycetes” (moulds and yeasts, mycobionts, mycoparasites). Moulds are thallophytic, sporogenic, non-chlorophyllous microorganisms, generally acidophilic (pH between 3 and 7) (Nicklin, J. et al., 2000) with the thallus of filamentous form septate (partitioned) or siphon (non-partitioned) and (Hyphomycetes and Zygomycetes) (Djossou Olga, 2011). Yeasts have unicellular thallus (*Candida sp.*, *Cryptococcus neoformans*). There are also dimorphic fungi that have filamentous thallus in the environment and thallus of yeast form in an organism (*Histoplasma capsulatum*). Thereafter, we will generally focus on micromycetes (molds and yeasts).

### **III.2.2. Mold classification and phylogeny**

Based on morphological analysis, fungi were divided into five orders. According to their modes of sexual reproduction, four of these orders were defined: Chytridiomycetes, Zygomycetes, Basidiomycetes and Ascomycetes. However, some molds, often or exclusively found in stages of asexual multiplication, have been grouped in the order Deuteromycetes, also called Adelomycetes or Fungi imperfecti. Building materials and surfaces inside or outside homes and buildings frequently represent growth conditions that favor only the asexual stage of molds. Thus, although this taxonomy is artificial, the criteria for classification of Deuteromycetes (based on the mode of production of asexual spores or conidia) are still used in practice as the basis for identification of indoor environmental contaminants.

With DNA sequencing, a multitude of new potential traits are available for classification of taxa. Gene sequencing involves determining the sequence of nitrogenous bases in genes (adenine, cytosine, guanine, thymine). For a given gene, the differences between species in these sequences represent distinctive characters: each successive position of the sequence is therefore a character. Sequences therefore provide a large quantity of characters, since each gene has several hundred, even thousands of positions. To be able to compare, it is necessary to find genes present in all taxa. Initially, to build the phylogenetic tree of Fungi, scientists used sequences of a single gene that encoded the subunit (18S) of ribosomal RNA, which allows the performance of basic cellular functions. The 18S data were insufficient to provide strong statistical support for many key branches in evolutionary trees (Bruns, 2006). That is why, (James et al., 2006) and (Hibbett et al.,

2007) provided a new classification of the kingdom Eumycota with their phylogenetic studies, based on the analysis of several genes (Figure 65).

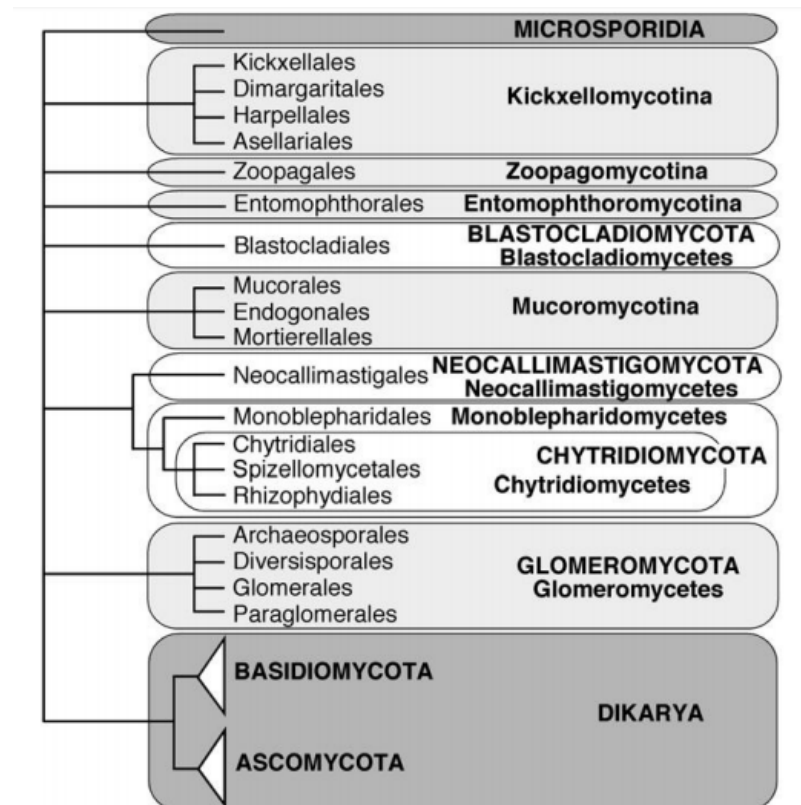


Figure 65. Phylogeny and classification of fungi based on the analysis of several genes (Hibbett et al., 2007)

The term Dikarya refers to the sub-division that includes the two most important phyla: Ascomycota and Basidiomycota. These are fungi whose life cycle stage is characterized by the presence of two nuclei within a cell. Most of the molds formerly belonging to the Deuteromycetes have been classified using molecular tools in the Ascomycota. This phylum includes more than 65,000 species, or 65% of the described fungal diversity (Méheust, 2012)

### III.2.3. Fungal reproduction

The nature of fungal reproduction is a challenge to understand because of the heterogeneity of their life style. Reproduction can be sexual or asexual, although some fungi alternate between the two types of reproduction depending on environmental conditions. As an example, the mold of the genus *Dictyostelium* performs a binary fission when conditions are favorable. But when these become unfavorable (desiccation, UV radiation, increase or decrease in temperature), the fungus proceeds to a sexual reproduction that leads to the formation of spores. Some fungi also exchange their genetic material by parasexual processes. The frequency and relative importance of this mode of reproduction is not clear and may be lower compared to sexual reproduction.

However, this mode of reproduction is necessary for the hybridization that is associated with the evolution of fungal species. It is important to know that fungi have neither male nor female, but different polarities (+ and -) (Bruns, 2006).

Asexual reproduction, as its name indicates, is done without fusion of reproductive cells. Most fungi use this mode of reproduction. Asexual reproduction can be done by budding (unequal division), binary fission (equal division), fragmentation, or by spore formation. To obtain sexual reproduction, it is necessary to have two haploid nuclei capable of fusion, or a single diploid nucleus. The fusion of two haploid nuclei results in a diploid nucleus which then undergoes meiosis. Meiosis is the origin of diversity within the fungal progeny and ends in the formation of spores (ascospores, basidiospores, zygospores), which varies according to the classes (Figure 66).

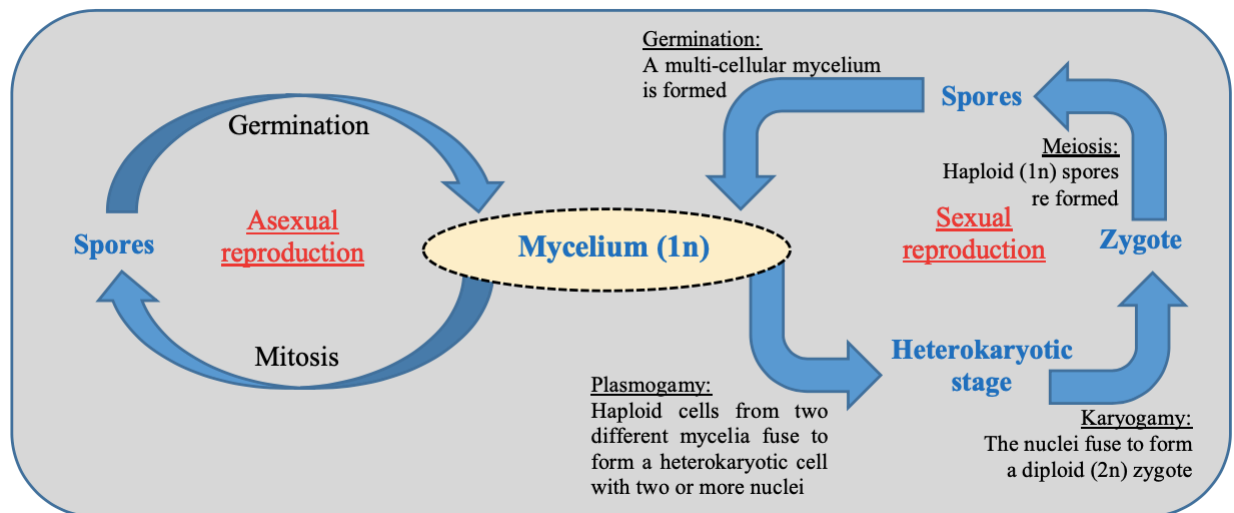


Figure 66. Diagram of fungal sexual and asexual reproduction

### III.2.4. Biological characteristics of molds

Molds are unable to synthesize their organic matter from atmospheric CO<sub>2</sub> because they do not have chlorophyll. They must therefore draw from the environment water, organic and mineral substances necessary for their own synthesis. This is how they degrade the complex organic matter of bio-based materials, through the excretion of enzymes and acids and then they absorb the digested components.

Molds produce, if the conditions are met, spores that can be transported anywhere. These spores are reproductive structures invisible to the naked eye that ensure the dissemination of molds, a key stage in their life cycle. The diameter of these resistance organs varies from 2 to 250 μm, with a majority between 2 and 20 μm (Méheust, 2012). The size, shape, and color of mold spores vary greatly between species. However, under microscopy, all spores of the same species are relatively consistent in color, size, and shape which is a taxonomic identifier.

### III.2.5. Conditions for mold growth

The phenomenon of mold growth has been a topic of research for many years and some work has been done to assess the risk of mold growth by calculating the mold growth index (M-index). Some research has also been done to apply mathematical mold growth models to construction simulations regarding climate change (Nik et al., 2012). According to this research the growth of molds on a given substrate, depends on the environmental conditions in which it is found, but also on the intrinsic properties of the substrate on which it grows. The development of molds depends on several parameters, such as biotic factors (viability of spores, the nature of fungal species, competition phenomena between fungi with other organisms), nutrients (sources of energy, nitrogen, mineral elements), physicochemical factors (pH level, presence of oxygen, light, temperature, humidity).

#### III.2.5.1. Physicochemical factors

##### *Temperature*

Temperature is one of the most important factors affecting the growth of microorganisms. Indeed, temperature plays a major role in mycelial growth, it is also involved in sporulation and spore germination (Bourgeois and Larpent, 1996). Each microorganism has an optimal temperature range for its development. Temperatures outside this range hinder its growth. According to their optimal temperature of growth, microorganisms into several groups whose names reflect the various areas of thermal tolerance. According to this classification we distinguish between thermoresistant, thermophilic, thermotolerant, mesophilic and psychrophilic molds.

Most molds are mesophilic. They multiply at temperatures ranging from 20 to 40 °C with with an optimum growth near that of the human body (37 °C) (Botton, 1990). Some species are thermotolerant or thermophilic and can grow at high temperature (above 50°C) with an optimal growth around 20 to 25°C, *Aspergillus fumigatus* is a good example (Bhabhra and Askew, 2005). Others are psychrophilic or psychrotolerant and grow at low temperatures (between -5 and 10°C) such as *Helicostylum pulchrum*, *Chrysosporium pannorum* and *Cladosporium herbarum*, these species can survive even at -60°C, they are found in cold stores (Botton, 1990). The list with all types of molds according to their temperature range is presented in Table 6.

Table 6. Fungi categories according to their development temperature range

Mold types	Temperature range	Optimal temperature
Thermophiles	20 à 50 °C	35 à 40 °C
Thermotolerant	0 à 50 °C	15 à 40 °C
Mesophilic	0 à 50 °C	15 à 30 °C
Psychrophiles	0 à 20 °C	0 à 17 °C

Apart from the four categories of Fungi listed in Table 6, there are molds that grow under extreme conditions. This is the case, for example, of the so-called thermoresistant fungi that can grow up to 80 °C, such as *Aspergillus fischeri* (Beuchat and Kuhn, 1997). Fungi with a wide range of growth temperatures have a competitive advantage over other organisms. This is particularly the case for *Aspergillus fumigatus* capable of growing at temperatures between 12 and 52 °C (Méheust, 2012).

### **Water activity**

In environments where biobased materials are used, nutrients are generally abundant and the temperature is also favorable. Thus, moisture is often the limiting parameter for spore germination and mold growth (Lähdesmäki et al., 2011). Water availability is necessary for fungi to sustain their physiological and metabolic activities (Méheust, 2012).

The materials are in equilibrium with the ambient relative humidity. Thus, fungal growth depends not only on the ambient relative humidity, but also on the water activity of the substrate  $a_w$ . The water activity measures the water availability of a given substrate (ISO 21807:2004). It is the ratio of the partial pressure of water of this substrate to the pressure of pure water at the same temperature according to the formula:

$$a_w = \frac{P_{H_2O \text{ substrate}}}{P_{H_2O \text{ pure}}} \quad (30)$$

Table 7. Moulds in building materials and their water activity (Li and Yang, 2004)

<b>Colonizer group</b>	<b><math>a_w</math> range</b>	<b>Classification</b>	<b>Examples de molds</b>
Primer (storage moulds)	< 0.80	<b>Xerophilic / Xerotolerant</b>	<i>Penicillium chrysogenum</i> ; <i>Aspergillus versicolor</i> : <i>A. fumigatus</i> , <i>A. niger</i> , <i>A. sydowii</i> , <i>A. ustus</i> , <i>Eurotium spp</i> , <i>P. brevicompactum</i> , <i>P. commune</i> , <i>P. corylophilum</i> , <i>P. palitans</i> , <i>Paecilomyces variotii</i> et <i>Wallemia sebi</i> .
Secondary	0.80– 0.90	<b>Mesophiles</b>	<i>Alternaria spp</i> , <i>Cladosporium spp</i> , <i>Epicoccum nigrum</i> , <i>Phoma spp</i> et <i>Ulocladium spp</i> .
Tertiary (water damage mold)	> 0.90	<b>Hydrophiles</b>	<i>Chaetomium globosum</i> , <i>Fusarium</i> , <i>Memnoniella echinata</i> , <i>Rhizopus stolonifer</i> , <i>Stachybotrys chartarum</i> , <i>Trichoderma spp</i> . ( <i>T. atroviride</i> , <i>T. citrinoviride</i> , <i>T. harzianum</i> et <i>T. longibrachiatum</i> )

The majority of molds grow at a water activity ( $a_w$ ) between 0.85 and 0.99 (Pitt and Hocking, 1977), with an absolute lower limit of 0.55 (Méheust, 2012). Fungi that grow at high moisture content are referred to as hygrophilic. This is the case, for example, of *Fusarium*. Other xerophilic fungi have the ability to grow at water activity below 0.85 (Pitt and Hocking, 1977). This is the case, for example, of certain fungal species: *Aspergillus penicillioides* or *Eurotium herbariorum*.



It has been shown that the latter two fungal species can grow from a water activity of 0.747 (Pitt and Hocking, 1977). Unfortunately, there is no in situ technique that can allow to determine the water activity of materials. The classification of molds in building materials according to their water activity  $a_w$  is presented in Table 7.

***pH level***

Every mold has a minimal, a maximal, and an optimal pH for growth. The vast majority of filamentous fungi grow in a pH range of 4.5 - 8.0 (Botton, 1990), although they are able to grow in a wide range of pH with a tendency to grow in slightly acidic environments. This is the case for *Fusarium culmorum*, *Trichoderma harzianum* and *Aspergillus oryzae* (Delgado-Jarana et al., 2002). However, extracellular enzymes produced in complex environments can have a very different pH optimum of activity (more acidic or more basic) (Botton, 1990). In addition, fungi are known to alter the pH of the environment by selective uptake and ion exchange, CO<sub>2</sub> or NH<sub>3</sub> production, or by acid production (Liaud et al., 2015, 2014).

***Presence of oxygen***

From a basic metabolic scheme whose center is glycolysis, the metabolism can be oriented, according to the organisms and, sometimes for the same cell according to the conditions of the environment, in an anaerobic metabolism (fermentations) or an aerobic metabolism (respiration) (Figure 67).

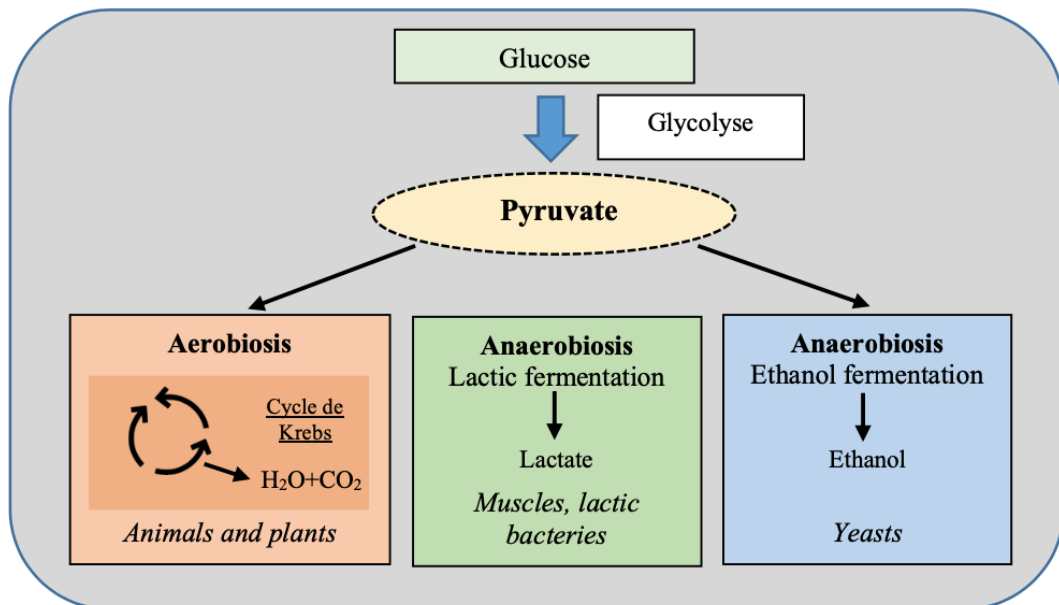


Figure 67. Metabolism scheme (aerobic and anaerobic)

Fungi are aerobic organisms for the vast majority. Therefore, the amount of oxygen available to the fungi is an important factor in their development. The most demanding live in the peripheral

regions of the substrates. But there are some yeasts that can be aero-anaerobic, participate in fermentative processes and, thus develop in depth as *Fusarium oxysporum* and *Aspergillus fumigatus*. Some can even withstand very strict anaerobiosis like *Neocallimastix* (Botton, 1990; Bourgeois and Larpent, 1996). Fungi can also exploit the oxygen dissolved in the substrate.

### ***Salts***

According to the reaction of molds towards salt concentration, 4 types of molds can be distinguished (Dassarma and Arora, 2002; Pitt and Hocking, 1977):

- Non-halophilic: do not tolerate more than 0.2 M of NaCl (>2%)
- Halotolerant: tolerate 0.2 to 0.85 M of NaCl (2-5%)
- Moderate halophiles: tolerate concentrations from 0.85 to 3.4 M of NaCl (5-20%)
- Extreme halophiles: grow in the range of 3.4 to 5.1 M of NaCl (20-30%)

Halophiles are defined as microorganisms that require the presence of salt (NaCl) in the environment for their growth (Dassarma and Arora, 2002). Indeed, salt has the ability to attract water and retain it. Therefore, in the presence of salt, microorganisms are deprived of water and can no longer grow. Most molds can withstand very high levels of salt and sugar. For example, *Debaromyces hansenii* is a halotolerant yeast, isolated from seawater, which can grow aerobically up to salinities of 4.5 mol.L<sup>-1</sup> NaCl. It produces glycerol as the compatible solution during the log phase growth and arabitol in the stationary phase. Another example - *Cladosporium glycolicum* (saprophytic hyphomycete) which can grow on submerged wood panels at salinity exceeding 4.5 mol.L<sup>-1</sup> NaCl in the Great Salt Lake. Other halophilic fungi, e.g., *Polypaecilum pisce* and *Basipetospora halophila* have also been isolated from salt fish (Dassarma and Arora, 2002).

### **III.2.5.2. Nutritive conditions**

The development of fungi on a given substrate, depends on the specificities of fungi such as the ability to produce metabolites (enzymes, pigments, toxin synthesis). But also, it depends on the composition of the substrate (Johansson et al., 2013). Indeed, the presence of atoms necessary for fungi, such as carbon or nitrogen promotes the growth of fungi. On the contrary, a very complex matrix with the presence of growth inhibitors, does not promote the growth of fungi.

Most molds are not very demanding in terms of nutrients necessary for their growth. Indeed, their enzymatic content allows them to use organic materials found in particular in bio-based materials. Some fungi, such as species of the genus *Aspergillus* and *Penicillium*, prefer sugars, they transform plant cellulose into simple sugars. These sugars allow them to grow very quickly. Others are able to degrade polymers (such as cellulose and lignin) or complex organic materials. Biobased materials are substrates easily degradable by molds, because of being materials that easily retain water. In addition, the presence of cellulosic products that make biobased materials,

excellent supports for the growth of molds. In addition, some authors made the link between the presence of soluble sugars in wood and surface quality: there are more sugars when the surface is rough than when it is sawn. That was also proven by (Lähdesmäki et al., 2011).

#### ***Source of carbon and energy***

Carbon is one of the most abundant elements in molds. The simplest of the compounds is carbon dioxide (CO<sub>2</sub>). This can be used by the mold for the synthesis of certain essential metabolites that would involve a carboxylation reaction. Virtually all organic compounds can be used as a source of carbon and energy by molds. Most molds can metabolize glucose and sucrose with some polysaccharides such as starch and cellulose (Nicklin, J. et al., 2000). Some molds produce extracellular lipases capable of hydrolyzing lipids into glycerol and fatty acid that can be assimilated by many fungal species, while some species use organic acids and ethanol (Tabuc, 2007).

#### ***Source of nitrogen and other mineral elements***

Molds need nitrogenous substances to synthesize their proteins. Most molds assimilate ammonia in the form of salts (NH<sup>4+</sup>) whose presence suppresses the use of other nitrogenous sources (nitrate, amino acids, proteins). Ammonia is transformed into glutamic acid, glutamine or other amino acids by transamination, while only some species use nitrate, others can only grow in the presence of organic nitrogen and no mold can fix atmospheric nitrogen.

The growth and reproduction of many fungal species require the use of mineral and metal ions in the culture medium, such as sulfate, magnesium, potassium, sodium and phosphorus with more or less different concentrations depending on the species (Uchikoba et al., 2001). Traces of elements such as iron, copper, manganese, zinc and molybdenum, are necessary for most molds for the production of cytochromes, pigments, organic acids, etc.

### **III.2.6. Interactions of molds with the environment**

Molds are heterotrophic and must therefore draw water, nutrients and minerals necessary for the synthesis of their own material from the environment. They absorb them through the wall of their vegetative apparatus. They are referred to be absorbotrophic. All molds are saprophytes developing on and to the detriment of inert materials very varied (paper, wood, food). Some can be "opportunistic", although naturally saprophytic, they can in some cases behave as parasites, develop on living organisms of animals or plants whose defenses are weakened, kill them and finally move to a saprophytic development.

### III.2.7. Ability of mold to degrade a material

As it was already mentioned in the previous sections, molds during their growth use certain metabolites (enzymes, pigments, synthesis of toxins) to receive nutrients from the environment. Among these metabolites we can distinguish organic acids for their extreme capacity to degrade different materials. Indeed, the natural fungal production of organic acids plays many key roles in nature depending on the type of fungi that produces them. These roles are either due to the decrease in pH as a result of their secretion or due to the direct interaction of the organic acid with the environment (Dutton and Evans, 2011; Jones, 1998). The decrease in pH level may give the competitive advantage to acid-tolerant molds, may enhance mineral alteration by solubilizing soil minerals thereby releasing nutrient ions for uptake (such as Ectomycorrhizae) (Plassard and Fransson, 2009) or may lead to acid-catalyzed hydrolysis of holocellulose (Green and Highley, 1997; Shimada et al., 1997; Tanaka et al., 1994). Regarding their direct interaction with the environment, organic acids participate in metal detoxification through metal complexation and oxalic acid plays a major role in biomass degradation (Jones, 1998). The ability to produce oxalic acid of certain types of molds has been extensively studied (Hastrup et al., 2012). (Guggiari et al., 2011) investigated the issue of biodegradation of different biobased materials by molds.

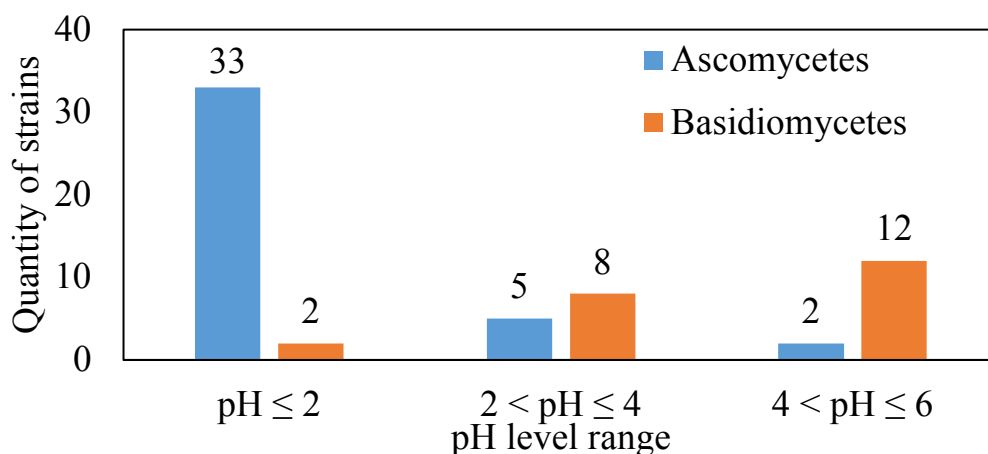


Figure 68. Distribution of Ascomycetes and Basidiomycetes strains according to the final pH of the growth medium after 6 days of incubation (Liaud et al., 2014)

The ability to produce acids and a type of acids depends on a type of mold. In general, all strains of Ascomycetes are able to grow in a medium with an initial pH of 5.5. All 33 strains of Ascomycetes (including all 22 strains of *Aspergillus*) studied by (Liaud et al., 2014) acidified the medium below pH 2. The 5 strains of other Ascomycetes acidified the medium to the range of 2 to 4 and just 2 strains did not or slightly acidify its media. Regarding Basidiomycetes, the work of Liaud et al. showed that there are four strains : (*Ischoderma benzoinum*, *Grifola frondosa*, *Panellus*

*serotinus* and *Polyporus squamosus*) that did not proliferate on a medium with pH 5.5 and made no influence (Liaud et al., 2014). Two strains strongly acidified the medium below pH 2, 8 strains of Basidiomycetes acidified the medium up to the range of 2 to 4 and 12 types of molds did not or slightly acidified the medium (Figure 68).

### **III.2.8. Effects of moulds on human health**

Air quality is very important for people's health and work productivity. Poor air quality in offices and schools can cause fatigue, unpleasant odor, irritations, respiratory symptoms and other short and long-term health problems (Lappalainen et al., 2015). One of the factors causing poor air quality is mold growth. Currently, the issue of adverse pathological effects due to fungal exposure is well studied. Exposure to molds in indoor environments is through inhalation or skin contact and ingestion (Mazur et al., 2006). As a result, immunological effects can occur due to allergic reactions, following exposure to allergenic proteins that activate or aggravate allergies. Some genera of fungi such as, *Cladosporium*, *Alternaria*, *Penicillium*, *Aspergillus*, would be frequently associated with allergies (Eduard, 2009; Nayak et al., 2018; Portnoy and Jara, 2015) and would aggravate rhinitis and asthma. Indeed, thanks to hydrophobic proteins (or hydrophobins) spores are able to disperse in the air (Bayry et al., 2012). Fungal components are likely to cause health effects in an exposed individual because of their size and characteristics. Fungal spore or hyphal fragments larger than 1  $\mu\text{m}$  can be deposited in the human airways (Górny, 2004), and those smaller than 1  $\mu\text{m}$  can reach the pulmonary alveoli (Eduard, 2009). Several clinical effects can be caused by volatile particles (irritations, intoxications, infections). This can be caused by the physical presence of the particles in the airways but also depends on the constituents of the volatile particles or because of elaborated substances (e.g. allergens, mVOCs, mycotoxins, glucans).

#### **III.2.8.1. Allergens**

Many studies show that molds can cause allergic reactions in humans (Green et al., 2006, 2003; Kurup et al., 2002). (Kurup, 2003) identified the production of immunoglobulin E (IgE) following allergic reactions. (Husman, 1996) demonstrated the presence of proteins, polysaccharides and lipopolysaccharides in spores. The question of the influence not only of spores but also of fungal fragments was studied by (Green et al., 2006) who showed that they are also an important source of aeroallergens. At the same time, (Green et al., 2003) highlighted the difference between the number of allergens released before and after germination.

### **III.2.8.2. Volatile Organic Compound (VOC)**

Molds produce microbial Volatile Organic Compounds (mVOCs) during their metabolism. (Pasanen et al., 1998) has shown that molds can cause exposure to mVOCs. From the musty smell of certain mVOCs one can predict the growth of molds (Schleibinger et al., 2008). Among the mVOCs, we can distinguish alcohols, aldehydes, esters, terpenes, etc. Symptoms of eye, nose and throat irritation have often been reported in the presence of strong odors produced by abundant mold growth. The synergistic and irritative effect of a mixture of compounds has been demonstrated in mice (Korpi et al., 1999). At the same time, the complexity of the indoor environment makes it difficult to isolate the specific role of fungal mVOCs in disease development, as many building materials also emit VOCs (Reboux et al., 2011).

### **III.2.8.3. Mycotoxins**

Mycotoxins are secondary metabolites of relatively low molecular weight, elaborated by various molds under certain environmental conditions. Their biosynthesis is dependent on several factors, including temperature, light intensity, carbon dioxide in the air, available nutrients and the presence of other competing species (Hendry and Cole, 1993). Each mycotoxin is not necessarily specific to a given mold (Li and Yang, 2004).

Many of these toxins are relatively stable and their toxicity can persist for a long time, even when the fungal elements are no longer viable. Mycotoxins are found in the mycelium and spores and can also diffuse into the substrate (Bloom et al., 2009). The size of the particles containing them (e.g. spores or mycelial fragments) or on which they are adsorbed (e.g. dust), will determine the depth of penetration of the toxic substances into the bronchial tree. Experimentally, deleterious effects have been proven in animals: immunosuppressive, mutagenic, teratogenic, carcinogenic, neurotoxic and hepatotoxic effects (Li and Yang, 2004). However, there is currently no evidence that mycotoxin levels in building air are high enough to cause adverse health effects.

Fungal growth is therefore a source of significant amounts of spores, cell fragments, allergens, mycotoxins, glucans and volatile organic compounds in indoor air. The agents responsible for adverse health effects have not been conclusively identified, but high levels of any of these agents in the indoor environment are a potential health risk.

### **III.2.8.4. Glucans**

Glucans, or  $\beta$ -1,3-glucans, are glucose polymers present in the cell wall of most molds, which may be associated with chitin or mannan molecules. They are non-allergenic compounds also found in some bacteria and plants (Bex and Squinazi, 2006). These complex sugars can, in some cases, have immunogenic effects and stimulate the function of macrophages and neutrophils.

They could be involved in inflammatory processes by triggering the production of specific type G immunoglobulins (IgG) (Douwes, 2005). Glucans would also be part of the complex mixture linked to the appearance of the toxic syndrome associated with exposure to organic dust (ODTS, organic dust toxic syndrome).

### **III.3. BIBLIOGRAPHIC STUDY OF THE MOLDS' IMPACT ON THE HEMP MORTAR**

Different authors have suggested the influence of mold growth on the physical and mechanical properties, as well as the microstructural integrity of building materials (Kazemian et al., 2019). Concerning hemp mortar, different characteristics such as microstructure, functional properties and thus durability are affected by microbiological growth (Zhu et al., 2016).

(Crawford et al., 2017) confirmed the decrease of its mechanical properties of hemp mortars due to fungal presence. Although different microorganisms are involved in microbial proliferation, a mold growth is the most critical criterion when assessing the degradation of biobased materials (Du et al., 2021; Kosiachevskiy et al., 2018).

First, it was suggested that mold growth affects negatively the air quality (Kosiachevskiy et al., 2018), as certain fungal strains produce toxins that are able to provoke different diseases such as asthma or cancer (Du et al., 2021).

Also, molds are known for their ability to degrade lignocellulosic biomass and produce different metabolites to get more minerals from environment (Zhu et al., 2016). Among these metabolites we can distinguish organic acids for their extreme capacity to degrade different materials, as detailed in section III.2.7 above. Indeed, the natural fungal production of organic acids plays many key roles in nature depending on the type of fungi that produces them. These roles are either due to the decrease in pH as a result of their secretion or due to the direct interaction of the organic acid with the environment (Jones, 1998; Dutton and Evans, 2011). The decrease in pH level may give the competitive advantage to acid-tolerant molds, may enhance mineral weathering by solubilizing soil minerals thereby releasing nutrient ions for uptake (such as Ectomycorrhizae) (Plassard and Fransson, 2009) or may lead to acid-catalyzed hydrolysis of holocellulose (Green and Highley, 1997; Shimada et al., 1997). Regarding their direct interaction with the environment, organic acids participate in metal detoxification through metal complexation while oxalic acid plays a major role in biomass degradation (Jones, 1998). The ability to produce oxalic acid of certain types of molds has been extensively studied. For example, in the case of saprophytic fungi, the decrease of pH level provokes an acid-catalyzed hydrolysis of holocellulose (Hastrup et al., 2012).

Most researchers are not interested in the influence of fungal growth on the chemical composition of hemp mortars. In fact, molds are able to modify the composition of the support that allow them to grow better. In order to better understand the behavior and the durability of hemp mortar towards the fungal growth, it is necessary to investigate the influence of the molds on its crystallographic composition. That is why, the main objectives of this chapter are first, to identify the depth of natural mold proliferation in hemp mortar after two years of its implementation and conditioning at laboratory in high humidity conditions. Then, to investigate the influence of the fungal growth on the crystallographic composition of the material. To attend these objectives, different experimental procedures were conducted for both benchmarks of samples: contaminated and non-contaminated with molds.

### **III.4. EXPERIMENTAL PROTOCOL**

In this section, the studied material, its conditioning and the experimental characterization methods are presented. Different methods of characterization of hemp mortar was conducted on both benchmarks: the first, exposed to laboratory conditions and the second, exposed to high humidity conditions. That allowed to compare the obtained results and study the influence of fungal growth on hemp mortar.

#### **III.4.1. Materials and conditioning**

One formulation of hemp mortar was used in this study. Hemp shives of French origin were used to make the hemp mortar samples. The granulometric curve of the used hemp particles is presented in the Section II. The binder represents a commercial mixture developed by ParexGroup SA. It is composed of Portland cement, hydrated lime and various additions to achieve the rheology suitable for spray application. The proportions of the hemp mortar mixture used are shown in Table 8. Chemical composition of mineral binder is present in Table 9. The mixing was done in two steps: first, the hemp shives were premixed with water for 1 minute at 140 rpm, secondly, the binder was added and mixed for 5 minutes at 140 rpm. The sample size adopted was  $4 \times 4 \times 16 \text{ cm}^3$ . After manual production (casting in the moulds), the samples of both benchmarks were dried for 28 days under laboratory conditions ( $23 \pm 2 \text{ }^\circ\text{C}$ ,  $50 \pm 5\% \text{ RH}$ ), as presented in Figure 69. Then, the samples from the first benchmark were placed in high humidity conditions ( $23 \pm 2 \text{ }^\circ\text{C}$ ,  $97 \pm 2\% \text{ RH}$ ) created by saturated salt solution for two years to facilitate mold growth (Figure 70). Mold growth is due to natural fungal contamination of hemp particles and mortar fabrication, no additional inoculation was used. The second benchmark's samples were kept under laboratory conditions as a reference for further comparison.



Table 8. Mass ratios of hemp mortar composition

Component	Hemp shives	Mineral binder	Water
Percent by mass (wt%)	12.5 %	25 %	62.5 %

Table 9. Oxide analysis of used lime-based binder with hydraulic additions

Oxide	CaO	Al <sub>2</sub> O <sub>3</sub>	Na <sub>2</sub> O	K <sub>2</sub> O	Fe <sub>2</sub> O <sub>3</sub>	SiO <sub>2</sub>	MgO	SO <sub>3</sub>
Percent by mass	57,40	2,20	0,15	0,27	0,92	25,40	0,50	3,09

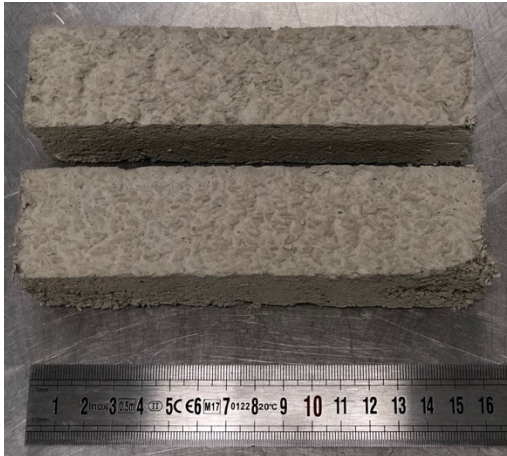


Figure 69. Hemp mortar samples before aging

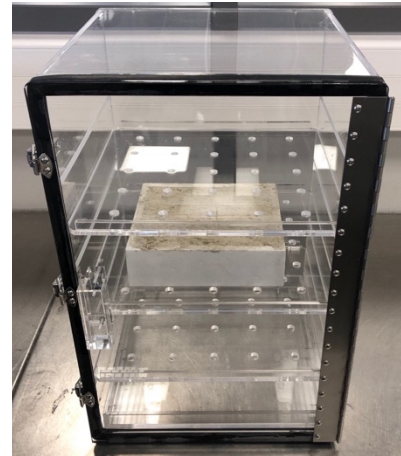


Figure 70. High humidity desiccator weathering ( $23 \pm 2$  °C,  $97 \pm 2\%$  RH) of hemp mortar samples

### III.4.2. Methods of characterization

#### III.4.2.1. Mold growth observation

First, the depth of fungal proliferation in hemp mortar and its influence on the mineralogical composition of the material were investigated. After two years of exposure two samples of size  $4 \times 4 \times 16$  cm<sup>3</sup> (conditioned at laboratory and high humidity conditions) were scanned using an attenuated total reflectance-Fourier-transform infrared spectroscopy (ATR-FTIR). It allowed to obtain information on the surface chemistry and confirm the presence of molds in the case of the sample conditioned at high humidity. It was performed with a PerkinElmer Spectrum Two spectrometer. For each sample, 4 measurements were accumulated with a resolution of 4 cm<sup>-1</sup>. The test was conducted by studding vibratory frequencies in the middle Infrared (4000-400 cm<sup>-1</sup>).

Then, scanning electron microscope (W-SEM) analysis using a Hitachi S-3400N device was conducted to evaluate the depth of the mold proliferation. Observations were conducted on the same specimens that were used for ATR-FTIR analysis. The special attention was devoted to the surface of the hemp mortar and the interface zone between cementitious matrix and hemp particles of two samples at different depth. Micrographs are recorded using secondary electrons detectors

at an acceleration voltage of 15 kV, in high vacuum mode (pressure <1 Pa). Before observations, the specimens were covered with carbon in order to improve the image quality.

### **III.4.2.2. Chemical characterization**

Then, the X-Ray Diffraction (XRD) was conducted for the samples of both benchmarks at two different areas (on the surface and interior part). Prior to XRD crystallography analysis, hemp mortar samples of the size 4x4x16 cm<sup>3</sup> were grinded and sieved to remove organic fibers. This step allowed to decrease the influence of the dilution on the final result as in this case we analyze only mineral matrix. Free water was removed using the acetone. Then, the specimens were dried at 40 °C in order not to modify the composition of the sample. XRD crystallography patterns were obtained using Cu K $\alpha$  anode tube ( $\lambda= 1.54182 \text{ \AA}$ ) radiation at 40 kV and 20 mA with a Bruker D8 diffractometer, that was presented above in Section II (Bruker, Karlsruhe, Germany). The diffractometer scanned from 5° to 60° (2 $\theta$ ) in step size of 0.015° and the counting time per step was 1.2 s.

The X-ray diffraction tests were accompanied by the measurements of pH at different position of the samples: the surface and interior parts. This step allowed to analyze the interconnection between the mold growth, pH level and mineralogical composition. For this test the specimens of the same composition, made with the same raw materials, of the size 16x4x4 cm<sup>3</sup> were used. For each value, three measures were performed at different positions on the specimen using the electrode WTW Sentix Sur. As the pH level measurements are possible just in solution, the constant volume of demineralized water (0.2 ml) was deposited on the studied surfaces. For the inner pH level measures the protocol is the same, but the measurements were conducted in the middle of the specimen.

Finally, the thermogravimetric analysis (TGA) test was conducted. The sample preparations were the same as described for XRD analysis. It allowed to quantify the material mass loss function of the temperature. Each mass variation reflects different phenomenon due to the effect of the temperature. The measurements were performed using the Perkin-Elmer TGA 8000 thermal analysis system. The test was conducted under a controlled helium atmosphere in a temperature range of 30-1000 °C with a heating rate of 10 °C/min.

## **III.5. MOLD GROWTH OBSERVATION**

First of all, in the case of specimen exposed to high humidity conditions, the mold growth was not visible to the naked eye during the first year of exposure. The validation of the presence of molds on the surface of hemp mortar samples was conducted by ATR-FTIR scanning. Figure 71 shows ATR-FTIR spectra for samples conditioned at high humidity and at laboratory

environment (23 °C, 50% RH). For both conditions, we note the intense peaks at around 3260 cm<sup>-1</sup> that are assigned to the stretching vibration of hydroxyl and -NH groups and at around 2920 cm<sup>-1</sup> - attributed to CH<sub>2</sub> methylene group stretching vibrations. Also, the vibration peak at 1750 cm<sup>-1</sup> is attributed to the C=O stretching and the peak at 1620 cm<sup>-1</sup> represents N-H vibrations. All these peaks are present only in the case of sample conditioned at high humidity and can be explained by the fungal contamination of its surface (Bayramoglu and Arica, 2018). Also, we note the intense peaks at 1400 and 870 cm<sup>-1</sup> that are attributed to the deposit of calcium carbonate. In order to verify if molds are able to grow inside the hemp mortar the SEM analysis was conducted at different depth of the sample.

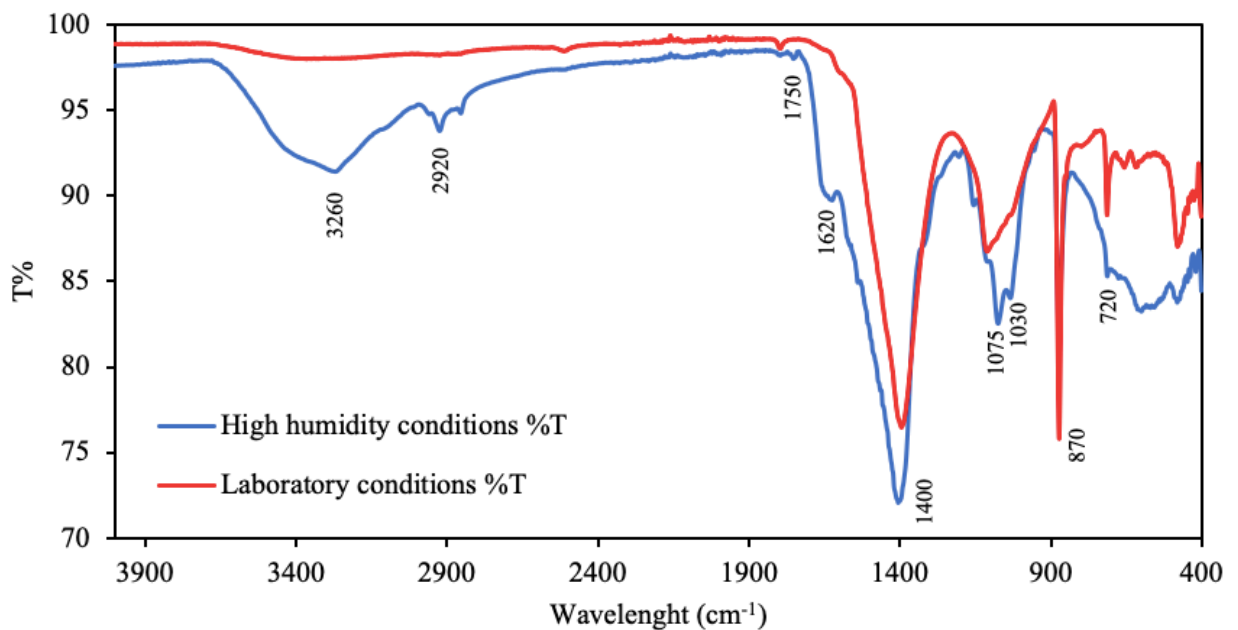


Figure 71. ATR-FTIR spectra obtained from hemp mortar samples conditioned during two years at high humidity and laboratory conditions

Then, W-SEM observations of the mold-contaminated hemp mortar sample were performed at different depths. This allowed to study the ability of molds to grow inside the hemp mortar. Figure 72 shows the results of the W-SEM observations at different depths: at the surface, at 1 mm, at 2 mm and at 4 mm depth. The presence of mold filaments on the hemp mortar surface was noted (Figure 72-a). They are flattened that allows better adhesion to the surface. Figure 72-b shows the presence of filaments at a depth of 1 mm in the hemp mortar sample. Indeed, mold growth occurs in the internal porosity of the sample. Molds were also noted at 2 and 4 mm depth. The presence of mold at a greater depth was not seen that is why the W-SEM images are not represented. The results of the W-SEM observations show the fungal ability to grow inside hemp mortars using their internal porosity.

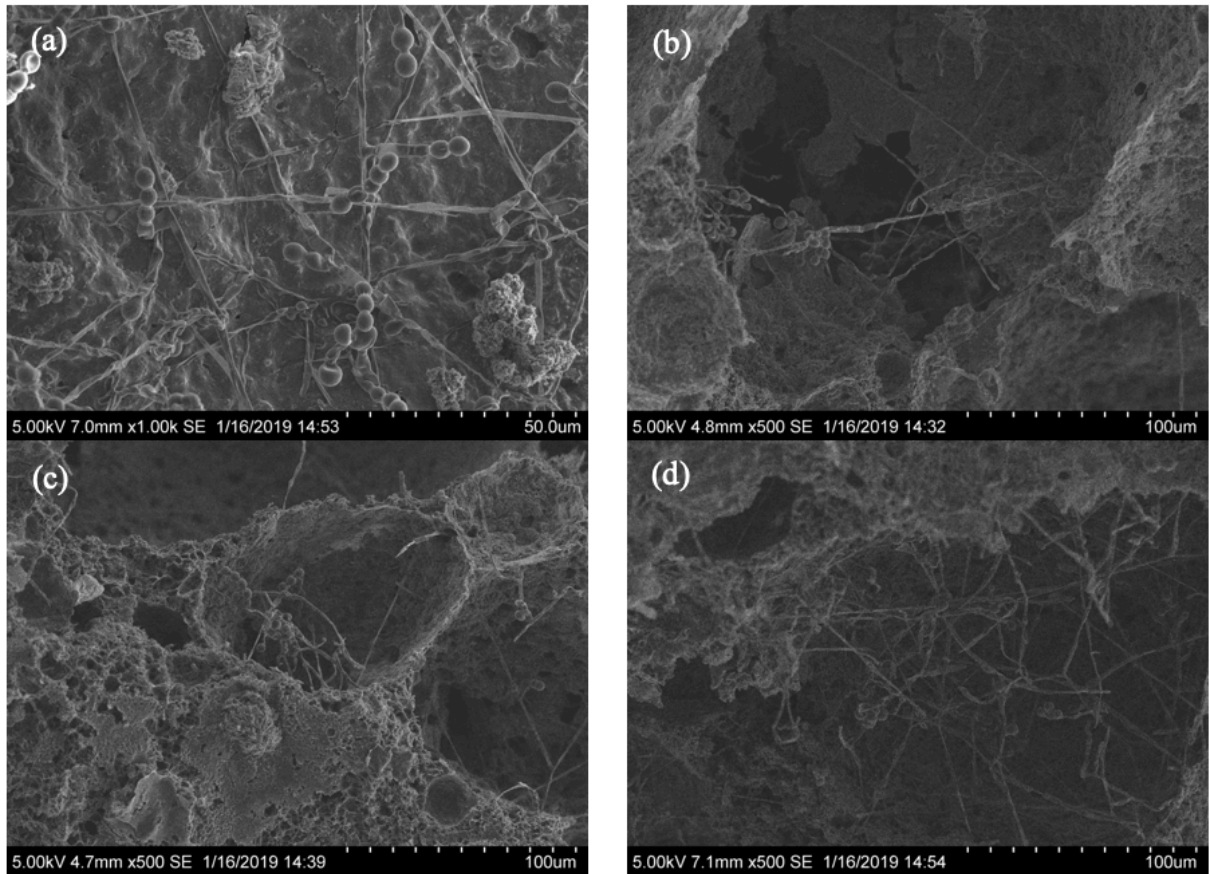


Figure 72. W-SEM observations of mould growth on the hemp mortar sample conditioned in a high humidity environment for two years at different depths: at the surface (a); at 1 mm (b); at 2 mm (c); and at 4 mm from the surface (d)

### III.6. CHEMICAL CHARACTERIZATION

In order to study the influence of molds on the mineral composition of hemp mortar, X-ray diffraction crystallography (XRD) was used. It was carried out on two samples conditioned for two years under high humidity (23 °C and 97% RH) and reference conditions (23 °C and 50% RH) respectively. For each sample, the crystallographic analysis of the surface and the interior part of the samples was carried out. This allowed a better comparison of the obtained results.

The XRD patterns for interior part (a) and surface part (b) of the hemp mortar reference sample; interior part (c) and surface part (d) of the hemp mortar sample conditioned at high relative humidity are presented in Figure 73. Results demonstrate that the main mineralogical compounds of both hemp mortars are  $\text{Ca}_6\text{Al}_2(\text{SO}_4)_3(\text{OH})_{12} \cdot 26\text{H}_2\text{O}$  (ettringite),  $\text{Ca}(\text{OH})_2$  (portlandite),  $\text{CaCO}_3$  (calcite),  $\text{SiO}_2$  (quartz),  $\text{Ca}_3\text{SiO}_5$  (tricalcium silicate) and  $\text{Ca}_2\text{SiO}_4$  (dicalcium silicate).

Figure 73, curves (a) and (b) represent, respectively, the crystallographic analysis of the interior part and surface part, of the hemp mortar specimen conditioned for two years at 23 °C and 50% RH (reference sample). The XRD spectrum of the interior part of the sample reveals the presence of ettringite and portlandite and low signal of calcite (Figure 73-a). On contrary at the

surface we note the great presence of calcite and low signals of portlandite and ettringite (Figure 73-b). It is explained by the carbonation of the mineral binder that occurs at 50% RH.

The XRD patterns of the sample conditioned at high humidity environment in the interior of the sample and at the surface (Figures 73-c and 73-d respectively) demonstrate the same pattern. The main difference is that the middle part of the sample conditioned at reference environment (Figure 73-a) represents lower signal of ettringite and calcite. Also, there are signals of non-hydrated  $\text{Ca}_3\text{SiO}_5$  (tricalcium silicate) and  $\text{Ca}_2\text{SiO}_4$  (dicalcium silicate), which means that hydration is not completed. Indeed, the hydration of the sample at 97% RH continues because of high relative humidity, and the hydration of the sample conditioned at 50% RH was not full due to drying and the lack of water.

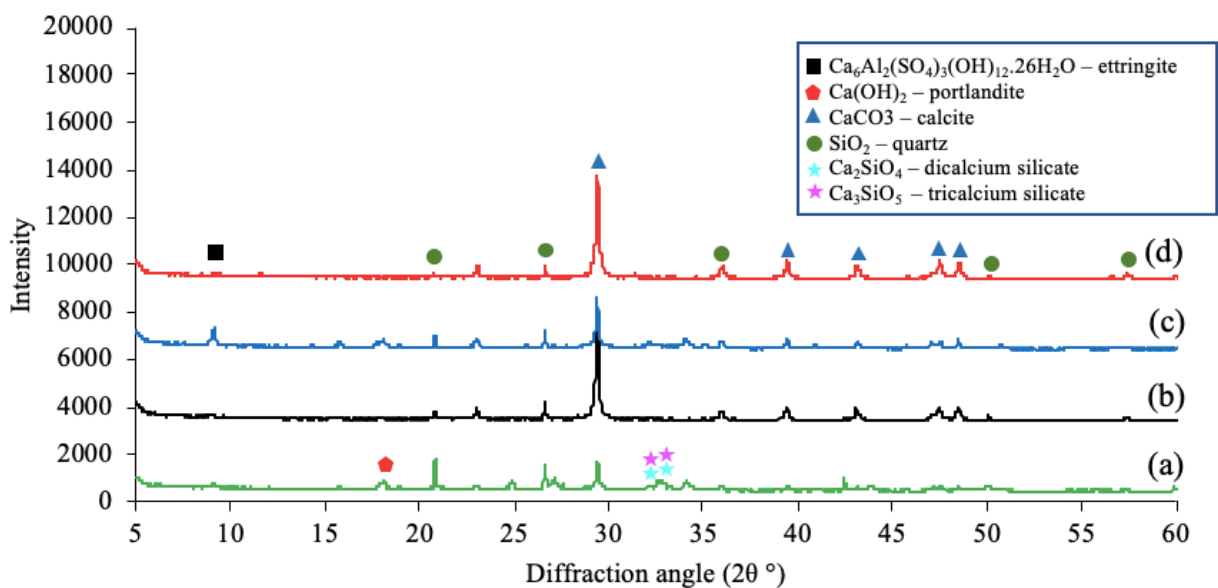


Figure 73. X-ray diffraction patterns of: interior part (a) and surface part (b) of the hemp mortar reference sample (23 °C and 50% RH); interior part (c) and surface part (d) of the hemp mortar sample conditioned at high humidity environment (23 °C and 97% RH)

The X-ray diffraction analysis was accompanied by the pH level measurements. The results represented in Figure 74 show that the interior part of the both samples represent higher pH level – 12.03 and 10.5 for the reference sample and the one conditioned at high humidity, respectively. At the same time, pH levels at the surface are lower – 8.24 and 8.53 respectively. It is consistent with the results of XRD analysis as the interior parts represent the portlandite signal. In fact, the diffusion of the air carbon dioxide in the hemp concrete provokes its reaction with the portlandite and decrease the pH level. Later, that leads to the degradation of the ettringite, as it is very sensible to the ambient pH level. Also, we note that the portlandite signal is higher for the interior part of the reference samples. Indeed, the carbonation occurs between 50% and 70% RH. Nevertheless, the high humidity allows the better dissolution of carbon dioxide in the material that can lead to such difference between pH levels of interior parts of the material.

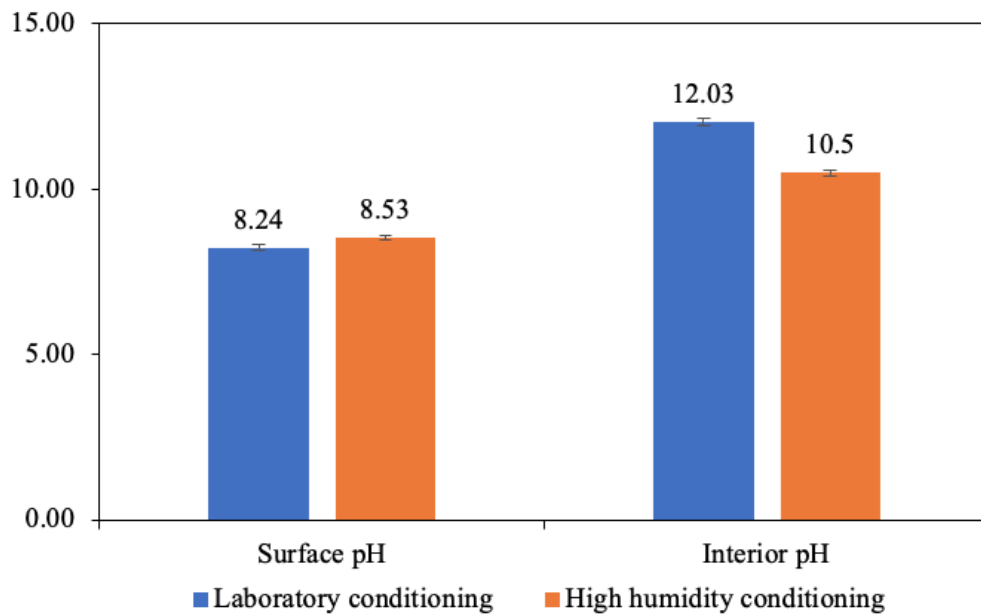


Figure 74. Diagram of pH level evolution on the surface and in the middle of the samples conditioned for two years at the laboratory and high humidity conditions

The TG/DTG curves show that samples of both types of conditioning represent four different thermal decomposition regions (Figure 75). The first thermal decomposition present in all samples occurs between 30 °C and 200 °C. This mass loss is caused by the evaporation of free water. These peaks of the interior of two samples are higher than those of the surface due to the drying of the material. At the same time, we note that the sample under high humidity conditions has a higher mass loss due to higher water content and its total hydration (see XRD results in Figure 73). The second decomposition phenomenon occurs between 250 °C and 350 °C. This mass loss is provoked by the departure of water bound to hydrates of CSH. The third mass loss is due to the thermal decomposition of  $\text{Ca}(\text{OH})_2$ . The last one is caused by the decarbonation of  $\text{CaCO}_3$  that occurs at the temperature range from 700 °C to 850 °C. Here, we note that the quantity of calcium carbonate is higher at the surface that is accordance with the XRD and pH level analysis.

Chemical characterization results show that after two years of exposure to different conditions, both conditioned samples represent a carbonation of the mineral binder on the surface. Nevertheless, the results show the presence of portlandite and ettringite inside both samples. Thus, we conclude that despite the ability of molds to grow inside the hemp mortar, it has little effect on the chemical composition of the material after two years of exposure.

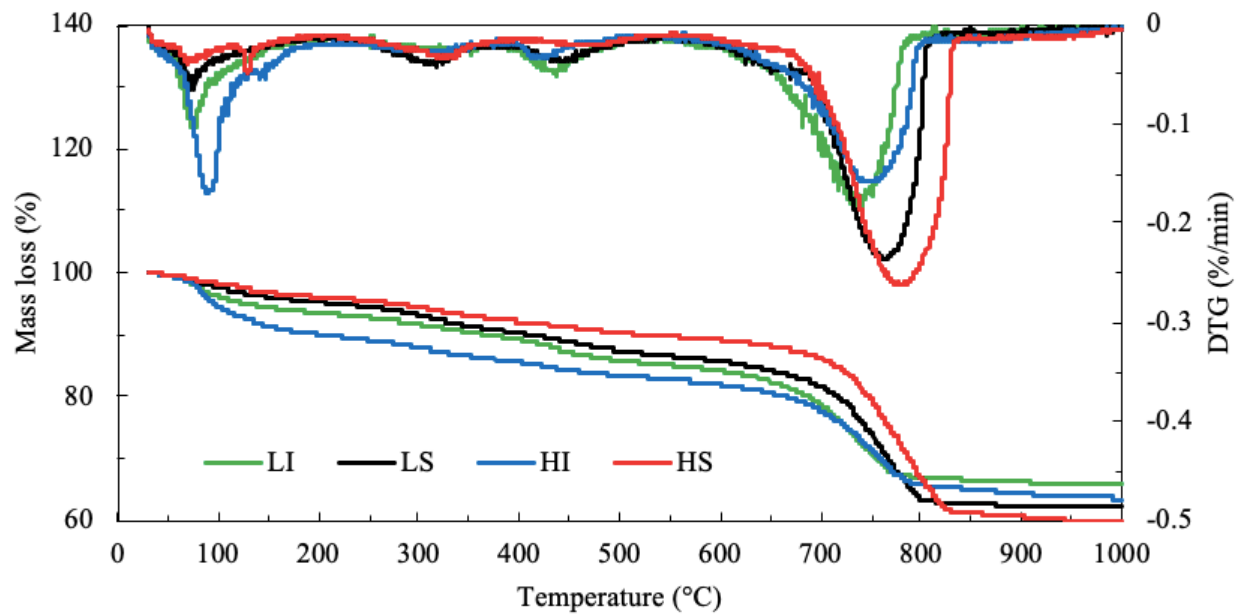


Figure 75. TG and DTG analysis performed in samples of two types of conditioning after 2 years: LI – interior part of laboratory conditioned sample, LS – surface part of laboratory conditioned sample, HI – interior part of the sample conditioned at high humidity, HS – surface part of the sample conditioned at high humidity

### III.7. CONCLUSION

In this chapter, the influence of mold proliferation on the hemp mortar and its durability was investigated. Also, the ability of molds to grow inside the hemp mortars was investigated. In order to provoke the mold growth, hemp mortar sample was exposed for two years to high humidity conditions. Another sample exposed to laboratory conditions was used as a reference. The ATR-FTIR analysis and W-SEM observations were used to study the mold growth on the surface and inside the hemp mortar sample. The XRD scanning allowed to investigate the difference of hemp mortar samples' chemical composition at different part. It was accompanied by the pH level measurements and thermogravimetric analysis.

Results revealed the ability of molds to grow inside the hemp mortar. Indeed, it was noted that molds occupy the inner porosity that is high in the case of studied material. The chemical composition analysis demonstrated the carbonation of the hemp mortar surface and thus the pH level decrease. At the same time, the interior part of the sample covered with molds represents the hydrates (ettringite and portlandite) that are responsible for mechanical properties and the durability. That is why despite the ability of molds to grow inside the hemp mortar, it has little effect on the chemical composition of the material after two years of exposure. This study provides future researchers with the sufficient refine information on the mold growth inside the hemp mortars and their influence on the chemical composition. Obtained results must be considered when studying the durability of hemp concrete under the accelerated aging protocol.

This chapter highlighted the influence of the mold growth on the evolution of the crystallographic composition of the hemp mortar. The results reveal the low effect of the fungal proliferation on the mineral composition of the hemp mortar. Therefore, the following chapter is devoted to the identification of the mold types.



CHAPTER IV.

FUNGAL RISK ANALYSIS IN HEMP MORTARS:  
IDENTIFICATION OF FUNGAL SPECIES

---

## **CHAPTER IV. FUNGAL RISK ANALYSIS IN HEMP MORTARS: IDENTIFICATION OF FUNGAL SPECIES**

---

### **IV.1. INTRODUCTION**

There are many types of fungi species that have different influence on the environment and growing conditions. In addition, due to the production of different volatile particles, spores and other allergens, molds are critical from the point of view of the air quality. The distinction between mold species is not considered when talking about contaminated materials in civil engineering.

That is why in this chapter, the analysis of fungal risk on hemp mortar was investigated and deals with the identification of mold types. To do so, a bibliographical study was carried out, which summarizes the different methods of the identification of mold species. Then, the phenotypic method of identification was used to investigate the fungal species present in hemp shives and hemp mortar. Two formulations were tested and compared. Finally, the conclusion on the proposed experimental method was made.

### **IV.2. PREDICTION AND QUANTIFICATION OF MOLD GROWTH**

In buildings, the real environmental conditions represent favorable parameters for mold growth. A temperature that is comfortable for humans is at the same time comfortable for the growth of most molds. In this case, one characteristic that can promote or limit the proliferation is humidity. According to the survey on the housing quality in France, about 20% of French inhabitants respectively mentioned that they have traces of moisture (Insee, 2017). This shows that the issue of mold contamination in buildings is a current one for the general public.

Several studies have been conducted for numerical prediction and quantification of mold growth on bio-based materials such as (Ojanen et al., 2010; Viitanen et al., 2010). Mold growth in these works is described by the index (M). The classification according to this index is presented in a Table 10.

The model of mold growth (for pine and spruce) is given in the following equation:

$$\frac{dM}{dt} = \frac{1}{7 \cdot \exp(-0.68 \ln T - 13.9 \ln RH + 0.14W - 0.33SQ + 66.02)} k_1 k_2 \quad (31)$$

Where T – temperature;

RH – relative humidity;

W – type de wood (0 – pine; 1 – spruce);

SQ – for the quality of the surface (0 – for sheared surfaces, 1 – oven-dried)

$$k_1 = \begin{cases} 1, & \text{when } M \leq 1 \\ \frac{2}{\frac{t_{M=3}}{t_{M=1}} - 1}, & \text{when } M > 1 \end{cases}$$

$$k_2 = \max[1 - \exp[2.3 \cdot (M - M_{max})], 0]$$

Table 10. Classification of mold growth index

Index value	Principle of classification
0	No growth
1	A few hyphae detectable in a few places, only with the microscope
2	Several hyphal colonies > 10% only visible with the microscope
3	Some spots (mycelium) cover less than 10% of the surface perceptible to the naked eye, less than 50% perceptible with the microscope
4	Some spots (mycelium) cover about 10-50% of the surface perceptible to the naked eye, more than 50% perceptible under the microscope
5	Mycelium covers more than 50% of the surface, detectable with the naked eye
6	Very high growth, mycelium coverage is nearly 100%

Where, the maximum index (M) is determined according to the following conditions:

$$M_{\max} = A + B \frac{RH_{\text{crit}} - RH}{RH_{\text{crit}} - 100} - C \left( \frac{RH_{\text{crit}} - RH}{RH_{\text{crit}} - 100} \right)^2 \quad (32)$$

$$\left\{ \begin{array}{l} \text{With } RH_{\text{crit}} = -0.00267 T^3 + 0.160 T^2 - 3.13 T + 100.0 \quad \text{si } T < 20^\circ \text{ C} \\ RH_{\text{crit}} = 80 \% \quad \text{si } T > 20^\circ \text{ C} \quad (\text{Hukka and Viitanen, 1999}) \end{array} \right.$$

And A, B, C, coefficients representing the sensitivity class of materials (Ojanen et al., 2010; Viitanen et al., 2010) are represented in Table 11.

Table 11. Values of the coefficients representing the material sensitivity class (Ojanen et al., 2010; Viitanen et al., 2010)

Sensitivity class	A	B	C
Very sensitive (pine sapwood)	1	7	2
Sensitive (spruce)	0.3	6	1
Resistant (concrete, glass wool)	0	5	1.5

Regarding the mold growth conditions, (Nik et al., 2012) found that when the temperature is below 0.1 °C or the relative humidity is below 75%, the conditions are unfavorable for mold growth. According to several studies (Lähdesmäki et al., 2011; Nik et al., 2012), at high relative humidity (97-98%), mold growth is observed in all materials, only the intensity changes from one material to another. At high humidity and low temperature (5°C), mold growth was somewhat slower and limited. However, at constant low relative humidity (89-90% RH / 20-22°C) mold growth was very limited with a growth index (0-1) except for pine sapwood. A decline in mold growth was examined by cold and dry conditions. Frost seemed to retard growth on several materials when it lasted for a long time. The impact of freezing also depended on the material. A dry period reduced the mold index in most cases (Lähdesmäki et al., 2011).

### **IV.3. IDENTIFICATION OF FUNGAL SPECIES**

#### **IV.3.1. Identification methods of molds strains**

It is important to identify the mold strains in order to know the health risks and to consider preventive methods to their development. One can distinguish several methods of identification of molds:

- Phenotypic methods
  - ✓ Microscopic observation
  - ✓ Mass spectrometry (Matrix Assisted Laser Desorption Ionization - Time of Flight (MALDI-TOF))
- Molecular methods
  - ✓ Comparative sequencing of genes encoding ribosomal RNA
  - ✓ Real time amplification (Reverse Transcription - Polymerase Chain Reaction (RT-PCR))

All the methods have certain number of disadvantages and advantages. In the next paragraphs these methods are briefly presented.

#### **IV.3.2. Phenotypic methods**

The most classical method - is the microscopic one. It consists in observing molds isolated from the surface under the microscope. This method is simple and inexpensive in reagents and materials (culture medium, incubator, adhesive tape, slide, dye, microscope). The identification is fast, it is not rare to identify directly with a single sample of the contaminated surface. Some criteria are still used as references for the description of the genera of the species. We can distinguish macroscopic and microscopic criterias.

### ***Macroscopic criteria***

Macroscopic criteria are based on the observation of colonies and their color, shape (round, star-shaped...), transparency (opaque, translucent), size (small or large), relief (flat, wrinkled...) and surface characteristics (fluffy, powdery, granular).

- The speed of colony development on Sabouraud's medium supplemented with antibiotics: as a rule, yeasts grow and sporulate in 24 to 48 hours; filamentous fungi, in 4 to 6 days.
- Optimal growth temperature: common contaminating fungi grow naturally at laboratory temperature, 20° to 27°C, and have difficulty with temperatures above 30-32°C. Growth at 37°C indicates an adaptation to the temperature of the human body and is therefore strongly in favor of the acquired pathogenicity of the fungus in question.
- Sensitivity to cycloheximide (Actidione). This antiseptic strongly inhibits the growth of contaminants. In certain cases (very high inoculum for example), this growth is however possible although very disturbed.
- The morphology of the rectum:
  - ✓ color, knowing that it evolves with the age of the colonies;
  - ✓ aspect: flat, raised or flat culture, wrinkled, cratered or hairless, plastery, powdery, granular, fluffy, flaky.
- Back morphology:
  - ✓ color;
  - ✓ existence of ridges or arborizations in the depth of the agar;
  - ✓ pigment diffusing in the medium.

### ***Microscopic criteria***

Microscopic criteria are based on the morphological aspect of the different structures of the fungi: the shape of the spores, the type of thallus (septate or not), the origin of the spores (endogenous or exogenous), the color of the hyphae (dark or light) and the shape of the heads (brush-like, aspergillate). Successively, next parts of molds must be observed:

- the thallus
  - ✓ thallus and shape of molds:
    - type of budding: axial or lateral, single or multiple, narrow or broad based,
    - existence or not of pseudomycelium, true mycelium,
    - possible presence of capsule.
  - ✓ filamentous thallus:
    - diameters of filaments, regular (upper fungi), wider and irregular (siphons of lower fungi);

- frequency of partitions: rare in lower fungi;
- pigmentation of the walls: dark (dematiaceous) or light (moniliaceous);
- ramifications and their mode: banal or dichotomous;
- particular formations: sclerotia, etc.
- the vegetative spore apparatus
  - ✓ mode of spore formation:
    - internal spores formed in sporangia (zygomycetes) or external spores (blastospores or thallospores) of higher fungi;
    - differentiation or not of conidiophores, branched or not, swollen or not, ornamented or not, with or without phialides;
    - spores isolated, in clusters, or in chains, at the end or along the filaments.
  - ✓ character of spores:
    - color;
    - size;
    - shape: oval, more or less elongated or round, with a wide (aleuria) or narrow (blastospores) base;
    - septa;
    - thickness and ornamentation of the walls (echinulations).
- the sexual apparatus (very rarely observed): perithecia (cleistothecia), asci and ascospores or particular formations (nut cells)

At the same time, this method has its disadvantages. Fungi often do not form vegetative multiplication structures on isolation media, for which only filaments are observable. It is then only possible to orientate towards higher and lower fungi. Nevertheless, macroscopic documentation of the cultures (shape, color, development) is a precious complement to establish possible correlations in time. Unfortunately, molds are polymorphic and polychromatic depending on the environmental conditions, which can complicate the process.

### **IV.3.3. Mass spectrometry method**

Another promising technique that has re-emerged in recent years, is mass spectrometry Matrix Assisted Laser Desorption Ionization - Time of Flight (MALDI-TOF). This technique allows to establish mass spectra in a defined range from a culture or a spore suspension and to compare them with a database of spectra of reference strains of different species. The algorithms for processing the spectra have progressed dramatically in last years. The results published recently are very interesting, with remarkable performances, but underline the low representativeness of the databases which cover only a few tens to a few hundreds of species, sometimes not very

representative of different environments and sometimes for a number of strains not very indicative. Indeed, it is necessary to use a large number of spectra of different strains of the same species in order to take into account the intra-species variability, so as to obtain a weak and robust identification result. Therefore, the creation, development and verification of databases is a complex and time-consuming process.

#### **IV.3.4. Molecular methods**

For more than 15 years, molecular methods have taken a prominent place in the taxonomy of fungal species in general and filamentous fungi in particular. The demonstration of ribosomal RNA coding gene sequences (18S, 28S variable region V3 D1:D2) for phylogenetic studies contributed to refine the distinction of taxonomic groups and species in fungi. The inter-gene non-transcribed regions of these genes (ITS1 and ITS2) have also proven useful for taxa distinction. These two types of markers rRNA28S or ITS1/ITS2 (unilocus analysis) allow a very good identification of genera, from nucleic acids extracted from any mycelium, after amplification with universal primers in lower and higher fungi, and comparison to reference sequences. The reference sequence databases are extremely rich since each new species description generates the sequence data of the various markers. Nevertheless, not all 28S rRNA or ITS1/ITS2 sequences are known simultaneously for all fungal species (about 10-20% are missing for each of the two types of markers). The 28S D1:D2 region is the reference for distinguishing many species of ascomycetes or basidiomycetes fungi. The combined ITS1-ITS2 intergenic regions, have been proposed as a "barcode of life" for animal species, plants, and fungi (Schoch et al., 2012). There is no consensus on a universal marker (unilocus). Indeed, many limitations have been documented for the identification of fungal species, with some different species showing 100% homologies for one or both markers. Thus, in genera important to the pharmaceutical industries, such as *Aspergillus*, *Penicillium*, *Cladosporium*, *Alternaria*, etc., accurate distinction of common species is not possible with 28S rRNA or ITS1/ITS2 sequences alone or combined. Combining the two ITS regions (ITS1/ITS2) has proven to be more efficient than using either one separately (ITS1 or ITS2). In all these cases, it is necessary to use other markers, to accurately differentiate species within genera (Schoch et al., 2012). These other markers consist of "housekeeping genes" on which the selection pressure is different, and which have therefore accumulated more mutations for species that have diverged more recently during evolution. The selected housekeeping genes vary according to the fungal groups and genera or even species, we can cite the genes coding for the elongation factor EF1a, actin, calmodulin, betatubulin, the different sub-units of RNA polymerases, etc. This "multilocus" approach, based on the simultaneous comparison of several marker sequences, allows

to overcome the limitations of unilocus approaches. Thus, the ability to distinguish species accurately is improved in many cases.

These molecular methods of identification by comparative sequencing remain expensive, because of the heavy investments and the reactive costs (multilocus > unilocus). However, they are faster than classical methods and can be applied to all fungi, even those that do not sporulate. They still require a good knowledge of mycology and in particular of fungal taxonomy, especially to manage the names of teleomorphs/anamorphs, two different names can correspond to the same species. Finally, with the development of real-time molecular amplification methods (PCR-RT), specific direct detection-identification tests are available for some particularly important species.

## **IV.4. EXPERIMENTAL PROTOCOL**

### **IV.4.1. Materials formulation and conditioning**

In this section hemp shive and hemp mortar fungal contamination was studied separately. It allowed to analyse the interconnection of the hemp shives and hemp mortar contaminations. To do so, the fungal contamination of 4 types of Hemp Shives (HS) from France was analysed. The apparent density of all the types of hemp shives was about 100-110 kg/m<sup>3</sup>. The question of repeatability has been the subject of particular attention. That's why, different samples from the same formulation, origin, conservation conditions and treatment were tested. Granulometric curves of 4 types of hemp shives are represented in Figure 76.

As for hemp shives, two different formulations were studied. The first formulation (F-1) was made according to the professional rules of execution of hemp concrete (SEBTP, 2012). The used binder is based on the lime, called Batichanvre, produced by French lime producers St. Astier. This binder is a mixture of: natural lime from Saint-Astier (Hydraulic lime: NHL and aerial one: CL), cement CEM I 52.5, and different adjuvants to improve the rheology and permeability of hemp concretes. Its density is of 500 kg/m<sup>3</sup>.

The second formulation of hemp mortar represents a commercial mix designed by ParexGroup SA. The mix proportion ratios of the used hemp mortar are represented in Table 12. The mixing was done in two stages: firstly, hemp shives were premixed with water during 1 minute at 140 rpm, secondly, the binder was added and it was mixed during 5 minutes at 140 rpm. After their manual manufacture, the specimens were dried for 28 days at laboratory conditions (23 ± 2°C, 50 ± 5%RH).



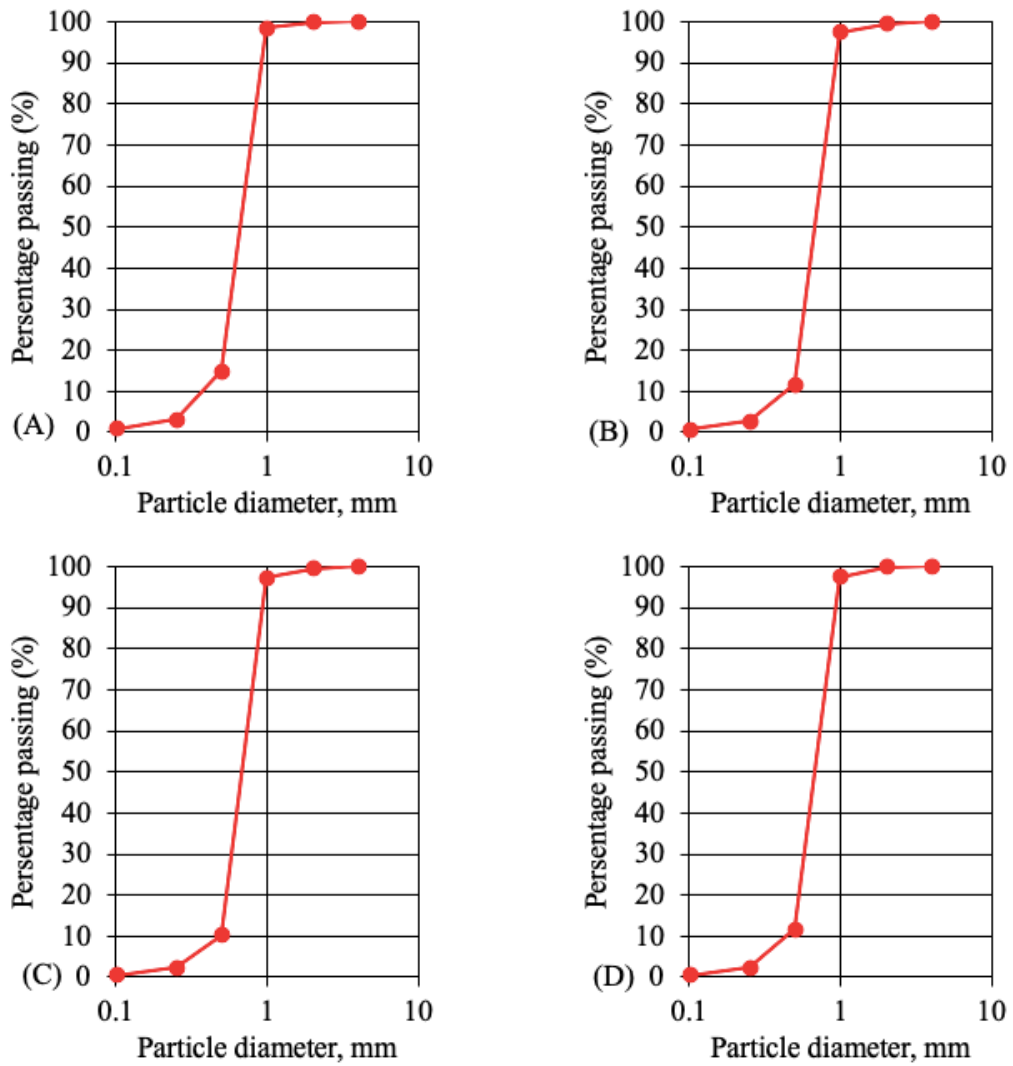


Figure 76. Granulometric curves of four hemp shives types: (A) HS-1, (B) HS-2, (C) HS-3, (D) HS-4

Table 12. Formulations of the studied hemp mortar

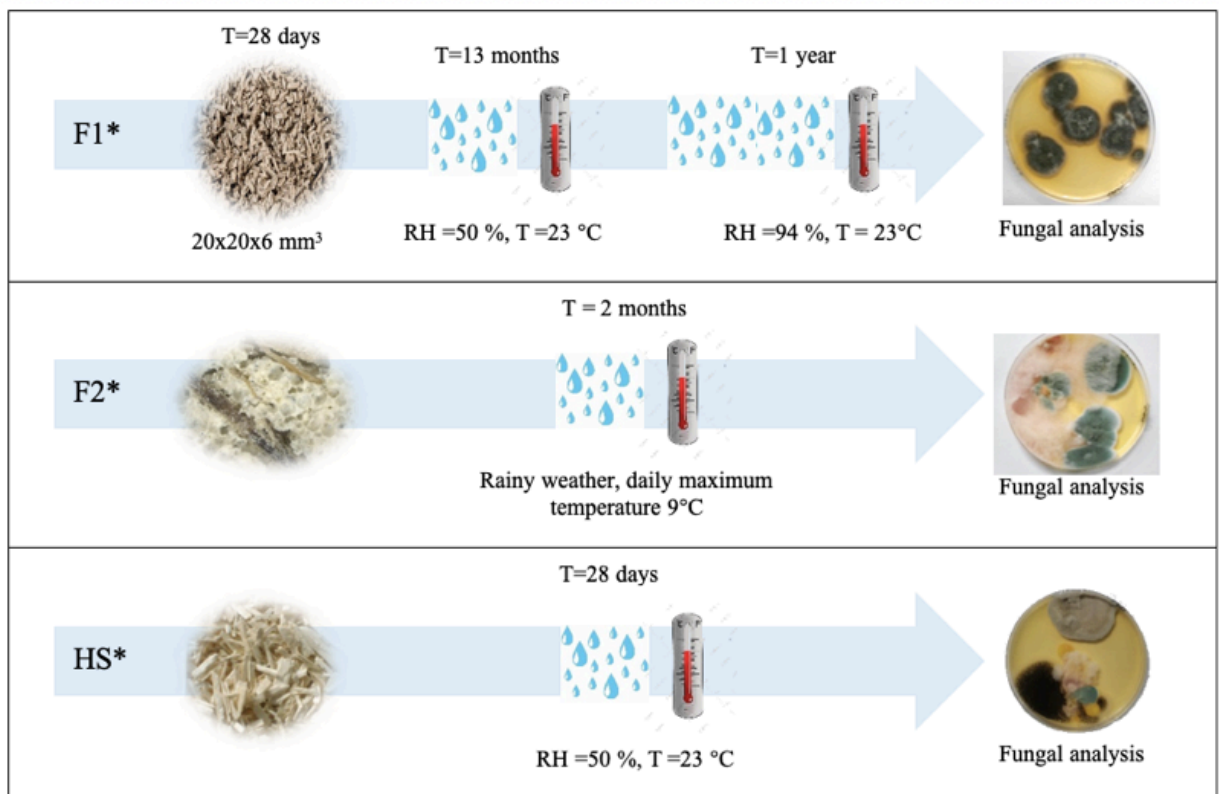
Material	F1	F2
Hemp shiv (kg)	10 kg	10 kg
Binder (kg)	25 kg	20 kg
Water (kg)	35 kg	50 kg
Water / binder (-)	1.4	2.5
Binder / hemp shiv (-)	2.5	2

#### IV.4.2. Conditioning

Hemp shives of all 4 types (HS-1, HS-2, HS-3, HS-4) were conditioned at laboratory conditions ( $23 \pm 2^\circ\text{C}$ ,  $50 \pm 5\%RH$ ) during one month before all experimental manipulations. As for hemp mortar samples, two different conditionings were applied. Indeed, specimens of the first formulation (F1) of dimensions of  $20 \times 20 \times 6 \text{ mm}^3$  have been produced on 31 January 2016. They were conditioned at  $23^\circ\text{C}$  and 50% of relative humidity to provoke the carbonatation of the binder

to decrease the pH level and favour the fungal development. After that, in March 2017 the specimen was put in a desiccator at 94% of relative humidity and 23°C which is a sufficient condition to provoke the mold growth. The mold proliferation was firstly visible to the naked eye one month after the conditioning at high humidity conditions and observed one year later.

As for second formulation (F2), it was naturally contaminated one month after its in situ application in November 2017. The in-situ application was represented by the thermal insulation of a house in the region of Pau. Samples were taken from the most contaminated areas observed in January 2018. We noticed that the first fungal proliferation was observed in December following a single month of exposure to extreme conditions. Indeed, it was applied inside an unheated building and exposed to high humidity, low temperature (about 9°C during the day) and no ventilation, conditions that do not correspond to the standard ones in which hemp mortar must be used. The schema of conditioning is represented in Figure 77.



- \*HS: Hemp Shivs
- \*F1: Hemp Mortar, Formulation 1
- \*F2: Hemp Mortar, Formulation 2

Figure 77. Conditioning schema of the hemp shives and hemp mortar samples

#### **IV.4.3. Cultivation conditions**

After the imposed conditioning period for the two hemp mortars formulations and the different hemp types, the fungi were visible to the naked eye. This allowed to apply the Phenotypic methods for the identification process of the species present in these contaminated samples. This method requires a preliminary culture of the fungal strains to grow. For this reason, Sabouraud's medium, which is adapted to the growth of molds which is a medium for the isolation of fungi (molds and yeasts), was used. It is also used in some environmental studies, it is known for its acceleration of the fungal growth but favors in a little more the growth of certain species and makes the enumerations difficult from the fifth day. Petri dishes with Sabouraud's medium (or Sabouraud's agar) were used. In fact, there are several culture media for the same family of fungi. Some genera have specific nutrient requirements (cellulotic, osmophilic) or specific incubation conditions. Thanks to the conditions (pH of 5.6, with added antibiotics) created by the traditional Sabouraud agar inhibits bacterial growth. The composition is as follows: peptone (10g), glucose (20g), agar-agar (15g), distilled water (1000ml), vitamins and growth factors.

#### **IV.4.4. Fungal identification procedure**

The fungal identification experimental protocol consists in sowing contaminated particles in Petri dishes on Sabouraud medium to let the present molds grow. The electrical burner (Figure 78) was used in order to protect against bacteria and to avoid possible fungal contamination from outside. The idea of using this device is to create a circuit of hot air that purifies our working area.

Before each manipulation, all tools were sterilized by heating on the burner to avoid the inter-contamination of samples. Under sterilized environment we put contaminated particles of hemp mortars and hemp shivs in Petri dishes. The manipulation is presented in Figure 79. Particles can be put in the middle or on the sides of the dish. In the first case it gives the best visibility, in the second one we can put more particles. We put particles of 4 different types of hemp in 4 different Petri dishes and 2 types of hemp mortars in 2 Petri dishes separately. To ensure the obtained results we studied the question of repeatability by seeding hemp mortar particles twice for each type of studied materials (hemp shivs and hemp mortars).

After seeding, the particles in Petri dishes were packed with parafilm and put in closed desiccator to avoid external contamination by air flow. The temperature of 25°C and relative humidity of 50% was controlled.

The identification of mold species was done at the 8<sup>th</sup> day by the Tape method which consists of the application on the surface of the culture of scotch tape and its examination between a slide and a cover glass, sandwiched between 2 drops of dyes (Figure 80) (Harris, 2000). The identification was done with the Keyence digital microscope which allows to have a magnification

from x100 to x1000. The interface and the morphology of the mold structures have been also studied for both hemp mortar formulations using the Hitachi S3400 Scanning Electronical Microscope. The acceleration voltage of 10 kV, the pressure of 50 Pa for the sample of the first formulation and of 70 Pa for the sample of the second one has been chosen for all the observations.



Figure 78. Electric burner



Figure 79. Isolation of molds

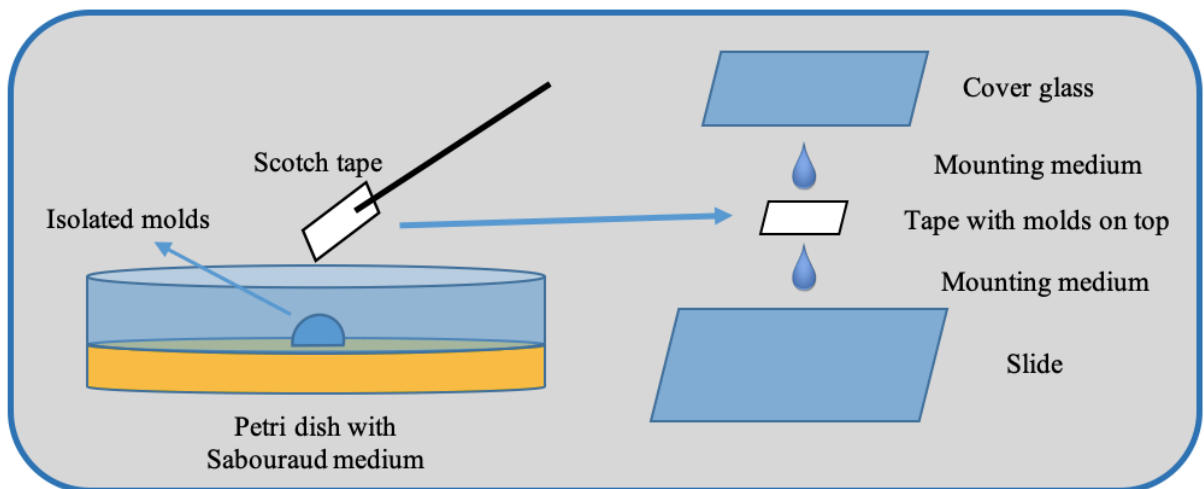


Figure 80. Representation of the scotch tape method for fungal identification

#### IV.5. HEMP SHIVE FUNGAL CONTAMINATION ANALYSIS

In the first part, mold strains of 4 types of hemp shives were identified. The monitoring of the growth was done visually. Figure 81 represents the growth of molds in Petri dishes at initial state and after 5 days.

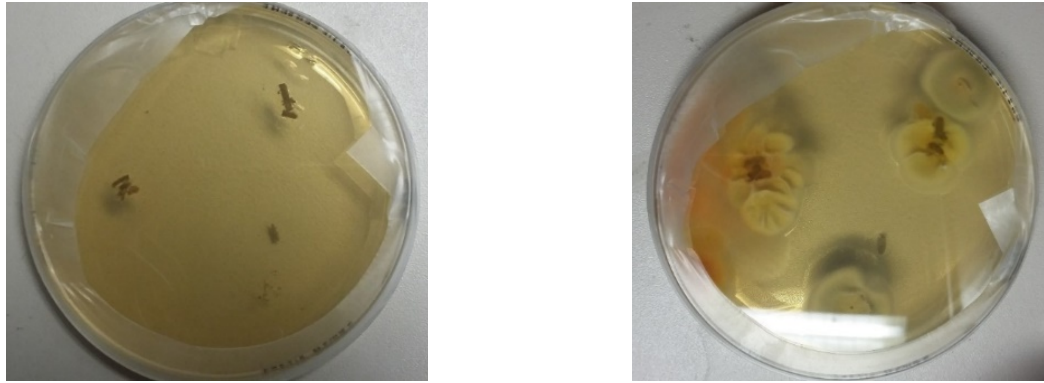


Figure 81. Monitoring of mold growth in a Petri dish (left - first day, right - after 5 days)

After 8 days of conditioning at 23°C, Petri dishes with different types of hemp shives visually showed different amounts of fungal strains (Figure 82). Using the scotch tape method described above, molds from each Petri dish were examined. Subsequently each type of hemp with its types of molds will be presented separately.

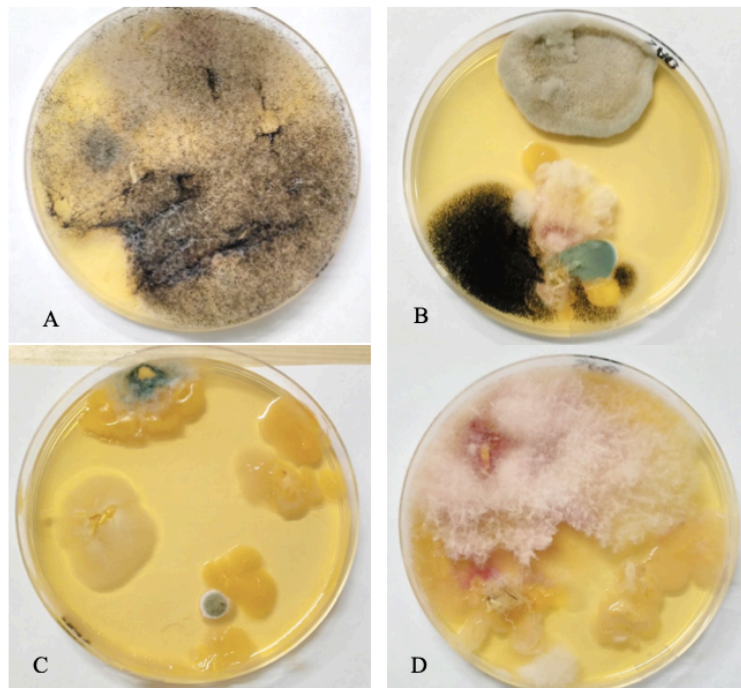


Figure 82. Images of Petri dishes with the shives of 4 hemp types after 8 days of cultivation: HS-1 (a), HS-2 (b), HS-3 (c), HS-4 (d)

First hemp type HS-1 represents 3 different types of species in the Petri dish (Fig. 82a): two species represented by two not too large yellow and grey spots on the agar and one raised species which filled the whole volume of the dish. Subsequently, the white voluminous mold was observed under a Keyence microscope. It was identified as *Rhizopus* sp. Yellow and gray mold thallus did not represent any morphological structures from which the determination was possible.

Second hemp type HS-2 visually represents 4 different types of species in Petri dishes (black, grey, yellow and white) (Fig. 82b). The black colored mold was identified as *Aspergillus niger*. The thallus of other molds did not represent morphological structures from which the determination was possible.

As for HS-3 and HS-4, they represent 3 species of molds (Fig. 82c and 82d). Just in the case of the white fungi in HS-4, it was identified as *Rhizopus sp.* Concerning others, no representative morphological structures were found. All the results are reported in Table 13.

Table 13. Results of hemp shive mold identification

Sample number	Species quantity	Identified species
HS-1	3: white, yellow and grey	White - <i>Rhizopus sp.</i> , N/D*
HS-2	4: white, yellow, grey and black	Black - <i>Aspergillus niger</i> , N/D*
HS-3	3: white, yellow, red	N/D*
HS-4	3: white, yellow, red	White - <i>Rhizopus sp.</i> , N/D*

\*N/D – non-identified species

## IV.6. HEMP MORTAR FUNGAL CONTAMINATION ANALYSIS

### IV.6.1. Morphology analysis and interface observation

After conditioning, hemp mortars were contaminated, so an analysis of their morphology and molds interface observation was conducted. Hemp mortars were observed with different magnifications. First, the numerical microscope images were used to analyse hemp mortars before and after mold growth. In figure 83, the hemp mortar of F2 formulation before and after fungal growth are proposed. Microscopical observations showed that both materials are heterogeneous, porous and represent a big quantity of microcracks (Fig. 83a) in the interface between hemp shives (1) and the cementitious part (2). Also, these images give us a better understanding of the procedure of the contamination and the mold growth. In figure 83b the mold proliferation on the surface of the contaminated sample (1) can be seen.

After the analysis of the numerical microscope observation, the results of the SEM observations were analyzed. Fig. 84 (a and b) represents the SEM images of fungal growth of the first formulation (F1) hemp mortar. Mold structures such as the filamentous thallus (1) and vesicles (2) are visible in Fig. 84a. Figure 84b shows that the cementitious part (1) covers and protects the hemp shiv (2). The mold thallus (3) is also visible. The images of the SEM observation of the contaminated sample of the second formulation F2 are presented in Fig. 85 (a and b). Analogically to the first case, we can see the mold structures with a huge number of the vesicles (Fig. 85a). Also, the mold thallus (1) is visible on the surface of the cementitious matrix (2) of our sample (Fig. 85b). Then we proceeded with the mold species identification.

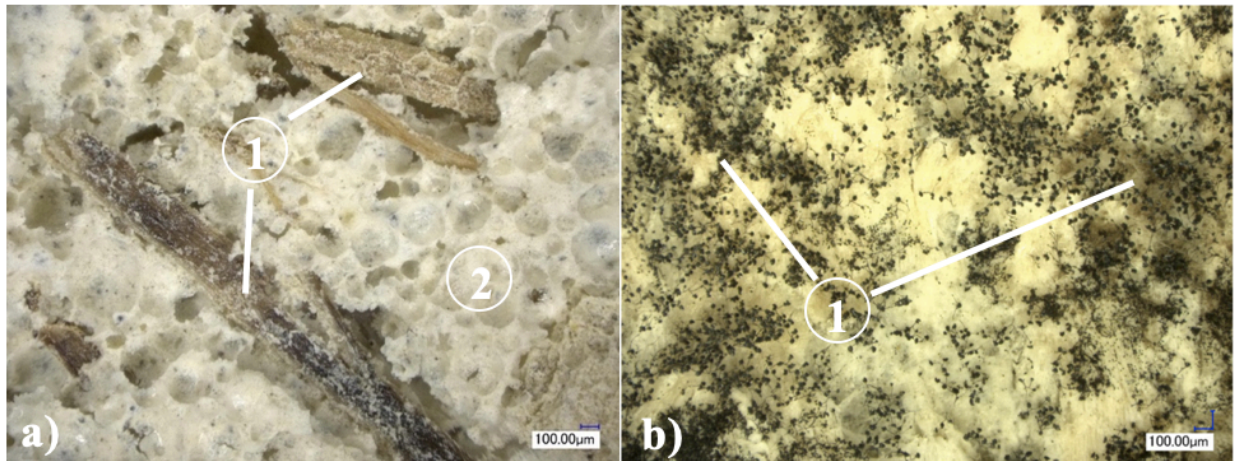


Figure 83. Numerical microscope photos of the hemp mortar (F2) before (a) and after (b) mold growth

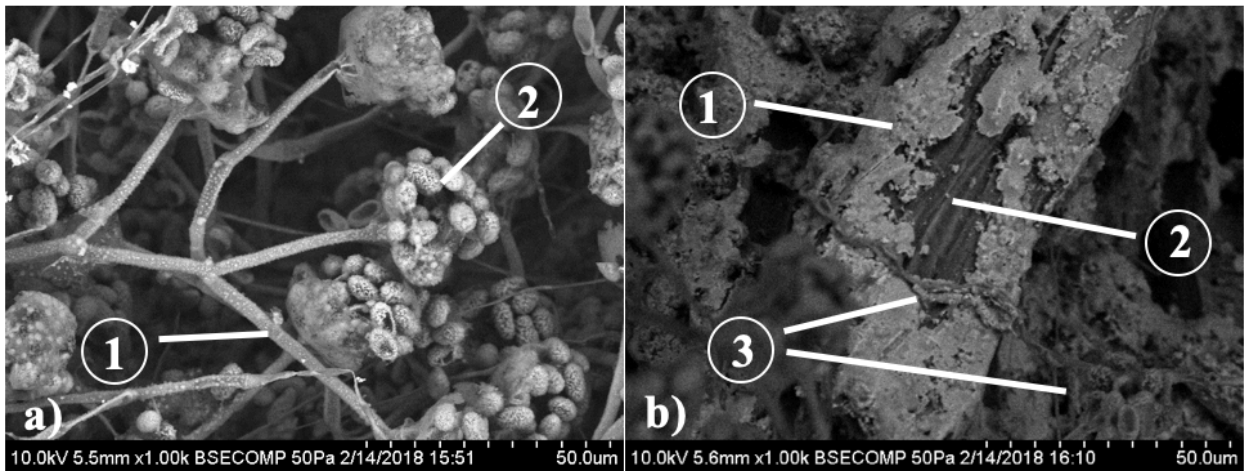


Figure 84. SEM images of the morphological structures of the mold present on the hemp concrete of the first formulation (F1)

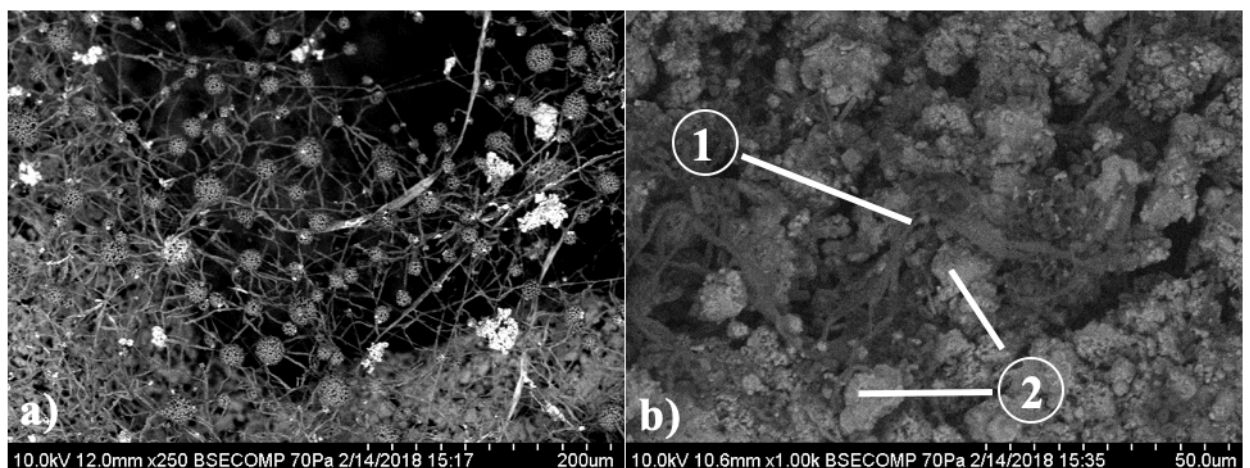


Figure 85. SEM images of the morphological structures of the mold present on the hemp concrete of the second formulation (F2)

## IV.6.2. Fungal species identification

After observation of the hemp mortar fungal contamination, species identification was conducted. Similar to the hemp shives, hemp mortar particles from the surface, most exposed to the environmental microorganism contamination, were isolated twice on the Sabouraud agar medium. The results showed that both mortars F1 and F2 represent molds of three colors. In the case of F1 there are white, red and grey molds and white, red and black for F2. The example of molds in Petri dish with F2 articles after 8 days at 15 °C and 50 %RH is proposed in Figure 86.



Figure 86. Image of Petri dish with F1 particles after 8 days at laboratory conditions

For better identification, all mold species were isolated one more time in other Petri dishes. Grey and red molds present in the mortar F1 and F2 respectively were not identified because of the limits of phenotypic method. As for black and white ones, they were identified as *Aspergillus niger* and *Rhizopus sp.* The Petri dishes with isolated molds are presented in Figures 87 and 88. The obtained identification results were reported in Table 14.



Figure 87. Image of Petri dish with isolated white fungal strain (identified as *Rhizopus sp.*) after 8 days at 25 °C and 50 %RH





Figure 88. Image of Petri dish with isolated white fungal strain (identified as *Aspergillus niger*) after 8 days at 25 °C and 50 %RH

Table 14. Results of hemp mortar mold identification

Sample number	Species quantity	Identified species
F1	3: white, red and grey	White - <i>Rhizopus sp.</i> , N/D
F2	3: white, red and black	White - <i>Rhizopus sp.</i> , Black - <i>Aspergillus niger</i> , N/D

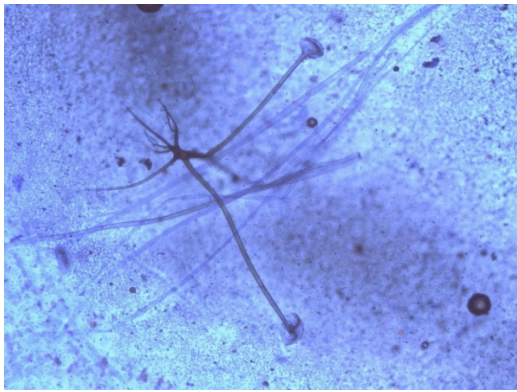
#### IV.7. ANALYSIS OF IDENTIFIED FUNGAL SPECIES

In this paragraph the analysis of the fungal species, identified previously in hemp and hemp mortar, is proposed. Their morphological and characteristic investigation were conducted as well as the literature study of their pathogenicity.

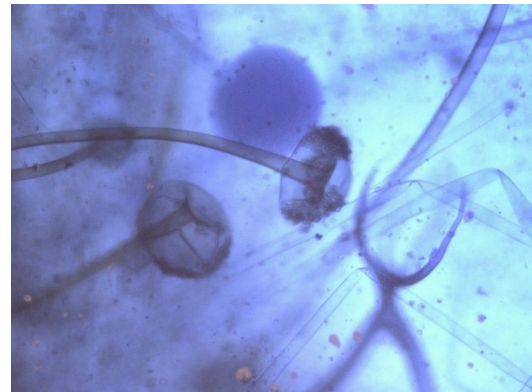
##### IV.7.1. *Rhizopus sp.*

After 8 days at 25°C, on Sabouraud medium, the diameter of the colony of *Rhizopus sp.* was 90 mm. It was raised, voluminous, filling the whole volume of the Petri dish. The hypha is filamentous rather regular siphoned without partitions, round blastospores. Microscopy images are shown in Figures 89. In order to study their development according to the temperature, Petri dishes were conserved at 5°C and 35°C. After 8 days at 5°C *Rhizopus sp.* represents moderate growth, diameter of the colony was about 13 mm (Figure 90). After 8 days at 35°C the colony was close to the one at 25°C (Figure 91). It was concluded that *Rhizopus sp.* was a mesophilic fungal species.

As for the pathogenicity, *Rhizopus sp.* is one of the most isolated species in cerebral and rhinofacial mucormycosis injuries. Patients are often diabetic patients with ketoacidosis, but also leukemic patients, sometimes AIDS patients. Also, *Rhizopus sp.* is dangerous for transplant surgery because of the great risk of the transplant rejection (Almyroudis et al., 2006).



(A)



(B)

Figure 89. Microscopical observation of *Rhizopus sp.*: (A) magnification 1:200 and (B) magnification 1:600

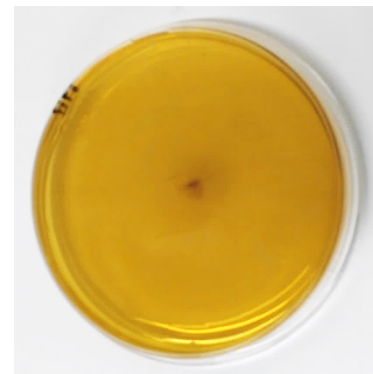
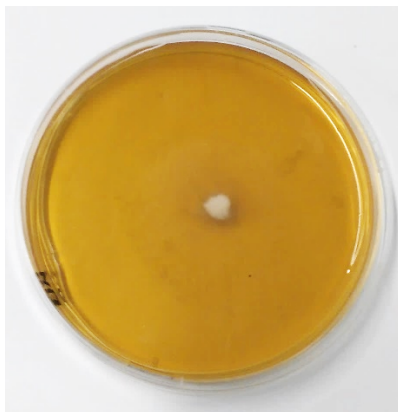


Figure 90. Isolated *Rhizopus sp.* after 8 days at 5°C

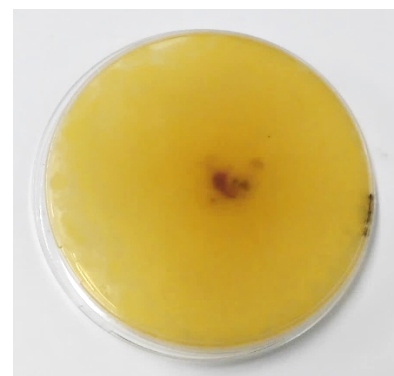


Figure 91. Isolated *Rhizopus sp.* after 8 days at 35°C

#### IV.7.2. *Aspergillus niger*

After 8 days at 25°C, on Sabouraud medium, the diameter of the colony of *Aspergillus niger* was 25-30 mm. It was flat, low, dense and velvety. During microscopic observation the

filamentous hyphae with conidiophores (a specialized filamentous stipe bearing the asexual reproductive organ) with the large amount of conidia on the vesicle were noticed (Figures 92, 93, 94). Conidia are black and dark brown. After 8 days at 5°C *Aspergillus niger* represents no growth (Figure 93). At 35°C the colony is larger than at 25°C and of the size 30-35 mm (Figure 94). Indeed, *Aspergillus niger* is thermophilic fungal species, that is why it represents more active growth at higher temperatures. According to the literature, the toxicity of *Aspergillus niger* comes from their production of oxalic acid, flavaspérone and aflatoxins (Botton, 1990).

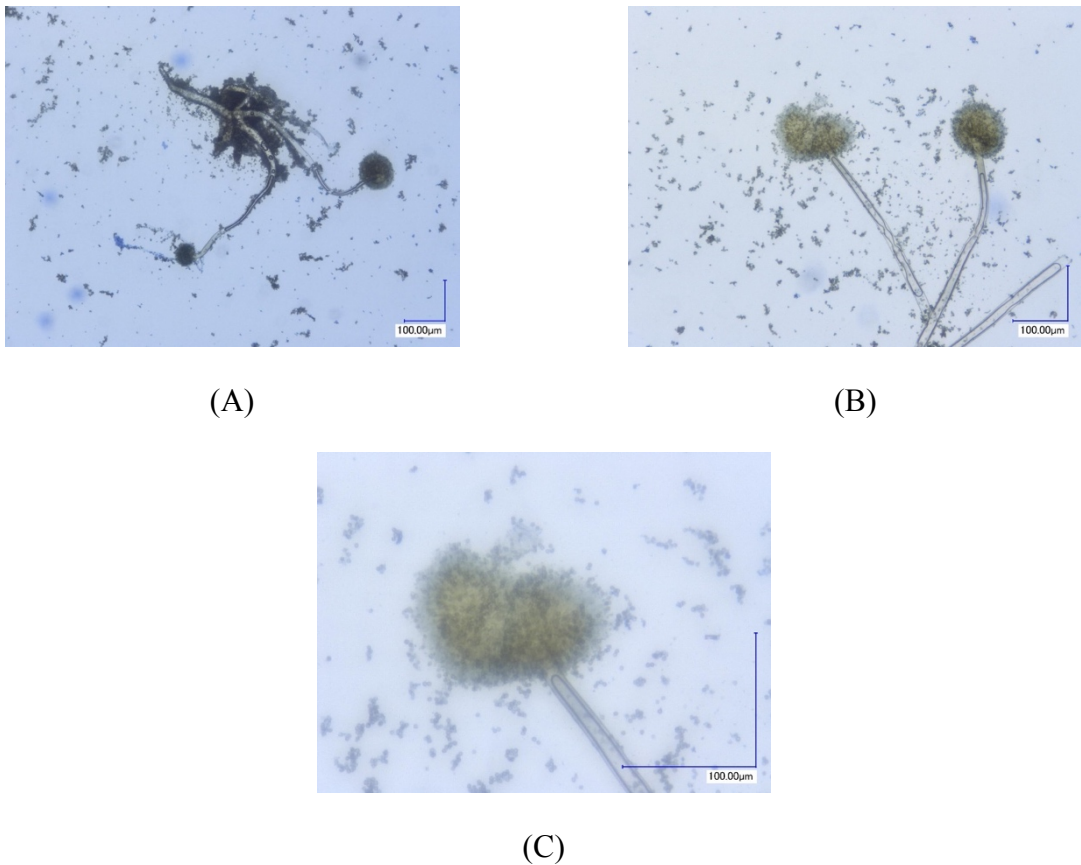


Figure 92. Microscopical observation of *Aspergillus niger*: (A) magnification 1:300, (B) magnification 1:400, (C) magnification 1:1000

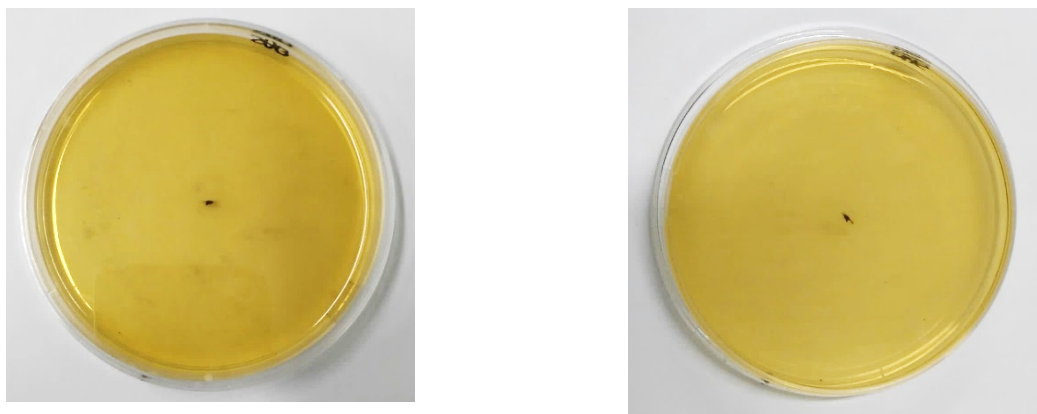


Figure 93. Isolated *Aspergillus niger* after 8 days at 5°C

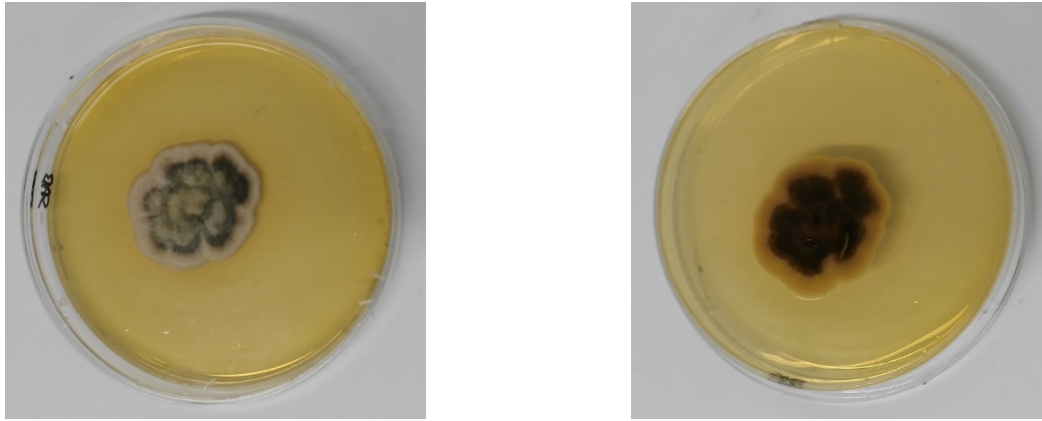


Figure 94. Isolated *Aspergillus niger* after 8 days at 35°C

#### IV.8. CONCLUSION

In this chapter, the fungal contamination of the hemp mortar was investigated. Firstly, the bibliographic study on molds was proposed, that showed the great variability of fungal species and their possible influence on hemp mortar durability. Then, different identification methods were reported that allowed to better choose a method basing on their advantages and disadvantages. Finally, a phenotypic method was applied to identify present in hemp shives and hemp mortar fungal species. Then, the analysis of identified species was proposed.

The obtained results show that:

- biobased mortars represents favorable conditions for fungal proliferation. The organic part is a good source of nutrients for growth and the aggressive influence of the cementitious matrix can be neglected with the help of specific metabolites like enzymes, acids, etc;
- there is a link between fungal strains present in hemp shives and hemp mortar made of it. It highlights the necessity of the quality control of the raw material;
- the fungal growth depends on the conditions. In order to successfully determine the strains, all organisms present must be identified, not just the ones which proliferated. It shows the disadvantages of the phenotypic method: (1) under certain conditions some mold strains do not form structures that allow to determine the strain family; (2) there is the strong possibility of contamination of Petri dishes, which distorts results; (3) due to the effect of synergy some strains may not proliferate which is not representative for the real case; (4) in a hemp mortar or in a hemp itself other microorganisms may be present which cannot be identified.

This chapter highlighted the necessity of application of other identification methods for more representative and reliable results. That is why in the next chapters the ribosomal RNA sequencing was used to get reliable fungal contamination profile.

CHAPTER V.

METAGENOMIC ANALYSIS OF HEMP MORTAR  
AND HEMP SHIVE FUNGAL CONTAMINATION

---

## **CHAPTER V. METAGENOMIC ANALYSIS OF HEMP MORTAR AND HEMP SHIVE FUNGAL CONTAMINATION**

---

### **V.1. INTRODUCTION**

In Chapter IV, the results of the phenotypic fungal identification were presented. It was shown that this method doesn't provide a complete mold contamination profile over the hemp mortars and hemp shives samples. That is why, in this chapter, we report new investigation using molecular method based on fungal DNA sequencing. To do so, the primary objectives of the present chapter are first, to investigate an accurate DNA extraction method that could be used for both bio-composite mortars and their fiber sources collected in situ; second, to understand the process of the proliferation of mold strains on both hemp shives and hemp mortar; and finally, to compare mold strains present in these phases to show their relationship to mold contamination. In situ hemp mortar contamination behavior was investigated in the region of Pau (France) two months after hemp mortar application in extreme conditions (high humidity, low temperature, no aeration), which did not match the standard conditions under which hemp mortar is used

### **V.2. BIBLIOGRAPHIC STUDY**

In recent years, the effects of molds on the degradation of bio-based mortars have piqued the interest of research communities, particularly in civil engineering. For example, Sinka et al. (Sinka, M. et al., 2019) showed that mold proliferation decreased pH levels. In fact, molds during growth use specific metabolites (enzymes, pigments, toxin synthesis, and organic acids) to uptake nutrients from the environment. Among these metabolites, organic acids can be distinguished by their extreme ability to degrade different materials (Liaud et al., 2014). Indeed, the natural fungal production of organic acids plays a critical role in nature and may give a competitive advantage to acid-tolerant filamentous fungi over other organisms by decreasing the ambient pH (Dutton and Evans, 2011; Jones, 1998; Liaud et al., 2014). In addition, decreasing the pH can improve mineral alteration by solubilizing soil minerals, thus releasing nutritive ions for absorption (e.g., ectomycorrhizas) (Plassard and Fransson, 2009) or can lead to acid-catalyzed holocellulose hydrolysis (Green and Highley, 1997; Shimada et al., 1997; Tanaka et al., 1994). Regarding their direct interaction with the environment, organic acids participate in metal detoxification by

complexation. Similarly, oxalic acid plays a significant role in the degradation of biomass (Jones, 1998), partially explaining the biodegradation of bio-composite materials derived from plant biomass such as hemp mortars.

However, a lack of information exists regarding mold population identification in general and mold species in hemp mortars, particularly with respect to their origin and how they survive under highly alkaline mortar conditions. Of the few studies available on this topic, Viel et al. (Viel et al., 2019) used a non-destructive method based on an optical evaluation of bio-composite mortar durability toward mold growth. However, this technique does not enable all mold species present in the material to be distinguished and quantified. This method does not detect the presence of bacteria and sources of external contamination related to the experimental environment, which may prevent true species related to contamination or fungal growth from being identified.

Accurate identification of mold species is necessary to characterize the interaction and possible influence of a mold's identified type on both mortar and hemp durability. Therefore, the main objective of this chapter is to evaluate the mold growth of contaminated hemp mortar collected in situ from a house located in the region of Pau in France. The study identifies mold species present in hemp shives before they are incorporated into the mortar and then examines the contaminated hemp mortar and compares the identified species. Particular attention was devoted to choosing of the deoxyribonucleic acid (DNA) extraction method and the subsequent metagenomics analysis of fungal community. A trophic cycle analysis was then conducted to determine how molds adapt to extreme environments such as that of fresh mortar.

### **V.3. EXPERIMENTAL PROCEDURE**

To better understand the nature of hemp shives and the biodegradation of whole hemp mortar, we carefully analyzed the behaviors of both materials. More specifically, hemp shive contamination was studied separately to identify mold strains already present before incorporation into the mortar. We then followed and evaluated the evolution of these fungal species after integration into the cement matrix (in hemp mortar). Analyzing how hemp fibers interact with the mortar and evaluating whether these vegetable plants are the main sources of contamination were critical in this study. In addition, we identified whether mortar affects the expansion of these mushrooms and if any species are already present in hemp mortars and not in hemp fibers. This experimental investigation aimed to answer all these questions.

#### **V.3.1. In situ conditioning and sample preparation**

The experimental protocol consisted of different treatments of naturally contaminated in situ collected samples of hemp mortar or hemp shives to extract DNA. Quantification was then

conducted to determine whether the extraction method functioned well. Finally, DNA sequencing was performed to identify the mold species.

Two types of samples were studied. The first was hemp mortar that was naturally contaminated one month after its in situ application in November 2017. The in-situ application was represented by the thermal insulation of a house in the region of Pau. Samples were taken from the most contaminated areas observed in January 2018. We noticed that the first fungal proliferation was observed in December following a single month of exposure to extreme conditions. Indeed, it was applied inside an unheated building and exposed to high humidity, low temperature (about 9°C during the day) and no ventilation, conditions that do not correspond to the standard ones in which hemp mortar must be used (Collectif SEBTP, 2012). This proliferation was visually determined by the fact that the mortar was covered with red spots and later validated by microscopic observation (Figure 95). The second sample was of hemp shives that were previously used in the application of hemp mortar in Pau. This “hemp mortar–raw material” link allowed us to compare the obtained results. The lime-based binder with hydraulic additions that we used is a commercial mix designed by ParexGroup SA (its composition is not disclosed by the manufacturer). The mix proportion ratios of the hemp mortar are presented in Figure 96.

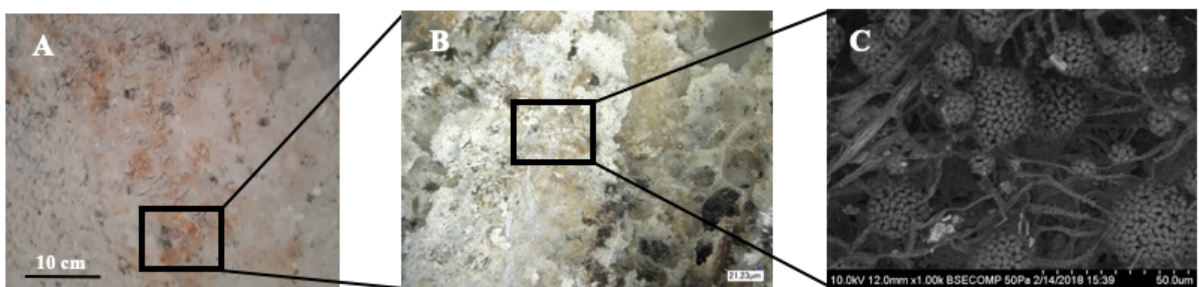


Figure 95. Images of mold proliferation on hemp mortar (A), in the optical microscope (B), and the electronic microscope (C)

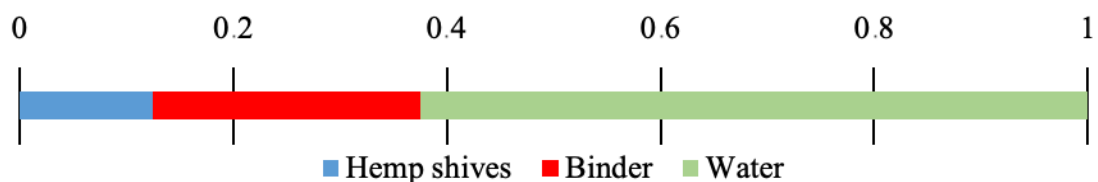


Figure 96. Mass ratios of hemp mortar composition

The DNA extraction experimental protocol (Figure 97) consisted of grinding samples to obtain fine particles. A benchtop mechanical grinder was used for grinding. Prior to each grinding session, all grinder surfaces were treated with acetone to avoid cross-contamination of the samples with possible DNA residues.



We then proceeded to the DNA extraction using specially dedicated kits. The following three kits were used after all precautions of the suppliers for extraction were considered: the FastDNA SPIN Kit, which is dedicated to soils (MP Biomedicals, Irvine, CA, USA), the EZNA High-Performance Fungal DNA Kit (Omega Bio-Tek, Norcross, GA, USA), and the DNeasy PowerPlant Pro Kit (Qiagen, Germantown, MD, USA). To verify the repeatability of the results, two replicates were performed for each kit. After each extraction, total DNA and fungal DNA quantification were performed to ensure the kit's ability to extract DNA from our material matrix. Finally, the FastDNA SPIN Kit (MP Biomedicals, Irvine, CA, USA) (Figure 97) was used for further treatments because it allowed the extraction of a greater total, particularly fungal DNA. This step was completed by the sequencing of 18S rDNA, which allowed us to identify mold strains in both hemp mortar and hemp shives. Each step is detailed in the following subsections.

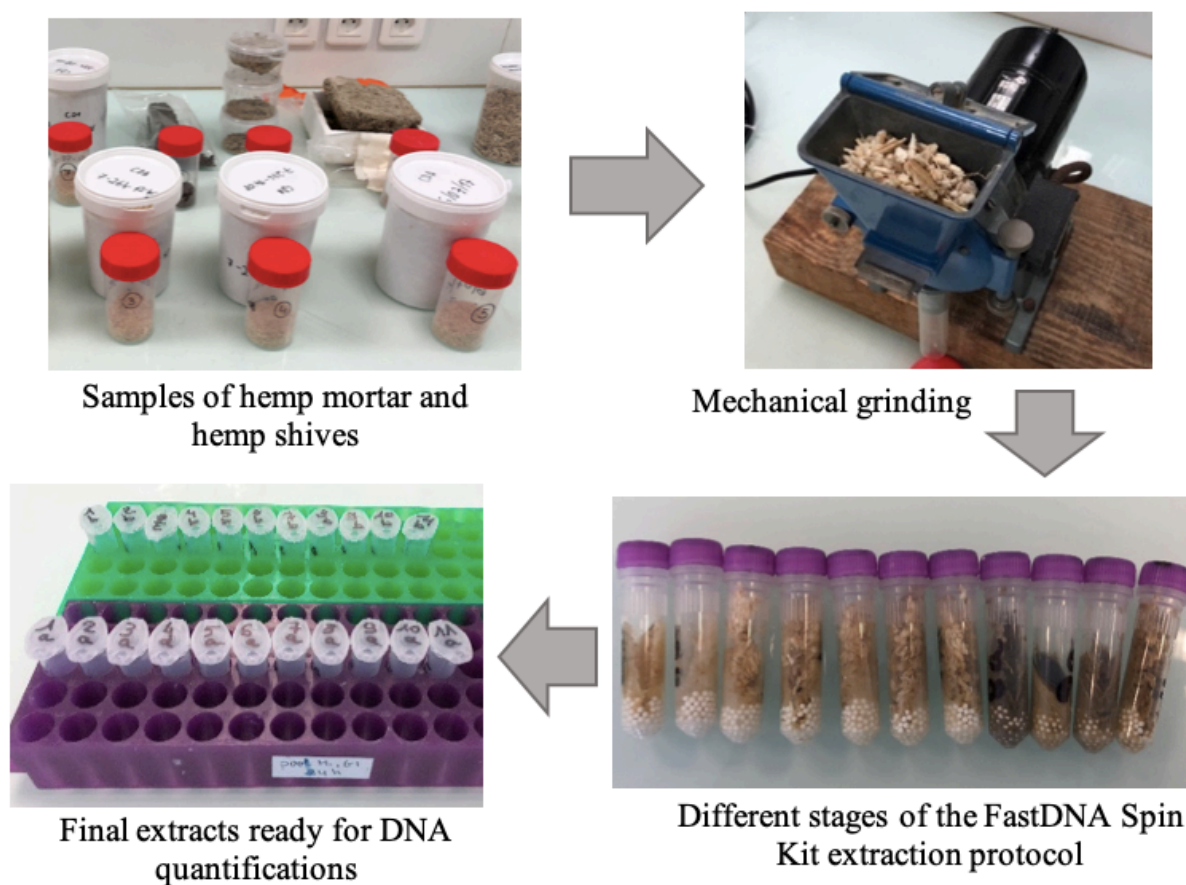


Figure 97. DNA extraction protocol schema

### V.3.2. Total DNA extraction and quantification

Nucleic acids were extracted from 0.1 g of hemp and 0.2 g of hemp mortar using a FastDNA SPIN Kit for Soil (MP Biomedicals, Irvine, CA, USA) according to manufacturer instructions. Two replicates were performed for each sample. DNA was quantified by a fluorimetric measurement using PicoGreen fluorochrome at 485/520-nm excitation/emission wavelengths with

a Fluorescent Quant-IT PicoGreen DS DNA assay Invitrogen P7589 Kit (Invitrogen, Grand Island, NY, USA) (Gangneux et al., 2011).

### **V.3.3. Real-time PCR amplification**

The 18S rDNA amplifications for fungal biomass estimation by 18S rDNA real-time quantitative polymerase chain reaction (qPCR) were conducted with a total volume of 25  $\mu$ L. The qPCR mix was prepared using: 10 ng of microbial DNA from our samples, 0.5  $\mu$ M of each primer [FU18S1 5'-GGAAACTCACCAGGTCCAGA-3' and Nu-SSU-1536 5'-ATTGCAATGCYCTATCCCCA-3'] (Borneman and Hartin, 2000), 25  $\mu$ l of absolute qPCR SYBR Green Mix (Thermo Scientific), and 0.25 mg/mL<sup>-1</sup> BSA (GeneOn). Standard curves were obtained using serial dilutions of linearized plasmids containing the cloned 18S rDNA gene of *Fusarium graminearum*. The results were expressed as the 18S rDNA gene copy number per  $\mu$ L. The amplification protocol (40 cycles of PCR, 40 s at 95 °C, 45 s at 64 °C, and 30 s at 72 °C) was performed using a thermocycler LightCycler® 480 (Roche Diagnostics, Penzberg, Germany). The efficiency of the qPCR ranged from 90% to 100%.

### **V.3.4. Metagenomic analysis of microbial community**

#### **V.3.4.1. Library construction and metagenomic sequencing**

The two highest DNA concentrations extracted from hemp and hemp mortar samples were analyzed using a metagenomic approach targeting the 18S region at the GenoScreen platform (Lille, France). A clone library was generated using the MetaBiote® kit. To prepare the amplicon libraries, Illumina MiSeq was used. To limit the amplification biases, the amplicon libraries included positive and negative controls named ABCv2-57049 and BF-57049, respectively. These controls were used and treated as samples during the stages of the MiSeq library process. The assays were conducted using a fluorimetric method, and the qualitative controls were performed by capillary electrophoresis. After library validation (10 libraries: six samples and four controls), they were diluted to 10 nM and controlled qualitatively and quantitatively by high-sensitivity capillary electrophoresis.

#### **V.3.4.2. Data metagenomic sequencing analyses**

Amplicons were sequenced on a MiSeq sequencer, and the quality of the generated sequence readings was evaluated using the Quantitative Insights into Microbial Ecology (QIIME) program (version 1.9.1) based on the Metabiote® pipeline (Bartram et al., 2011; Caporaso et al., 2011). The similarity data and phylogenetic analysis were combined to define the operational taxonomic units

(OTUs). An OTU was defined as when the percentage of similarity exceeded 97%. These sufficient and high-quality 18S full-length sequences enabled us to achieve affiliation to obtain the taxonomic profile of eukaryotic populations identified within the studied samples. As the DNA of the negative control was sequenced, the fungal genera present in the control sample were subtracted from the hemp shive and hemp mortar extraction. Further identification and classification of sequences were conducted by (Greengenes, version 13.8; [www.greengenes.gov](http://www.greengenes.gov)) using v2.2 of the RDP classifier (Wang et al., 2007). A Venn diagram was plotted to compare the obtained results from a source/material point of view. This represented the number of genera present in hemp shives, in hemp mortar, and in both materials.

## **V.4. FUNGAL DNA SEQUENCING DATA ANALYSIS**

### **V.4.1. DNA extraction**

Following the extraction step, a fluorimeter analysis was conducted to determine whether the DNA extraction kit was well chosen. Two replicates were performed for each sample. The samples with the highest total DNA concentration were 7.53, 46.49, and 0.23 ng/ $\mu$ L for the hemp shives, hemp mortar, and control sample, respectively. These samples were used for DNA sequencing. Based on the total concentrations, it was determined that the extraction method worked well, and a sufficient quantity of DNA was extracted. Simultaneously, because the FastDNA SPIN Kit used for DNA extraction is designed to extract all DNA from the soil (i.e., plant, bacterial, and fungal DNA) in the resulting mixture, all were extracted. The qPCR analysis of the extracts from hemp shives and hemp mortar was conducted to identify the mold DNA concentration. The number of copies of  $5.42 \times 10^5$  and  $3.94 \times 10^6 \mu\text{L}^{-1}$  for hemp shives and hemp mortar, respectively, were obtained. The extracts of total DNA were used after rDNA sequencing.

### **V.4.2. Rarefaction analysis**

To validate the representativeness of our hemp mortar and hemp shive samplings across the entire sample, the diversity was studied. To do this, the OTUs observed for hemp shives, hemp mortar, and negative control samples as a function of an increasing number of sequences were plotted (see Figure 98). Thus, we considered a detailed description of the sample diversity when the curve reached the plateau. The so-called “plateau” phase was reached for all samples by demonstrating a detailed description of eukaryotic diversity.

However, we should note that the diversity of hemp shives was more significant than what was possible due to less auspicious conditions in the hemp mortar. This could also be explained by the nature of the vegetal fibers, which are very heterogeneous from a dimensional point of view

(aggregate hemp size) and where we risk finding traces of dust and contamination (due to the industrial process of retting).

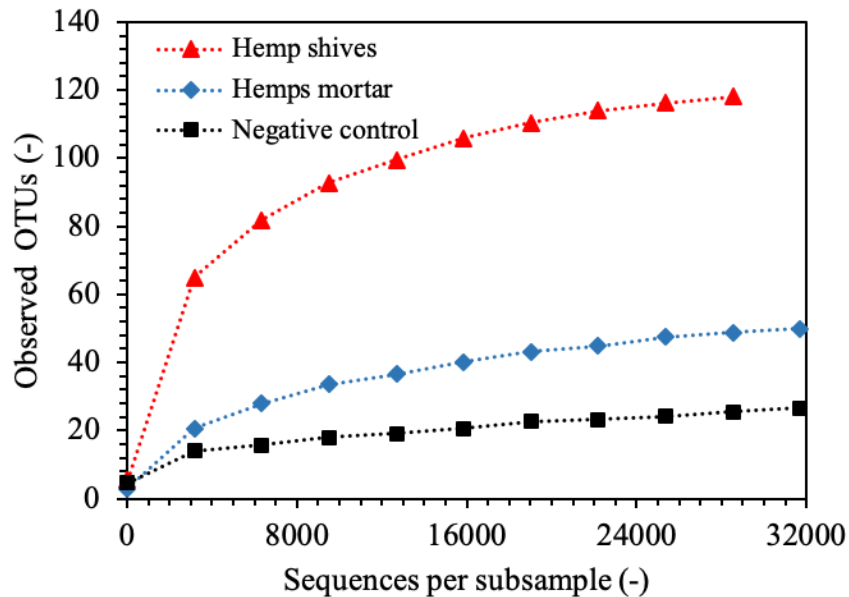


Figure 98. Rarefaction analysis of the observed OTUs for the hemp shives, the hemp mortar, and the negative control as a function of an increasing number of sequences

#### V.4.3. Mold species identified

Following the subtraction of fungal genera present in the negative control, four phyla remained in the studied samples of hemp shives and hemp mortar. As Figure 99 shows, *Opisthokonta* was the major phylum in both cases, with 83.6% in hemp shives and 99.97% in hemp mortar. This suggested that the *Opisthokonta* phylum species, initially present in the hemp shives, could survive under the fresh hemp mortar's aggressive conditions and dominate following the application.

The second most abundant phylum was *Archaeplastida*, representing 16.3% of hemp shives. However, it decreased to 0.004% in the mortar. This showed that the conditions of fresh mortar are not suitable for these species. A decrease in abundance was also noted for *SAR* phylum strains (from 0.1% to 0.02%). However, it could be observed that *Incertae Sedis* phylum microorganisms were present at 0.007% in the hemp mortar samples and were not found in hemp shives. This may have been due to external contamination following the hemp mortar application (Figure 99).

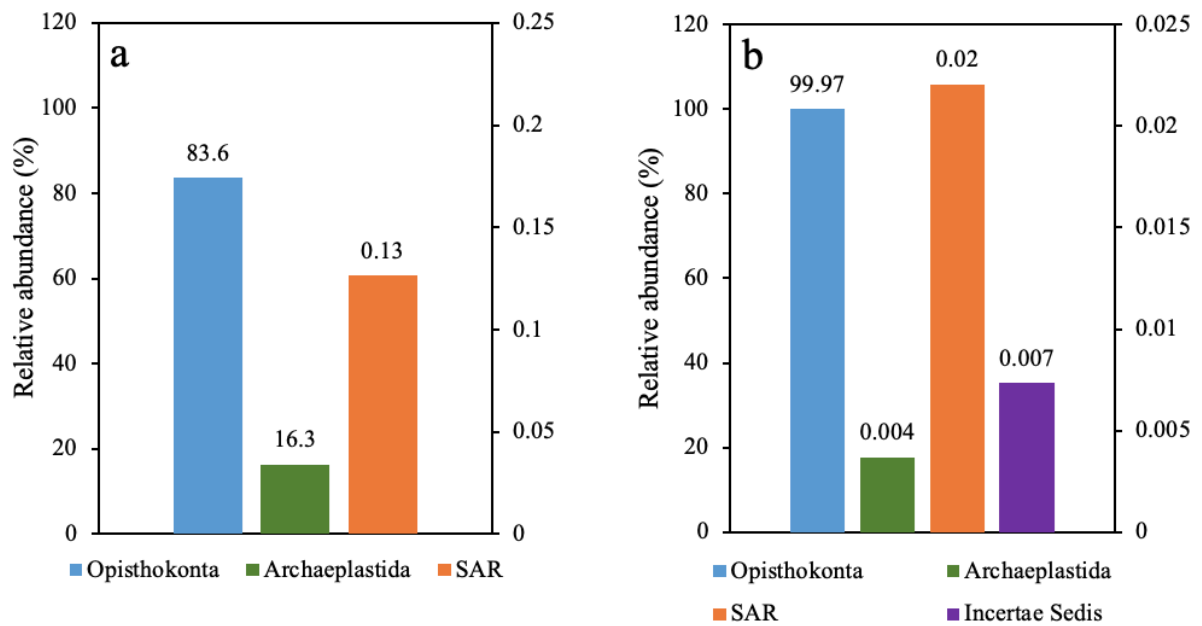


Figure 99. Relative abundance levels of each fungal phylum for hemp shives (a) and hemp mortar (b)

Next, mold strain abundances from hemp shives and hemp mortar were analyzed separately. Thirty-seven and twenty-five genera of mold were identified in hemp shives and hemp mortar samples, respectively (see Figures 100-101). Some fungi have not been identified up to the genus, but they are reported to the phylum represented in Figure 99. For example, eight undefined (17% total abundance) and four undefined (0.05% total abundance) fungi exist in hemp shives and hemp mortar, respectively, which had not been previously identified and are represented by "other/unclassified" (Figures 100-101).

In hemp shives, the majority of identified genera (abundance greater than 1%) are representatives of the *Opisthokonta* phylum: *Acrostalagmus* (42%), *Tremellales* (24%), *Filobasidiacacae* (9%), and *Alternaria* (6%). In the case of the hemp mortar samples, *Acrostalagmus* (96%) and *Auricularia* (3%) genera are major (also belonging to the *Opisthokonta* phylum) (Figures 100-101). A trophic cycle analysis of these genera was conducted and is described later in this section.

In addition, the Venn diagram shows that a greater number of genera exist in hemp shives than in hemp mortar, which can be explained by the extreme conditions of the alkaline medium such as mortar after mixing. There are 87.4% sequences that have not been identified up to the genus in hemp shives. They are represented by "other/unclassified" (Figure 8). Simultaneously, 95% of these sequences belong to the *Charophyta* order of *Archaeplastida* phylum and 5% to the fungi order of the *Opisthokonta* phylum. The most abundant genera identified are *Kondoa* (2.8%),

*Diaporthe* (1.9%), and *Cystofilobasidiaceae* (1.2%) of the *Opisthokonta* phylum and *Panax* (2.5%) of the *Archaeplastida* phylum.

Among the genera that are present only in hemp mortar, we distinguish two major ones: *Auricularia* (96%) and *Geosmithia* (2%) (Figure 102). These genera belong to the *Fungi* order. Regarding the fungal genera present in both hemp shives and hemp mortar, we distinguish 7 genera. 6 genera belong to the *Fungi* order and one to the phylum SAR, order *Cercozoa*. Four genera in hemp shives are considered major: *Acrostalagmus* (51%), *Tremellales* (30%), *Filobasidiaceae* (11%), and *Alternaria* (7%) (Figure 102). By contrast, only one genus dominates in hemp mortar, namely, *Acrostalagmus* (99.9%). We note that the *Acrostalagmus* genus representatives are the majority of mold species in hemp shives and dominate in hemp mortar (Figure 102).

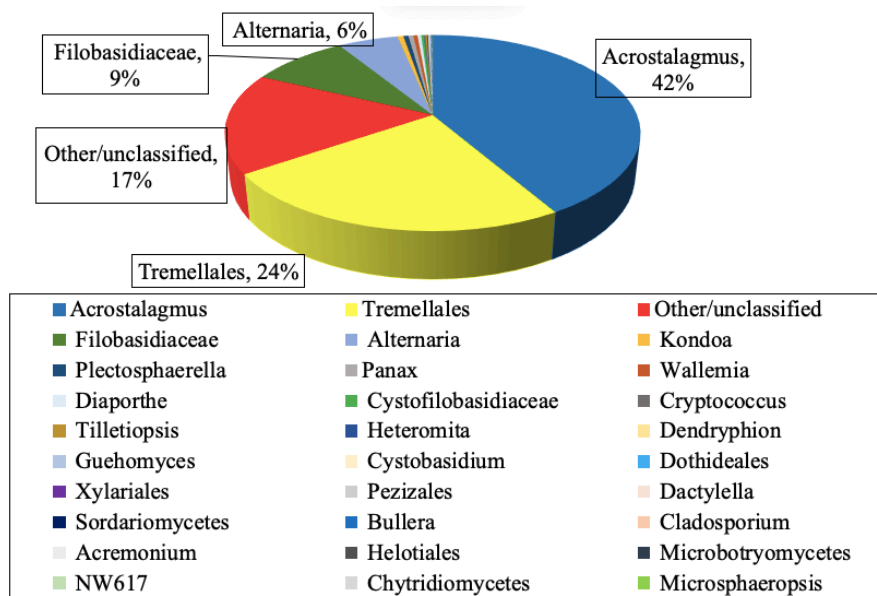


Figure 100. Fungal community analysis in hemp shives (18S rDNA)

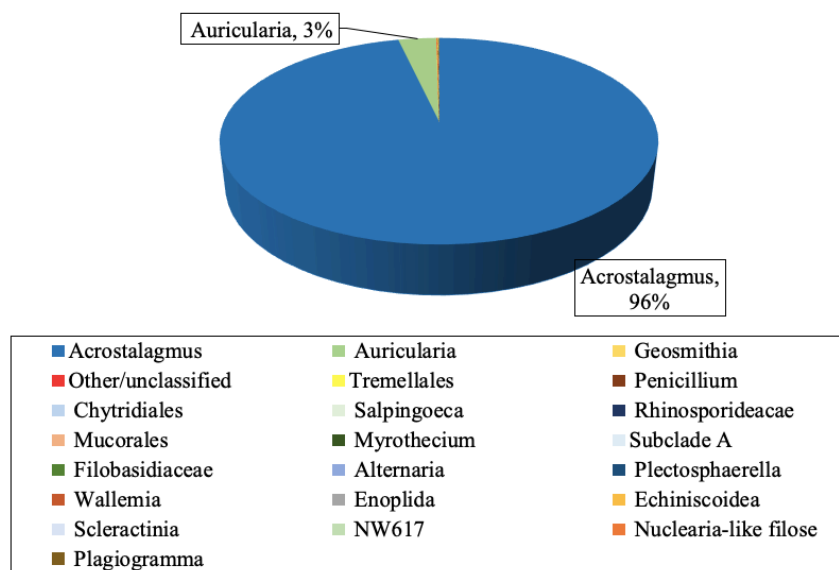


Figure 101. Fungal community analysis in hemp mortar (18S rDNA)

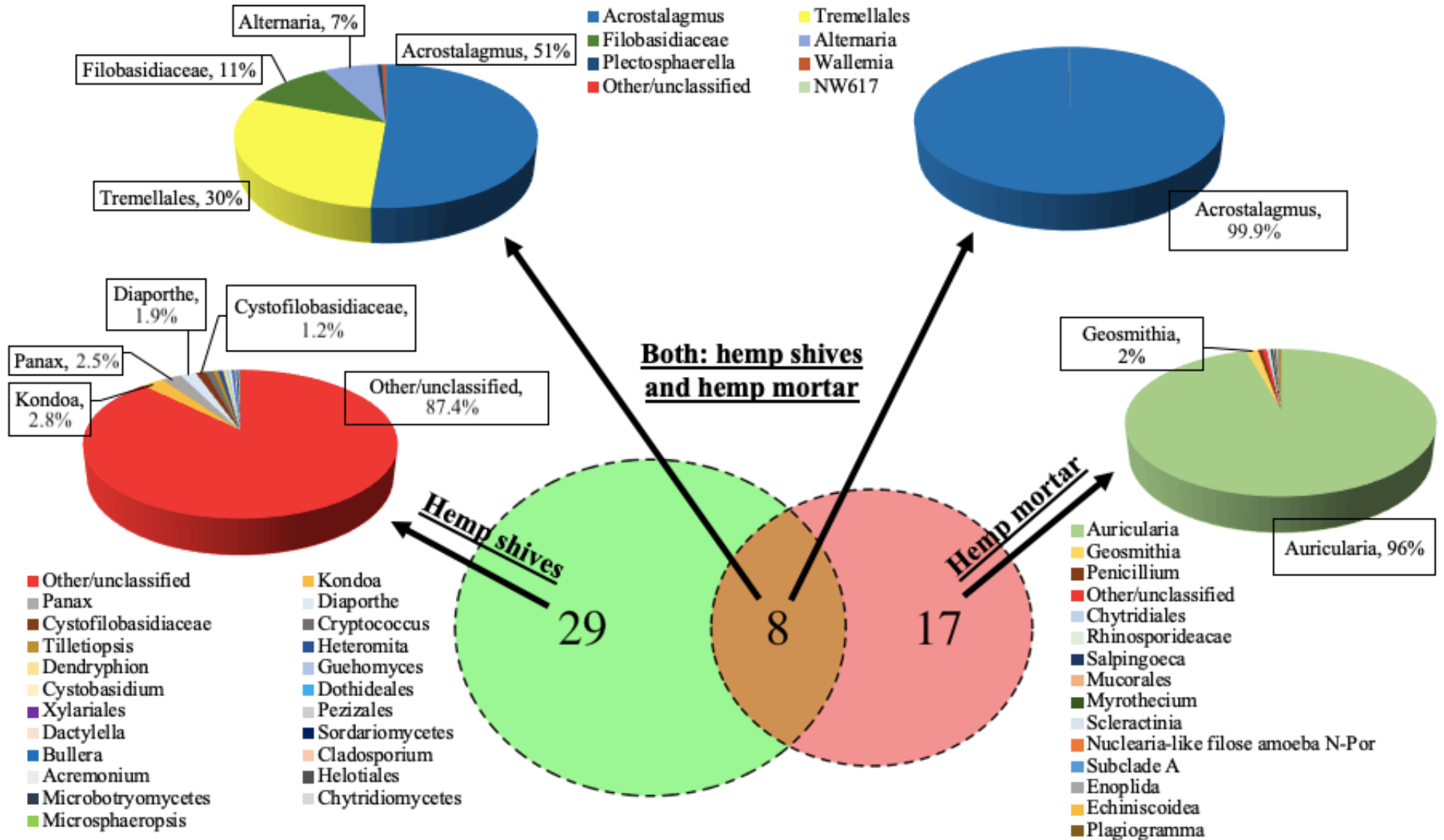


Figure 102. Venn Diagram evaluating the concentration of mold contamination of hemp shives, hemp mortar and both

## V.5. ANALYSIS OF MAJOR FUNGI GENERA AND DISCUSSION

To better understand the proliferation of mold strains in hemp mortar, major genera representative trophic cycle analysis is proposed. As previously noted, the major genera of hemp shives are represented by the *Acrostalagmus*, *Tremellales*, *Filobasidiaceae*, and *Alternaria*. For hemp mortar, the two major genera of *Acrostalagmus* and *Auricularia* exist.

According to (Giraldo and Crous, 2019), 54 records are listed in the nomenclatural databases Index Fungorum and Myco-Bank under the name *Acrostalagmus* with 29 included species, six forms, and eight varieties. The authors (Giraldo and Crous, 2019) also reported that the representatives of the *Acrostalagmus* genus are cosmopolitan fungi and could be isolated from various soil types, including alkaline soils in Europe, Russia, Turkey, Sri Lanka, Nepal, Japan, Australia, Hawaii, Canada, and the continental USA, or from a great variety of types of plant debris as well as from dung (for example, *Acrostalagmus luteoalbusis*). They could also be saprophytic on wood, bark, leaves, and herbaceous stems. They are occasionally isolated from tropical and subtropical soils (for example, *Acrostalagmus annulatusis* (Seifert and Gams, 2011)). Simultaneously, *Acrostalagmus luteoalbusis* is reported to be a mycoparasite on *Alternaria brassicae*, *Cronartium comandrae*, *Daldinia concentrica*, and *Flammulina velutipes* (Domsch et al., 2007; Grum-Grzhimaylo et al., 2016; Seifert and Gams, 2011; Zhang and Tang, 2015).

The *Tremellales* genus representatives are characterized by dolipore septa with vesiculate parenthesomes (Bandoni, 1984). This order includes more than 50 lichenicolous species (Diederich et al., 2014; Millanes et al., 2014, 2012, 2011; Werth et al., 2013). They are cosmopolitan fungi that have been isolated in different countries (Brazil, Europe, Russia, Mexico, Panama, and Greenland).

Using Bayesian analysis on the seven-gene dataset for the *Filobasidiaceae*, we could distinguish five strongly supported clades named *Aerius*, *Albidus*, *Cylindricus*, *Filobasidium*, and *Gastricus* (Boekhout et al., 2011). The representatives of this order are mostly different species and varieties of *Cryptococcus*. It has been reported that *Filobasidiaceae* species can grow in extreme conditions. For example, three species of *Gastricus* were isolated from acid rock drainage from a pyrite mine in Portugal (Gadanhó and Sampaio, 2009; Liu et al., 2015), and another three species were isolated from hypersaline soil of the Urmia Lake National Park in Iran that also showed the possibility of growing in saline environments (10–15% of NaCl) (Mokhtarnejad et al., 2016).

*Alternaria* species are fungi distributed worldwide as saprophytes, endophytes, and plant pathogens in soil, atmosphere, plant materials, and food commodities because of their ability to adapt and survive in environmental conditions that are far from optimal (Aust et al., 1980). As



plant pathogens, *Alternaria* spp. have been reported on crops, including cereals, oil crops, ornamentals, vegetables, and fruits (Logrieco et al., 2009). *Alternaria* spp. are also known to produce many secondary metabolites such as host-specific toxins required for pathogenicity, a vast number of mycotoxins, and several allergens (Thomma, 2003).

The *Auricularia* genus representatives are cosmopolitan fungi reported in eastern Asia, North America, Europe, and elsewhere (Lowy, 1951). *Auricularia* is a major genus among the jelly fungi because of its widespread consumption and medicinal (antibacterial) properties. For example, *Auricularia heimuer* is one of the most famous traditional Chinese foods and medicines and is the third most cultivated mushroom worldwide (Yuan et al., 2019).

Thus, results of rDNA sequencing showed that the major fungal genera from hemp shives and hemp mortar are cosmopolitan and widely present in the world. Some of them (*Acrostalagmus*, *Filobasidiaceae*) can reportedly grow in extreme environments. Mortar (high pH, high salinity) is one example. We should also note that the number of representatives of the two orders *Tremellales* (mostly parasitic fungi) and *Alternaria* (mostly saprophytic fungi) was greatly reduced in hemp mortar as compared to hemp shives. We could hypothesize that this was due to environmental conditions and the inaccessibility of food because of enrobing hemp shives by mortar. By contrast, the *Acrostalagmus* representatives accustomed to alkaline environments preserved their viability and maintained their ability to grow. As a result, they had an advantage over other mold strains. Strains from the *Auricularia* genus proliferated after mortar casting, as they were present only in the hemp mortar, which could be explained by further external contamination. In addition, we observed that environmental conditions played a critical role in determining the durability of hemp mortars and particularly fungal growth because of the conditions of mold proliferation (humidity, temperature, pH level, etc.) and even greater external contamination.

## **V.6. CONCLUSION**

In this chapter, a metagenomic analysis and identification of fungal communities present in in situ collected hemp mortar and its raw organic material were conducted. Thus, this study developed a detailed protocol for DNA extraction and sequencing for hemp shives and hemp mortar that could be used for composite cementitious materials. A real case involving in situ collected samples of hemp mortar and its source (hemp shives) were studied separately to understand the interaction between the mold contamination of raw hemp shives and final hemp mortar. First, a DNA extraction method was carefully selected based on total and fungal extracted DNA quantification. Second, the diversity of studied samples using rarefaction analysis was evaluated to ensure representativeness of the results. Finally, the mold genera present in hemp shives and hemp mortar were then accurately identified to analyze the trophic cycle of major fungi.

Hemp mortar mold proliferation was noted after one month of exposure to extreme conditions that did not match the standard conditions under which hemp mortar is used (high humidity, low temperature, no aeration). The results of DNA sequencing showed a difference between mold contamination of hemp shives and composite hemp mortar. The relative abundance levels of fungal phyla present in hemp shives and hemp mortar revealed that the most abundant phylum was Opisthokonta. It represented 83.6% of hemp shives and 99.97% of hemp mortar mold contamination. Analysis of the identified species emphasized the interconnection between the mold strain characteristics (particularly the ability to grow in extreme environments) and their presence in hemp mortar. For example, the most abundant identified genus was *Acrostalagmus*, that represented 42% of hemp shives and 96% of hemp mortar mold contamination. This was explained by its ability to survive in alkaline environments (e.g., alkaline soils). Because more genera exist in hemp shives than in hemp mortar (37 against 25, respectively) and because the *Acrostalagmus* genus present in hemp shives is the most abundant in hemp mortar, we could conclude that the hemp shives are the main source of hemp mortar contamination. However, their use conditions were also found to be significant. As a result, only eight species exist in both hemp shives and hemp mortar, and 17 species are not present in hemp shives (but instead derive from external contamination).

The chosen DNA extraction method could be used to characterize other types of mortars and their raw materials under different conditions. The present study opens the possibility of using a molecular rDNA screening method for building materials that could help in understanding the consistent patterns of proliferation of different microbiological flora and fauna types. The obtained in this chapter results should be considered when studying the durability of hemp mortars and their interaction with fungal communities. In addition, we observed that the most crucial origin of fungal contamination was hemp shives. This adds to the urgency of further studies on protecting hemp mortars from initial or external contamination, for example, by applying different treatments of hemp shives or by using essential oil additives. Apart from mold contamination, hemp mortar represents also a risk of bacterial proliferation. That is why in the next chapter, the bacterial contamination analyze was reported.

CHAPTER VI.

EVALUATION OF HEMP MORTAR AND HEMP  
SHIV BACTERIAL CONTAMINATION BY  
METAGENOMIC INVESTIGATION

---

## **CHAPTER VI. EVALUATION OF HEMP MORTAR AND HEMP SHIV BACTERIAL CONTAMINATION BY METAGENOMIC INVESTIGATION**

---

### **VI.1. INTRODUCTION**

In Chapter V, the results of the fungal identification using the metagenomic analysis were presented. It was shown that hemp shives are the main source of mold contamination. Indeed, apart from molds there are also other microorganisms that can affect the durability of the hemp mortars. Also, such microorganisms as bacteria represent the first proliferation on hemp mortars as the range of their growth is bigger. That is why, in this chapter, we report the results of molecular method based on bacteria DNA sequencing. For this purpose, first a bibliographic study is presented. Then, the experimental protocols for DNA extraction and sequencing are presented. Finally, the analysis of the obtained results with the trophic cycles of the identified major strains are reported.

### **VI.2. BIBLIOGRAPHIC STUDY**

Bacteria are the most common organisms accounting about 50% of all dry biomass of the Earth (Kallmeyer et al., 2012). These are unicellular prokaryotic organisms; whose average size varies between 0.5 and 1.5  $\mu\text{m}$ . There are autotrophic or heterotrophic bacteria, i.e. they can use the mineral or organic source of carbon and proliferate on any type of support. Apart from this cosmopolitan nutrition, they could be aerobic or anaerobic which allow them to draw energy from different sources (oxidation of  $\text{Fe}^{2+}$ ,  $\text{H}_2\text{S}$  or  $\text{NH}_4^+$ ) and to colonize surfaces in contact with the oxygen in the air or the entire volume of the material without access to oxygen. Moreover, bacteria have another type of adaptation to different environmental conditions - the growth of a biofilm. The biofilm is a three-dimensional structure composed of microorganisms covered by the matrix of extracellular polymeric substances (EPS) that could represent 50 to 90% of the total organic carbon of the biofilm (Donlan, 2002)).

In fact, the extracellular bacterial matrix is drained by the channels that provide nutrients and electron acceptors ( $\text{O}_2$ ) (Costerton et al., 1994). All these factors give them the advantage over other species and the possibility to live in wide ranges of environmental conditions (1 to

1000 atm, -5°C to 113°C, 0 to 12 pH or even extreme radioactivity) (Kulakov et al., 2002; Rothschild and Mancinelli, 2001).

The effect of bacteria on the durability of materials is beginning to interest the research community, particularly in the field of civil engineering. Certain species of bacteria are used in concrete structures as a self-healing factor because of their ability to close porosity by precipitating calcium carbonate during their life cycle. In fact, the encapsulated bacteria are added to the concrete during its pouring process. When cracks appear, the bacteria around them are activated by moisture, access the oxygen in the air and precipitate CaCO<sub>3</sub>, which closes the cracks (Lee and Park, 2018; Wang et al., 2014).

At the same time, bacteria are known for their ability to cause the degradation of concrete structures. That's why, (Maresca et al., 2017) studied the identification of the surface and internal bacterial population of concrete samples. Results show that live bacteria are present in concrete samples after one year of in situ exposure and that there is a difference between inside and outside bacterial species. However, there is no information on the identification of the biofilm population in general and the bacterial species in particular in hemp mortars. In fact, all surfaces of the material are colonized by different types of microorganisms, and bacteria is the most important one. Thus, the precise identification of bacterial species is a necessary step to characterize the possible influence of the type of the identified bacteria on the durability of both mortar and hemp and the interaction between bacterial species and other microorganisms.

That's why, the main objective of this chapter is to evaluate the bacteria growth of hemp mortar contaminated by molds, collected in situ in a stone masonry castle located in the region of Pau in France. The originality is the identification of bacterial species present in the hemp shives, before their incorporation in the mortar, and in the contaminated hemp mortar and the comparison of these species. Particular attention was devoted to the choice of the deoxyribonucleic acid extraction method and the subsequent metagenomics analysis of the microbial community. In order to realize how they adapt to such extreme environment as the mortar, an analyze of the trophic cycle of the major strains was conducted.

### **VI.3. EXPERIMENTAL PROCEDURE**

In order to better understand the behavior of the hemp shivs and the biodegradation of whole hemp mortar, the behavior of both materials was analyzed carefully in this study, i.e. the hemp shivs contamination was studied separately to identify the bacterial strains already present before incorporation into the mortar. Indeed, we proposed to follow and evaluate the development of these bacterial species after the colonization of the cement matrix by molds in

the hemp mortar. In fact, it was essential to analyze how the hemp fibers interact with the mortar and to evaluate whether these vegetable plants are the main sources of bacterial contamination. We also proposed to determine if the mortar affects the expansion of these bacteria, if there are some species already present in hemp mortars and not in hemp fibers. This experimental research aims to provide answers to all these questions.

### VI.3.1. In situ conditioning

For a better representativeness of the study, we investigated real samples contaminated in situ. The in situ application was represented by the inside insulation of the stone masonry castle in the region of Pau, in France (Figure 103). The castle was insulated from inside using the hemp mortar in November 2017 (Figure 104). Samples were taken from the most contaminated areas observed in January 2018.



Figure 103. Study case: stone masonry castle in the region of Pau (France)



Figure 104. Image of the wall before the hemp mortar insulation (a) and the application process (b)

### VI.3.2. Sample preparation

Two types of samples were studied (Figure 105). The first one is the hemp mortar that was naturally contaminated one month later after its in situ application in November 2017. It is noticed here that the first fungal proliferation was observed in December after a month of exposure to extreme conditions (Figure 106). Indeed, it was applied inside an unheated building and exposed to high humidity, low temperature (about 9°C during the day) and no ventilation, conditions that do not correspond to the standard ones in which hemp mortar must be used (Collectif SEBTP, 2012). This proliferation was determined visually by the fact that the mortar was covered with red spots. It was later verified by microscopic observations (Figure 107). SEM and optical microscopic observations show a strong contamination of these samples. On the SEM image the filamentous structures of the molds are clearly visible, indicating a strong presence of fungal species. The second sample consists of the hemp shivs that were previously used during the application of the hemp mortar in the stone masonry castle in situ in Pau.



Figure 105. Example of two samples: hemp mortar (left) and hemp shivs (right)



Figure 106. In situ mold proliferation on inside insulation hemp mortar

The choice to study these two samples was legitimate in order to establish comparisons between hemp mortar - raw material (hemp aggregates). The idea is to evaluate the influence of the bacterial contribution of hemp fibers on the mortar and also to analyze the interaction between them after application. The binder used, based on lime with hydraulic additions, is a commercial mix designed by ParexGroup S.A. Its composition is not commercially disclosed by the manufacturer, for privacy reasons. However, the mix proportion ratios of the used hemp mortar are shown in Table 15.

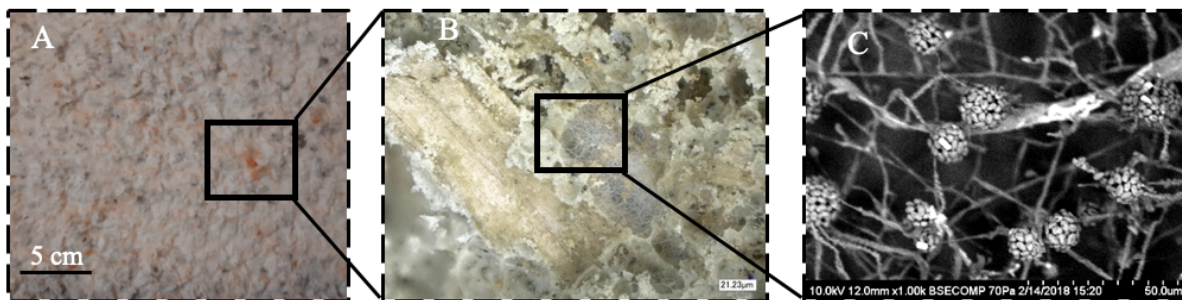


Figure 107. Images of bacterial proliferation on hemp mortar (A), in optical microscope (B) and in electronic microscope (C)

Table 15. Mass ratios of hemp mortar composition

Hemp shives	Binder	Water
12,5%	25%	62,5%

### VI.3.3. Total DNA extraction and quantification

The identification of microorganisms in hemp mortar and hemp fibers is an essential step to analyze them and then to prevent the degradation of this material. It also helps to prevent any health risk for the inhabitants. In this work, the finest method of metagenomic analysis of the bacterial community was used. It consists of extracting and sequencing DNA to identify all the bacteria present in the samples.

The different stages of experimental protocol of DNA extraction are represented in Fig. 6. The first step consists of grinding samples to receive fine particles. The benchtop mechanical grinder was used for grinding samples. Before and after each grinding, all grinder surfaces were treated with acetone to avoid cross-contamination of the samples with possible DNA residues. Then, we proceeded to a total extraction of the DNA using specially conceived kits. Three kits were used following all the suppliers' precautions for extraction: the FastDNA Spin Kit which is dedicated to soils (MP Biomedicals, Irvine, CA, USA), the E.Z.N.A. High Performance Fungal DNA Kit (Omega Bio-Tek, Norcross, GA, USA) and the DNeasy PowerPlant Pro Kit (Qiagen, Germantown, MD, USA).

In order to verify the repeatability of results two replicates were performed for each kit. After each extraction, total DNA and bacterial DNA quantification were performed to insure the kit's ability to extract DNA from the material matrix. Finally, the FastDNA™ Spin Kit (MP Biomedicals, Irvine, CA, USA) has been adopted for further treatments because it allows the extraction of a larger quantity of total and especially bacterial DNA. Nucleic acids were extracted from 0.1 g of hemp and 0.2 g of hemp mortar. DNA was quantified by a fluorimetric



measurement using Picogreen fluorochrome at 485/ 520 nm excitation/emission wavelengths with a Fluorescent Quant-IT PicoGreen DS DNA assay Invitrogen P7589 Kit (Invitrogen, Grand Island, NY, USA) (Gangneux et al., 2011). This step was completed by the sequencing of 16S rDNA which allowed us to identify bacterial strains for both hemp mortar and hemp shivs. Each step will be detailed later in the following subsections.

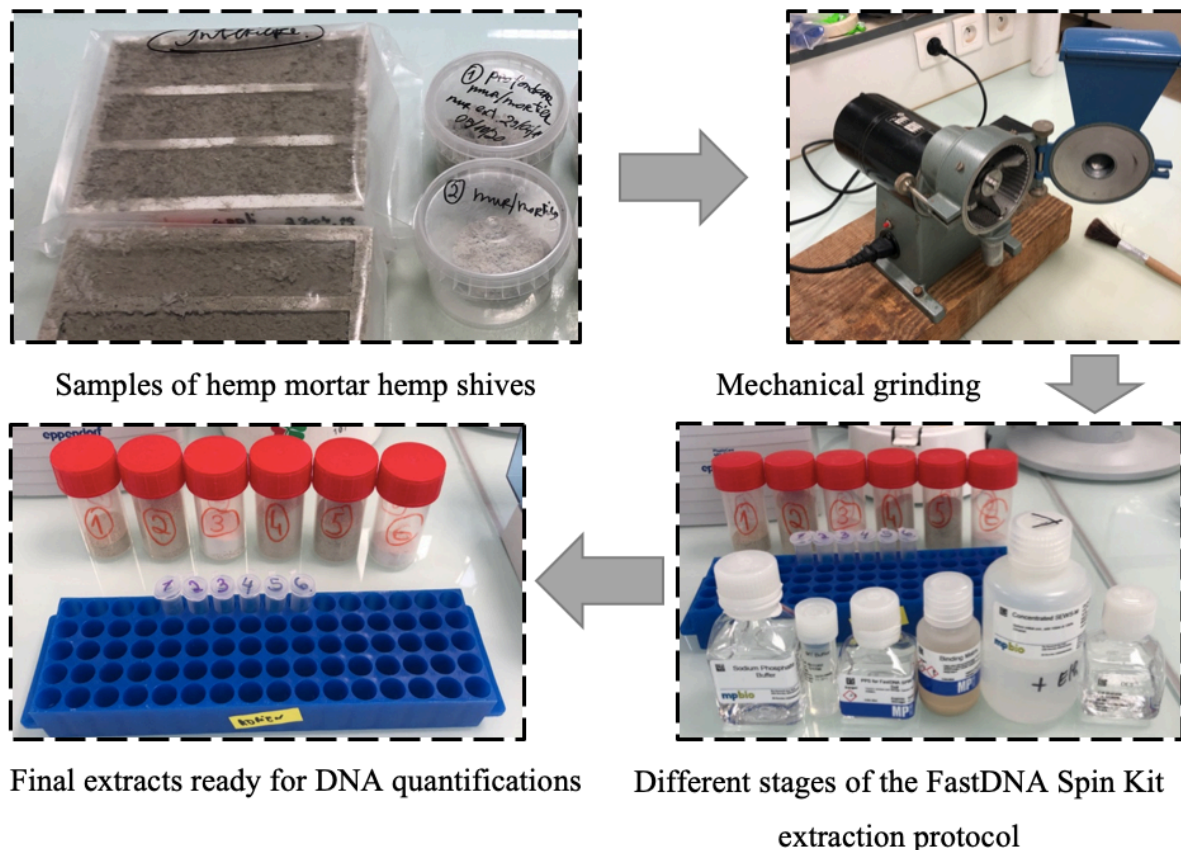


Figure 108. DNA extraction protocol schema

### VI.3.4. Real-time polymerase chain reaction (PCR) amplification

The 16S rDNA amplifications for fungal biomass estimation by 16S rDNA real-time quantitative polymerase chain reaction (hereinafter - qPCR) were performed with a total volume of 25  $\mu$ l. The qPCR mixture was prepared as follows: 10 ng of microbial DNA from our samples, 0.5  $\mu$ M of each primer [63f 5'-CAGGCCTAACA CATGCAAGTC-3' (Marchesi et al., 1998) and BU16S4 5' CTGCTGCCTCCCGTAGG-3'] derived from 341F (Muyzer et al., 1993), 25  $\mu$ l of absolute qPCR SYBR Green Mix (Thermo Scientific) and 0.25  $\text{mg}\cdot\text{ml}^{-1}$  BSA (GeneOn). Standard curves were obtained using serial dilutions of linearized plasmids containing the cloned 16S rRNA genes from the *Pseudomonas aeruginosa*. The results are expressed as the number of copies of the 16S rDNA gene per  $\mu$ l. The amplification protocol

(40 cycles of PCR, 40 s at 95 °C, 45 s at 64 °C and 30 s at 72 °C) was performed in the qPCR (LightCycler® 480, Roche Diagnostics, Penzberg, Germany). The efficiency of the qPCR ranged from 90 % to 100 %.

### **VI.3.5. Metagenomic analysis of microbial community**

#### **VI.3.5.1. Library construction, and metagenomic sequencing**

The two highest concentration of DNA extracted from hemp and hemp mortar samples were analyzed by a metagenomic approach targeting the 16S region at Genoscreen platform (Lille, France). A clone library was generated by the MetaBiote® kit. Illumina MiSeq was used for the preparation of the amplicon libraries. In order to limit the amplification bias, the amplicon libraries include a positive and negative control named ABCv2-57049 and BF-57049. These controls were used and treated as samples during the MiSeq libraries process stages. The assays are performed by a fluorimetric method and the qualitative controls by capillary electrophoresis. After validation of the libraries (10 libraries: 6 samples and 4 controls), they were diluted to 10 nM and controlled qualitatively and quantitatively by high-sensitivity capillary electrophoresis.

#### **VI.3.5.2. Data metagenomic sequencing analyses**

Amplicons were sequenced on MiSeq sequencer and the quality of the generated sequence readings was evaluated using the QIIME (Quantitative Insights into Microbial Ecology) program (version 1.9.1) based on Metabiote® pipeline (Bartram et al., 2011; Caporaso et al., 2011). Similarity data and phylogenetic analysis were combined to defined operational taxonomic units (OTUs). An OTU was defined when the percentage of similarity exceeded 97 %. These sufficient, complete and high quality 16S full length sequences allowed us to perform affiliation in order to obtain the taxonomic profile of prokaryotic populations identified within the studied samples. Since the DNA of the negative control has been sequenced, the bacterial genera present in the control sample were subtracted from the results of the extraction of the hemp shivs and hemp mortar. Further sequence identification and classification was conducted by Greengenes<sup>7</sup> (version 13.8) using v2.2 of RDP classifier (Wang et al., 2007). In order to compare results obtained from the source / material point of view, the

---

<sup>7</sup> [www.greengenes.gov](http://www.greengenes.gov)

Venn diagram was plotted, which represents the number of genera present in hemp shivs, in a hemp mortar and in both materials.

## **VI.4. BACTERIAL DNA SEQUENCING DATA ANALYSIS**

### **VI.4.1. DNA extraction**

After the extraction step, quantification of the fluorimeter analysis was conducted to determine if the DNA extraction kit was properly selected. Two replicates were performed for each sample. The samples with the highest total DNA concentration were 7.53, 46.49 and 0.23 ng/ $\mu$ l for the hemp shivs, hemp mortar and control sample, respectively. These samples were used for the DNA sequencing. Based on the total concentrations, it was noted that the extraction method worked well and that sufficient DNA was extracted. At the same time, as the FastDNA SPIN Kit used for DNA extraction is dedicated to extract all the DNA from soil, i.e. plant, bacterial and fungal DNA, in the resulting mixture all have been extracted. Then, in order to identify the concentration of the bacterial DNA, the qPCR analysis of the extracts from hemp shivs and hemp mortar was conducted. The quantity of copies of  $3.64 \cdot 10^6$  and  $1.09 \cdot 10^4 \mu\text{l}^{-1}$  for hemp shivs and hemp mortar respectively was obtained. The extracts of total DNA were used after for the rDNA sequencing.

### **VI.4.2. Rarefaction analysis**

To validate the representativeness of the hemp mortar and hemp shivs sampling across the entire sample, the diversity was studied. To do so, the OTUs observed for hemp shivs, hemp mortar and negative control samples as a function of an increasing number of sequences were plotted (Figure 109). As the number of the sequences for negative control sample is too low, the curve for this sample is not presented. Thus, we consider an exhaustive description of the diversity of the samples when the curve reaches the plateau. The so-called "plateau" phase is attained for all samples by demonstrating an exhaustive description of the prokaryotic diversity.

Nevertheless, we note that the diversity for hemp shivs is greater, which could be due to less favorable conditions in hemp mortar. It can also be explained by the nature of plant fibers which are heterogeneous dimensionally (hemp aggregate size) and where traces of dust and contamination (due to industrial retting process) can be found.

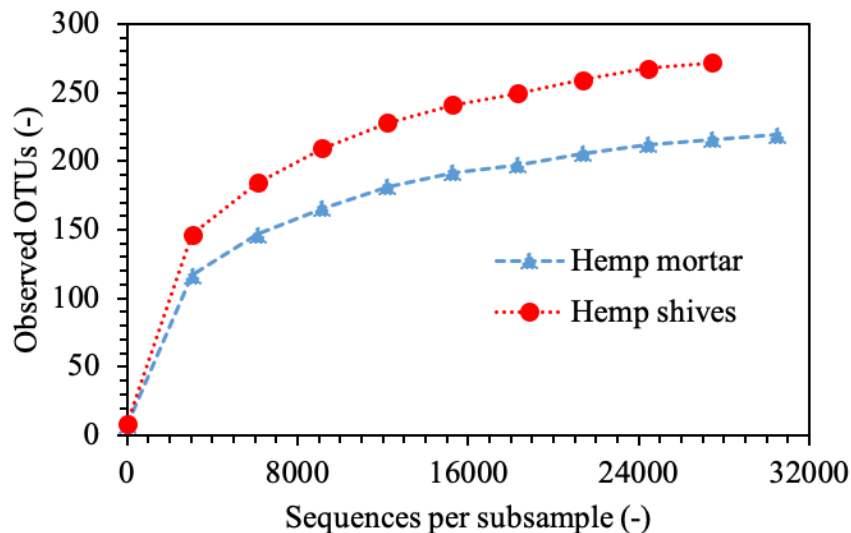


Figure 109. Rarefaction analysis of the observed OTUs for the hemp shivs, the hemp mortar and the negative control as a function of an increasing number of sequences

### VI.4.3. Identification of bacterial species

After subtraction of the bacterial genera present in the negative control, 7 different phyla remain present in the studied samples of hemp shivs and hemp mortar.

We can see in Figure 110 that Proteobacteria and Bacteroidetes are the dominant phylum with 77.05% and 18.5% in the hemp shivs and decreased to 35.3% and 2.9% in the hemp mortar respectively. At the same time, Actinobacteria and Firmicutes phyla increased their abundance in hemp mortar (42.2% and 19.6%) compared to hemp shivs (3.5% and 0.9 respectively). Representatives of other phyla stay minor with little changes in abundance: FBP and Elusimicrobia phyla decreased their presence after mortar production from 0.05% and 0.012% to 0.022% and 0% respectively. Similarly, microorganisms that were not classified until the genus represented 0.006% in hemp shivs and totally disappeared in hemp concrete. However, Verrucomicrobia that is not present in hemp shivs represents 0.015% in hemp mortar due to external contamination (Figure 110).

For further investigation, the bacterial abundances from hemp shivs and hemp mortar were analyzed separately. 111 and 108 bacterial genera were identified in hemp shivs and hemp mortar samples respectively (Fig. 111 - 113). Some bacteria were not identified up to the genus, but are reported to the phylum, which is represented in the figure above. For example, there are 40 undefined fungi (12% total abundance) and 34 undefined fungi (19% total abundance) in hemp shivs and hemp mortar respectively that have not been identified and are represented as "Other/unclassified" (Fig. 111 - 113).

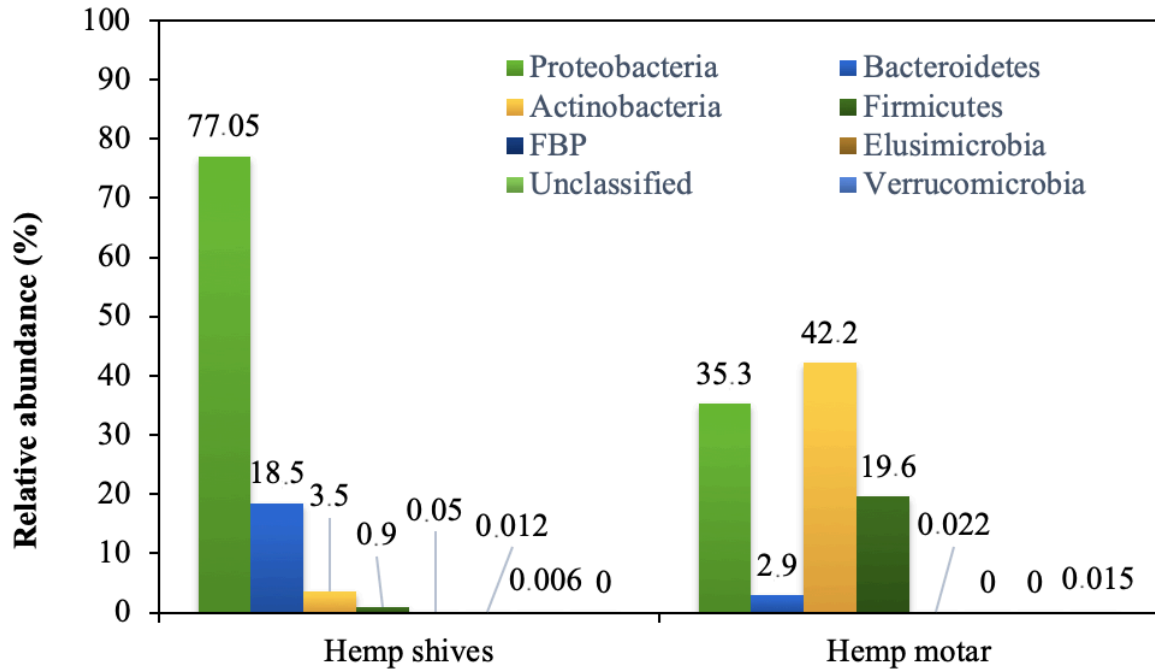


Figure 110. Relative abundance levels of each bacterial phylum for hemp shivs (left) and hemp mortar (right)

In hemp shivs, the majority of the identified genera (abundance over 1%) are the representatives of the Proteobacteria phylum: *Janthinobacterium* (29%), *Agrobacterium* (17%), *Rhodobacter* (7%), *Devosia* (4%), *Brevundimonas* (4%) and *Luteimonas* (3%). The second most abundant branch is that of Bacteroidetes with four genera: *Chryseobacterium* (7%), *Pedobacter* (5%), *Flavobacterium* (3%) and *Sphingobacterium* (1%) (Fig. 9).

In the case of the hemp mortar samples, Proteobacteria phylum remains its high abundance with 3 major genera: *Burkholderia* (26%), *Janthinobacterium* (4%) and *Agrobacterium* (2%). The *Burkholderia* genus is also present in hemp shivs, but after the application it has considerably increased its abundance. At the same time, *Janthinobacterium* and *Agrobacterium* genera decreased. The phylum Actinobacteria increased its abundance and started to dominate. The main genera are *Streptomyces* (17%), *Actinoalloteichus* (11%), *Nocardiopsis* (10%) and *Promicromonospora* (3%). The principal representatives of the phyla Bacteroidetes and Firmicutes are *Chryseobacterium* (1%) and *Paenibacillus* (1%) respectively (Figure 112). The trophic cycles analysis of these genera was conducted further in the paragraph 4.

In addition, the Venn Diagram shows that there is almost the same quantity of bacterial genera in hemp shivs and mortar (Figure 113). It is different from the mold population analyses where hemp shivs represented more genera, which could be explained by stronger ability of

bacteria to survive even in extreme alkaline conditions. As for the bacterial population that is present in hemp shivs and that was not isolated in hemp mortar, there are 39% of sequences that were not identified before the genus in hemp shivs. They are represented by "Other/unclassified" (Figure 113). The major genera present only in hemp shivs are *Enterococcus* (20%) and *Carnobacterium* (3%) from the phylum Firmicutes, *Brevibacterium* (8%) and *Williamsia* (5%) from the phylum Actinobacteria and *Ewingella* (6%) from Proteobacteria.

As for bacteria present in both hemp shivs and the hemp mortar, there are 10 and 8 major genera (abundance more than 1%) respectively. Hemp shivs represent bacteria from two phyla: *Chryseobacterium* (7%), *Pedobacter* (5%), *Flavobacterium* (3%) and *Sphingobacterium* (1%) from Bacteroidetes phylum and *Janthinobacterium* (30%), *Agrobacterium* (18%), *Rhodobacter* (7%), *Devosia* (4%), *Brevundimonas* (4%) and *Luteimonas* (3%) from Proteobacteria. After the mortar cast and consecutive contamination by molds, the bacterial population changed and we note that there are the major representatives of four phyla in hemp mortar: *Burkholderia* (29%), *Janthinobacterium* (4%), *Agrobacterium* (2%) from Proteobacteria, *Streptomyces* (19%), *Actinoalloteichus* (12%) and *Promicromonospora* (3%) from Actinobacteria, *Chryseobacterium* (1%) from Bacteroidetes and *Paenibacillus* (1%) from Firmicutes.

Among the bacteria that are present only in the hemp mortar, two genera from the phylum Actinobacteria can be distinguish: *Nocardiopsis* (93%) and *Jiangella* (1%). Also, there are 2% of unclassified bacteria (Figure 113).

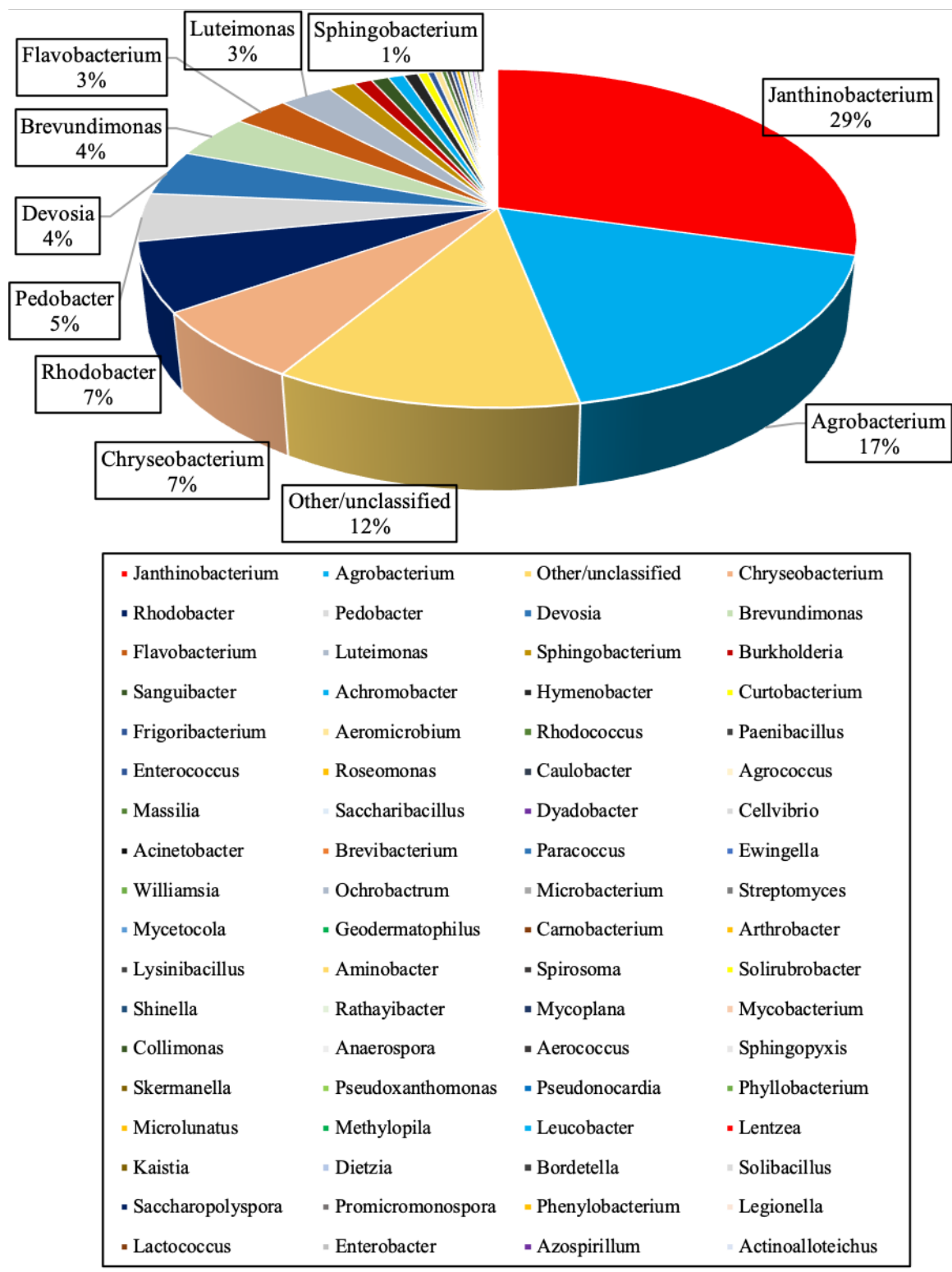


Figure 111. Bacterial community analysis in hemp shivs (16S rDNA)

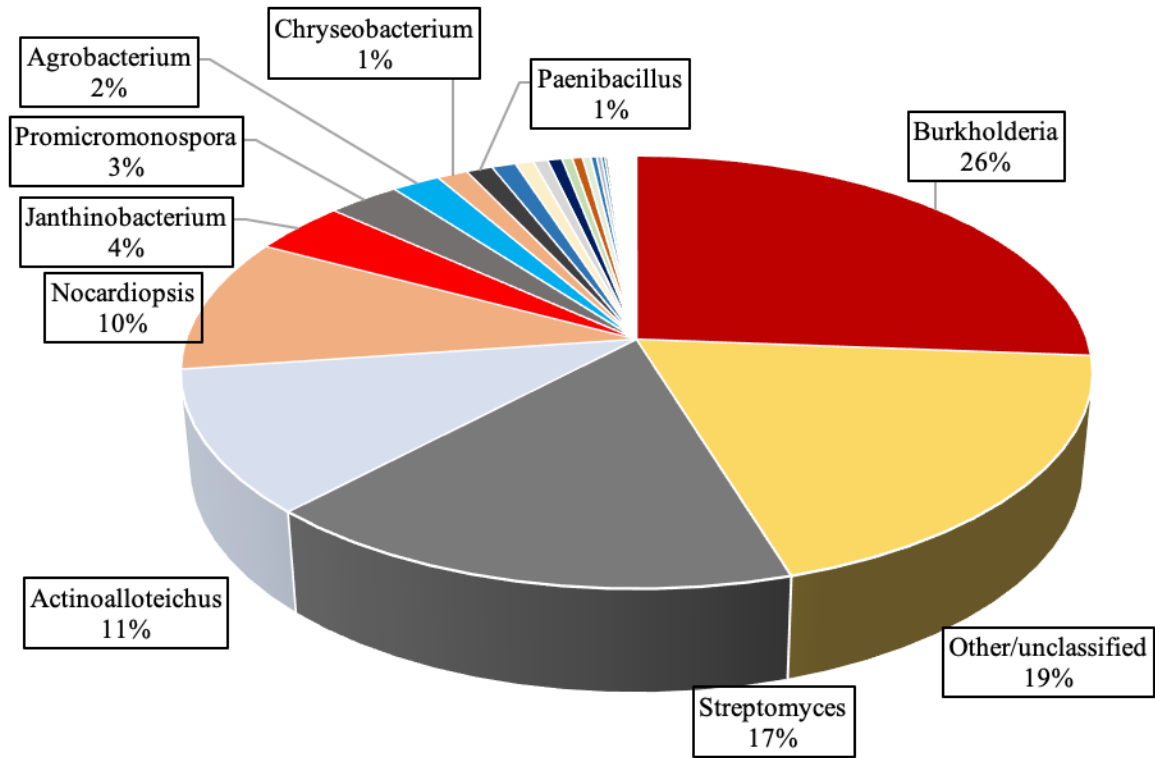


Figure 112. Bacterial community analysis in hemp mortar (16S rDNA)



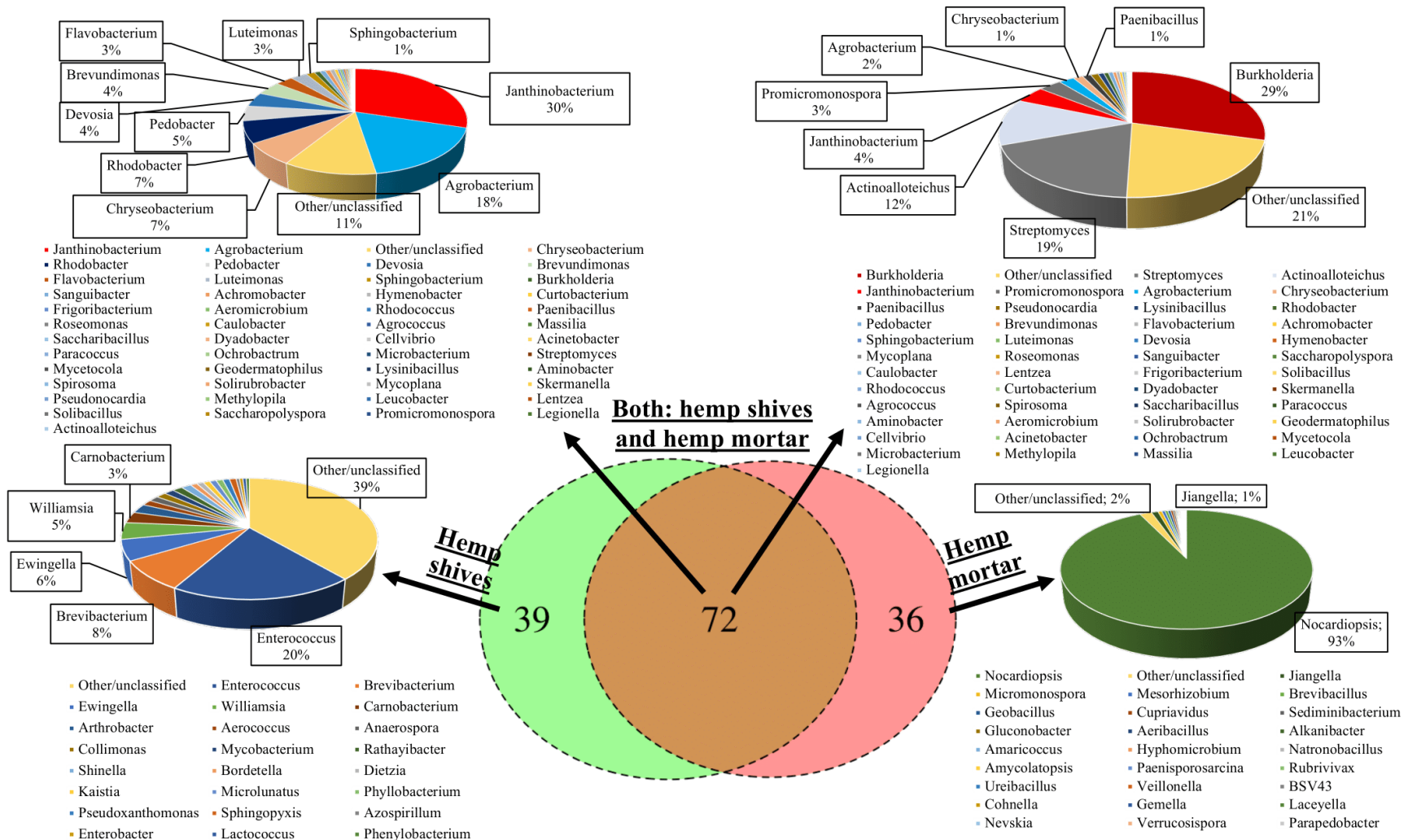


Figure 113. Venn Diagram evaluating the concentration of bacterial contamination of hemp shivs, hemp mortar and both hemp shivs and mortar

## VI.5. ANALYZE OF MAJOR BACTERIAL GENERA AND DISCUSSION

To better understand the bacterial population in hemp shivs and mortar, the analyze of trophic cycle of the representatives of major genera is proposed in this section. First of all, it should notice that the bacterial genera present only in hemp shivs are not major (their abundance is lower than 1%) in the total bacterial population of hemp shivs. For example, the most abundant genus *Enterococcus* represents only 0.23% among total bacterial community. We have therefore chosen here the majority criterion of 3% between the genera present only in hemp shivs.

### VI.5.1. Hemp shivs bacterial contamination

By applying this criterion, besides *Enterococcus*, we can distinguish *Brevibacterium* (8%), *Ewingella* (6%), *Williamsia* (5%) and *Carnobacterium* (3%). Also, we note that there are 16 types of bacteria that have not been identified before the species, they are regrouped in “Other/unclassified”.

*Enterococcus* spp. are Gram-positive opportunistic anaerobic bacteria, that are cosmopolitan and can be found in different natural habitats such as soil and water, but are known to inhabit predominantly gastrointestinal tract of humans and animals (Isnard, 2017; Micallef SA et al., 2013; Schloissnig et al., 2013). Representatives of this genus, mainly *Enterococcus faecium* and *Enterococcus faecalis* are known to provoke the different infections worldwide (Guzman Prieto et al., 2016; Hooton, 2012). The authors of the study (Fisher and Phillips, 2009; Sykes, 2014) reported that *Enterococcus* spp. are able to survive at a range of stresses and hostile environments, including those with extreme temperature (5–65 °C), pH (4.5–10.0). At the same time, (Mubarak and Soraya, 2018) discovered that *Enterococcus faecalis* is capable to adapt to acidic environments (pH 2.9–4.2).

*Brevibacteria* are nonmotile, nonspore-forming, nonacid fast, Gram-positive, obligate aerobe organisms with a growth temperature range of 4–42 °C and an optimum temperature of 21–28 °C. *Brevibacteria* grow over a wide pH range, starting at pH 5.5 and continuing to 10 with the optimum being about 7.0. Representatives of genus *Brevibacterium* have the capability to metabolize different sources of carbon and nitrogen for growth, they use glucose and galactose as a source of carbon and ammonium sulfate as nitrogen and sulfur source (Forquin and Weimer, 2014; Huang and Tang, 2007).

The genus *Ewingella* is represented by its type-species *Ewingella americana* known as Gram-negative, facultative anaerobic, lactose fermenting, oxidase negative, catalase positive bacillus, first described in 1983 by Grimont et al. (Grimont et al., 1983). It was classified in a new

group in the *Enterobacteriaceae* family. Rarely, but *Ewingella americana* is known to provoke different human infections like peritonitis (Kati et al., 1999), conjunctivitis (Da Costa et al., 2000) or pneumonia (Pound et al., 2007). It has been isolated from intestinal contents of snails and slugs (Müller et al., 1995), fresh nutria carcasses, vacuum packaged meat (Helps et al., 1999), and mushrooms (Reyes et al., 2004) as well.

The genus *Williamsia* is represented by colonies of Gram-positive, aerobic, rod-like and coccoid bacteria, smooth and pigmented, orange-red in color (in some species) and not acid-resistant. Representatives of the genus *Williamsia*, e.g. *Williamsia aurantiacus* sp., *Williamsia muralis*, and *Williamsia serinedens* sp., were reported to growth at 10-45°C (optimum 28 °C), in a pH from 4.0 to 10.0 (optimum pH 5–8) (de Menezes et al., 2019; Kämpfer et al., 1999; Yassin et al., 2007).

The genus *Carnobacterium* is represented by Gram-positive rod-shaped acetate sensitive bacteria that have an ability to grow in chiller temperature (Cailliez-Grimal et al., 2014). Although they are lactic acid-producing bacteria, they grow in a pH range of 7–9. Most of the species produce lactic acid by fermenting carbohydrates such as glucose (Lorenzo et al., 2018). Representatives of this genus are known for their potential use in the food industry because of production of bacteriocins (Davidson and Zivanovic, 2003).

We note that all these bacteria were minor in the hemp shivs and didn't survive in the extreme environment like fresh hemp mortar (pH>12.5). Also, these microorganisms are pathogens for human, that's why we conclude that the use of hemp in combination with the alkaline mineral binder is one of the factors to decrease the bacterial contamination of the hemp mortar. This is important when it comes to the industrial use of the material in contact with humans from the point of view of air quality and hygiene.

### **VI.5.2. Hemp shives and hemp mortar contamination**

Nevertheless, there are representatives of 72 genera that are present in the hemp shivs and survived after hemp mortar cast. Hemp shivs represent 10 major genera: *Janthinobacterium* (30%), *Agrobacterium* (18%), *Chryseobacterium* (7%), *Rhodobacter* (7%), *Pedobacter* (5%), *Devosia* (4%), *Brevundimonas* (4%), *Flavobacterium* (3%), *Luteimonas* (3%) and *Sphingobacterium* (1%) and hemp mortar 7 major genera: *Burkholderia* (29%), *Streptomyces* (19%), *Actinoalloteichus* (12%), *Janthinobacterium* (4%), *Promicromonospora* (3%), *Agrobacterium* (2%), *Chryseobacterium* (1%) and *Paenibacillus* (1%).

The genus *Janthinobacterium* is represented by Gram-negative soil bacteria, they are also named violet or violet-blue bacteria because of their ability to produce the purple-violet pigment. These microorganisms are tolerant of cold and ultraviolet radiation. Some species as

*Janthinobacterium lividum* can grow in extreme conditions of Antarctic peninsula at pH 4 to 9 with optimum at pH 6.8 and from 2 to 28°C with an optimum at 15°C (Shivaji et al., 1991). Also, representatives of the genus *Janthinobacterium* were isolated from different habitats as rainbow trout in Korea (Oh et al., 2019), inner elbows of healthy people (Grice et al., 2008) or western Himalayan subglacial lakes (Yadav et al., 2019).

*Agrobacteria* are a genus of Gram-negative, motile (up to six flagella per cell), aerobic (using oxygen as a final electron acceptor during cellular respiration), rod-shaped, non-spore-forming soil bacteria. These microorganisms are often isolated from abnormally proliferating plant tissues. *Agrobacteria* are able to catabolize a large variety of metabolites. They exhibit chemotactic behavior for some plant exudates, which they use in nature to initiate colonization of susceptible plant tissue (Lacroix and Citovsky, 2013). *Agrobacteria* show a remarkable resistance to desiccation. A bacterial colony left on an agar plate, at room temperature, can survive more than 6 months (Van Montagu, 2001). They are pathogens of the plants, the optimal temperature for their growth being 24 - 28°C.

*Chryseobacterium* spp. is represented by gram-negative, aerobic rods that are pigmented yellowish orange (O'Rourke and Rosenbaum, 2015). They usually grow between 5° and 30° C, but strains isolated from human specimens, including *E. meningoseptica*, grow readily at 37 °C (Wisplinghoff, 2017). *Chryseobacterium* species are inhabitants of soil and water and can be recovered from a variety of foods. They can be found in municipal water supplies despite adequate chlorination and have been recovered from the hospital environment, often in conjunction with clusters of clinical isolates. *Chryseobacterium* species are organisms of low virulence, and their presence in clinical specimens usually represents colonization and not infection (Steinberg and Burd, 2015).

The genus *Rhodobacter* spp. regroups aquatic photosynthetic bacteria, found in the marine environment or fresh water. *Rhodobacter* expresses different respiratory modes (aerobic or anaerobic), allowing it to survive in a large number of habitats. One of the example of this genus are *Rhodobacter sphaeroides* and *Rhodobacter capsulatus* that are well-studied species in fundamental research, in particular on the study of bacterial photosynthesis, adaptation to the environment and evolution (Gürkan et al., 2020; "06/00850 Hydrogen photosynthesis by *Rhodobacter capsulatus* and its coupling to a PEM fuel cell," 2006; Jeong et al., 2020; Magnin and Deseure, 2019). *Rhodobacter sphaeroides* WS8 is known to grow in a pH range of 6-9. Sustained motility was, however, observed in resuspended cell populations at pH values between 4.9 and 10.4 (Packer et al., 1994).

*Pedobacter* spp. is a genus of Gram-negative soil-associated bacteria that were isolated worldwide, from cold to temperate climatic conditions, and most have been isolated from

environmental terrestrial and aquatic habitats (Zhang et al., 2010; Margesin and Zhang, 2013; Chaudhary et al., 2017; He et al., 2020; Kangale et al., 2020). It has been reported that *Pedobacter bauzanensis* sp. nov. can grow at a temperature of 5-25 °C (Zhang et al., 2010). *Pedobacter kyonggii* sp. nov. grows at 0–32 °C, at pH 5.0–10.0 and with 0–1.5 % (w/v) NaCl (Chaudhary et al., 2017). *Pedobacter indicus* sp. nov. grows at 15–40 °C (optimum, 28 °C), at pH 5.0–9.0 (optimum, pH 6.0–7.0) and with 0–8% (w/v) NaCl (optimum, 1.5%) (He et al., 2020).

The genus *Devosia* is represented by Gram-negative, motile (by flagella), aerobic, oval or rod-shaped and non-spore forming bacteria. The microorganisms were isolated from different habitats worldwide (Rivas et al., 2003, 2002; Talwar et al., 2020; Xu et al., 2017; Yoon et al., 2007). *Devosia insulae* sp. nov. was reported to grow at optimal pH of 6.5-7.5 and between 10 and 31 °C (with an optimum at 25°C) in the presence of 0.5 % (w/v) NaCl (Yoon et al., 2007). *Devosia nitraria* sp. nov. showed the optimal growth at 30°C (and was inhibited at pH of 4.37 and 40°C) and at pH 7 with some growth up to a pH level of 11 (Xu et al., 2017).

*Brevundimonas* spp. is represented by Gram-negative, non-fermenting, aerobic bacteria. Some strains has been isolated from clinical samples and are known to provoke several human infections (Panasiti et al., 2008; Lee et al., 2011; Ryan and Pembroke, 2018). At the same time, another representative of the genus, *Brevundimonas terrae* sp. nov. was isolated from alkaline soil in Korea. It grew optimally at pH 7.5-8.0 and 30°C without NaCl (Yoon et al., 2006).

*Flavobacterium* species are Gram-negative rods, non-spore-forming, strictly aerobic and motile by gliding. Representatives of this genus were isolated worldwide from various habitats such as diseased fish, microbial mats, freshwater and river sediments, seawater and marine sediments, soil, glaciers, and Antarctic lakes (Waśkiewicz and Irzykowska, 2014). They have been isolated from many chilled foods (Betts, 2006). Most *Flavobacterium* are harmless, but some are opportunistic or true pathogens and cause disease in a wide variety of organisms, including plants, fish, and humans (Waśkiewicz and Irzykowska, 2014).

*Luteimonas* spp. is represented by Gram-reaction negative, aerobic, rod-shaped bacillus. They were isolated from wormcast (Cha et al., 2020), intertidal macroalga (Verma et al., 2016), granules of wastewater treatment plant (Siddiqi et al., 2020) or food waste (Young et al., 2007). *Luteimonas lumbrici* sp. nov. showed an optimal grow at 30 °C, pH 7.0 and with 0% (w/v) NaCl (Cha et al., 2020). *Luteimonas granuli* sp. nov. grew optimally at 30 °C and at pH 7.0 (Siddiqi et al., 2020). *Luteimonas composti* sp. nov. was referenced to grow at 20-45°C (optimum at 30°C) at pH 7.0-10 with optimum at 7.0 (Young et al., 2007).

The genus *Sphingobacterium* consists of Gram-negative environmental bacilli rarely involved in human infections (“Bacteremia caused by a novel species of *Sphingobacterium* | Elsevier Enhanced Reader,” n.d.). Nevertheless, several representatives of the genus

*Sphingobacterium* spp. are known to provoke different human infections (Lambiase et al., 2009; Barahona and Slim, 2015; Abro et al., 2016). Meanwhile, other members of the genus were isolated from soil (Fu et al., 2017), lake water (Albert et al., 2013) or deep subsurface aquifer (He et al., 2019). *Sphingobacterium soli* sp. nov., isolated from soil grew optimally at 30°C, at pH 7.0 and with 0–3 % (w/v) NaCl (Fu et al., 2017). For *Sphingobacterium puteale* sp. nov. the optimal growth was obtained at pH 7.0 (range: 6.0–9.0), 28 °C (range: 15–37 °C) and 0% NaCl (range: 0–1.5%, w/v) (He et al., 2019).

The genus *Burkholderia* is very heterogenous group and contains more than 30 species isolated from many places such as water, soil, plants, insects, animals, and also human beings (Horinouchi et al., 2010, p.; Van Dommelen and Vanderleyden, 2007). Bacteria of the genus *Burkholderia* are often symbiotic and sometimes have negative effects on their hosts, for example *Burkholderia cepacia* is known to infect a range of hosts, including insects (Uehlinger et al., 2009). *Burkholderia vietnamiensis* sp. was the first species found to fix atmospheric azote, it was discovered in association with roots of rice, maize roots and coffee plants (Van Tran et al., 1996). The invasive *Burkholderia* species, *Burkholderia pseudomallei* and *Burkholderia mallei*, cause a remarkably wide range of disease outcomes, varying from subacute, localized inflammation to severe organ system damage and overwhelming septicaemia. *Burkholderia pseudomallei* can be isolated from environmental samples such as soil and water (Inglis and Merritt, 2015; Wisplinghoff, 2017). For instance, *Burkholderia unamae* could only be isolated from the rhizosphere of plants growing in soils, with a pH ranging from 4.5 to 7.1, but not from soils with a pH higher than 7.5 (Caballero-Mellado et al., 2004; Stopnisek et al., 2014).

The *Streptomyces* species are Gram-positive bacteria that grow in different environments. They grow as network of filaments that resemble to filamentous fungi. The morphological differentiation of *Streptomyces* involves the formation of a layer of hyphae that can differentiate into a chain of spores (de Lima Procópio et al., 2012). Most members of *Streptomyces* are saprophytes, but several strains may infect and cause disease to humans, including wound contamination and abscess formation. Only a few *Streptomyces* have been isolated from pathological material (Sharma et al., 2014). *Streptomyces* bacteria are the most important source of antibiotics (Chater, 2013). Most representatives of the genus grow optimally at 25-35°C and a pH of 6.5-8.0 (Kontro et al., 2005; Mohammadipanah et al., 2014).

Although the characteristics of *Actinoalloteichus* spp. were firstly described by Liu et al. (Liu, Z. et al., 1984) at 1984, the genus name was validly published by Tamura et al. (Tamura et al., 2000). Representatives of the genus were isolated from different environments like different soils (Liu, Z. et al., 1984; Singla et al., 2005), marine sponge (Nouioui et al., 2017; Zhang et al., 2006) or fig tree (Xiang et al., 2011). The *Actinoalloteichus* species grow at 20-37°C with the

optima at 25-28°C, and pH level 6-11 (optimum at pH 8) (Nouioui et al., 2017; Singla et al., 2005; Tamura et al., 2000; Xiang et al., 2011; Zhang et al., 2006).

The genus *Promicromonospora* is represented by the Gram-positive aerobic bacteria (Schumann and Stackebrandt, 2015). They were isolated from soil (Mohammadipanah et al., 2017), marine sediments (Thawai and Kudo, 2015), air (Busse et al., 2003) or medicinal plants (Qin et al., 2012). Most of the species grow at the range of 20 - 37°C and pH level 5-9 (Busse et al., 2003; Mohammadipanah et al., 2017; Qin et al., 2012; Thawai and Kudo, 2015).

*Paenibacillus* is a genus of facultative aerobic or anaerobic bacteria, forming rod-like endospores with Gram-positive or variable Gram. They were isolated worldwide from fresh and salt water, alkaline soil, sediments, compost, plants, food or clinical samples (Beno et al., 2020; Grady et al., 2016; Sáez-Nieto et al., 2017). The representatives are known for their ability to promote the plant growth or to produce different extracellular enzymes such as polysaccharide-degrading enzymes, so they are used in agriculture, horticulture and cosmetic industry. Depending on the species, the growth occurs at wide range from 15 - 45°C (some species were isolated from Antarctic soil (Dsouza et al., 2014)) and pH level of 5.5 to 9.5 (Kämpfer et al., 2012; Yoon et al., 2005).

### **VI.5.3. Hemp mortar contamination**

As one can see in Figure 113, there are 36 genera of bacteria that are present only in hemp mortar and are due to external contamination after the mortar cast. 10 bacterial types have not been identified before the genus, so they are referenced as “Other/unclassified”. We note the most present and abundant genus is *Nocardiopsis*.

*Nocardiopsis* spp. is represented by aerobic, Gram-positive, non-acid-fast, catalase-positive soil bacteria. Members of the genus are ecologically versatile and biotechnologically important. They produce a variety of bioactive compounds such as antimicrobial agents, anticancer substances, tumorinducers, toxins and immunomodulators (Bennur et al., 2016, 2015; Ibrahim et al., 2018). Representatives of the genus are ubiquitously distributed in the environment (Kroppenstedt and Evtushenko, 2006). Many of these species prefer moderately alkaline conditions. For example, *Nocardiopsis algeriensis* sp. nov. showed a good growth at 20–45°C and pH 7.0–12.0, with optima at 25–35°C and pH 7.0–10.0 (Bouras et al., 2015) or *Nocardiopsis sediminis* sp. nov. that grew at the temperature range 20-40°C (with optimum at 25-28°C) and pH 6-11 (with optimum at pH 7-10) (Muangham et al., 2016).

The *Jiangella* genus was firstly proposed by Song et al. (Song, L et al., 2005) and is represented by aerobic, Gram-positive bacteria that grow at temperature between 15-45°C (optimum 28°C) and at pH 6.5-9 (optima at pH 7) depending on the strain. The representatives

were isolated from plant stems (Qin et al., 2012), rhizosphere soil or rhizome of plants (Han et al., 2019; Niemhom et al., 2019) and soil (Hilal Ay et al., 2019).

So, we noticed that there are 39 bacterial species that didn't survive in the hemp mortar. This is a positive effect of the hemp matrix due to its high alkalinity and the possibility to eradicate the pathogenic bacterial species (like the representatives of the genus *Enterococcus* spp. or *Ewingella* spp.). Meanwhile, the results of the rDNA sequencing show that hemp shivs are the main source of bacterial contamination for hemp mortar. Also, we note that the major bacterial genera from hemp shivs and hemp mortar are cosmopolitan and widely present in the world. Some of them grow better under alkaline conditions (as for example, *Burkholderia* spp., *Streptomyces* spp., *Actinoalloteichus* spp.), which explain their presence in final hemp mortar (high alkalinity – pH about 12.5). The following contamination by *Nocardiopsis* spp. could be provoked by its possibility at the same time to grow in alkaline environments and produce different antimicrobial agents (inhibits other bacteria). That gives to *Nocardiopsis* species an advantage for its proliferation. Finally, we note that environmental conditions play a crucial role in the durability of hemp mortars and especially the bacterial growth due to the conditions of bacterial proliferation (humidity, temperature, pH level, etc.) and even more so due to the external contamination.

## **VI.6. CONCLUSION**

This chapter focuses on the metagenomics analysis and identification of bacterial communities present in hemp mortar collected in situ after its contamination by molds and its raw materials - hemp shivs. To better understand the studied bacterial communities, an accurate protocol based on DNA extraction and sequencing of hemp shivs and hemp mortar has been developed. This protocol could also be used for other composite cementitious materials. In this study, samples of hemp mortar collected in situ and its source - hemp shivs - were analyzed to understand the interconnection between the bacterial contamination of raw hemp shivs and final hemp mortar. Firstly, the DNA extraction method was carefully selected basing on the results of the quantification of total DNA and extracted bacterial DNA. Secondly, the diversity of the studied samples using the rarefaction analysis was evaluated to guarantee the representativeness of the results. Then, the accurate identification of the bacterial genera that are present in hemp shivs and hemp mortar was conducted, allowing the analysis of the trophic cycle of the main fungi.

Mold proliferation on the hemp mortar was observed after one month of exposure to extremely aggressive conditions (high humidity, low temperature, no ventilation) which are not appropriate for biobased insulating materials. That is promising for studied use of hemp mortar.

According to the results of the bacterial DNA sequencing, the largest number (72) of representatives of genera present in the hemp shivs survived and became major in the hemp mortar.



So, hemp shivs are the most important source of bacterial contamination of hemp mortar. We found that the species of the 39 genera were eradicated due to addition of the mineral binder, which decrease the bacterial contamination of the hemp mortar, especially by pathogenic bacterial species (like the representatives of the genus *Enterococcus* spp. or *Ewingella* spp.). Moreover, the analyze of the trophic cycles of the major genera allowed to explain the proliferation of bacteria. We mentioned that most bacteria are cosmopolitan and most live in soils and have the ability to survive in alkaline environments, for example alkaline soils or hemp mortar in our case (pH about 12.5) (such as *Burkholderia* spp., *Streptomyces* spp. and *Actinoalloteichus* spp.).

The chosen DNA extraction method could be used to characterize other types of mortars and their raw materials in different conditions. The present study opens the subject of the use of non-destructive molecular rDNA screening method for building materials that could help to understand the consistent patterns of proliferation of different types of microbiological flora and fauna. Obtained results represent an important database that must be considered when studding the durability of hemp mortars and its interaction with bacterial communities. These results also build an important database for the study of air quality in environments built with these hemp mortars. Since hemp shivs are the most important source of bacterial contamination, it is necessary to continue the study of the protection of hemp mortars against initial or external contamination (such as the different treatments of hemp shivs or the use of the essential oil additives).

## CONCLUSIONS AND PERSPECTIVES

---

## CONCLUSIONS AND PERSPECTIVES

---

The main objective of this thesis was to analyze the durability of hemp mortars and to investigate the microbiological contamination of hemp mortars in order to better understand its behavior and deterioration risk during its life cycle.

The originality of this work resides in several aspects. On the one hand, it is the study of the durability of hemp mortar using the accelerated aging cycles, which revealed different phenomenon that occur in the material during its use. This required the adoption of the experimental protocol of accelerated aging which is representative of the natural conditions. This led to the adaptation to our material use of the existing ETICS accelerated aging protocol.

On the other hand, the precise analysis of the microbiological proliferation of the hemp mortar was conducted. Firstly, the influence of molds on the chemical composition of the hemp mortars was investigated. Then, the identification of fungal and bacterial contamination of the in situ collected was conducted. This required the use of several experimental techniques of DNA extraction and sequencing rarely adopted for building materials and moreover for bio-based ones. They allowed the refine identification of the microbiological contamination profile.

First, a refine characterization of the microstructure, chemical composition and hygro-thermal properties under accelerated aging cycles was accomplished. The aging protocol was adopted taking into account different protocols available in the literature and allowed to couple different solicitations (hygric, thermal). Thus, the great complexity of the phenomena that take place at the microscopic scale was demonstrated. Indeed, two main reactions occurred: the carbonation of the mineral matrix and the mineral matrix / hemp particle interface cracking. It was revealed that these two phenomena are in contest and provoke the evolution of the hemp mortar microstructural characteristics and properties.

As for microbiological proliferation, different aspects were investigated. On the one hand, the influence of the fungal proliferation on the chemical composition of the hemp mortar was studied. First, different techniques as the scanning electron microscope (W-SEM) and the attenuated total reflectance-Fourier-transform infrared spectroscopy (ATR-FTIR) allowed to identify the fungal growth of the hemp mortar specimens. Then, other characterization methods as the X-Ray Diffraction (XRD) and the thermogravimetric analysis (TGA) were applied to analyze the chemical composition of the contaminated and non-contaminated specimens. The comparison

of obtained results demonstrated no particular influence of mold proliferation on the chemical composition of the mineral matrix of hemp mortar.

On the other hand, the identification of the microbiological species using different methods were conducted. Indeed, the phenotypical identification method was suggested as not reliable enough to get the complete profile of fungal contamination of hemp mortar because of the dependence of the results on the conditions of the growth and mold types. That is why, the metagenomic identification method was adopted that proposed the refine screening of fungal and bacterial species. The results of fungal DNA sequencing showed that the most abundant phylum was Opisthokonta. It represented 83.6% of hemp shives and 99.97% of hemp mortar mold contamination. Analysis of the identified species emphasized the interconnection between the mold strain characteristics (particularly the ability to grow in extreme environments) and their presence in hemp mortar. For example, the most abundant identified genus was *Acrostalagmus*, that represented 42% of hemp shives and 96% of hemp mortar mold contamination. This was explained by its ability to survive in alkaline environments (e.g., alkaline soils). Because more genera exist in hemp shives than in hemp mortar (37 against 25, respectively) and because the *Acrostalagmus* genus present in hemp shives is the most abundant in hemp mortar, we could conclude that hemp shives are the main source of hemp mortar contamination. However, their use conditions were also found to be significant. As a result, only eight species exist in both hemp shives and hemp mortar, and 17 species are not present in hemp shives (but instead derive from external contamination).

As for results of bacterial DNA sequencing, it was demonstrated that the largest number (72) of representatives of genera present in the hemp shivs survived and became major in the hemp mortar. So, hemp shivs are the most important source of bacterial contamination of hemp mortar. We found that the species of the 39 genera were eradicated due to addition of the mineral binder, which decrease the bacterial contamination of the hemp mortar, especially by pathogenic bacterial species (like the representatives of the genus *Enterococcus* spp. or *Ewingella* spp.). Moreover, the analyze of the trophic cycles of the major genera allowed to explain the proliferation of bacteria. We mentioned that most bacteria are cosmopolitan and most live in soils and have the ability to survive in alkaline environments, for example alkaline soils or hemp mortar in our case (pH about 12.5) (such as *Burkholderia* spp., *Streptomyces* spp. and *Actinoalloteichus* spp.).

The chosen DNA extraction method could be used to characterize other types of mortars and their raw materials under different conditions. The present study opens the possibility of using a molecular rDNA screening method for building materials that could help in understanding the consistent patterns of proliferation of different microbiological flora and fauna types. The obtained in this chapter results should be considered when studying the durability of

hemp mortars and their interaction with fungal communities. In addition, we observed that the most crucial origin of fungal contamination was hemp shives. This adds to the urgency of further studies on protecting hemp mortars from initial or external contamination, for example, by applying different treatments of hemp shives or by using essential oil additives.

Obtained results opened a lot of perspectives as a complementary to the accomplished works in the meaning of both the evaluation of the durability using the accelerated aging protocols and the study of the microbiological contamination risk assessment of biobased materials, in particular hemp mortars:

- Results of the accelerated aging study and proposed hypothesis (closing of the microporosity by the carbonation of the mineral binder and hemp particles / mineral binder interface cracking) should be verified by the analysis of the microstructure or sorption/desorption isotherms.
- Also, the results of the accelerated aging should be compared to the natural aging in situ in order to better understand the representativeness of the proposed experimental protocol.
- More refine analysis of mold influence on the microstructure and moreover on the hygro-thermal properties should be investigated.
- As the microbiological contamination depends on the region, the obtained results of the fungal and bacterial DNA sequencing should be compared to other regions.
- Moreover, the influence of the treatment with essential oils should be evaluated and the possible methods of the control of organic particles should be investigated.

## REFERENCES

- Abahri, K., Bourdot, A., Langlois, S., Alhaik, G., 2020. Impact of the accelerated aging protocols on the hemp concrete durability, in: 3rd RILEM Spring Convention and Conference, RSCC2020. Guimaraes, Portugal.
- Abro, A.H., Rahimi Shahmirzadi, M.R., Jasim, L.M., Badreddine, S., Al Deesi, Z., 2016. *Sphingobacterium multivorum* Bacteremia and Acute Meningitis in an Immunocompetent Adult Patient: A Case Report. *Iran Red Crescent Med J* 18. <https://doi.org/10.5812/ircmj.38750>
- ADEME, 2018. Climat, Air et Energie. Chiffres clés - édition 2018.
- AFN, 2010. NF P18-459 - Concrete - testing hardened concrete - testing porosity and density.
- AFSSE, 2004. Impacts sanitaires du bruit 30.
- Agence Qualité Construction, 2016. Isolants biosourcés : points de vigilance.
- Akbarnezhad, A., Xiao, J., 2017. Estimation and Minimization of Embodied Carbon of Buildings: A Review 24.
- Albert, R.A., Waas, N.E., Pavlons, S.C., Pearson, J.L., Ketelboeter, L., Rosselló-Móra, R., Busse, H.-J., 2013. *Sphingobacterium psychroaquaticum* sp. nov., a psychrophilic bacterium isolated from Lake Michigan water. *International Journal of Systematic and Evolutionary Microbiology*, 63, 952–958. <https://doi.org/10.1099/ij.s.0.043844-0>
- Almyroudis, N.G., Sutton, D.A., Linden, P., Rinaldi, M.G., Fung, J., Kusne, S., 2006. Zygomycosis in solid organ transplant recipients in a tertiary transplant center and review of the literature. *Am J Transplant* 6, 2365–2374. <https://doi.org/10.1111/j.1600-6143.2006.01496.x>
- Alonso, C., Fernandez Luco, L., García, J., Hidalgo, A., Huertas, F., 2007. Low-pH Cementitious Materials Design and Characterisation.
- Amaducci, S., Scordia, D., Liu, F.H., Zhang, Q., Guo, H., Testa, G., Cosentino, S.L., 2015. Key cultivation techniques for hemp in Europe and China. *Industrial Crops and Products, FIBRE CROPS: from production to end use* 68, 2–16. <https://doi.org/10.1016/j.indcrop.2014.06.041>
- Arizzi, A., Brümmer, M., Martín-Sánchez, I., Cultrone, G., Viles, H., 2015. The Influence of the Type of Lime on the Hygric Behaviour and Bio-Receptivity of Hemp Lime Composites Used for Rendering Applications in Sustainable New Construction and Repair Works. *PLOS ONE* 10, e0125520. <https://doi.org/10.1371/journal.pone.0125520>
- Arizzi, A., Viles, H., Martín-Sánchez, I., Cultrone, G., 2016. Predicting the long-term durability of hemp–lime renders in inland and coastal areas using Mediterranean, Tropical and Semi-arid climatic simulations. *Science of The Total Environment* 542, 757–770. <https://doi.org/10.1016/j.scitotenv.2015.10.141>
- Arnaud, L., Gourlay, E., 2012. Experimental study of parameters influencing mechanical properties of hemp concretes. *Construction and Building Materials* 28, 50–56. <https://doi.org/10.1016/j.conbuildmat.2011.07.052>
- Asprone, D., Durante, M., Prota, A., Manfredi, G., 2011. Potential of structural pozzolanic matrix–hemp fiber grid composites. *Construction and Building Materials* 25, 2867–2874. <https://doi.org/10.1016/j.conbuildmat.2010.12.046>
- Aust, H.J., Bashi, E., Rotem, J., 1980. Flexibility of plant pathogens in exploiting ecological and

biotic conditions in the development of epidemics. Presented at the Comparative epidemiology - a tool for better disease management. Muenchen (Germany, F.R.). 16-23 Aug 1978.

- Bacteremia caused by a novel species of *Sphingobacterium* | Elsevier Enhanced Reader [WWW Document], n.d. <https://doi.org/10.1111/j.1469-0691.2003.00801.x>
- Bandoni, R.J., 1984. The Tremellales and Auriculariales: An alternative classification. *Transactions of the Mycological Society of Japan (Japan)*.
- Barahona, F., Slim, J., 2015. *Sphingobacterium multivorum*: case report and literature review. *New Microbes New Infect* 7, 33–36. <https://doi.org/10.1016/j.nmni.2015.04.006>
- Bartram, A.K., Lynch, M.D.J., Stearns, J.C., Moreno-Hagelsieb, G., Neufeld, J.D., 2011. Generation of multimillion-sequence 16S rRNA gene libraries from complex microbial communities by assembling paired-end illumina reads. *Appl. Environ. Microbiol.* 77, 3846–3852. <https://doi.org/10.1128/AEM.02772-10>
- Bayramoglu, G., Arica, M.Y., 2018. Adsorption of Congo Red dye by native amine and carboxyl modified biomass of *Funalia trogii*: Isotherms, kinetics and thermodynamics mechanisms. *Korean J. Chem. Eng.* 35, 1303–1311. <https://doi.org/10.1007/s11814-018-0033-9>
- Bayry, J., Aïmanianda, V., Guijarro, J.I., Sunde, M., Latgé, J.-P., 2012. Hydrophobins—Unique Fungal Proteins. *PLoS Pathog* 8, e1002700. <https://doi.org/10.1371/journal.ppat.1002700>
- Bendavid, R., Chasles-Parot, M., 2014. Les français et les nuisances sonores. Principaux résultats - 2014.
- Bengtsson, E., 2009. Obtaining high quality textile fibre from industrial hemp through organic cultivation 41.
- Benmahiddine, F., Bennai, F., Cherif, R., Belarbi, R., Tahakourt, A., Abahri, K., 2020. Experimental investigation on the influence of immersion/drying cycles on the hygrothermal and mechanical properties of hemp concrete. *Journal of Building Engineering* 32, 101758. <https://doi.org/10.1016/j.jobe.2020.101758>
- Bennai, F., El Hachem, C., Abahri, K., Belarbi, R., 2019. Influence of hydric solicitations on the morphological behavior of hemp concrete. *RILEM Technical Letters* 4, 16–21. <https://doi.org/10.21809/rilemtechlett.2019.80>
- Bennai, F., Nabil, I., Abahri, K., Belarbi, R., Tahakourt, A., 2017. Experimental characterization of thermal and hygric properties of hemp concrete with consideration of the material age evolution. *Heat and Mass Transfer*. <https://doi.org/10.1007/s00231-017-2221-2>
- Bennur, T., Kumar, A.R., Zinjarde, S., Javdekar, V., 2015. *Nocardiopsis* species: Incidence, ecological roles and adaptations. *Microbiological Research* 174, 33–47. <https://doi.org/10.1016/j.micres.2015.03.010>
- Bennur, T., Kumar, A.R., Zinjarde, S.S., Javdekar, V., 2016. *Nocardiopsis* species: a potential source of bioactive compounds. *Journal of Applied Microbiology* 120, 1–16. <https://doi.org/10.1111/jam.12950>
- Beno, S.M., Cheng, R.A., Orsi, R.H., Duncan, D.R., Guo, X., Kovac, J., Carroll, L.M., Martin, N.H., Wiedmann, M., 2020. *Paenibacillus odorifer*, the Predominant *Paenibacillus* Species Isolated from Milk in the United States, Demonstrates Genetic and Phenotypic Conservation of Psychrotolerance but Clade-Associated Differences in Nitrogen Metabolic Pathways. *mSphere* 5. <https://doi.org/10.1128/mSphere.00739-19>
- Betts, G., 2006. Other spoilage bacteria, in: Blackburn, C. de W. (Ed.), *Food Spoilage Microorganisms*, Woodhead Publishing Series in Food Science, Technology and Nutrition. Woodhead Publishing, pp. 668–693. <https://doi.org/10.1533/9781845691417.5.668>

- Beuchat, L.R., Kuhn, G.D., 1997. Thermal Sensitivity of *Neosartorya fischeri* Ascospores in Regular and Reduced-Sugar Grape Jelly. *J Food Prot* 60, 1577–1579. <https://doi.org/10.4315/0362-028X-60.12.1577>
- Bevan, R., Woolley, T., 2008. Hemp lime construction – a guide to building with hemp lime composites.
- Bex, V., Squinazi, F., 2006. Mise en évidence de moisissures des ambiances intérieures par la mesure des (1→3)-β-D-glucanes. *Revue Française d'Allergologie et d'Immunologie Clinique*, 1er Congrès Français d'Allergologie 46, 184–187. <https://doi.org/10.1016/j.allerg.2006.01.018>
- Bhabhra, R., Askew, D.S., 2005. Thermotolerance and virulence of *Aspergillus fumigatus*: role of the fungal nucleolus. *Medical Mycology* 43, S87–S93. <https://doi.org/10.1080/13693780400029486>
- Bilba, K., Arsene, M.-A., 2008. Silane treatment of bagasse fiber for reinforcement of cementitious composites. *Composites Part A: Applied Science and Manufacturing* 39, 1488–1495. <https://doi.org/10.1016/j.compositesa.2008.05.013>
- Bleuze, L., Chabbert, B., Lashermes, G., Recous, S., 2020. Hemp harvest time impacts on the dynamics of microbial colonization and hemp stems degradation during dew retting. *Industrial Crops and Products* 145, 112122. <https://doi.org/10.1016/j.indcrop.2020.112122>
- Bleuze, L., Lashermes, G., Alavoine, G., Recous, S., Chabbert, B., 2018. Tracking the dynamics of hemp dew retting under controlled environmental conditions. *Industrial Crops and Products* 123, 55–63. <https://doi.org/10.1016/j.indcrop.2018.06.054>
- Bloom, E., Nyman, E., Must, A., Pehrson, C., Larsson, L., 2009. Molds and mycotoxins in indoor environments--a survey in water-damaged buildings. *J Occup Environ Hyg* 6, 671–678. <https://doi.org/10.1080/15459620903252053>
- Bócsa, I., Karus, M., 1998. *The Cultivation of Hemp: Botany, Varieties, Cultivation and Harvesting*. Hemptech.
- Boekhout, T., Fonseca, Á., Sampaio, J.P., Bandoni, R.J., Fell, J.W., Kwon-Chung, K.J., 2011. Discussion of teleomorphic and anamorphic basidiomycetous yeasts. <https://doi.org/10.1016/B978-0-444-52149-1.00100-2>
- Borneman, J., Hartin, R.J., 2000. PCR Primers That Amplify Fungal rRNA Genes from Environmental Samples. *Appl. Environ. Microbiol.* 66, 4356–4360. <https://doi.org/10.1128/AEM.66.10.4356-4360.2000>
- Botton, B., 1990. *Moisissures utiles et nuisibles: importance industrielle*. Masson, Paris.
- Bouras, N., Meklat, A., Zitouni, A., Mathieu, F., Schumann, P., Spröer, C., Sabaou, N., Klenk, H.-P., 2015. *Nocardiosis algeriensis* sp. nov., an alkalitolerant actinomycete isolated from Saharan soil. *Antonie van Leeuwenhoek* 107, 313–320. <https://doi.org/10.1007/s10482-014-0329-7>
- Bourdot, A., Abahri, K., Bennai, F., Pefouo, R.F., Rateau, O., Rateau, O., Belarbi, R., 2020. Analysis of the response of flax concrete submitted to intense hygrothermal solicitations. *Academic Journal of Civil Engineering* 38, 173–176. <https://doi.org/10.26168/ajce.38.1.42>
- Bourgeois, C.M., Larpent, J.-P., 1996. *Microbiologie alimentaire - Tome 1*.
- Brümmer, M., Saez-Perez, M.P., Suarez, J.D., 2017. Hemp fibre based light weight concretes for environmental building – parameters that influence the mechanical strength. Presented at the 3rd International Conference on Natural Fibres ICNF 2017.
- Bruns, T., 2006. Evolutionary biology: a kingdom revised. *Nature* 443, 758–761.



<https://doi.org/10.1038/443758a>

- Bucher, R., Cyr, M., Escadeillas, G., 2021. Performance-based evaluation of flash-metakaolin as cement replacement in marine structures – Case of chloride migration and corrosion. *Construction and Building Materials* 267, 120926. <https://doi.org/10.1016/j.conbuildmat.2020.120926>
- Bullard, J.W., Jennings, H.M., Livingston, R.A., Nonat, A., Scherer, G.W., Schweitzer, J.S., Scrivener, K.L., Thomas, J.J., 2011. Mechanisms of cement hydration. *Cement and Concrete Research* 41, 1208–1223. <https://doi.org/10.1016/j.cemconres.2010.09.011>
- Bullerjahn, F., Boehm-Courjault, E., Zajac, M., Ben Haha, M., Scrivener, K., 2019a. Hydration reactions and stages of clinker composed mainly of stoichiometric ye'elimite. *Cement and Concrete Research* 116, 120–133. <https://doi.org/10.1016/j.cemconres.2018.10.023>
- Bullerjahn, F., Zajac, M., Ben Haha, M., Scrivener, K.L., 2019b. Factors influencing the hydration kinetics of ye'elimite; effect of mayenite. *Cement and Concrete Research* 116, 113–119. <https://doi.org/10.1016/j.cemconres.2018.10.026>
- Busse, H.-J., Zlamala, C., Buczolits, S., Lubitz, W., Kämpfer, P., Takeuchi, M., 2003. *Promicromonospora vindobonensis* sp. nov. and *Promicromonospora aerolata* sp. nov., isolated from the air in the medieval “Virgilkapelle” in Vienna. *Int J Syst Evol Microbiol* 53, 1503–1507. <https://doi.org/10.1099/ijms.0.02522-0>
- Bütschi, P.-Y., Deschenaux, C., Miao, B., Srivastava, N.K., 2004. Caractérisation d'une maçonnerie composée d'éléments en aggloméré de chanvre. *Can. J. Civ. Eng.* 31, 526–529. <https://doi.org/10.1139/104-028>
- Caballero-Mellado, J., Martínez-Aguilar, L., Paredes-Valdez, G., Santos, P.E.L., 2004. *Burkholderia unamae* sp. nov., an N<sub>2</sub>-fixing rhizospheric and endophytic species. *International Journal of Systematic and Evolutionary Microbiology* 54, 1165–1172. <https://doi.org/10.1099/ijms.0.02951-0>
- Cailliez-Grimal, C., Afzal, M.I., Revol-Junelles, A.-M., 2014. *Carnobacterium*, in: Batt, C.A., Tortorello, M.L. (Eds.), *Encyclopedia of Food Microbiology* (Second Edition). Academic Press, Oxford, pp. 379–383. <https://doi.org/10.1016/B978-0-12-384730-0.00381-5>
- Caporaso, J.G., Lauber, C.L., Walters, W.A., Berg-Lyons, D., Lozupone, C.A., Turnbaugh, P.J., Fierer, N., Knight, R., 2011. Global patterns of 16S rRNA diversity at a depth of millions of sequences per sample. *PNAS* 108, 4516–4522. <https://doi.org/10.1073/pnas.1000080107>
- Cerezo, V., 2005. Propriétés mécaniques, thermiques et acoustiques d'un matériau à base de particules végétales : approche expérimentale et modélisation théorique 248.
- Cha, Q.-Y., Zhou, X.-K., Zhang, X.-F., Li, M., Wei, Y.-Q., Zhang, T.-K., Qin, S.-C., Liu, Z.-Y., Wang, X.-J., Liu, J.-J., Zhu, M.-L., Mo, M.-H., 2020. *Luteimonas lumbrici* sp. nov., a novel bacterium isolated from wormcast. *International Journal of Systematic and Evolutionary Microbiology*, 70, 604–610. <https://doi.org/10.1099/ijsem.0.003799>
- Chabannes, M., 2015. Formulation et étude des propriétés mécaniques d'agrobétons légers isolants à base de balles de riz et de chènevotte pour l'éco-construction. Université de Montpellier.
- Chabannes, M., Garcia-Diaz, E., Clerc, L., Bénézet, J.-C., 2015. Studying the hardening and mechanical performances of rice husk and hemp-based building materials cured under natural and accelerated carbonation. *Construction and Building Materials* 94, 105–115. <https://doi.org/10.1016/j.conbuildmat.2015.06.032>
- Chabannes, M., Garcia-Diaz, E., Clerc, L., Bénézet, J.-C., Becquart, F., 2018. Lime and Hemp or Rice Husk Concretes for the Building Envelope: Applications and General Properties, in: Chabannes, M., Garcia-Diaz, E., Clerc, L., Bénézet, J.-C., Becquart, F. (Eds.), *Lime Hemp*

and Rice Husk-Based Concretes for Building Envelopes, SpringerBriefs in Molecular Science. Springer International Publishing, Cham, pp. 45–98. [https://doi.org/10.1007/978-3-319-67660-9\\_4](https://doi.org/10.1007/978-3-319-67660-9_4)

- Chamoin, J., 2013. Optimisation des propriétés (physiques, mécaniques et hydriques) de bétons de chanvre par la maîtrise de la formulation 206.
- Chater, K.F., 2013. Streptomyces, in: Maloy, S., Hughes, K. (Eds.), *Brenner's Encyclopedia of Genetics* (Second Edition). Academic Press, San Diego, pp. 565–567. <https://doi.org/10.1016/B978-0-12-374984-0.01483-2>
- Chaudhary, D.K., Lee, S.D., Kim, J., 2017. *Pedobacter kyonggii* sp. nov., a psychrotolerant bacterium isolated from forest soil. *International Journal of Systematic and Evolutionary Microbiology* 67, 5120–5127. <https://doi.org/10.1099/ijsem.0.002428>
- Cizer, Ö., Van Balen, K., Elsen, J., Van Gemert, D., 2012. Real-time investigation of reaction rate and mineral phase modifications of lime carbonation. *Construction and Building Materials* 35, 741–751. <https://doi.org/10.1016/j.conbuildmat.2012.04.036>
- Codina, M., 2007. Les bétons bas pH - Formulation, caractérisation et étude à long terme (phdthesis). INSA de Toulouse.
- Colinart, T., Glouannec, P., Chauvelon, P., 2012. Influence of the setting process and the formulation on the drying of hemp concrete. *Construction and Building Materials* 30, 372–380. <https://doi.org/10.1016/j.conbuildmat.2011.12.030>
- Collectif SEBTP, 2012. *Construire en chanvre - SEBTP*, SEBTP. ed.
- Collet, F., Bart, M., Serres, L., Miriel, J., 2008. Porous structure and water vapour sorption of hemp-based materials. *Construction and Building Materials* 22, 1271–1280. <https://doi.org/10.1016/j.conbuildmat.2007.01.018>
- Collet, F., Chamoin, J., Pretot, S., Lanos, C., 2013. Comparison of the hygric behaviour of three hemp concretes. *Energy and Buildings* 62, 294–303. <https://doi.org/10.1016/j.enbuild.2013.03.010>
- Collet, F., Pretot, S., 2014. Thermal conductivity of hemp concretes: Variation with formulation, density and water content. *Construction and Building Materials* 65, 612–619. <https://doi.org/10.1016/j.conbuildmat.2014.05.039>
- Collet, F., Pretot, S., 2012. Experimental investigation of moisture buffering capacity of sprayed hemp concrete. *Construction and Building Materials* 36, 58–65. <https://doi.org/10.1016/j.conbuildmat.2012.04.139>
- Costerton, J.W., Lewandowski, Z., DeBeer, D., Caldwell, D., Korber, D., James, G., 1994. Biofilms, the customized microniche. *Journal of Bacteriology* 176, 2137–2142. <https://doi.org/10.1128/JB.176.8.2137-2142.1994>
- Costigan, A., Pavia, S., 2012. Influence of the Mechanical Properties of Lime Mortar on the Strength of Brick Masonry, in: Válek, J., Hughes, J.J., Groot, C.J.W.P. (Eds.), *Historic Mortars*, RILEM Bookseries. Springer Netherlands, Dordrecht, pp. 359–372. [https://doi.org/10.1007/978-94-007-4635-0\\_28](https://doi.org/10.1007/978-94-007-4635-0_28)
- Coutinho, M.L., Miller, A.Z., Rogerio-Candelera, M.A., Mirão, J., Alves, L.C., Veiga, J.P., Águas, H., Pereira, S., Lyubchik, A., Macedo, M.F., 2016. An integrated approach for assessing the bioreceptivity of glazed tiles to phototrophic microorganisms. *Biofouling* 32, 243–259. <https://doi.org/10.1080/08927014.2015.1135242>
- Crawford, B., Pakpour, S., Kazemian, N., Klironomos, J., Stoeffler, K., Rho, D., Denault, J., Milani, A.S., 2017. Effect of Fungal Deterioration on Physical and Mechanical Properties of Hemp and Flax Natural Fiber Composites. *Materials* (Basel) 10.

<https://doi.org/10.3390/ma10111252>

- Da Costa, P.S., Tostes, M.M., de Carvalho Valle, L.M., 2000. A case of keratoconjunctivitis due to *Ewingella americana* and a review of unusual organisms causing external eye infections. *Braz J Infect Dis* 4, 262–267.
- Dartois, S., Mom, S., Dumontet, H., Ben Hamida, A., 2017. An iterative micromechanical modeling to estimate the thermal and mechanical properties of polydisperse composites with platy particles: Application to anisotropic hemp and lime concretes. *Construction and Building Materials* 152, 661–671. <https://doi.org/10.1016/j.conbuildmat.2017.06.181>
- Dassarma, S., Arora, P., 2002. Halophiles, in: ELS. <https://doi.org/10.1038/npg.els.0000394>
- Davidson, P.M., Zivanovic, S., 2003. The use of natural antimicrobials, in: Zeuthen, P., Bøgh-Sørensen, L. (Eds.), *Food Preservation Techniques*, Woodhead Publishing Series in Food Science, Technology and Nutrition. Woodhead Publishing, pp. 5–30. <https://doi.org/10.1533/9781855737143.1.5>
- de Bruijn, P.B., Jeppsson, K.-H., Sandin, K., Nilsson, C., 2009. Mechanical properties of lime-hemp concrete containing shives and fibres. *Biosystems Engineering* 103, 474–479. <https://doi.org/10.1016/j.biosystemseng.2009.02.005>
- de Lima Procópio, R.E., da Silva, I.R., Martins, M.K., de Azevedo, J.L., de Araújo, J.M., 2012. Antibiotics produced by *Streptomyces*. *The Brazilian Journal of Infectious Diseases* 16, 466–471. <https://doi.org/10.1016/j.bjid.2012.08.014>
- de Menezes, C.B.A., Afonso, R.S., de Souza, W.R., Parma, M.M., de Melo, I.S., Fugita, F.L.S., Moraes, L.A.B., Zucchi, T.D., Fantinatti-Garboggini, F., 2019. *Williamsia aurantiacus* sp. nov. a novel actinobacterium producer of antimicrobial compounds isolated from the marine sponge. *Arch Microbiol* 201, 691–698. <https://doi.org/10.1007/s00203-019-01633-z>
- Delannoy, G., Marceau, S., Glé, P., Gourlay, E., Guéguen-Minerbe, M., Amziane, S., Farcas, F., 2020a. Durability of hemp concretes exposed to accelerated environmental aging. *Construction and Building Materials* 252, 119043. <https://doi.org/10.1016/j.conbuildmat.2020.119043>
- Delannoy, G., Marceau, S., Glé, P., Gourlay, E., Guéguen-Minerbe, M., Diafi, D., Amziane, S., Farcas, F., 2020b. Impact of hemp shiv extractives on hydration of Portland cement. *Construction and Building Materials* 244, 118300. <https://doi.org/10.1016/j.conbuildmat.2020.118300>
- Delannoy, G., Marceau, S., Glé, P., Gourlay, E., Guéguen-Minerbe, M., Diafi, D., Nour, I., Amziane, S., Farcas, F., 2018. Aging of hemp shiv used for concrete. *Materials & Design* 160, 752–762. <https://doi.org/10.1016/j.matdes.2018.10.016>
- Delgado-Jarana, J., Rincón, A.M., Beni Tez, T.A., 2002. Aspartyl protease from *Trichoderma harzianum* CECT 2413: cloning and characterization. *Microbiology (Reading, Engl.)* 148, 1305–1315. <https://doi.org/10.1099/00221287-148-5-1305>
- Diederich, P., Ertz, D., Eichler, M., Cezanne, R., Boom, P. van den, Broeck, D.V. den, Sérusiaux, E., 2014. New or interesting lichens and lichenicolous fungi from Belgium, Luxembourg and northern France. *Bull. Soc. Nat. luxemb.*
- Djossou Olga, 2011. Mycoflore post-récolte du café robusta et utilisation des bactéries lactiques pour le contrôle des moisissures mycotoxinogènes et de l'Ochratoxine A. L'Université Paul Cezanne, Aix Marseille III.
- Domsch, K.H., Gams, W., Anderson, T.-H., 2007. *Compendium of soil fungi*. IHW, Munchen.
- Donlan, R.M., 2002. Biofilms: Microbial Life on Surfaces. *Emerg. Infect. Dis.* 8, 881–890. <https://doi.org/10.3201/eid0809.020063>

- Douwes, J., 2005. (1→3)-Beta-D-glucans and respiratory health: a review of the scientific evidence. *Indoor Air* 15, 160–169. <https://doi.org/10.1111/j.1600-0668.2005.00333.x>
- Dsouza, M., Taylor, M.W., Turner, S.J., Aislabie, J., 2014. Genome-based comparative analyses of Antarctic and temperate species of *Paenibacillus*. *PLoS One* 9, e108009. <https://doi.org/10.1371/journal.pone.0108009>
- Du, C., Li, B., Yu, W., 2021. Indoor mould exposure: Characteristics, influences and corresponding associations with built environment—A review. *Journal of Building Engineering* 35, 101983. <https://doi.org/10.1016/j.jobbe.2020.101983>
- Dubosc, A., 2000. Etude du developpement de salissures biologiques sur les parements en beton : mise au point d'essais acceleres de vieillissement (These de doctorat). Toulouse, INSA.
- Dutton, M., Evans, C., 2011. Oxalate production by fungi: its role in pathogenicity and ecology in the soil environment. *Canadian Journal of Microbiology* 42, 881–895. <https://doi.org/10.1139/m96-114>
- Eduard, W., 2009. Fungal spores: a critical review of the toxicological and epidemiological evidence as a basis for occupational exposure limit setting. *Crit Rev Toxicol* 39, 799–864. <https://doi.org/10.3109/10408440903307333>
- El Hachem, C., Abahri, K., Bennacer, R., 2019. Original experimental and numerical approach for prediction of the microscopic hygro-mechanical behavior of spruce wood. *Construction and Building Materials* 203, 258–266. <https://doi.org/10.1016/j.conbuildmat.2019.01.107>
- El Hachem, C., Ye, P., Abahri, K., Bennacer, R., 2017. Fiber's hygromorphic effect on thermal conductivity of wooden fibrous insulation characterized by X-ray tomography. *Construction and Building Materials* 150, 758–765. <https://doi.org/10.1016/j.conbuildmat.2017.06.013>
- Elfordy, S., Lucas, F., Tancret, F., Scudeller, Y., Goudet, L., 2008. Mechanical and thermal properties of lime and hemp concrete (“hempcrete”) manufactured by a projection process. *Construction and Building Materials* 22, 2116–2123. <https://doi.org/10.1016/j.conbuildmat.2007.07.016>
- EOTA, 2013. Guideline for European technical approval of external thermal insulation composite systems (ETICS) with rendering.
- Evrard, A., De Herde, A., 2005. Bioclimatic envelopes made of lime and hemp concrete. Presented at the CISBAT 2005 - Renewables in a Changing Climate - Innovation in Building Envelopes and Environmental Systems.
- Fisher, K., Phillips, C., 2009. The ecology, epidemiology and virulence of *Enterococcus*. *Microbiology*, 155, 1749–1757. <https://doi.org/10.1099/mic.0.026385-0>
- Forquin, M.-P., Weimer, B.C., 2014. *Brevibacterium*, in: *Encyclopedia of Food Microbiology*. Carl A. Batt, Mary Lou Tortorello, pp. 324–330.
- Fourmentin, M., Faure, P., Pelupessy, P., Sarou-Kanian, V., Peter, U., Lesueur, D., Rodts, S., Daviller, D., Coussot, P., 2016. NMR and MRI observation of water absorption/uptake in hemp shives used for hemp concrete. *Construction and Building Materials* 124, 405–413. <https://doi.org/10.1016/j.conbuildmat.2016.07.100>
- Fu, Y.-S., Hussain, F., Habib, N., Khan, I.U., Chu, X., Duan, Y.-Q., Zhi, X.-Y., Chen, X., Li, W.-J., 2017. *Sphingobacterium soli* sp. nov., isolated from soil. *International Journal of Systematic and Evolutionary Microbiology* 67, 2284–2288. <https://doi.org/10.1099/ijsem.0.001946>
- Gadanho, M., Sampaio, J.P., 2009. *Cryptococcus ibericus* sp. nov., *Cryptococcus aciditolerans* sp. nov. and *Cryptococcus metallitolerans* sp. nov., a new ecoclade of anamorphic basidiomycetous yeast species from an extreme environment associated with acid rock

- drainage in São Domingos pyrite mine, Portugal. *International Journal of Systematic and Evolutionary Microbiology*, 59, 2375–2379. <https://doi.org/10.1099/ij.s.0.008920-0>
- Gangneux, C., Akpa-Vinceslas, M., Sauvage, H., Desaire, S., Houot, S., Laval, K., 2011. Fungal, bacterial and plant dsDNA contributions to soil total DNA extracted from silty soils under different farming practices: Relationships with chloroform-labile carbon. <https://doi.org/10.1016/j.soilbio.2010.11.012>
- Garikapati, K.P., Sadeghian, P., 2020. Mechanical behavior of flax-lime concrete blocks made of waste flax shives and lime binder reinforced with jute fabric. *Journal of Building Engineering* 29, 101187. <https://doi.org/10.1016/j.job.2020.101187>
- Gibson, L.J., 2003. Cellular Solids. *MRS Bulletin* 28, 270–274. <https://doi.org/10.1557/mrs2003.79>
- Giraldo, A., Crous, P.W., 2019. Inside Plectosphaerellaceae. *Studies in Mycology* 92, 227–286. <https://doi.org/10.1016/j.simyco.2018.10.005>
- Glé, P., 2013. *Acoustique des Matériaux du Bâtiment à base de Fibres et Particules Végétales - Outils de Caractérisation, Modélisation et Optimisation.*
- Glé, P., Gourdon, E., Arnaud, L., 2011. Acoustical properties of materials made of vegetable particles with several scales of porosity. *Applied Acoustics* 72, 249–259. <https://doi.org/10.1016/j.apacoust.2010.11.003>
- Górny, R.L., 2004. Filamentous microorganisms and their fragments in indoor air--a review. *Ann Agric Environ Med* 11, 185–197.
- Gourlay, E., Glé, P., Marceau, S., Foy, C., Moscardelli, S., 2017. Effect of water content on the acoustical and thermal properties of hemp concretes. *Construction and Building Materials* 139, 513–523. <https://doi.org/10.1016/j.conbuildmat.2016.11.018>
- Grady, E.N., MacDonald, J., Liu, L., Richman, A., Yuan, Z.-C., 2016. Current knowledge and perspectives of *Paenibacillus*: a review. *Microb Cell Fact* 15. <https://doi.org/10.1186/s12934-016-0603-7>
- Gram, H.-E., 1983. Durability of natural fibres in concrete. *Cement- och betonginst.*
- Grant, C., 1982. Fouling of terrestrial substrates by algae and implications for control - a review. *International biodeterioration bulletin.*
- Green, B.J., Mitakakis, T., Tovey, E., 2003. Allergen detection from 11 fungal species before and after germination. *The Journal of allergy and clinical immunology.* <https://doi.org/10.1067/MAI.2003.57>
- Green, B.J., Tovey, E.R., Sercombe, J.K., Blachere, F.M., Beezhold, D.H., Schmechel, D., 2006. Airborne fungal fragments and allergenicity. *Med Mycol* 44 Suppl 1, S245-255. <https://doi.org/10.1080/13693780600776308>
- Green, F., Highley, T.L., 1997. Mechanism of brown-rot decay: Paradigm or paradox. *International Biodeterioration & Biodegradation, Biodegradation of Wood* 39, 113–124. [https://doi.org/10.1016/S0964-8305\(96\)00063-7](https://doi.org/10.1016/S0964-8305(96)00063-7)
- Grice, E.A., Kong, H.H., Renaud, G., Young, A.C., NISC Comparative Sequencing Program, Bouffard, G.G., Blakesley, R.W., Wolfsberg, T.G., Turner, M.L., Segre, J.A., 2008. A diversity profile of the human skin microbiota. *Genome Research* 18, 1043–1050. <https://doi.org/10.1101/gr.075549.107>
- Grimont, P.A.D., Farmer, J.J., Grimont, F., Asbury, M.A., Brenner, D.J., Deval, C., 1983. *Ewingella americana* gen.nov., sp. nov., a new Enterobacteriaceae isolated from clinical specimens. *Annales de l'Institut Pasteur / Microbiologie* 134, 39–52.

[https://doi.org/10.1016/0769-2609\(83\)90102-3](https://doi.org/10.1016/0769-2609(83)90102-3)

- Grum-Grzhimaylo, A.A., Georgieva, M.L., Bondarenko, S.A., Debets, A.J.M., Bilanenko, E.N., 2016. On the diversity of fungi from soda soils. *Fungal Diversity* 76, 27–74. <https://doi.org/10.1007/s13225-015-0320-2>
- Guggiari, M., Bloque, R., Aragno, M., Verrecchia, E., Job, D., Junier, P., 2011. Experimental calcium-oxalate crystal production and dissolution by selected wood-rot fungi. *International Biodeterioration & Biodegradation* 65, 803–809. <https://doi.org/10.1016/j.ibiod.2011.02.012>
- Guillitte, O., 1995. Bioreceptivity: a new concept for building ecology studies. *Science of The Total Environment* 167, 215–220. [https://doi.org/10.1016/0048-9697\(95\)04582-L](https://doi.org/10.1016/0048-9697(95)04582-L)
- Guillitte, O., Dreesen, R., 1995. Laboratory chamber studies and petrographical analysis as bioreceptivity assessment tools of building materials. *Science of The Total Environment* 167, 365–374. [https://doi.org/10.1016/0048-9697\(95\)04596-S](https://doi.org/10.1016/0048-9697(95)04596-S)
- Gürgan, M., Koku, H., Eroglu, I., Yücel, M., 2020. Transcriptome analysis of the effects of light and dark cycle on hydrogen production metabolism of *Rhodobacter capsulatus* DSM1710. *International Journal of Hydrogen Energy*. <https://doi.org/10.1016/j.ijhydene.2020.03.108>
- Guzman Prieto, A.M., van Schaik, W., Rogers, M.R.C., Coque, T.M., Baquero, F., Corander, J., Willems, R.J.L., 2016. Global Emergence and Dissemination of Enterococci as Nosocomial Pathogens: Attack of the Clones? *Front. Microbiol.* 7. <https://doi.org/10.3389/fmicb.2016.00788>
- Hamidi, M., 2013. Evaluation and improvement of pozzolanic activity of andesite for its use in eco-efficient cement. *Construction and Building Materials* 10.
- Han, C., Zhao, J., Shi, H., Tian, Y., Zhang, C., Guo, X., Xiang, W., Wang, X., 2019. *Jiangella rhizosphaerae* sp. nov., an actinomycete isolated from the rhizosphere soil of wheat (*Triticum aestivum* L.). *International Journal of Systematic and Evolutionary Microbiology*, 69, 1320–1326. <https://doi.org/10.1099/ijsem.0.003314>
- Harris, J.L., 2000. Safe, Low-Distortion Tape Touch Method for Fungal Slide Mounts. *Journal of Clinical Microbiology* 38, 4683–4684. <https://doi.org/10.1128/JCM.38.12.4683-4684.2000>
- Hastrup, A.C.S., Green, F., Lebow, P.K., Jensen, B., 2012. Enzymatic oxalic acid regulation correlated with wood degradation in four brown-rot fungi. *International Biodeterioration & Biodegradation* 75, 109–114. <https://doi.org/10.1016/j.ibiod.2012.05.030>
- Haugaard-Nielsen, H., Barron, A., Coutinho, J., English, A., Gergely, S., Lidouren, E., 2003. INTEGRATING HEMP IN ORGANIC FARMING SYSTEMS: 137.
- Hawksworth, D.L., 2001. The magnitude of fungal diversity : the 1.5 million species estimate revisited. *Mycological Research* 11.
- He, W., Guo, J., Guo, H., An, M., Huang, W., Wang, Y., Cai, H., 2019. *Sphingobacterium puteale* sp. nov., isolated from a deep subsurface aquifer. *International Journal of Systematic and Evolutionary Microbiology*, 69, 3356–3361. <https://doi.org/10.1099/ijsem.0.003521>
- He, X., Li, N., Chen, X., Zhang, Y., Zhang, X., Song, X., 2020. *Pedobacter indicus* sp. nov., isolated from deep-sea sediment. *Antonie van Leeuwenhoek* 113, 357–364. <https://doi.org/10.1007/s10482-019-01346-9>
- Helps, C.R., Harbour, D.A., Corry, J.E.L., 1999. PCR-based 16S ribosomal DNA detection technique for *Clostridium estertheticum* causing spoilage in vacuum-packed chill-stored beef. *International Journal of Food Microbiology* 52, 57–65. [https://doi.org/10.1016/S0168-1605\(99\)00116-6](https://doi.org/10.1016/S0168-1605(99)00116-6)

- Hendry, K.M., Cole, E.C., 1993. A review of mycotoxins in indoor air. *Journal of Toxicology and Environmental Health* 38, 183–198. <https://doi.org/10.1080/15287399309531711>
- Hibbett, D.S., Binder, M., Bischoff, J.F., Blackwell, M., Cannon, P.F., Eriksson, O.E., Huhndorf, S., 2007. A higher-level phylogenetic classification of the Fungi. *Mycological Research* 111, 509–547. <https://doi.org/10.1016/j.mycres.2007.03.004>
- Hilal Ay, Imen Nouioui, Lorena Carro, Hans-Peter Klenk, Demet Cetin, Igual, J.M., Sahin, N., Isik, K., 2019. *Jiangella anatolica* sp. nov. isolated from coastal lake soil. *Antonie van Leeuwenhoek* 112, 887–895. <https://doi.org/10.1007/s10482-018-01222-y>
- Hooton, T.M., 2012. Clinical practice. Uncomplicated urinary tract infection. *N. Engl. J. Med.* 366, 1028–1037. <https://doi.org/10.1056/NEJMcp1104429>
- Horinouchi, S., Ueda, K., Nakayama, J., Ikeda, T., 2010. Cell-to-Cell Communications among Microorganisms, in: Liu, H.-W. (Ben), Mander, L. (Eds.), *Comprehensive Natural Products II*. Elsevier, Oxford, pp. 283–337. <https://doi.org/10.1016/B978-008045382-8.00098-8>
- Horne, M.R.L., 2020. Bast fibres: hemp cultivation and production, in: Kozłowski, R.M., Mackiewicz-Talarczyk, M. (Eds.), *Handbook of Natural Fibres (Second Edition)*, Woodhead Publishing Series in Textiles. Woodhead Publishing, pp. 163–196. <https://doi.org/10.1016/B978-0-12-818398-4.00007-4>
- Huang, W.-C., Tang, I.-C., 2007. Chapter 8 - Bacterial and Yeast Cultures – Process Characteristics, Products, and Applications, in: Yang, S.-T. (Ed.), *Bioprocessing for Value-Added Products from Renewable Resources*. Elsevier, Amsterdam, pp. 185–223. <https://doi.org/10.1016/B978-044452114-9/50009-8>
- Hukka, A., Viitanen, H.A., 1999. A mathematical model of mould growth on wooden material. *Wood Science and Technology* 33, 475–485. <https://doi.org/10.1007/s002260050131>
- Husman, T., 1996. Health effects of indoor-air microorganisms. *Scand J Work Environ Health* 22, 5–13. <https://doi.org/10.5271/sjweh.103>
- Hussain, A., Calabria-Holley, J., Lawrence, M., Jiang, Y., 2019. Hygrothermal and mechanical characterisation of novel hemp shiv based thermal insulation composites. *Construction and Building Materials* 212, 561–568. <https://doi.org/10.1016/j.conbuildmat.2019.04.029>
- Hydrogen photosynthesis by *Rhodobacter capsulatus* and its coupling to a PEM fuel cell: He, D. et al. *Journal of Power Sources*, 2005, 141, (1), 19–23., 2006. . *Fuel and Energy Abstracts* 47, 125. [https://doi.org/10.1016/S0140-6701\(06\)80852-0](https://doi.org/10.1016/S0140-6701(06)80852-0)
- Ibrahim, A.H., Desoukey, S.Y., Fouad, M.A., Kamel, M.S., Gulder, T.A.M., Abdelmohsen, U.R., 2018. Natural Product Potential of the Genus *Nocardiopsis*. *Mar Drugs* 16. <https://doi.org/10.3390/md16050147>
- Inglis, T.J.J., Merritt, A.J., 2015. Chapter 42 - *Burkholderia pseudomallei* and *Burkholderia mallei*, in: Tang, Y.-W., Sussman, M., Liu, D., Poxton, I., Schwartzman, J. (Eds.), *Molecular Medical Microbiology (Second Edition)*. Academic Press, Boston, pp. 769–791. <https://doi.org/10.1016/B978-0-12-397169-2.00042-1>
- Insee, 2017. Les conditions de logement en France.
- IPCC, 2013. *Climate Change 2013: The Physical Science Basis*.
- Isnard, C., 2017. *Enterococcus* spp. : entre pathogènes opportunistes et probiotiques Genetic basis for in vitro and in vivo resistance to lincosamides, streptogramins A, and pleuromutilins (LSAP phenotype) in *Enterococcus faecium* Genomic analysis of reduced susceptibility to tigecycline in *Enterococcus faecium* Impact of caspofungin against *Enterococcus faecium* : deciphering the versatile effect of echinocandins *Enterococcus hirae* and *Barnesiella intestinihominis* Facilitate Cyclophosphamide-Induced Therapeutic Immunomodulatory

Effects (These de doctorat). Normandie.

- ISO 12571, 2000. ISO 12571:2000(E) Hygrothermal performance of building materials and products. Determination of hygroscopic sorption properties: <https://doi.org/10.3403/30259581>
- ISO 12572, 2016. ISO 12572:2016 Hygrothermal performance of building materials and products — Determination of water vapour transmission properties — Cup method.
- ISO 14040, 2006. ISO 14040:2006 Environmental management — Life cycle assessment — Principles and framework.
- ISO 14044, 2006. ISO 14044:2006 Environmental management — Life cycle assessment — Requirements and guidelines.
- ISO 14067, 2018. ISO 14067:2018 Greenhouse gases — Carbon footprint of products — Requirements and guidelines for quantification.
- ISO 15686, 2011. ISO 15686-1:2011 Buildings and constructed assets — Service life planning — Part 1: General principles and framework.
- James, T.Y., Kauff, F., Schoch, C.L., Matheny, P.B., Hofstetter, V., Cox, C.J., Celio, G., 2006. Reconstructing the early evolution of Fungi using a six-gene phylogeny. *Nature* 443, 818–822. <https://doi.org/10.1038/nature05110>
- Jami, T., Karade, S.R., Singh, L.P., 2019. A review of the properties of hemp concrete for green building applications. *Journal of Cleaner Production* 239, 117852. <https://doi.org/10.1016/j.jclepro.2019.117852>
- Jankauskienė, Z., Butkutė, B., Gruzdevienė, E., Cesevičienė, J., Fernando, A.L., 2015. Chemical composition and physical properties of dew- and water-retted hemp fibers. *Industrial Crops and Products, Advances in Industrial Crops and Products Worldwide: AAIC 2014 international conference* 75, 206–211. <https://doi.org/10.1016/j.indcrop.2015.06.044>
- Jeong, E.-L., Broad, S.J., Moody, R.G., Phillips-Jones, M.K., 2020. The adherence-associated Fdp fasciclin I domain protein of the biohydrogen producer *Rhodobacter sphaeroides* is regulated by the global Prr pathway. *International Journal of Hydrogen Energy* 45, 26840–26854. <https://doi.org/10.1016/j.ijhydene.2020.07.108>
- Jerónimo, A., Soares, C., Aguiar, B., Lima, N., 2020. Hydraulic lime mortars incorporating micro cork granules with antifungal properties. *Construction and Building Materials* 255, 119368. <https://doi.org/10.1016/j.conbuildmat.2020.119368>
- Johansson, P., Svensson, T., Ekstrand-Tobin, A., 2013. Validation of critical moisture conditions for mould growth on building materials. *Building and Environment* 62, 201–209. <https://doi.org/10.1016/j.buildenv.2013.01.012>
- Jones, D.L., 1998. Organic acids in the rhizosphere – a critical review. *Plant and Soil* 205, 25–44. <https://doi.org/10.1023/A:1004356007312>
- Kallmeyer, J., Pockalny, R., Adhikari, R.R., Smith, D.C., D’Hondt, S., 2012. Global distribution of microbial abundance and biomass in subseafloor sediment. *Proceedings of the National Academy of Sciences of the United States of America (PNAS)* 109, 16213–16216. <https://doi.org/10.1073/pnas.1203849109>
- Kämpfer, P., Andersson, M.A., Rainey, F.A., Kroppenstedt, R.M., Salkinoja-Salonen, M., 1999. *Williamsia muralis* gen. nov., sp. nov., isolated from the indoor environment of a children’s day care centre. *International Journal of Systematic and Evolutionary Microbiology* 49, 681–687. <https://doi.org/10.1099/00207713-49-2-681>
- Kämpfer, P., Falsen, E., Lodders, N., Martin, K., Kassmannhuber, J., Busse, H.-J., 2012.



- Paenibacillus chartarius* sp. nov., isolated from a paper mill. *International Journal of Systematic and Evolutionary Microbiology* 62, 1342–1347. <https://doi.org/10.1099/ijs.0.035154-0>
- Kangale, L.J., Raoult, D., Ghigo, E., Fournier, P.-E., 2020. *Pedobacter schmidtea* sp. nov., a new bacterium isolated from the microbiota of the planarian *Schmidtea mediterranea*. *Scientific Reports* 10, 6113. <https://doi.org/10.1038/s41598-020-62985-x>
- Kati, C., Bibashi, E., Kokolina, E., Sofianou, D., 1999. Case of Peritonitis Caused by *Ewingella americana* in a Patient Undergoing Continuous Ambulatory Peritoneal Dialysis. *Journal of Clinical Microbiology* 37, 3733–3734. <https://doi.org/10.1128/JCM.37.11.3733-3734.1999>
- Kazemian, N., Pakpour, S., Milani, A.S., Klironomos, J., 2019. Environmental factors influencing fungal growth on gypsum boards and their structural biodeterioration: A university campus case study. *PLOS ONE* 14, e0220556. <https://doi.org/10.1371/journal.pone.0220556>
- Khalil, N., Aouad, G., El Cheikh, K., Rémond, S., 2017. Use of calcium sulfoaluminate cements for setting control of 3D-printing mortars. *Construction and Building Materials* 157, 382–391. <https://doi.org/10.1016/j.conbuildmat.2017.09.109>
- Kinnane, O., Reilly, A., Grimes, J., Pavia, S., Walker, R., 2016. Acoustic absorption of hemp-lime construction. *Construction and Building Materials* 122, 674–682. <https://doi.org/10.1016/j.conbuildmat.2016.06.106>
- Kontro, M., Lignell, U., Hirvonen, M.-R., Nevalainen, A., 2005. pH effects on 10 *Streptomyces* spp. growth and sporulation depend on nutrients. *Letters in Applied Microbiology* 41, 32–38. <https://doi.org/10.1111/j.1472-765X.2005.01727.x>
- Korpi, A., Kasanen, J.P., Alarie, Y., Kosma, V.M., Pasanen, A.L., 1999. Sensory irritating potency of some microbial volatile organic compounds (MVOCs) and a mixture of five MVOCs. *Arch Environ Health* 54, 347–352. <https://doi.org/10.1080/00039899909602499>
- Kosiachevskiy, D., Abahri, K., Chaouche, M., Prat, E., Daubresse, A., Bousquet, C., 2018. Risk assessment of mold growth in hemp concrete, in: *Conference Proceedings of SynerCrete'18: Interdisciplinary Approaches for Cement-Based Materials and Structural Concrete: Synergizing Expertise and Bridging Scales of Space and Time*. Funchal, Portugal, p. 6. <https://doi.org/10.5281/zenodo.1405563>
- Kosiachevskiy, D., Maryna Babenko, Savytskyi, M., Schmidt, M., Perehinets, I., 2017. The main insulation parameters for the design of nzeb from biosourced materials 99, 7.
- Kounetas, K.E., 2021. Measurement of eco-efficiency and convergence: Evidence from a non-parametric frontier analysis. *European Journal of Operational Research* 14.
- Kroppenstedt, R.M., Evtushenko, L.I., 2006. The Family Nocardioptaceae, in: Dworkin, M., Falkow, S., Rosenberg, E., Schleifer, K.-H., Stackebrandt, E. (Eds.), *The Prokaryotes: Volume 3: Archaea. Bacteria: Firmicutes, Actinomycetes*. Springer, New York, NY, pp. 754–795. [https://doi.org/10.1007/0-387-30743-5\\_29](https://doi.org/10.1007/0-387-30743-5_29)
- Kulakov, L.A., McAlister, M.B., Ogden, K.L., Larkin, M.J., O'Hanlon, J.F., 2002. Analysis of Bacteria Contaminating Ultrapure Water in Industrial Systems. *AEM* 68, 1548–1555. <https://doi.org/10.1128/AEM.68.4.1548-1555.2002>
- Kurup, V.P., 2003. Fungal allergens. *Curr Allergy Asthma Rep* 3, 416. <https://doi.org/10.1007/s11882-003-0078-6>
- Kurup, V.P., Shen, H.-D., Vijay, H., 2002. Immunobiology of fungal allergens. *Int Arch Allergy Immunol* 129, 181–188. <https://doi.org/10.1159/000066780>
- Lacroix, B., Citovsky, V., 2013. *Agrobacterium*, in: Maloy, S., Hughes, K. (Eds.), *Brenner's Encyclopedia of Genetics (Second Edition)*. Academic Press, San Diego, pp. 52–54.

<https://doi.org/10.1016/B978-0-12-374984-0.00025-5>

- Lähdesmäki, K., Salminen, K., Vinha, J., Viitanen, H., Ojanen, T., Peuhkuri, R., 2011. Fungi and the history of mycology. Presented at the 9th Nordic Symposium on Building Physics, Finland.
- Lambiase, A., Rossano, F., Del Pezzo, M., Raia, V., Sepe, A., de Gregorio, F., Catania, M.R., 2009. Sphingobacterium respiratory tract infection in patients with cystic fibrosis. *BMC Research Notes* 2, 262. <https://doi.org/10.1186/1756-0500-2-262>
- Lappalainen, V., Sohlberg, E., Järnström, H., Laamanen, J., Viitanen, H., Pasanen, P., 2015. IAQ Simulator Tests: VOC Emissions from Hidden Mould Growth. *Energy Procedia*, 6th International Building Physics Conference, IBPC 2015 78, 1212–1217. <https://doi.org/10.1016/j.egypro.2015.11.187>
- Latif, E., Lawrence, M., Shea, A., Walker, P., 2015. Moisture buffer potential of experimental wall assemblies incorporating formulated hemp-lime. *Building and Environment* 93, 199–209. <https://doi.org/10.1016/j.buildenv.2015.07.011>
- Le-Bihan, T., Georgin, J.F., Michel, M., Ambroise, J., Morestin, F., 2012. Measurements and modeling of cement base materials deformation at early age: The case of sulfo-aluminous cement. *Cement and Concrete Research* 42, 1055–1065. <https://doi.org/10.1016/j.cemconres.2012.04.004>
- Lee, M.R., Huang, Y.T., Liao, C.H., Chuang, T.Y., Lin, C.K., Lee, S.W., Lai, C.C., Yu, C.J., Hsueh, P.R., 2011. Bacteremia caused by *Brevundimonas* species at a tertiary care hospital in Taiwan, 2000–2010. *Eur J Clin Microbiol Infect Dis* 30, 1185–1191. <https://doi.org/10.1007/s10096-011-1210-5>
- Lee, Y.S., Park, W., 2018. Current challenges and future directions for bacterial self-healing concrete. *Appl Microbiol Biotechnol* 102, 3059–3070. <https://doi.org/10.1007/s00253-018-8830-y>
- Li, D.-W., Yang, C.S., 2004. Fungal contamination as a major contributor to sick building syndrome. *Adv Appl Microbiol* 55, 31–112. [https://doi.org/10.1016/S0065-2164\(04\)55002-5](https://doi.org/10.1016/S0065-2164(04)55002-5)
- Liaud, N., Ginies, C., Navarro, D., Fabre, N., Crapart, S., Gimbert, I., Levasseur, A., Raouche, S., Sigoillot, J.-C., 2014. Exploring fungal biodiversity: organic acid production by 66 strains of filamentous fungi. *Fungal Biology and Biotechnology* 1, 1. <https://doi.org/10.1186/s40694-014-0001-z>
- Liaud, N., Rosso, M.-N., Fabre, N., Crapart, S., Herpoël-Gimbert, I., Sigoillot, J.-C., Raouche, S., Levasseur, A., 2015. L-lactic acid production by *Aspergillus brasiliensis* overexpressing the heterologous *ldha* gene from *Rhizopus oryzae*. *Microbial Cell Factories* 14, 66. <https://doi.org/10.1186/s12934-015-0249-x>
- Liu, X.-Z., Wang, Q.-M., Theelen, B., Groenewald, M., Bai, F.-Y., Boekhout, T., 2015. Phylogeny of tremellomycetous yeasts and related dimorphic and filamentous basidiomycetes reconstructed from multiple gene sequence analyses. *Stud Mycol* 81, 1–26. <https://doi.org/10.1016/j.simyco.2015.08.001>
- Liu, Z., Zhang, Y., Yan, X., 1984. A new genus of the order Actinomycetales. *Acta Microbiol Sin* 24, 295–298.
- Logrieco, A., Moretti, A., Solfrizzo, M., 2009. *Alternaria* toxins and plant diseases: an overview of origin, occurrence and risks.
- Lorenzo, J.M., Munekata, P.E., Dominguez, R., Pateiro, M., Saraiva, J.A., Franco, D., 2018. Chapter 3 - Main Groups of Microorganisms of Relevance for Food Safety and Stability:

- General Aspects and Overall Description, in: Barba, F.J., Sant'Ana, A.S., Orlie, V., Koubaa, M. (Eds.), *Innovative Technologies for Food Preservation*. Academic Press, pp. 53–107. <https://doi.org/10.1016/B978-0-12-811031-7.00003-0>
- Lowy, B., 1951. A Morphological Basis for Classifying the Species of *Auricularia*. *Mycologia* 43, 351–358. <https://doi.org/10.1080/00275514.1951.12024135>
- Luo, H., Xiong, G., Ma, C., Li, D., Wan, Y., 2014. Preparation and performance of long carbon fiber reinforced polyamide 6 composites injection-molded from core/shell structured pellets. *Materials & Design* 64, 294–300. <https://doi.org/10.1016/j.matdes.2014.07.054>
- Magnin, J.-P., Deseure, J., 2019. Hydrogen generation in a pressurized photobioreactor: Unexpected enhancement of biohydrogen production by the phototrophic bacterium *Rhodobacter capsulatus*. *Applied Energy* 239, 635–643. <https://doi.org/10.1016/j.apenergy.2019.01.204>
- Magwood, C., 2014. *Making Better Buildings: A Comparative Guide to Sustainable Construction for Homeowners and Contractors*. New Society Publishers.
- Marceau, S., Delannoy, G., 2017. Durability of Bio-based Concretes, in: Amziane, S., Collet, F. (Eds.), *Bio-Aggregates Based Building Materials : State-of-the-Art Report of the RILEM Technical Committee 236-BBM*, RILEM State-of-the-Art Reports. Springer Netherlands, Dordrecht, pp. 167–187. [https://doi.org/10.1007/978-94-024-1031-0\\_8](https://doi.org/10.1007/978-94-024-1031-0_8)
- Marceau, S., Glé, P., Guéguen-Minerbe, M., Gourlay, E., Moscardelli, S., Nour, I., Amziane, S., 2017. Influence of accelerated aging on the properties of hemp concretes. *Construction and Building Materials* 139, 524–530. <https://doi.org/10.1016/j.conbuildmat.2016.11.129>
- Marchesi, J.R., Sato, T., Weightman, A.J., Martin, T.A., Fry, J.C., Hiom, S.J., Dymock, D., Wade, W.G., 1998. Design and Evaluation of Useful Bacterium-Specific PCR Primers That Amplify Genes Coding for Bacterial 16S rRNA. *Appl. Environ. Microbiol.* 64, 2333–2333. <https://doi.org/10.1128/AEM.64.6.2333-2333.1998>
- Maresca, J.A., Moser, P., Schumacher, T., 2017. Analysis of bacterial communities in and on concrete. *Mater Struct* 50, 25. <https://doi.org/10.1617/s11527-016-0929-y>
- Margesin, R., Zhang, D.-C., 2013. *Pedobacter ruber* sp. nov., a psychrophilic bacterium isolated from soil. *International Journal of Systematic and Evolutionary Microbiology* 63, 339–344. <https://doi.org/10.1099/ijs.0.039107-0>
- Martinet, G., Souchu, P., 2009. La chaux Définitions et histoire. *Techniques de l'ingénieur Les matériaux de construction*.
- Mazur, L.J., Kim, J., Committee on Environmental Health, American Academy of Pediatrics, 2006. Spectrum of noninfectious health effects from molds. *Pediatrics* 118, e1909-1926. <https://doi.org/10.1542/peds.2006-2829>
- Méheust, D., 2012. Exposition aux moisissures en environnement intérieur: méthodes de mesure et impacts sur la santé.
- Melo Filho, J. de A., Silva, F. de A., Toledo Filho, R.D., 2013. Degradation kinetics and aging mechanisms on sisal fiber cement composite systems. *Cement and Concrete Composites* 40, 30–39. <https://doi.org/10.1016/j.cemconcomp.2013.04.003>
- Micallef SA, Goldstein RE, George A, Ewing L, Tall BD, Ms, B., Sw, J., Ar, S., 2013. Diversity, distribution and antibiotic resistance of *Enterococcus* spp. recovered from tomatoes, leaves, water and soil on U.S. Mid-Atlantic farms. *Food Microbiol* 36, 465–474. <https://doi.org/10.1016/j.fm.2013.04.016>
- Millanes, A.M., Diederich, P., Ekman, S., Wedin, M., 2011. Phylogeny and character evolution in the jelly fungi (Tremellomycetes, Basidiomycota, Fungi). *Mol. Phylogenet. Evol.* 61, 12–

28. <https://doi.org/10.1016/j.ymprev.2011.05.014>

- Millanes, A.M., Truong, C., Westberg, M., Diederich, P., Wedin, M., 2014. Host switching promotes diversity in host-specialized mycoparasitic fungi: uncoupled evolution in the *Biatoropsis-usnea* system. *Evolution* 68, 1576–1593. <https://doi.org/10.1111/evo.12374>
- Millanes, A.M., Westberg, M., Wedin, M., Diederich, P., 2012. *Tremella diploschistina* (Tremellales, Basidiomycota, Fungi), a new lichenicolous species growing on *Diploschistes*. *The Lichenologist* 44, 321–332. <https://doi.org/10.1017/S0024282911000788>
- Miller, A.Z., Sanmartín, P., Pereira-Pardo, L., Dionísio, A., Saiz-Jimenez, C., Macedo, M.F., Prieto, B., 2012. Bioreceptivity of building stones: A review. *Science of The Total Environment* 426, 1–12. <https://doi.org/10.1016/j.scitotenv.2012.03.026>
- Mohammadipanah, F., Hamedi, J., Spröer, C., Rohde, M., Montero-Calasanz, M. del C., Klenk, H.-P., 2014. *Streptomyces zagrosensis* sp. nov., isolated from soil. *International Journal of Systematic and Evolutionary Microbiology* 64, 3434–3440. <https://doi.org/10.1099/ijms.0.064527-0>
- Mohammadipanah, F., Montero-Calasanz, M. del C., Schumann, P., Spröer, C., Rohde, M., Klenk, H.-P., 2017. *Promicromonospora kermanensis* sp. nov., an actinobacterium isolated from soil. *International Journal of Systematic and Evolutionary Microbiology*, 67, 262–267. <https://doi.org/10.1099/ijsem.0.001613>
- Mokhtarnejad, L., Arzanlou, M., Babai-Ahari, A., Di Mauro, S., Onofri, A., Buzzini, P., Turchetti, B., 2016. Characterization of basidiomycetous yeasts in hypersaline soils of the Urmia Lake National Park, Iran. *Extremophiles* 20, 915–928. <https://doi.org/10.1007/s00792-016-0883-1>
- Moujalled, B., Aït Ouméziane, Y., Moissette, S., Bart, M., Lanos, C., Samri, D., 2018. Experimental and numerical evaluation of the hygrothermal performance of a hemp lime concrete building: A long term case study. *Building and Environment* 136, 11–27. <https://doi.org/10.1016/j.buildenv.2018.03.025>
- Muangham, S., Suksaard, P., Mingma, R., Matsumoto, A., Takahashi, Y., Duangmal, K., 2016. *Nocardiostrictum diminis* sp. nov., isolated from mangrove sediment. *International Journal of Systematic and Evolutionary Microbiology*, 66, 3835–3840. <https://doi.org/10.1099/ijsem.0.001273>
- Mubarak, Z., Soraya, C., 2018. The acid tolerance response and pH adaptation of *Enterococcus faecalis* in extract of lime *Citrus aurantiifolia* from Aceh Indonesia. *F1000Research* 7. <https://doi.org/10.12688/f1000research.13990.2>
- Müller, H.E., Fanning, G.R., Brenner, D.J., 1995. Isolation of *Ewingella americana* from mollusks. *Current Microbiology* 31, 287–290. <https://doi.org/10.1007/BF00314581>
- Muyzer, G., de Waal, E.C., Uitterlinden, A.G., 1993. Profiling of complex microbial populations by denaturing gradient gel electrophoresis analysis of polymerase chain reaction-amplified genes coding for 16S rRNA. *Applied and Environmental Microbiology* 59, 695–700. <https://doi.org/10.1128/AEM.59.3.695-700.1993>
- Nadif, A., Hunkeler, D., Käuper, P., 2002. Sulfur-free lignins from alkaline pulping tested in mortar for use as mortar additives. *Bioresource Technology* 84, 49–55. [https://doi.org/10.1016/S0960-8524\(02\)00020-2](https://doi.org/10.1016/S0960-8524(02)00020-2)
- Nayak, A.P., Croston, T.L., Lemons, A.R., Goldsmith, W.T., Marshall, N.B., Kashon, M.L., Germolec, D.R., Beezhold, D.H., Green, B.J., 2018. *Aspergillus fumigatus* viability drives allergic responses to inhaled conidia. *Ann Allergy Asthma Immunol* 121, 200-210.e2. <https://doi.org/10.1016/j.anai.2018.04.008>

- Nguyen, S.T., Tran-Le, A.D., Vu, M.N., To, Q.D., Douzane, O., Langlet, T., 2016. Modeling thermal conductivity of hemp insulation material: A multi-scale homogenization approach. *Building and Environment* 107, 127–134. <https://doi.org/10.1016/j.buildenv.2016.07.026>
- Nguyen, T.T., 2014. Contribution à l'étude de la formulation et du procédé de fabrication d'éléments de construction en béton de chanvre 169.
- Nguyen, T.T., Picandet, V., Carre, P., Lecompte, T., Amziane, S., Baley, C., 2010. Effect of compaction on mechanical and thermal properties of hemp concrete. *European Journal of Environmental and Civil Engineering* 14, 545–560. <https://doi.org/10.1080/19648189.2010.9693246>
- Nicklin, J., Graeme-Cook, K., Paget, T., Killington, R., 2000. *L'essentiel en microbiologie*. Berti.
- Niemhom, N., Chutrakul, C., Suriyachadkun, C., Tadtong, S., Thawai, C., 2019. *Jiangella endophytica* sp. nov., an endophytic actinomycete isolated from the rhizome of *Kaempferia elegans*. *Int J Syst Evol Microbiol* 69, 454–459. <https://doi.org/10.1099/ijsem.0.003175>
- Nik, V.M., Sasic Kalagasidis, A., Kjellström, E., 2012. Assessment of hygrothermal performance and mould growth risk in ventilated attics in respect to possible climate changes in Sweden. *Building and Environment* 55, 96–109. <https://doi.org/10.1016/j.buildenv.2012.01.024>
- NORDTEST project, 2005. BYG DTU R-126 Moisture buffering of building materials.
- Nouioui, I., Rückert, C., Willemse, J., van Wezel, G.P., Klenk, H.-P., Busche, T., Kalinowski, J., Bredholt, H., Zotchev, S.B., 2017. *Actinoalloteichus fjordicus* sp. nov. isolated from marine sponges: phenotypic, chemotaxonomic and genomic characterisation. *Antonie van Leeuwenhoek* 110, 1705–1717. <https://doi.org/10.1007/s10482-017-0920-9>
- Oh, W.T., Giri, S.S., Yun, S., Kim, H.J., Kim, S.G., Kim, S.W., Kang, J.W., Han, S.J., Kwon, J., Jun, J.W., Park, S.C., 2019. *Janthinobacterium lividum* as An Emerging Pathogenic Bacterium Affecting Rainbow Trout (*Oncorhynchus mykiss*) Fisheries in Korea. *Pathogens* 8, 146. <https://doi.org/10.3390/pathogens8030146>
- Ojanen, T., Viitanen, H., Peuhkuri, R., Lähdesmäki, K., Vinha, J., Salminen, K., 2010. Mold growth modeling of building structures using sensitivity classes of materials. ASHRAE Buildings XI Conference, Dec. 5-9, 2010 Cleawater Beach, Florida 1–10.
- O'Rourke, D.P., Rosenbaum, M.D., 2015. Chapter 18 - Biology and Diseases of Amphibians, in: Fox, J.G., Anderson, L.C., Otto, G.M., Pritchett-Corning, K.R., Whary, M.T. (Eds.), *Laboratory Animal Medicine (Third Edition)*, American College of Laboratory Animal Medicine. Academic Press, Boston, pp. 931–965. <https://doi.org/10.1016/B978-0-12-409527-4.00018-3>
- Östbom, G., 2007. Hampa - ett textilt material: undersökning av styrka och finlek hos gotländsk hampfiber. Högskolan i Borås, Textilhögskolan.
- Packer, H.L., Harrison, D.M., Dixon, R.M., Armitage, J.P., 1994. The effect of pH on the growth and motility of *Rhodobacter sphaeroides* WS8 and the nature of the driving force of the flagellar motor. *Biochimica Et Biophysica Acta* 1188, 101–107. [https://doi.org/10.1016/0005-2728\(94\)90027-2](https://doi.org/10.1016/0005-2728(94)90027-2)
- Panasiti, V., Devirgiliis, V., Mancini, M., Curzio, M., Rossi, M., Fioriti, D., Pietropaolo, V., Nicosia, R., Gallinelli, C., Chiarini, F., Pecorini, G., Calvieri, S., 2008. A cutaneous infection caused by *Brevundimonas vesicularis*: a case report. *International Journal of Immunopathology and Pharmacology* 21, 457–461. <https://doi.org/10.1177/039463200802100226>
- Parexlanko, 2020. Corps d'enduit chanvre - emploi et mise en oeuvre.
- Pasanen, A.-L., Korpi, A., Kasanen, J.-P., Pasanen, P., 1998. Critical aspects on the significance

- of microbial volatile metabolites as indoor air pollutants. *Environment International* 24, 703–712. [https://doi.org/10.1016/S0160-4120\(98\)00065-8](https://doi.org/10.1016/S0160-4120(98)00065-8)
- Piot, A., Béjat, T., Jay, A., Bessette, L., Wurtz, E., Barnes-Davin, L., 2017a. Study of a hempcrete wall exposed to outdoor climate: Effects of the coating. *Construction and Building Materials* 139, 540–550. <https://doi.org/10.1016/j.conbuildmat.2016.12.143>
- Piot, A., Béjat, T., Jay, A., Bessette, L., Wurtz, E., Barnes-Davin, L., 2017b. Study of a hempcrete wall exposed to outdoor climate: Effects of the coating. *Construction and Building Materials* 139, 540–550. <https://doi.org/10.1016/j.conbuildmat.2016.12.143>
- Pitt, J.I., Hocking, A.D., 1977. Influence of solute and hydrogen ion concentration on the water relations of some xerophilic fungi. *J Gen Microbiol* 101, 35–40. <https://doi.org/10.1099/00221287-101-1-35>
- Plassard, C., Fransson, P., 2009. Regulation of low-molecular weight organic acid production in fungi. *Fungal Biology Reviews* 23, 30–39. <https://doi.org/10.1016/j.fbr.2009.08.002>
- Portnoy, J.M., Jara, D., 2015. Mold allergy revisited. *Ann Allergy Asthma Immunol* 114, 83–89. <https://doi.org/10.1016/j.anai.2014.10.004>
- Pound, M.W., Tart, S.B., Okoye, O., 2007. Multidrug-resistant *Ewingella americana*: a case report and review of the literature. *Ann Pharmacother* 41, 2066–2070. <https://doi.org/10.1345/aph.1K398>
- Qin, S., Jiang, J.-H., Klenk, H.-P., Zhu, W.-Y., Zhao, G.-Z., Zhao, L.-X., Tang, S.-K., Xu, L.-H., Li, W.-J., 2012. *Promicromonospora xylanilytica* sp. nov., an endophytic actinomycete isolated from surface-sterilized leaves of the medicinal plant *Maytenus austroyunnanensis*. *Int J Syst Evol Microbiol* 62, 84–89. <https://doi.org/10.1099/ij.s.0.032185-0>
- Rackley, S.A., 2017. Mineral carbonation, in: Rackley, S.A. (Ed.), *Carbon Capture and Storage (Second Edition)*. Butterworth-Heinemann, Boston, pp. 253–282. <https://doi.org/10.1016/B978-0-12-812041-5.00010-6>
- Rahim, M., Douzane, O., Tran Le, A.D., Promis, G., Laidoudi, B., Crigny, A., Dupre, B., Langlet, T., 2015. Characterization of flax lime and hemp lime concretes: Hygric properties and moisture buffer capacity. *Energy and Buildings* 88, 91–99. <https://doi.org/10.1016/j.enbuild.2014.11.043>
- Ranalli, P., 1999. *Advances in Hemp Research*. CRC Press.
- Reboux, G., Bellanger, A.-P., Dalphin, J.-C., 2011. Contre : les composés organiques volatils d'origine fongique ont un impact sur la santé. *Revue Française d'Allergologie*, 6ème Congrès Francophone d'Allergologie 51, 350–353. <https://doi.org/10.1016/j.reval.2011.01.017>
- Ren, J., Zhao, Z., Zhang, J., Wang, J., Guo, S., Sun, J., 2019. Study on the hygrothermal properties of a Chinese solar greenhouse with a straw block north wall. *Energy and Buildings* 193, 127–138. <https://doi.org/10.1016/j.enbuild.2019.03.040>
- Reyes, J.E., Venturini, M.E., Oria, R., Blanco, D., 2004. Prevalence of *Ewingella americana* in retail fresh cultivated mushrooms (*Agaricus bisporus*, *Lentinula edodes* and *Pleurotus ostreatus*) in Zaragoza (Spain). *FEMS Microbiol Ecol* 47, 291–296. [https://doi.org/10.1016/S0168-6496\(03\)00283-6](https://doi.org/10.1016/S0168-6496(03)00283-6)
- Rima, A., Abahri, K., Bennai, F., El Hachem, C., Bonnet, M., 2021. Microscopic estimation of swelling and shrinkage of hemp concrete in response to relative humidity variations. *Journal of Building Engineering* 43, 102929. <https://doi.org/10.1016/j.job.2021.102929>
- Rivas, R., Velázquez, E., Willems, A., Vizcaíno, N., Subba-Rao, N.S., Mateos, P.F., Gillis, M., Dazzo, F.B., Martínez-Molina, E., 2002. A New Species of *Devosia* That Forms a Unique

Nitrogen-Fixing Root-Nodule Symbiosis with the Aquatic Legume *Neptunia natans* (L.f.) Druce. *Appl Environ Microbiol* 68, 5217–5222. <https://doi.org/10.1128/AEM.68.11.5217-5222.2002>

- Rivas, R., Willems, A., Subba-Rao, N.S., Mateos, P.F., Dazzo, F.B., Kroppenstedt, R.M., Martínez-Molina, E., Gillis, M., Velázquez, E., 2003. Description of *Devosia neptuniae* sp. nov. that nodulates and fixes nitrogen in symbiosis with *Neptunia natans*, an aquatic legume from India. *Systematic and Applied Microbiology* 26, 47–53. <https://doi.org/10.1078/072320203322337308>
- Rodrigues, A., Gutierrez-Patricio, S., Miller, A.Z., Saiz-Jimenez, C., Wiley, R., Nunes, D., Vilarigues, M., Macedo, M.F., 2014. Fungal biodeterioration of stained-glass windows. *International Biodeterioration & Biodegradation* 90, 152–160. <https://doi.org/10.1016/j.ibiod.2014.03.007>
- Rothschild, L.J., Mancinelli, R.L., 2001. Life in extreme environments. *Nature* 409, 1092–1101. <https://doi.org/10.1038/35059215>
- Roulet, C.-A., 2004. Santé et qualité de l'environnement intérieur dans les bâtiments. PPUR presses polytechniques.
- Ryan, M.P., Pembroke, J.T., 2018. *Brevundimonas* spp: Emerging global opportunistic pathogens. *Virulence* 9, 480–493. <https://doi.org/10.1080/21505594.2017.1419116>
- Sáez-Nieto, J.A., Medina-Pascual, M.J., Carrasco, G., Garrido, N., Fernandez-Torres, M.A., Villalón, P., Valdezate, S., 2017. *Paenibacillus* spp. isolated from human and environmental samples in Spain: detection of 11 new species. *New Microbes and New Infections* 19, 19–27. <https://doi.org/10.1016/j.nmni.2017.05.006>
- Sáez-Pérez, M.P., Brümmer, M., Durán-Suárez, J.A., 2020. A review of the factors affecting the properties and performance of hemp aggregate concretes. *Journal of Building Engineering* 31, 101323. <https://doi.org/10.1016/j.job.2020.101323>
- Sanmartín, P., Miller, A.Z., Prieto, B., Viles, H.A., 2021. Revisiting and reanalysing the concept of bioreceptivity 25 years on. *Science of The Total Environment* 770, 145314. <https://doi.org/10.1016/j.scitotenv.2021.145314>
- Schleibinger, H., Lausmann, D., Bornehag, C.-G., Eis, D., Rueden, H., 2008. Microbial volatile organic compounds in the air of moldy and mold-free indoor environments. *Indoor Air* 18, 113–124. <https://doi.org/10.1111/j.1600-0668.2007.00513.x>
- Schloissnig, S., Arumugam, M., Sunagawa, S., Mitreva, M., Tap, J., Zhu, A., Waller, A., Mende, D.R., Kultima, J.R., Martin, J., Kota, K., Sunyaev, S.R., Weinstock, G.M., Bork, P., 2013. Genomic variation landscape of the human gut microbiome. *Nature* 493, 45–50. <https://doi.org/10.1038/nature11711>
- Schoch, C.L., Seifert, K.A., Huhndorf, S., Robert, V., Spouge, J.L., Levesque, C.A., Chen, W., Fungal Barcoding Consortium, Fungal Barcoding Consortium Author List, 2012. Nuclear ribosomal internal transcribed spacer (ITS) region as a universal DNA barcode marker for Fungi. *Proc Natl Acad Sci U S A* 109, 6241–6246. <https://doi.org/10.1073/pnas.1117018109>
- Schumann, P., Stackebrandt, E., 2015. *Promicromonospora*, in: *Bergey's Manual of Systematics of Archaea and Bacteria*. American Cancer Society, pp. 1–10. <https://doi.org/10.1002/9781118960608.gbm00130>
- SEBTP, 2012. Construire en chanvre - Règles professionnelles d'exécution.
- Sedan, D., Pagnoux, C., Smith, A., Chotard, T., 2008. Mechanical properties of hemp fibre reinforced cement: Influence of the fibre/matrix interaction. *Journal of the European Ceramic Society* 28, 183–192. <https://doi.org/10.1016/j.jeurceramsoc.2007.05.019>

- Seifert, K.A., Gams, W., 2011. The genera of Hyphomycetes – 2011 update. *Persoonia*. <https://doi.org/10.3767/003158511X617435>
- Sentenac, C., Sonebi, M., Amziane, S., Pascal, U.B., Pascal, I., Clermont-Ferrand, P., 2017. Investigation on the performance and durability of treated hemp concrete with linseed oil 35, 9.
- Sharma, A., Gautam, S., Saxena, S., 2014. Streptomyces, in: Batt, C.A., Tortorello, M.L. (Eds.), *Encyclopedia of Food Microbiology (Second Edition)*. Academic Press, Oxford, pp. 560–566. <https://doi.org/10.1016/B978-0-12-384730-0.00326-8>
- Shimada, M., Akamtsu, Y., Tokimatsu, T., Mii, K., Hattori, T., 1997. Possible biochemical roles of oxalic acid as a low molecular weight compound involved in brown-rot and white-rot wood decays. *Journal of Biotechnology, Low Molecular Weight Compounds in Lignin Degradation* 53, 103–113. [https://doi.org/10.1016/S0168-1656\(97\)01679-9](https://doi.org/10.1016/S0168-1656(97)01679-9)
- Shivaji, S., Ray, M.K., Kumar, G.S., Reddy, G.S.N., Saisree, L., 1991. Identification of *Janthinobacterium fividum* from the soils of the islands of Scotia Ridge and from Antarctic peninsula 5.
- Shuvo, I.I., 2020. Fibre attributes and mapping the cultivar influence of different industrial cellulosic crops (cotton, hemp, flax, and canola) on textile properties. *Bioresources and Bioprocessing* 7, 51. <https://doi.org/10.1186/s40643-020-00339-1>
- Siddiqi, M.Z., Yeon, J.M., Choi, H., Lee, J.H., Kim, S.Y., Wee, J.-H., Im, W.T., 2020. *Luteimonas granuli* sp. nov., Isolated from Granules of the Wastewater Treatment Plant. *Curr Microbiol* 77, 2002–2007. <https://doi.org/10.1007/s00284-020-02066-4>
- Singla, A.K., Mayilraj, S., Kudo, T., Krishnamurthi, S., Prasad, G.S., Vohra, R.M., 2005. *Actinoalloteichus spitiensis* sp. nov., a novel actinobacterium isolated from a cold desert of the Indian Himalayas. *International Journal of Systematic and Evolutionary Microbiology* 55, 2561–2564. <https://doi.org/10.1099/ijs.0.63720-0>
- Sinka, M., Obuka, V., Bajare, D., Jakovics, A., 2019. Durability and hygrothermal performance of bio-based materials in northern European climate. <https://doi.org/10.26168/icbbm2019.53>
- Sinka, M., Sahmenko, G., Korjakins, A., 2014. Mechanical Properties of Pre-Compressed Hemp-Lime Concrete. *Journal of Sustainable Architecture and Civil Engineering* 8, 92–99. <https://doi.org/10.5755/j01.sace.8.3.7451>
- Song, L, Li, W. J., Wang, Q. L., Chen, G. Z., Zhang, Y. S., Xu, L. H., 2005. *Jiangella gangsuensis* gen. nov., sp. nov., a novel actinomycete from a desert soil in north-west China. *Int J Syst Evol Microbiol* 55, 881–884.
- Steinberg, J.P., Burd, E.M., 2015. Other Gram-Negative and Gram-Variable Bacilli, in: Bennett, J.E., Dolin, R., Blaser, M.J. (Eds.), *Mandell, Douglas, and Bennett's Principles and Practice of Infectious Diseases (Eighth Edition)*. Content Repository Only!, Philadelphia, pp. 2667-2683.e4. <https://doi.org/10.1016/B978-1-4557-4801-3.00238-1>
- Stevulova, N., Kidalova, L., Junak, J., Cigasova, J., Terpakova, E., 2012. Effect of Hemp Shive Sizes on Mechanical Properties of Lightweight Fibrous Composites. *Procedia Engineering, CHISA 2012* 42, 496–500. <https://doi.org/10.1016/j.proeng.2012.07.441>
- Stopnisek, N., Bodenhausen, N., Frey, B., Fierer, N., Eberl, L., Weisskopf, L., 2014. Genus-wide acid tolerance accounts for the biogeographical distribution of soil Burkholderia populations: Preference of Burkholderia sp. for acid soils. *Environ Microbiol* 16, 1503–1512. <https://doi.org/10.1111/1462-2920.12211>
- Sykes, J.E., 2014. Chapter 34 - Streptococcal and Enterococcal Infections, in: Sykes, J.E. (Ed.), *Canine and Feline Infectious Diseases*. W.B. Saunders, Saint Louis, pp. 334–346.



<https://doi.org/10.1016/B978-1-4377-0795-3.00034-X>

- Tabuc, C., 2007. Flore fongique de différents substrats et conditions optimales de production des mycotoxines (phd).
- Talon, A., 2006. Evaluation des scénarii de dégradation des produits de construction 322.
- Talwar, C., Nagar, S., Kumar, R., Scaria, J., Lal, R., Negi, R.K., 2020. Defining the Environmental Adaptations of Genus *Devosia*: Insights into its Expansive Short Peptide Transport System and Positively Selected Genes. *Scientific Reports* 10, 1151. <https://doi.org/10.1038/s41598-020-58163-8>
- Tamura, T., Zhiheng, L., Yamei, Z., Hatano, K., 2000. *Actinoalloteichus cyanogriseus* gen. nov., sp. nov. *International Journal of Systematic and Evolutionary Microbiology*, 50, 1435–1440. <https://doi.org/10.1099/00207713-50-4-1435>
- Tanaka, N., Akamatsu, Y., Hattori, T., Shimada, M., 1994. Effect of Oxalic Acid on the Oxidative Breakdown of Cellulose by the Fenton Reaction 81, 4.
- Terres Inovia, 2020. Guide de culture: Chanvre.
- Tettey, U.Y.A., Dodoo, A., Gustavsson, L., 2014. Effects of different insulation materials on primary energy and CO<sub>2</sub> emission of a multi-storey residential building. *Energy and Buildings* 82, 369–377. <https://doi.org/10.1016/j.enbuild.2014.07.009>
- Thawai, C., Kudo, T., 2015. *Promicromonospora thailandica* sp. nov., isolated from marine sediment 6.
- Thomma, B.P.H.J., 2003. *Alternaria* spp.: from general saprophyte to specific parasite. *Mol. Plant Pathol.* 4, 225–236. <https://doi.org/10.1046/j.1364-3703.2003.00173.x>
- Tolêdo Filho, R.D., Scrivener, K., England, G.L., Ghavami, K., 2000. Durability of alkali-sensitive sisal and coconut fibres in cement mortar composites. *Cement and Concrete Composites* 22, 127–143. [https://doi.org/10.1016/S0958-9465\(99\)00039-6](https://doi.org/10.1016/S0958-9465(99)00039-6)
- Tran Le, A.D., 2010. Etude des transferts hygrothermiques dans le béton de chanvre et leur application au bâtiment (sous titre: simulation numérique et approche expérimentale) 220.
- Tran, T.H., Govin, A., Guyonnet, R., Grosseau, P., Lors, C., Damidot, D., Deves, O., Ruot, B., 2014. Influence of the intrinsic characteristics of mortars on their biofouling by pigmented organisms: Comparison between laboratory and field-scale experiments. *International Biodeterioration & Biodegradation* 86, 334–342. <https://doi.org/10.1016/j.ibiod.2013.10.005>
- Tran, T.H., Govin, A., Guyonnet, R., Grosseau, P., Lors, C., Garcia-Diaz, E., Damidot, D., Devès, O., Ruot, B., 2012. Influence of the intrinsic characteristics of mortars on biofouling by *Klebsormidium flaccidum*. *International Biodeterioration & Biodegradation* 70, 31–39. <https://doi.org/10.1016/j.ibiod.2011.10.017>
- Uchikoba, T., Mase, T., Arima, K., Yonezawa, H., Kaneda, M., 2001. Isolation and characterization of a trypsin-like protease from *Trichoderma viride*. *Biol Chem* 382, 1509–1513. <https://doi.org/10.1515/BC.2001.185>
- Uehlinger, S., Schwager, S., Bernier, S.P., Riedel, K., Nguyen, D.T., Sokol, P.A., Eberl, L., 2009. Identification of specific and universal virulence factors in *Burkholderia cenocepacia* strains by using multiple infection hosts. *Infection and Immunity* 77, 4102–4110. <https://doi.org/10.1128/IAI.00398-09>
- Van Dommelen, A., Vanderleyden, J., 2007. Chapter 12 - Associative Nitrogen Fixation, in: Bothe, H., Ferguson, S.J., Newton, W.E. (Eds.), *Biology of the Nitrogen Cycle*. Elsevier, Amsterdam, pp. 179–192. <https://doi.org/10.1016/B978-044452857-5.50013-8>

- Van Montagu, M., 2001. *Agrobacterium*, in: Brenner, S., Miller, J.H. (Eds.), *Encyclopedia of Genetics*. Academic Press, New York, pp. 23–25. <https://doi.org/10.1006/rwgn.2001.0018>
- Van Tran, V., Mavingui, P., Berge, O., Balandreau, J., Heulin, T., 1996. *Burkholderia vietnamiensis*, a new nitrogen-fixing species associated with rice roots, isolated from an acid sulphate soil in Vietnam: plant-growth-promoting effects on rice, in: Rahman, M., Podder, A.K., Van Hove, C., Begum, Z.N.T., Heulin, Thierry, Hartmann, A. (Eds.), *Biological Nitrogen Fixation Associated with Rice Production: Based on Selected Papers Presented in the International Symposium on Biological Nitrogen Fixation Associated with Rice*, Dhaka, Bangladesh, 28 November– 2 December, 1994, *Developments in Plant and Soil Sciences*. Springer Netherlands, Dordrecht, pp. 181–190. [https://doi.org/10.1007/978-94-015-8670-2\\_20](https://doi.org/10.1007/978-94-015-8670-2_20)
- Vázquez-Nion, D., Silva, B., Prieto, B., 2018. Influence of the properties of granitic rocks on their bioreceptivity to subaerial phototrophic biofilms. *Science of The Total Environment* 610–611, 44–54. <https://doi.org/10.1016/j.scitotenv.2017.08.015>
- Verma, A., Ojha, A.K., Kumari, P., Sundharam, S.S., Mayilraj, S., Krishnamurthi, S., 2016. *Luteimonas padinae* sp. nov., an epiphytic bacterium isolated from an intertidal macroalga. *International Journal of Systematic and Evolutionary Microbiology* 66, 5444–5451. <https://doi.org/10.1099/ijsem.0.001539>
- Viel, M., Collet, F., Lecieux, Y., François, M.L.M., Colson, V., Lanos, C., Hussain, A., Lawrence, M., 2019. Resistance to mold development assessment of bio-based building materials. *Composites Part B: Engineering* 158, 406–418. <https://doi.org/10.1016/j.compositesb.2018.09.063>
- Viitanen, H., Vinha, J., Salminen, K., Ojanen, T., Peuhkuri, R., Paajanen, L., Lähdesmäki, K., 2010. Moisture and Bio-deterioration Risk of Building Materials and Structures. *Journal of Building Physics* 33, 201–224. <https://doi.org/10.1177/1744259109343511>
- Walker, R., Pavia, S., Mitchell, R., 2014. Mechanical properties and durability of hemp-lime concretes. *Construction and Building Materials* 61, 340–348. <https://doi.org/10.1016/j.conbuildmat.2014.02.065>
- Wang, J.Y., Soens, H., Verstraete, W., De Belie, N., 2014. Self-healing concrete by use of microencapsulated bacterial spores. *Cement and Concrete Research* 56, 139–152. <https://doi.org/10.1016/j.cemconres.2013.11.009>
- Wang, Q., Garrity, G.M., Tiedje, J.M., Cole, J.R., 2007. Naïve Bayesian Classifier for Rapid Assignment of rRNA Sequences into the New Bacterial Taxonomy. *Appl Environ Microbiol* 73, 5261–5267. <https://doi.org/10.1128/AEM.00062-07>
- Waśkiewicz, A., Irzykowska, L., 2014. *Flavobacterium* spp. – Characteristics, Occurrence, and Toxicity, in: Batt, C.A., Tortorello, M.L. (Eds.), *Encyclopedia of Food Microbiology (Second Edition)*. Academic Press, Oxford, pp. 938–942. <https://doi.org/10.1016/B978-0-12-384730-0.00126-9>
- Wei, J., Meyer, C., 2015. Degradation mechanisms of natural fiber in the matrix of cement composites. *Cement and Concrete Research* 73, 1–16. <https://doi.org/10.1016/j.cemconres.2015.02.019>
- Werth, S., Millanes, A.M., Wedin, M., Scheidegger, C., 2013. Lichenicolous fungi show population subdivision by host species but do not share population history with their hosts. *Fungal Biol* 117, 71–84. <https://doi.org/10.1016/j.funbio.2012.11.007>
- Williams, J.S., Dungait, J.A.J., Bol, R., Abbott, G.D., 2016. Comparison of extraction efficiencies for water-transportable phenols from different land uses. *Organic Geochemistry* 102, 45–51. <https://doi.org/10.1016/j.orggeochem.2016.09.010>

- Wisplinghoff, H., 2017. *Pseudomonas* spp., *Acinetobacter* spp. and Miscellaneous Gram-Negative Bacilli, in: Cohen, J., Powderly, W.G., Opal, S.M. (Eds.), *Infectious Diseases* (Fourth Edition). Elsevier, pp. 1579-1599.e2. <https://doi.org/10.1016/B978-0-7020-6285-8.00181-7>
- Xiang, W., Liu, C., Wang, X., Du, J., Xi, L., Huang, Y., 2011. *Actinoalloteichus nanshanensis* sp. nov., isolated from the rhizosphere of a fig tree (*Ficus religiosa*). *International Journal of Systematic and Evolutionary Microbiology*, 61, 1165–1169. <https://doi.org/10.1099/ijs.0.023283-0>
- Xu, L., Zhang, Y., Read, N., Liu, S., Friman, V.-P., 2017. *Devosia nitraria* sp. nov., a novel species isolated from the roots of *Nitraria sibirica* in China. *Antonie van Leeuwenhoek* 110, 1475–1483. <https://doi.org/10.1007/s10482-017-0901-z>
- Yadav, A.N., Yadav, N., Kour, D., Kumar, Akhilesh, Yadav, K., Kumar, Amit, Rastegari, A.A., Sachan, S.G., Singh, B., Chauhan, V.S., Saxena, A.K., 2019. Chapter 1 - Bacterial community composition in lakes, in: Bandh, S.A., Shafí, S., Shameem, N. (Eds.), *Freshwater Microbiology*. Academic Press, pp. 1–71. <https://doi.org/10.1016/B978-0-12-817495-1.00001-3>
- Yassin, A.F., Young, C.C., Lai, W.-A., Hupfer, H., Arun, A.B., Shen, F.-T., Rekha, P.D., Ho, M.-J., 2007. *Williamsia serinedens* sp. nov., isolated from an oil-contaminated soil. *International Journal of Systematic and Evolutionary Microbiology* 57, 558–561. <https://doi.org/10.1099/ijs.0.64691-0>
- Yoon, J.-H., Kang, S.-J., Lee, J.-S., Oh, T.-K., 2006. *Brevundimonas terrae* sp. nov., isolated from an alkaline soil in Korea. *International Journal of Systematic and Evolutionary Microbiology* 56, 2915–2919. <https://doi.org/10.1099/ijs.0.64253-0>
- Yoon, J.-H., Kang, S.-J., Park, S., Oh, T.-K., 2007. *Devosia insulae* sp. nov., isolated from soil, and emended description of the genus *Devosia*. *International Journal of Systematic and Evolutionary Microbiology* 57, 1310–1314. <https://doi.org/10.1099/ijs.0.65028-0>
- Yoon, J.-H., Kang, S.-J., Yeo, S.-H., Oh, T.-K., 2005. *Paenibacillus alkaliterrae* sp. nov., isolated from an alkaline soil in Korea. *International Journal of Systematic and Evolutionary Microbiology* 55, 2339–2344. <https://doi.org/10.1099/ijs.0.63771-0>
- Young, C.-C., Kämpfer, P., Chen, W.-M., Yen, W.-S., Arun, A.B., Lai, W.-A., Shen, F.-T., Rekha, P.D., Lin, K.-Y., Chou, J.-H., 2007. *Luteimonas composti* sp. nov., a moderately thermophilic bacterium isolated from food waste. *International Journal of Systematic and Evolutionary Microbiology* 57, 741–744. <https://doi.org/10.1099/ijs.0.64701-0>
- Yuan, Y., Wu, F., Si, J., Zhao, Y.-F., Dai, Y.-C., 2019. Whole genome sequence of *Auricularia heimuer* (Basidiomycota, Fungi), the third most important cultivated mushroom worldwide. *Genomics* 111, 50–58. <https://doi.org/10.1016/j.ygeno.2017.12.013>
- Yüksel, N., 2016. The Review of Some Commonly Used Methods and Techniques to Measure the Thermal Conductivity of Insulation Materials. *Insulation Materials in Context of Sustainability*. <https://doi.org/10.5772/64157>
- Zhang, D.-C., Schinner, F., Margesin, R., 2010. *Pedobacter bauzanensis* sp. nov., isolated from soil. *International Journal of Systematic and Evolutionary Microbiology* 60, 2592–2595. <https://doi.org/10.1099/ijs.0.018903-0>
- Zhang, G.Z., Tang, C.Y., 2015. First Report of *Acrostalagmus luteo-albus* Causing Red Rust of Needle Mushroom (*Flammulina velutipes*) in China. *Plant Dis.* 99, 158. <https://doi.org/10.1094/PDIS-07-14-0728-PDN>
- Zhang, H., Zheng, W., Huang, J., Luo, H., Jin, Y., Zhang, W., Liu, Z., Huang, Y., 2006. *Actinoalloteichus hymeniacidonis* sp. nov., an actinomycete isolated from the marine sponge *Hymeniacidon perleve*. *International Journal of Systematic and Evolutionary Microbiology*,

56, 2309–2312. <https://doi.org/10.1099/ijms.0.64217-0>

Zhao, D., Liu, P., Pan, C., Du, R., Ping, W., Ge, J., 2016. Bacterial succession and metabolite changes during flax (*Linum usitatissimum* L.) retting with *Bacillus cereus* HDYM-02. *Sci Rep* 6. <https://doi.org/10.1038/srep31812>

Zhu, Y., Zhuang, L., Goodell, B., Cao, J., Mahaney, J., 2016. Iron sequestration in brown-rot fungi by oxalate and the production of reactive oxygen species (ROS). *International Biodeterioration & Biodegradation* 109, 185–190. <https://doi.org/10.1016/j.ibiod.2016.01.023>



**Titre :** Approches micro-macroscopiques pour l' valuation des m canismes fongiques impliqu s dans la d gradation des mortiers biosourc s : impact sur les propri t s hygrothermiques

**Mots cl s :** mat riaux biosourc s, b ton de chanvre, durabilit , cycles de vieillissement, biod terioration, contamination microbienne

**R sum  :** L'objectif principal de ce travail de th se  tait l' tude de la durabilit  de mat riaux biosourc s tel que le mortier de chanvre dans le sens large. La prise en compte des aspects de vieillissement et de diff rents facteurs influant sur la performance de mortier de chanvre au cours de son p riode d'utilisation a  t  faite.

L'originalit  de ce travail r side dans plusieurs aspects. D'une part, il s'agit d'une  tude du vieillissement du mortier de chanvre. Pour ce faire, il est n cessaire   la fois d'adopter un protocole de vieillissement repr sentatif des conditions d'utilisation du mortier de chanvre et d'utiliser diff rentes m thodes exp rimentales de suivi de l' volution des caract ristiques et propri t s. L'ensemble de ces travaux a conduit   la mise en place de montages sp cifiques pour l'application des cycles de vieillissement.

D'autre part, l' tude approfondie de la prolif ration microbienne est n cessaire pour pallier le fait que le mortier de chanvre repr sente un grand risque de croissance microbienne en raison de sa nature organique.

Dans ce but, l'utilisation de m thodes analytiques rarement utilis es dans le milieu du g nie civil a  t  adopt e (extraction et s quen age de l'ADN).

Premi rement, le protocole de vieillissement acc l r  a  t  propos  qui visait   mieux repr senter les conditions d'utilisation compte tenu des informations constructives de l'installation de mortier de chanvre. Pour analyser l'influence du vieillissement, plusieurs dispositifs exp rimentaux ont  t  adopt s. Cela a permis d' tudier l' volution de la microstructure, de la composition chimique et des propri t s hygrothermiques.

Ensuite, la contamination microbienne a  t   tudi e de diff rents points de vue. Tout d'abord, l'influence de la prolif ration fongique sur la composition chimique a  t   tudi e. Ce travail a n cessit  l' tude des conditions de croissance des moisissures et la mise en place d'un protocole exp rimental permettant l'analyse et la comparaison de l' volution de la composition des mortiers bruts et contamin s. Ensuite, diff rentes m thodes d'identification ont  t  propos es pour comprendre la nature de la contamination fongique. Dans un premier temps, l'identification ph notypique a  t  appliqu e pour l'analyse de la contamination fongique. Ensuite, une autre m thode, proposant une technique de criblage fin de la contamination fongique et bact rienne, a  t  utilis e pour obtenir les r sultats les plus fiables.

**Title :** Micro-macroscopic approaches for evaluation of fungal mechanisms involved in the degradation of bio-sourced mortars: the impact on hygrothermal properties

**Keywords :** bio-based materials, hemp mortar, durability, aging cycles, biodeterioration, microbial contamination

**Abstract :** The main objective of this thesis work was the study of the durability of bio-based materials such as hemp mortar in the broad sense. The aspects of aging and different factors influencing the performance of hemp mortar during its period of use were taken into account. The originality of this work lies in several aspects. On the one hand, it is a study of the aging of hemp mortar. To do this, it is necessary both to adopt an aging protocol representative of the conditions of use of hemp mortar and to use different experimental methods to monitor the evolution of characteristics and properties. All this work has led to the implementation of specific setups for the application of aging cycles.

On the other hand, the in-depth study of the microbial proliferation is necessary to palliate the fact that the hemp mortar represents a great risk of microbial growth because of its organic nature. For this purpose, the use of analytical methods rarely used in the civil engineering environment was adopted (DNA extraction and sequencing).

First, the accelerated aging protocol was proposed which aimed to better represent the usage conditions considering the constructive information of the hemp mortar installation. To analyze the influence of aging, several experimental devices were adopted. This allowed to study the evolution of microstructure, chemical composition and hygrothermal properties.

Then, the microbial contamination was studied from different points of view. First, the influence of fungal growth on the chemical composition was studied. This work required the study of the conditions of growth of moulds and the implementation of an experimental protocol allowing the analysis and the comparison of the evolution of the composition of raw and contaminated mortars. Then, different identification methods were proposed to understand the nature of the fungal contamination. First, phenotypic identification was applied to analyze the fungal contamination. Then, another method, proposing a fine screening technique of fungal and bacterial contamination, was used to obtain the most reliable results.